Taming Flavor in Two Higgs Doublet Models

VNIVERSITAT DE VALÈNCIA

Fernando Cornet Gómez

IFIC, Universitat de València - CSIC

Tesi

Programa de Doctorat en Física

Juliol 2021

Directors

Francisco José Botella Olcina
Miguel Ruben Nebot Gómez

La única diferencia entre un científico y un niño
es el precio de sus juguetes.

A Sara

Francisco José Botella Olcina, catedràtic de la Universitat de València i **Miguel Rubén Nebot Gómez**, PI Investigador Distingit d'Excel.lencia CV de la Universitat de València

certifican:

Que la present memòria "Taming Flavor in Two Higgs Doublet Models" ha sigut realitzada sota la seua direcció a lInstitut de Física Corpuscular, centre mixt de la Universitat de València i del CSIC, per **Fernando Cornet Gómez** i constitueix la seua Tesi per a optar al grau de Doctor en Física. I perquè així conste, en compliment de la legislació vigent, presenta en el Departament de Física Teòrica de la Universitat de València la referida Tesi Doctoral, i firma el present certificat.

València, a 30 de juliol de 2021.

Francisco José Botella Olcina

Miguel Rubén Nebot Gómez

Contents

List of Abbreviations

The following abbreviations will be used throughout the thesis

2HDM . . . . . Two Higgs Doublet Model.

A2HDM . . . . Aligned Two Higgs Doublet Model.

BGL . . . . . Branco-Grimus-Lavoura

CKM . . . . . Cabibbo-Kobayashi-Maskawa.

DM . . . . . Dark Matter

EDMs . . . . . Electric Dipole Moments

EW . . . . . Electroweak

EWSB . . . . . Electroweak Symmetry Breaking.

FCNC . . . . . Flavor Changing Neutral Currents.

gBGL . . . . . Generalized Branco-Grimus-Lavoura

gFC . . . . . General Flavour Conservation

HEP . . . . . High Energy Physics

LHC . . . . . Large Hadron Collider

NFC . . . . . Natural Flavor Conservation

NP . . . . . New Physics

PDG . . . . . Particle Data Group

PMNS . . . . . Pontecorvo-Maki-Nakagawa-Sakata.

QCD . . . . . Quantum Chromodynamics

QED . . . . . Quantum Electrodynamics

RGE . . . . . Renormalization Group Evolution

SCPV . . . . . Spontaneous CP Violation

SFCNC . . . . Scalar Flavor Changing Neutral Couplings.

SM . . . . . Standard Model.

SSB . . . . . Spontaneous Symmetry Breaking

VEV . . . . . Vacuum expectation value

WB . . . . . Weak Basis

List of Publications

This Ph.D thesis is based on the following publications:

[1] J. M. Alves, F. J. Botella, G. C. Branco, F. Cornet-Gomez, and M. Nebot. "Controlled Flavour Changing Neutral Couplings in Two Higgs Doublet Models". In: *Eur. Phys. J. C* 77.9 (2017), p. 585. arXiv: 1703.03796 [hep-ph].

[2] F. J. Botella, F. Cornet-Gomez, and M. Nebot. "Flavor conservation in two-Higgs-doublet models". In: *Phys. Rev. D* 98.3 (2018), p. 035046. arXiv: 1803.08521 [hep-ph].

[3] J. M. Alves, F. J. Botella, G. C. Branco, F. Cornet-Gomez, M. Nebot, and J. P. Silva. "Symmetry Constrained Two Higgs Doublet Models". In: *Eur. Phys. J. C* 78.8 (2018), p. 630. arXiv: 1803.11199 [hep-ph].

[4] F. J. Botella, F. Cornet-Gomez, and M. Nebot. "Electron and muon $g-2$ anomalies in general flavour conserving two Higgs doublets models". In: *Phys. Rev. D* 102.3 (2020), p. 035023. arXiv: 2006.01934 [hep-ph].

[5] J. M. Alves, F. J. Botella, G. C. Branco, F. Cornet-Gomez, and M. Nebot. "The framework for a common origin of δ_{CKM} and δ_{PMNS}". In: *Eur. Phys. J. C* 81.8 (2021), p. 727. arXiv: 2105.14054 [hep-ph].

and this proceeding:

[6] F. J. Botella Olcina, F. Cornet-Gomez, and M. Nebot. "(g-2)l in the General Flavour Conserving 2HDM". In: *PoS* CORFU2019 (2020), p. 038.

–It would be the death of you to come with me, SAM,–
said Frodo– and I could not have borne that.
–Not as certain as being left behind– said SAM.
–But I am going to Mordor.
–I know that well enough, Mr. Frodo. Of course you are. And I'm coming with you.

— SAMwise Gamgee and Frodo Baggins
The Lord of the Rings, J. R. R. Tolkien

Preface

While the observation of the Higgs Boson at the Large Hadron Collider (LHC) completes the Standard Model, it is not the end of the story at all. Vibrant times concerning particle physics are to come, mainly in two directions. The first one is the SM precision calculations that could be tested as the experimental technology improves. This topic is not going to be covered in this thesis. The second one is to spot the aspects where the Standard Model fails and look for an explanation. This PhD thesis is focused on the second path i.e. the study of New Physics models that could solve some of the theoretical questions together with some of the experimental hints of physics beyond the Standard Model. The dissertation is divided in four parts.

With the goal of being as much self-contained as possible, part I contains all the theoretical foundations in which the thesis is based. This part also sets the notation that will be used. Chapter 1 contains a general overview of the Standard Model. After that, in chapter 2, the general Two Higgs Doublet Model is introduced and the notation concerning this class of models is set. This chapter also includes a review of some of the most studied types of Two Higgs Doublet Models.

Part II is dedicated to the theoretical aspects of the works developed during the doctoral period [1–3, 5]. More precisely, in chapter 3 we study the one loop renormalization group evolution of the simultaneous diagonalizability condition of the two Yukawa matrices (in the quark sector). Such condition would prevent the appearance of Flavor Changing Neutral Couplings. Chapter 4 contains a generalization of the so called Branco-Grimus-Lavoura models. In chapter 5, our most recent work is presented. There we propose a framework, based on the same symmetry that generates the generalized Branco-Grimus-Lavoura model, in which it

is possible to relate the complex phases of the quarks and leptons mixing matrices. Chapter 6 contains a systematic analysis of the different flavor structures obtained once extra abelian symmetries have been introduced into Two Higgs Doublet Models.

Part III is dedicated to the phenomenological aspects of the thesis. Chapter 7 collects all the different experimental observables that are going to be used as constraints in the fits presented in this part. The first analysis, presented in chapter 8, studies the general phenomenology of the generalized Flavor Conserving models introduced in chapter 3. Finally, in chapter 9 we show how one of the models presented in chapter 3 can reproduce both the electron and muon $(g-2)$ anomalies.

At the end it is possible to find the conclusions and a summary written in Catalan.

Part I

Theoretical Bases

–Snow's all right on a fine morning, but I like to be in bed while it's falling

— SAMwise Gamgee, *The Lord of the Rings*, J. R. R. Tolkien

1 The Standard Model

The Standard Model (SM)[7–10] of particle physics is currently the simplest and most successful theory that can explain the fundamental matter content and its interactions. The SM Lagrangian is invariant under the local symmetry group $SU(3)_c \times SU(2)_L \times U(1)_Y$ making it a gauge theory. The elementary particles, which are the fundamental degrees of freedom, can be classified into fermions (quarks and leptons) with spin 1/2 and bosons (gauge and Higgs bosons) with spin 1 and 0 respectively, that are representations of the Lorentz symmetry. These features provide a complete framework that is capable of explaining and predict in great detail most of the results obtained from the performed experiments. Therefore, the SM is seen as one of the greatest achievements in Modern Physics. In this chapter the theory will be briefly reviewed firstly. Then, both the most important phenomenological results as well as the open questions will be presented. For a full review of the SM see Refs. [11–13].

1.1 The SM particle content and interactions

The Standard Model is a gauge theory, based on the symmetry group $SU(3)_c \times SU(2)_L \times U(1)_Y$ which describes the interactions between the fundamental matter content. These fundamental matter *bricks* are the elementary particles that can

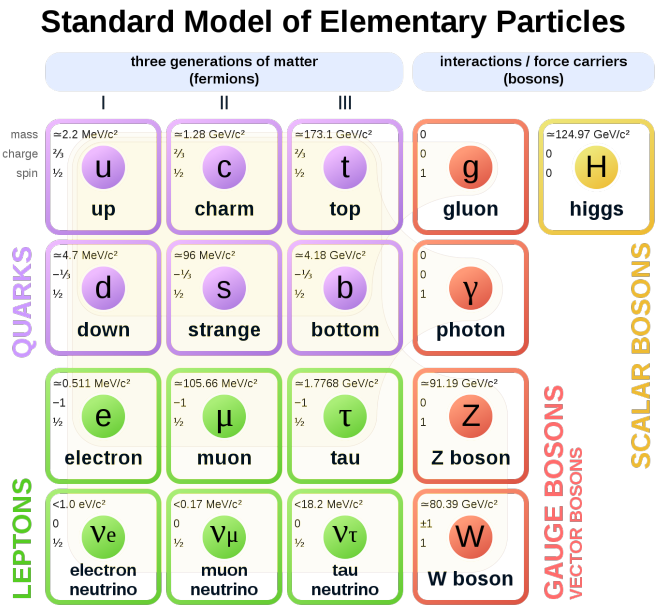

Table 1.1: Elementary particles of the Standard Model [14]

be divided in two groups based on their charge under the $SU(3)_c$ group, quarks and leptons. Both of them are fermions which mean that they have spin 1/2 and form what it is called the *observable matter*. Fermions interact with each other via exchange of bosons (spin 1 and 0) associated to the different forces. Fermions appear with a defined chirality in five different representations of the SM symmetry group. Left-handed fermions form $SU(2)_L$ doublets while their right-handed partners are singlets under the $SU(2)_L$ symmetry group

$$\begin{aligned} Q_L^0 &= \begin{pmatrix} u_L^0 \\ d_L^0 \end{pmatrix}, \qquad u_R^0\,, \qquad d_R^0\,, \\ L_L^0 &= \begin{pmatrix} \nu_L^0 \\ \ell_L^0 \end{pmatrix}, \qquad \ell_R^0\,. \end{aligned} \tag{1.1}$$

For every fermion in Eq. (1.1) there are three different copies, usually known as families or flavors. In table 1.1 all the flavors for both quarks and leptons can be found. Each copy has the same quantum numbers except for the mass, in other words, as we will see in following sections, that they have the same gauge interactions but different Yukawa couplings. The fact that gauge interactions among the different families are equal is known as flavor universality.

Type	Particle	$SU(3)_c$	$SU(2)_L$	$U(1)_Y$
Quarks	Q_L	3	2	1/6
	u_R	3	1	2/3
	d_R	3	1	-1/3
Leptons	L_L	1	2	-1/2
	ℓ_R	1	1	-1
Higgs	Φ	1	2	1/2

Table 1.2: Charges of the quarks, leptons and Higgs under the SM symmetry group.

The rest of the particles in table 1.1 are bosons which are responsible for the interaction between particles such as the Higgs or gauge bosons. The matter particles interact with each other via exchange of one of these bosons. As will be explained in following sections, bosons can interact with themselves as well. The gauge fields are defined in terms of the SM symmetry group generators. The $SU(3)_c$ has eight generators so there are eight massless gluons (G^{α}_{μ}). Associated to the $SU(2)_L \times U(1)_Y$ there are four bosons, the massless photon (A_μ), the mediator of electromagnetism, and the $W^{\pm}_{\mu}$ and Z_μ massive bosons that carry the weak force.

The interaction between quarks and gluons is described by Quantum Chromodynamics (QCD) the non-abelian gauge theory based on the $SU(3)_c$ group. QCD will be briefly reviewed in section 1.1.1. Weak and electromagnetic interactions are unified in the so-called Electroweak (EW) theory, discussed in section 1.1.2. In table 1.2 the charges of the fermions and the Higgs boson under the SM symmetry group can be found.

1.1.1 Quantum Chromodynamics

The non-abelian gauge theory that rules the interactions among quarks via exchange of gluons is known as Quantum Chromodynamics [15–18]. As it is shown in table 1.1 there are six different quark flavors, three with electric charge (in units of minus the electron charge) equals 2/3 (up, charm and top) and three with -1/3 (down, strange and bottom). Each of them can carry three different colors ($N_C = 3$) where color is the name that the number of degrees of freedom in the quark multiplet of the $SU(3)_c$ group receives.

The quarks' free Lagrangian reads

$$\mathscr{L}_0 = \sum_f \bar{q}_f \left(i\partial\!\!\!/ - m_f \right) q_f \,, \tag{1.2}$$

where q_f is a three-dimensional vector in color space and f runs over the six different quark flavors. The Lagrangian in eq. (1.2) is invariant under global $\mathrm{SU}(3)_c$ transformations

$$q_f^\alpha \longrightarrow q_f^{\alpha'} \equiv \mathcal{U}_\beta^\alpha q_f^\beta \,, \tag{1.3}$$

where

$$\mathcal{U} = \exp\left[\frac{i\lambda_a \theta_a}{2} \right] , \tag{1.4}$$

is an $\mathrm{SU}(3)_c$ rotation and λ_a the eight Gell-Mann matrices that are the generators of the group in the fundamental representation and θ_a are eight arbitrary constants. We are assuming summation over the repeated indices, which in this case is color. However, the Lagrangian in eq. (1.2) is not invariant under local transformations of this symmetry. This feature can be achieved by promoting the partial derivative to a covariant derivative. This process of promoting the derivative is usually mentioned as *to gauge the Lagrangian* since it is done to preserve local gauge symmetry in the Lagrangian The introduction of a spin-one field for each of the generators of the group is needed, that is, the gauge bosons that in the case of QCD are the gluons G_μ^α. The covariant derivative

$$D_\mu \equiv \left(\partial_\mu + i g_c G_\mu^\alpha \frac{\lambda_\alpha}{2} \right) , \tag{1.5}$$

where g_c is the $\mathrm{SU}(3)_c$ coupling, leads finally to the QCD Lagrangian

$$\mathscr{L}_{\mathrm{QCD}} = -\frac{1}{4} G_\alpha^{\mu\nu} G_{\mu\nu}^\alpha + \sum_f \bar{q}_f \left(i D\!\!\!/ - m_f \right) q_f \,, \tag{1.6}$$

where $G_\alpha^{\mu\nu}$ is the field stregths defined by

$$G_\alpha^{\mu\nu} = \partial^\mu G_\alpha^\nu - \partial^\nu G_\alpha^\mu - g_c f^{\alpha\beta\gamma} G_\beta^\mu G_\gamma^\nu \,, \tag{1.7}$$

and $f^{\alpha\beta\gamma}$ the totally antisymmetric structure constants of $\mathrm{SU}(3)_c$. This new derivative is responsible for the generation of the interaction terms among gauge fields

and fermions which are proportional to the gauge coupling g_c. These interactions are flavor universal, i.e. they are the same for all the fermion families. The first term in eq. (1.6) correspond yo the (gauge invariant) gluon kinetic term.

1.1.2 Electroweak theory

The electroweak [7–9] theory unifies both electromagnetic and weak interactions under the structure of the group $\mathrm{SU}(2)_L \times \mathrm{U}(1)_Y$. Analogously to the case of QCD, the interactions in the EW sector are mediated by gauge bosons, photons for the electromagnetic interactions and the $W^{\pm}$ and Z^0 for the weak ones. For compactness let us rename the fermion fields in eq. (1.1)

$$\begin{aligned} Q_1(x) \equiv Q_L^0 &= \begin{pmatrix} u_L^0 \\ d_L^0 \end{pmatrix}, \qquad Q_2 \equiv d_R^0\,, \qquad Q_3 \equiv u_R^0\,, \\ L_1(x) \equiv L_L &= \begin{pmatrix} \nu_L^0 \\ \ell_L^0 \end{pmatrix}, \qquad L_2(x) \equiv \ell_R^0\,, \end{aligned} \tag{1.8}$$

and consider the free Lagrangian for the fermions

$$\mathscr{L}_0 = i\sum_{j=1}^{3} \bar{Q}_j \not{\partial} Q_j + i\sum_{j=1}^{2} \bar{L}_j \not{\partial} L_j\,, \tag{1.9}$$

invariant under global $G \equiv \mathrm{SU}(2)_L \times \mathrm{U}(1)_Y$ transformations

$$\begin{aligned} Q_1(x) &\xrightarrow{G} Q_1'(x) = \exp\left[iY_1^q\beta\right]\mathcal{U}_L Q_1(x)\,, \\ Q_2(x) &\xrightarrow{G} Q_2'(x) = \exp\left[iY_2^q\beta\right] Q_2(x)\,, \\ Q_3(x) &\xrightarrow{G} Q_3'(x) = \exp\left[iY_3^q\beta\right] Q_3(x)\,, \\ L_1(x) &\xrightarrow{G} L_1'(x) = \exp\left[iY_1^\ell\beta\right]\mathcal{U}_L L_1(x)\,, \\ L_2(x) &\xrightarrow{G} L_2' = \exp\left[iY_2^\ell\beta\right] L_2(x)\,, \end{aligned} \tag{1.10}$$

where $\mathcal{U}_L$ is an $\mathrm{SU}(2)_L$ transformation defined by

$$\mathcal{U}_L = \exp\left[i\frac{\sigma_j}{2}\alpha^j\right], \tag{1.11}$$

being σ_j the Pauli matrices that are the generators of the $\mathrm{SU}(2)_L$ group in the doublet representation and α^j and β arbitrary constants. Transformation $\mathcal{U}_L$ is non-abelian and only acts on left-handed doublets. The hypercharge Y_j^f is the charge under the $\mathrm{U}(1)_Y$ transformation named in this way by analogy with the

Quantum Electrodynamics (QED) electric charge. At this point it is important to notice that there is no mass term in the Lagrangian in eq. (1.9). The only way of having a Dirac mass term is by mixing left-handed doublets with right-handed singlets, and that would break the symmetry.

We must require now the Lagrangian to be invariant under local $\mathrm{SU}(2)_L \times \mathrm{U}(1)_Y$ gauge transformations. This is achieved substituting $\alpha^j \to \alpha^j(x)$ and $\beta \to \beta(x)$. As in the QCD case, in order to keep the Lagrangian invariant under these new transformations, it is required to gauge it by promoting the partial derivatives to covariant ones. Now, as was anticipated before, four gauge bosons are needed since $\mathrm{SU}(2)_L$ has 3 generators and $\mathrm{U}(1)_Y$ has one generator. The covariant derivatives read

$$\begin{aligned}
D_\mu Q_1(x) &\equiv \left(\partial_\mu + ig\widetilde{W}_\mu(x) + ig' Y_1^q B_\mu(x)\right) Q_1(x)\,, \\
D_\mu Q_2(x) &\equiv \left(\partial_\mu + ig' Y_2^q B_\mu(x)\right) Q_2(x)\,, \\
D_\mu Q_3(x) &\equiv \left(\partial_\mu + ig' Y_3^q B_\mu(x)\right) Q_3(x)\,, \\
D_\mu L_1(x) &\equiv \left(\partial_\mu + ig\widetilde{W}_\mu(x) + ig' Y_1^\ell B_\mu(x)\right) L_1(x)\,, \\
D_\mu L_2(x) &\equiv \left(\partial_\mu + ig' Y_2^\ell B_\mu(x)\right) L_2(x)\,,
\end{aligned} \tag{1.12}$$

where $\widetilde{W}_\mu(x) = \frac{\sigma_j}{2} W_\mu^j(x)$ and g and g' are the $\mathrm{SU}(2)_L$ and $\mathrm{U}(1)_Y$ couplings respectively. The definition of the covariant derivatives automatically fixes the transformation of the gauge fields under the symmetry group

$$\begin{aligned}
\widetilde{W}_\mu(x) &\xrightarrow{G} \widetilde{W}'_\mu(x) \equiv \mathcal{U}_L \widetilde{W}_\mu(x) \mathcal{U}_L^\dagger + \tfrac{i}{g} \partial_\mu \mathcal{U}_L(x) \mathcal{U}_L^\dagger(x)\,, \\
B_\mu(x) &\xrightarrow{G} B'_\mu(x) \equiv B_\mu(x) - \tfrac{i}{g'} \partial_\mu \beta(x)\,,
\end{aligned} \tag{1.13}$$

where $\mathcal{U}_L(x)$ is just the substitution of α^j by $\alpha^j(x)$ in eq. (1.11). Now, in order to build a gauge invariant kinetic term, we must define the field strengths

$$\begin{aligned}
\widetilde{W}_{\mu\nu} &\equiv \partial_\mu \widetilde{W}_\nu - \partial_\nu \widetilde{W}_\mu + ig\left[\widetilde{W}_\mu, \widetilde{W}_\nu\right], \\
B_{\mu\nu} &\equiv \partial_\mu B_\nu - \partial_\nu B_\mu\,,
\end{aligned} \tag{1.14}$$

where the contraction $\widetilde{W}_{\mu\nu}$ is defined by

$$\widetilde{W}_{\mu\nu} = \frac{\sigma_i}{2} W_{\mu\nu}^i\,, \quad W_{\mu\nu}^i = \partial_\mu W_\nu^i - \partial_\nu W_\mu^i - g\,\epsilon^{ijk}\, W_{\mu,j} W_{\nu,k}\,, \tag{1.15}$$

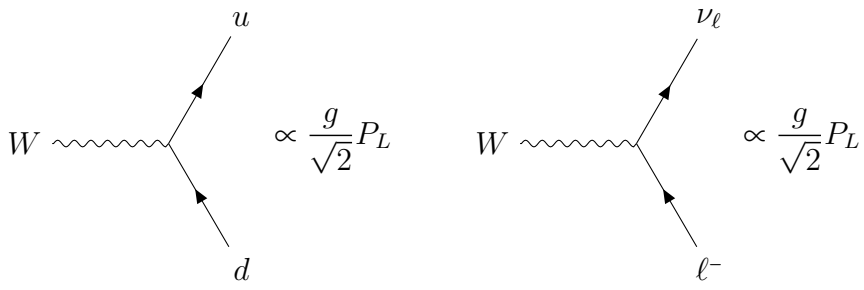

Figure 1.1: Charged current vertices [19]

being ϵ^{ijk} the totally antisymmetric tensor. Here, $\widetilde{W}_{\mu\nu}$ transforms in a covariant way under G transformations while $B_{\mu\nu}$ remains invariant

$$\widetilde{W}_{\mu\nu} \xrightarrow{G} \widetilde{W}'_{\mu\nu} \equiv \mathcal{U}_L \widetilde{W}_{\mu\nu} \mathcal{U}_L^\dagger \,, \qquad B_{\mu\nu} \xrightarrow{G} B'_{\mu\nu} \equiv B_{\mu\nu} \,. \tag{1.16}$$

The Lagrangian including the kinetic term reads

$$\mathscr{L}_{\text{EW}} = -\frac{1}{4} W^a_{\mu\nu} W_a^{\mu\nu} - \frac{1}{4} B_{\mu\nu} B^{\mu\nu} + i \sum_{j=1}^{3} \bar{Q}_j \not{D} Q_j + i \sum_{j=1}^{2} \bar{L}_j \not{D} L_j \,. \tag{1.17}$$

This Lagrangian generates cubic and quartic self interactions among gauge bosons. Furthermore, it contains charged and neutral fermionic currents

$$\begin{aligned} \mathscr{L}_{\text{EW}} \supset & - g \bar{Q}_1(x) \gamma^\mu \widetilde{W}_\mu Q_1(x) - g' B_\mu \sum_{j=1}^{3} Y_j^q \bar{Q}_j(x) \gamma^\mu Q_j(x) \\ & - g \bar{L}_1(x) \gamma^\mu \widetilde{W}_\mu L_1(x) - g' B_\mu \sum_{j=1}^{3} Y_j^\ell \bar{L}_j(x) \gamma^\mu L_j(x) \,, \end{aligned} \tag{1.18}$$

which are going to be studied in the following.

Charged Currents

The EW Lagrangian in eq. (1.18) contains interactions between fermions and $W^\pm$ bosons known as charged currents. In order to preserve electric charge, these terms must couple fermions of different charge, that is, an up-type and a down-type quark (figure 1.1 left) or a charged lepton with a neutrino (figure 1.1 right). These currents arise from the term containing the $\text{SU}(2)_L$ transformation matrix in eq. (1.18), that is

$$\widetilde{W}_\mu = \frac{\sigma_j}{2} W_\mu^j = \frac{1}{2} \begin{pmatrix} W_\mu^3 & \sqrt{2} W_\mu^\dagger \\ \sqrt{2} W_\mu & -W_\mu^3 \end{pmatrix} , \tag{1.19}$$

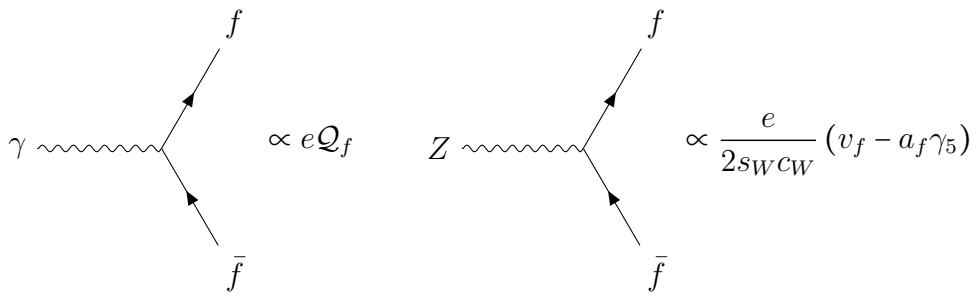

Figure 1.2: Neutral current vertices

where W_μ^1 and W_μ^2 are combined into $W_\mu \equiv \left(W_\mu^1 + iW_\mu^2\right)/\sqrt{2}$ and its hermitian-conjugate $W_\mu^\dagger \equiv \left(W_\mu^1 - iW_\mu^2\right)/\sqrt{2}$. Thus, the Lagrangian for the charged currents reads

$$\mathscr{L}_{\mathrm{CC}} = -\frac{g}{\sqrt{2}}\left\{W_\mu^\dagger\left[\bar{u}\gamma^\mu P_L d + \bar{\nu}_\ell \gamma^\mu P_L \ell\right] + \mathrm{h.c.}\right\}, \tag{1.20}$$

where P_L is the left-handed chirality projector

$$P_L = \frac{1-\gamma_5}{2}, \quad P_R = \frac{1+\gamma_5}{2}. \tag{1.21}$$

These terms correspond to the Feynman diagrams in figure 1.1 . It is important to notice that, for the moment we cannot use these vertices to explain the observed dynamics since we have not been able to build a mass term neither for the gauge bosons nor for the quarks and charged leptons and we know from experiments [20] that all of them have a non-zero mass.

Neutral Currents

In addition to the charge currents just presented, the Lagrangian in eq. (1.18) also contains terms that do not mix fermions of different charges. Those ones are known as neutral currents and are mediated by the photon (γ) and Z^0 neutral gauge bosons. After identifying the terms involving W_μ^1 and W_μ^2 with the charged currents, the remaining ones are those that involve W_μ^3 and B_μ. It is not straightforward to identify the photon with B_μ even though both B_μ and QED photon are the gauge bosons of a U(1) group. This can be easily understood by noticing that photons must couple in the same way to both fermion chiralities. In order to achieve that

for B_μ, in eq. (1.18), we would have to impose $Y_1^q = Y_2^q = Y_3^q$ and $Y_1^\ell = Y_2^\ell = Y_3^\ell$ as well as $g' Y_j^f = e\mathcal{Q}_j^f$ (with $\mathcal{Q}$ the electric charge) which cannot be simultaneously satisfied. This problem can be solved by combining the fields like

$$\begin{pmatrix} W_\mu^3 \\ B_\mu \end{pmatrix} = \begin{pmatrix} \cos\theta_W & \sin\theta_W \\ -\sin\theta_W & \cos\theta_W \end{pmatrix} \begin{pmatrix} Z_\mu \\ A_\mu \end{pmatrix}, \tag{1.22}$$

where θ_W is known as the *weak angle*. This transformation makes the Lagrangian for the neutral currents

$$\begin{aligned} \mathscr{L}_{\text{NC}} = &\sum_{j=1}^{3} \bar{Q}_j \left\{ \gamma^\mu A_\mu \left[g\frac{\sigma_3}{2} s_{\theta_W} + g' Y_j^q c_{\theta_W} \right] + \gamma^\mu Z_\mu \left[g\frac{\sigma_3}{2} c_W - g' Y_j^q s_W \right] \right\} Q_j \\ &+ \sum_{j=1}^{2} \bar{L}_j \left\{ \gamma^\mu A_\mu \left[g\frac{\sigma_3}{2} s_{\theta_W} + g' Y_j^\ell c_W \right] + \gamma^\mu Z_\mu \left[g\frac{\sigma_3}{2} c_W - g' Y_j^\ell s_{\theta_W} \right] \right\} L_j , \end{aligned} \tag{1.23}$$

where for compactness we have defined $c_W \equiv \cos\theta_W$ and $s_W \equiv \sin\theta_W$ Now, if we want that the field A_μ describes the QED photon, we must match the couplings

$$g \sin\theta_W = g' \cos\theta_W = e \quad \text{and} \quad Y = \mathcal{Q} - T_3 , \tag{1.24}$$

where $T_3 = \sigma_3/2$ is the weak isospin and $\mathcal{Q}$ the electromagnetic charge operator

$$\mathcal{Q}_1 \equiv \begin{pmatrix} \mathcal{Q}_{u(\nu)} & 0 \\ 0 & \mathcal{Q}_{d(\ell)} \end{pmatrix}, \quad \mathcal{Q}_2 \equiv \mathcal{Q}_{d(\ell)} , \quad \mathcal{Q}_3 \equiv \mathcal{Q}_u . \tag{1.25}$$

Eq. (1.24) provides the desired relation between $\text{SU}(2)_L \times \text{U}(1)_Y$ couplings and electromagnetism and fixes the hypercharge in terms of the electric charge and the weak isospin. Thus, the hypercharges, as was anticipated in table 1.2, read

$$\begin{aligned} Y_1^q &= \begin{cases} Y_1^u = \mathcal{Q}_u - \frac{1}{2} = \frac{1}{6} \\ Y_1^d = \mathcal{Q}_d + \frac{1}{2} = \frac{1}{6} \end{cases}, \qquad Y_2^q = \mathcal{Q}_d = -\frac{1}{3} , \quad Y_3^q = \mathcal{Q}_u = \frac{2}{3} , \\ Y_1^\ell &= \begin{cases} Y_1^\nu = \mathcal{Q}_\nu - \frac{1}{2} = -\frac{1}{2} \\ Y_1^\ell = \mathcal{Q}_\ell + \frac{1}{2} = -\frac{1}{2} \end{cases}, \qquad Y_2^\ell = \mathcal{Q}_\ell = -1 . \end{aligned} \tag{1.26}$$

At this point it is interesting to notice that if we had included a right-handed neutrino both the electric charge and the hypercharge would have equaled zero. That means that it does not couple to any other field neither via charged currents nor neutral currents. In QED the right neutrino field would be sterile and for that reason, along with the fact that historically neutrinos where assumed to be

massless[1], a right-handed neutrino was not included in the SM context. All the pieces of the neutral currents Lagrangian have been presented, in particular

$$\mathscr{L}_{\mathrm{NC}} = \mathscr{L}_{\mathrm{QED}} + \mathscr{L}^{Z}_{\mathrm{NC}}\,, \tag{1.27}$$

where the QED Lagrangian is

$$\mathscr{L}_{\mathrm{QED}} = -eA_\mu \sum_f \bar{\psi}_f \gamma^\mu \mathcal{Q}_f \psi_f\,, \tag{1.28}$$

where ψ_f represents the five possible fermions fields Q_L, L_L, u_R, d_R and ℓ_R. The Z_μ boson part has the well-known V-A (*vector minus axial*) structure

$$\mathscr{L}^{Z}_{\mathrm{NC}} = \frac{e}{2\sin\theta_W \cos\theta_W} Z_\mu \sum_f \bar{f}\gamma^\mu \left(v_f - a_f\gamma_5\right) f\,, \tag{1.29}$$

where the vector coupling is defined as $v_f \equiv T_3^f \left(1 - 4|\mathcal{Q}_f|\sin^2\theta_W\right)$ and the axial as $a_f \equiv T_3^f$.

At this point it is important to remember that we may have been missing something. It is known that the $W^\pm$ and Z^0 bosons are massive but in the EW Lagrangian in eq. (1.17) there is no possible mass term for these fields without breaking the symmetry. This problem is solved through the Brout-Englert-Higgs[2] [22, 23] and it will be presented in section 1.1.3.

Gauge Sector

In addition to charged and neutral currents just reviewed, the Lagrangian in eq. (1.17) contains gauge boson self-interactions, in particular there are cubic and quartic vertices (see figure 1.3). The Lagrangian for the cubic interactions reads

$$\begin{aligned}\mathscr{L}_3 = ie\cot\theta_W \Big\{ &\left(\partial^\mu W^\nu - \partial^\nu W^\mu\right) W^\dagger_\mu Z_\nu \quad - \left(\partial^\mu W^{\nu\dagger} - \partial^\nu W^{\mu\dagger}\right) W_\mu Z_\nu \\ &\qquad + W_\mu W^\dagger_\nu \left(\partial^\mu Z^\nu - \partial^\nu Z^\mu\right)\Big\} \\ + ie\Big\{ &\left(\partial^\mu W^\nu - \partial^\nu W^\mu\right) W^\dagger_\mu A_\nu \quad - \left(\partial^\mu W^{\nu\dagger} - \partial^\nu W^{\mu\dagger}\right) W_\mu A_\nu \\ &\qquad + W_\mu W^\dagger_\nu \left(\partial^\mu A^\nu - \partial^\nu A^\mu\right)\Big\}\,,\end{aligned} \tag{1.30}$$

[1] Without a right-handed neutrino a Dirac mass term cannot be built but being the neutrino a chargeless particle we can add a Majorana mass term, via a non-renormalizable interaction, (that violates lepton number conservation) to the Lagrangian.

[2] Some authors refers to this as the Englert-Brout-Higgs-Guralnik-Hagen-Kibble mechanism giving credit to a slightly later, but independent, contribution of Guralnik, Hagen and Kibble[21].

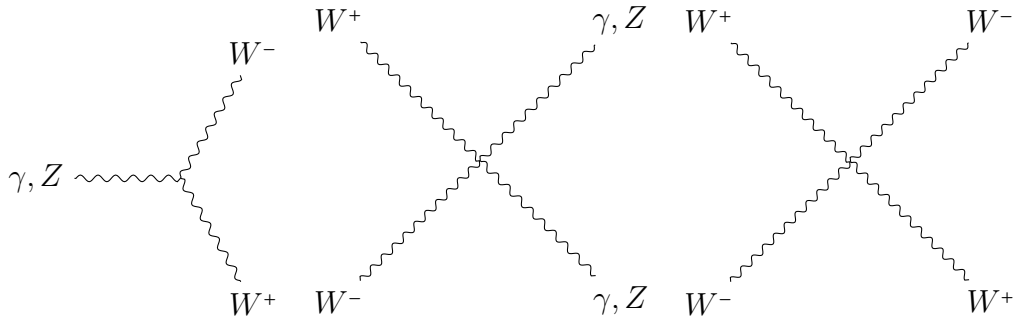

Figure 1.3: Gauge bosons cubic and quartic self interactions

and for the quartic

$$\mathscr{L}_4 = -\frac{e^2}{2\sin^2\theta_W}\left\{\left(W_\mu^\dagger W^\mu\right)^2 - W_\mu^\dagger W^{\mu\dagger} W_\nu W^\nu\right\} - e^2\cot^2\theta_W\left\{W_\mu^\dagger W^\mu Z_\nu Z^\nu - W_\mu^\dagger Z^\mu W_\nu Z^\nu\right\}. \quad (1.31)$$

1.1.3 The Scalar Sector

As mentioned above, the EW theory cannot explain by its own that the $W^\pm$ and Z bosons are massive as experimental evidence dictates. The insertion of a mass term would break the gauge symmetry making the Lagrangian non-renormalizable. This problem will be solved in this section with what is called Spontaneous Symmetry Breaking (SSB)[21–24]. As we will see, the Lagrangian will remain invariant under the symmetry group but the state with minimal energy will be degenerate. If one of the set of degenerate states is arbitrarily selected as the ground state of the system, the symmetry will be *spontaneously* broken. In Quantum Field Theory, the fact that there are flat directions connecting the different minima implies the existence of massless degrees of freedom. This result is known as Goldstone theorem [25, 26] and it is going to be reviewed in general next. After that, it will be applied to the EW theory.

Goldstone Theorem

Let us study the Lagrangian of a complex scalar field $\Phi(x)$

$$\mathscr{L} = \partial_\mu\Phi^\dagger\partial^\mu\Phi - V(\Phi), \quad \text{where} \quad V(\Phi) = \mu^2\Phi^\dagger\Phi + \lambda\left(\Phi^\dagger\Phi\right)^2, \quad (1.32)$$

being λ and μ arbitrary parameters. This Lagrangian is invariant under global phase transformations of the scalar field

$$\Phi(x) \to \Phi'(x) \equiv \exp[i\theta]\Phi(x)\,, \tag{1.33}$$

where θ is an arbitrary constant. We must require the parameter λ to be positive in order to have a ground state in the potential $V(\Phi)$. There are two possibilities depending on the value of μ^2.

- **If $\mu^2 > 0$** the potential only has the minimum $\Phi = 0$. The Lagrangian contains two terms, a mass term with mass equals μ for the scalar field Φ and a quartic self-interaction term with coupling λ.

- **If $\mu^2 < 0$** there is a degenerate set of minima satisfying

$$|\Phi_0| = \sqrt{\frac{-\mu^2}{2\lambda}} \equiv \frac{v}{\sqrt{2}} > 0 \quad \text{and} \quad V(\Phi_0) = -\frac{\lambda}{4}v^4\,. \tag{1.34}$$

  The invariance under phase transformations provokes the existence of infinite ground states $\Phi_0(x) = \frac{v}{\sqrt{2}}\exp[i\theta]$ with the same energy.

We are interested in the second scenario ($\mu^2 < 0$). By choosing one of the possible states, for simplicity $\Phi_0(x) = \frac{v}{\sqrt{2}}$ the symmetry breaks *spontaneously*. It is possible to parametrize the scalar field as excitations over the ground state

$$\Phi(x) = \frac{v + \rho(x) + i\eta(x)}{\sqrt{2}}\,, \tag{1.35}$$

where now $\rho(x)$ and $\eta(x)$ are real scalar fields. If we expand the potential in term of the real fields

$$V(\rho,\eta) = -\frac{\lambda}{4}v^4 - \mu^2\rho^2(x) + \lambda v\rho(x)\left(\rho^2(x) + \eta^2(x)\right) + \frac{\lambda}{4}\left(\rho^2(x) + \eta^2(x)\right)^2\,, \tag{1.36}$$

we can clearly see that while there is a mass term for ρ with mass $m_\rho^2 = -2\mu^2$ there is not such a term for η. That is, a massless particle has emerged after SSB. This is easy to understand (see 1.4) since η is describing excitations around a flat direction in the potential i.e. from one ground state to another. These transitions do not cost any energy so they correspond to massless states. This is a general result and it is known as Goldstone Theorem [25, 26]

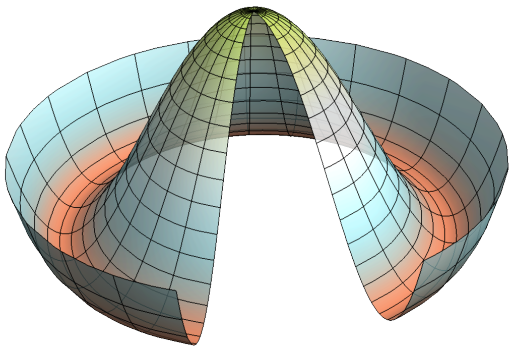

Figure 1.4: Higgs potential for the $\mu^2 < 0$ case. The horizontal lines correspond to the flat directions.

> *If a Lagrangian is invariant under a continuous symmetry group G, but the vacuum is only invariant under a subgroup $H \subset G$, then there must exist as many massless spin-0 particles (Nambu-Goldstone bosons) as broken generators (i.e. generators of G which do not belong to H).*

Brout-Englert-Higgs mechanism

Let us remember that our goal was to generate masses for the gauge bosons. It is clear that the Goldstone theorem as it is formulated in the previous section cannot do this for us given that it generates massless fields. However, when a local gauge symmetry, instead of a global one, is broken we can achieve our goal. The simplest way of implementing this mechanism is by introducing an $\mathrm{SU}(2)_L$ doublet

$$\Phi(x) = \begin{pmatrix} \varphi^+(x) \\ \varphi^0(x) \end{pmatrix}, \tag{1.37}$$

and the gauged Lagrangian

$$\begin{aligned}\mathscr{L}_S &= (D_\mu\Phi)^\dagger D_\mu\Phi - \mu^2\Phi^\dagger\Phi - \lambda(\Phi^\dagger\Phi)^2\,, \quad (\lambda>0,\,\mu^2<0),\\ D^\mu\Phi &= \left(\partial^\mu + ig\widetilde{W}^\mu + ig'Y_\Phi B^\mu\right)\Phi,\end{aligned} \tag{1.38}$$

that is invariant under $\mathrm{SU}(2)_L \times \mathrm{U}(1)_Y$ transformations. Requiring that the photon A_μ does not couple to φ^0 and that φ^+ has the right electric charge, the hypercharge of the doublet is fixed

$$Y_\Phi = \mathcal{Q}_\Phi - T_3 = \frac{1}{2}\,. \tag{1.39}$$

As in the case studied in the Goldstone theorem (eq. (1.36)), the scalar potential has an infinite set of minima

$$|\langle 0|\Phi|0\rangle| = \begin{pmatrix} 0 \\ |\langle 0|\varphi^0|0\rangle| \end{pmatrix} = \begin{pmatrix} 0 \\ \sqrt{\frac{-\mu^2}{2\lambda}} \end{pmatrix}, \tag{1.40}$$

where we can define

$$\sqrt{\frac{-\mu^2}{2\lambda}} \equiv \frac{v}{\sqrt{2}}\,, \tag{1.41}$$

being v the vacuum expectation value (VEV). Here, since the electric charge must be conserved, the VEV of the charged field must vanish so only the neutral component can acquire a vacuum expectation value different from zero. Thus, the original $\mathrm{SU}(2)_L \times \mathrm{U}(1)_Y$ symmetry group gets broken to the electromagnetic $U(1)_{\mathcal{Q}}$.

At the beginning, the Lagrangian was symmetric under $\mathrm{SU}(2)_L \times \mathrm{U}(1)_Y$ that has four generators, three corresponding to $\mathrm{SU}(2)_L$ and one from the $\mathrm{U}(1)_Y$ symmetry group. After spontaneously breaking the symmetry we end up with just one unbroken generator from the $U(1)_{\mathcal{Q}}$ group, that is, three generators have been broken. Attending to the Goldtone theorem, three massless Goldstone bosons will arise. But now we can parametrize the doublet as excitations around the vacuum

$$\Phi(x) = \begin{pmatrix} \varphi^+(x) \\ \frac{1}{\sqrt{2}}\left(v + \rho(x) + i\eta(x)\right) \end{pmatrix}, \tag{1.42}$$

or analogously

$$\Phi(x) = \exp\left[i\frac{\sigma_j}{2}\theta^j(x)\right]\frac{1}{\sqrt{2}}\begin{pmatrix} 0 \\ v + \mathrm{h}(x) \end{pmatrix}, \tag{1.43}$$

where $\mathrm{h}(x)$ is a real scalar field as well as $\theta^j(x)$ that are precisely the Goldstone bosons. But now, as we saw in eqs. (1.10)–(1.11), by a local $\mathrm{SU}(2)_L$ transformation it is possible to *gauge away* any dependence on $\theta^j(x)$ by

$$\Phi(x) \xrightarrow{\mathrm{SU}(2)_L} H_{SM}(x) = \exp\left[i\tfrac{\sigma_j}{2}\alpha^j(x)\right]\Phi(x)\,, \tag{1.44}$$

and matching $\alpha^j(x) = -\theta_j(x)$. Here we have chosen a particular gauge which is known as the unitary gauge. We are left with

$$H_{SM}(x) = \frac{1}{\sqrt{2}}\begin{pmatrix} 0 \\ v + \mathrm{h}(x) \end{pmatrix}. \tag{1.45}$$

It might seem that there are three missing degrees of freedom but if we expand the kinetic term of the Lagrangian in eq. (1.38) in terms of the real scalar field $h(x)$ and the VEV

$$(D_\mu\Phi)^\dagger D_\mu\Phi = \frac{1}{2}\partial_\mu\mathrm{h}\partial^\mu\mathrm{h} + (v+\mathrm{h})^2\left\{\frac{g^2}{4}W_\mu^\dagger W^\mu + \frac{g^2}{8\cos^2\theta_W}Z_\mu Z^\mu\right\}, \tag{1.46}$$

we can see that mass terms for the W and Z gauge bosons have appeared. That is to say, the degrees of freedom from the *would-be Goldstone bosons* become the longitudinal polarizations of the $W^\pm$ and Z^0 gauge bosons. The masses are related by the weak mixing angle

$$M_W = \frac{1}{2}vg = M_Z\cos\theta_W. \tag{1.47}$$

Moreover the Brout-Englert-Higgs [21–23] mechanism predicts the appearance of a scalar particle h, known as the Higgs boson and described by the Lagrangian

$$\mathscr{L}_{\mathrm{S}} = \frac{1}{4}\lambda v^4 + \mathscr{L}_{\mathrm{h}} + \mathscr{L}_{\mathrm{h\text{-}G}}\,, \tag{1.48}$$

where

$$\begin{aligned}
\mathscr{L}_{\mathrm{h}} &= \frac{1}{2}\partial_\mu\mathrm{h}\partial^\mu\mathrm{h} - \frac{1}{2}\mathrm{m}_{\mathrm{h}}^2\mathrm{h}^2 - \frac{\mathrm{m}_{\mathrm{h}}^2}{2v}\mathrm{h}^3 - \frac{\mathrm{m}_{\mathrm{h}}^2}{8v^2}\mathrm{h}^4\,,\\
\mathscr{L}_{\mathrm{h\text{-}G}} &= M_W^2 W_\mu^\dagger W^\mu\left\{1 + \frac{2}{v}\mathrm{h} + \frac{1}{v^2}\mathrm{h}^2\right\} + \frac{1}{2}M_Z^2 Z_\mu Z^\mu\left\{1 + \frac{2}{v}\mathrm{h} + \frac{1}{v^2}\mathrm{h}^2\right\},
\end{aligned} \tag{1.49}$$

and

$$\mathrm{m}_{\mathrm{h}} = \sqrt{-2\mu^2} = \sqrt{2\lambda}\,v\,. \tag{1.50}$$

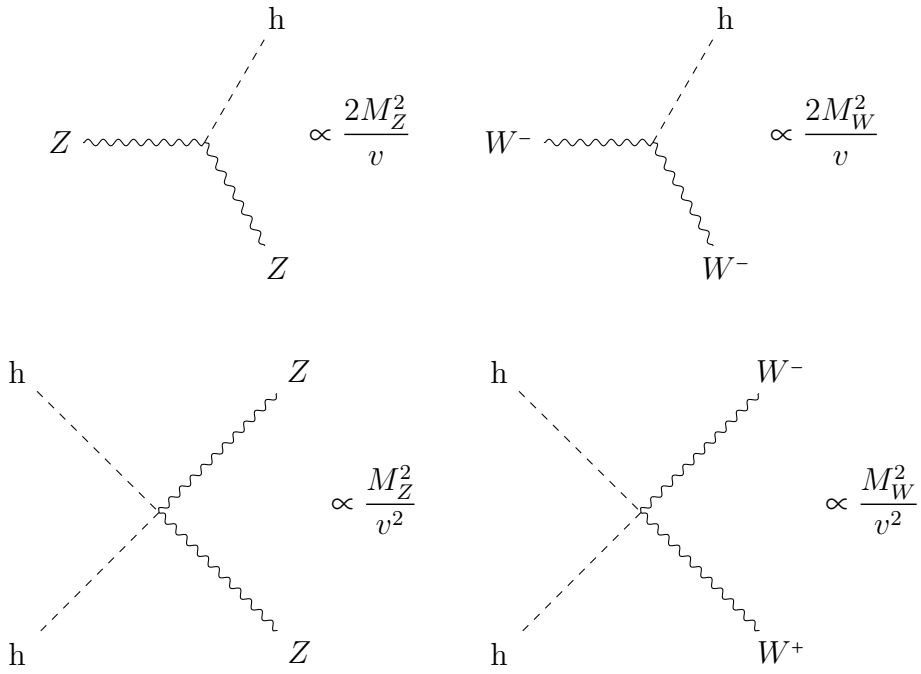

Figure 1.5: Higgs couplings to the gauge bosons

The Higgs mechanism implies the existence of the Higgs boson but it does not predict its mass, that is, it is a free parameter of the theory. In figure 1.5 the vertices that involve the Higgs and gauge bosons described by the Lagrangian in eq. (1.49) can be found.

The Higgs boson was the last missing particle predicted by the Standard Model. It was discovered in 2012 by ATLAS [27] and CMS [28]. As we have seen, it was a crucial piece since it was necessary to explain the gauge bosons masses. The Higgs boson does not only accomplish this mission but also it is necessary to build the structures that provide mass to the fermions. Without the scalar doublet, a fermionic mass term in the Lagrangian would break gauge invariance. This is going to be reviewed in the next section.

Yukawa Sector

The straightforward way of explaining fermion masses is by introducing a mass term in the Lagrangian of the form

$$\mathscr{L}_m = -m\bar{\psi}\psi = -m\left(\bar{\psi}_L\psi_R + \bar{\psi}_R\psi_L\right), \tag{1.51}$$

but this structure, that mixes left and right-handed fields which are in different $\mathrm{SU}(2)_L$ representations is not invariant under gauge symmetry transformations. Nevertheless, and making use of the Higgs doublet introduced in the previous section, it is possible to build fermion-scalar couplings that are gauge invariant and read

$$\mathscr{L}_{\mathrm{Y}} = -\bar{Q}^0_L\, Y_d \Phi \;\; d^0_R - \bar{Q}^0_L\, Y_u \tilde{\Phi} \;\; u^0_R - \bar{L}^0_L\, Y_\ell \Phi \;\; \ell^0_R + \mathrm{h.c.}\,, \tag{1.52}$$

as in 1.37 the scalar doublet is defined as

$$\Phi = \begin{pmatrix} \varphi^+ \\ \varphi^0 \end{pmatrix}, \tag{1.53}$$

and its $\mathcal{C}$-conjugate

$$\tilde{\Phi} \;\equiv i\sigma_2 \Phi^* = \begin{pmatrix} \varphi^{0\dagger} \\ -\varphi^- \end{pmatrix}. \tag{1.54}$$

Once SSB is performed, in the unitary gauge, the Lagrangian reads

$$\mathscr{L}_{\mathrm{Y}} = -\frac{1}{\sqrt{2}}\,(v+h)\left\{\bar{d}^0_L\, Y_d\, d^0_R + \bar{u}^0_L\, Y_u\, u^0_R + \bar{\ell}^0_L\, Y_\ell\, \ell^0_R\right\} + \mathrm{h.c.}\,, \tag{1.55}$$

where clearly the terms proportional to the vev provide the fermion mass matrices

$$\mathrm{M}^0_d = \frac{v}{\sqrt{2}} Y_d\,, \quad \mathrm{M}^0_u = \frac{v}{\sqrt{2}} Y_u\,, \quad \mathrm{M}^0_\ell = \frac{v}{\sqrt{2}} Y_\ell\,, \tag{1.56}$$

that are 3×3 matrices since there are three flavors of each fermion type. These mass matrices are not, in principle, diagonal, what adds a total of 54 new real parameters coming from nine complex elements of each matrix.

The Lagrangians in eqs. (1.17)–(1.48) are invariant under what is known as Weak Basis (WB) transformations. That is, transformations of the symmetry group $\mathrm{U}(3)_{Q_L} \times \mathrm{U}(3)_{d_R} \times \mathrm{U}(3)_{u_R} \times \mathrm{U}(3)_{L_L} \times \mathrm{U}(3)_{\ell_R}$. However, the one in eq. (1.55) it is not. This feature will be used to diagonalize the mass matrices absorbing some of the parameters into the fermionic fields.

As we know experimentally [20] that none of the quark neither the charge lepton masses are zero, the rank of the mass matrices in eq. (1.56) must be three. That is their determinant cannot vanish $\det(\mathrm{M}^0_f) \neq 0$. Any complex square matrix can be polar decomposed as

$$\mathrm{M}^0_f = \mathrm{H}_f\, \mathrm{S}_f\,, \tag{1.57}$$

where H_f is a positive semidefinite hermitian matrix and S_f a unitary matrix. As the determinant of M_f^0 is different from zero, H_f is unique

$$\mathrm{H}_f = \sqrt{\mathrm{M}_f^0 \mathrm{M}_f^{0\dagger}}\,, \tag{1.58}$$

and can be diagonalized by a unitary matrix $\mathcal{U}_{f_L}$ as

$$\mathrm{H}_f = \mathcal{U}_{f_L} \mathrm{M}_f \mathcal{U}_{f_L}^\dagger\,, \tag{1.59}$$

being M_f a diagonal matrix with all its elements positive. Thus, the diagonal mass matrix reads

$$\mathrm{M}_f = \mathcal{U}_{f_L}^\dagger \mathrm{H}_f \mathcal{U}_{f_L} = \mathcal{U}_{f_L}^\dagger \mathrm{M}_f^0 \mathcal{U}_{f_R}\,, \tag{1.60}$$

where $\mathcal{U}_{f_R} = \mathrm{S}_f^\dagger \mathcal{U}_{f_L}$ is also a unitary matrix. The diagonal mass matrices for each fermion type are

$$\begin{aligned}
\mathrm{M}_d &= \mathcal{U}_{d_L}^\dagger \mathrm{M}_d^0 \mathcal{U}_{d_R} = \mathrm{diag}(m_d, m_s, m_b)\,,\\
\mathrm{M}_u &= \mathcal{U}_{u_L}^\dagger \mathrm{M}_u^0 \mathcal{U}_{u_R} = \mathrm{diag}(m_u, m_c, m_t)\,,\\
\mathrm{M}_\ell &= \mathcal{U}_{\ell_L}^\dagger \mathrm{M}_\ell^0 \mathcal{U}_{\ell_R} = \mathrm{diag}(m_e, m_\mu, m_\tau)\,.
\end{aligned} \tag{1.61}$$

Finally, thanks to WB invariance the fermion fields can be redefined in order to absorb some of the bi-diagonalization matrices:

$$\begin{aligned}
Q_L = \mathcal{U}_{u_L}^\dagger Q_L^0\,, \quad & d_R = \mathcal{U}_{d_R}^\dagger d_R^0\,,\\
& u_R = \mathcal{U}_{u_R}^\dagger u_R^0\,,\\
L_L = \mathcal{U}_{\ell_L}^\dagger L_L^0\,, \quad & \ell_R = \mathcal{U}_{\ell_R}^\dagger \ell_R\,,
\end{aligned} \tag{1.62}$$

giving rise, already in the unitary gauge, to

$$\mathscr{L}_\mathrm{Y} = -\left(1 + \frac{h}{v}\right)\left\{\bar{d}'_L\, V \mathrm{M}_d\, d_R + \bar{u}_L\, \mathrm{M}_u\, u_R + \bar{\ell}_L\, \mathrm{M}_\ell\, \ell_R\right\} + \mathrm{h.c.}\,, \tag{1.63}$$

where we have introduced the Cabibbo-Kobayashi-Maskawa (CKM)[29, 30] matrix $V \equiv \mathcal{U}_{u_L}^\dagger \mathcal{U}_{d_L}$ as the clash between the left-handed matrices needed to bring to its diagonal forms M_d and M_u, the quark mass matrices. The entries of the CKM matrix are usually labeled as

$$V = \begin{pmatrix} V_{ud} & V_{us} & V_{ub} \\ V_{cd} & V_{cs} & V_{cb} \\ V_{td} & V_{ts} & V_{tb} \end{pmatrix}. \tag{1.64}$$

Therefore from the flavor structures in the quark sector we are left just with the quark masses (inside M_d and M_u) and the CKM matrix V. The traditional way of doing perturbation theory makes convenient to diagonalize VM_d by means of the transformation

$$\bar{d}'_L = \bar{d}_L V^\dagger \,, \tag{1.65}$$

that is not a WB transformation. Therefore V will become observable in general. In particular V will appear in the charged currents but not in the neutral. In the leptonic sector we have managed to diagonalize the mass matrix with a WB transformation because neutrinos are massless.

In this basis where the mass matrices are diagonal, the neutral currents Lagrangian in eq. (1.27) does not change since $\bar{f}^0_L \gamma_\mu f^0_L = \bar{f}_L \gamma_\mu f_L$ and $\bar{f}^0_R \gamma_\mu f^0_R = \bar{f}_R \gamma_\mu f_R$. However, the charged currents in eq. (1.20) do change given that

$$\bar{u}^0_L \gamma_\mu d^0_L = \bar{u}_L \mathcal{U}^\dagger_{u_L} \gamma_\mu \, \mathcal{U}_{d_L} d_L = \bar{u}_L \gamma_\mu V \, d_L \,. \tag{1.66}$$

Taking this into account, the charged current Lagrangian reads

$$\mathscr{L}_{\rm CC} = -\frac{g}{\sqrt{2}} \left\{ W^\dagger_\mu \left[\sum_{jk} \bar{u}_j \gamma^\mu P_L V_{jk} d_k + \sum_\ell \bar{\nu}_\ell \gamma^\mu P_L \ell \right] + \text{h.c.} \right\} . \tag{1.67}$$

At this point it is important to remember that in the SM framework the neutrinos are assumed to be massless. For this reason, it is always possible to rotate the lepton fields in the flavor space in order to eliminate the analogous to the CKM matrix for the leptonic sector. In the lepton sector we can diagonalize all the flavor structures with a WB transformation. That means that flavor is conserved in the SM leptonic sector if neutrinos are massless. We will see in 1.2 that in fact, neutrinos are not massless particles and then a mixing matrix will appear. This matrix is known as the Pontecorvo-Maki-Nakagawa-Sakata (PMNS) matrix [31, 32].

The CKM matrix is a unitary matrix so in principle it contains nine real parameters, three moduli and six phases. Nevertheless, not all of them are physical since it is always possible to choose arbitrary quark phases by

$$u_j \to \exp[i\theta_j] u_j \,, \qquad d_k \to \exp[i\omega_k] d_k \,, \tag{1.68}$$

Collaboration	λ	A	$\bar{\rho}$	$\bar{\eta}$
CKMfitter[34]	$0.224837^{+0.000251}_{-0.000060}$	$0.8235^{+0.0056}_{-0.0145}$	$0.1569^{+0.0102}_{-0.0061}$	$0.3499^{+0.0079}_{-0.0065}$
UTfit [35]	0.22534 ± 0.00065	0.821 ± 0.012	0.132 ± 0.023	0.352 ± 0.014

Table 1.3: Experimental values for the Wolfenstein parameters from flavor fits where the barred parameters are defined as $(\bar{\rho}, \bar{\eta}) = (1 - \lambda^2/2)(\rho, \eta)$.

that transform the CKM matrix as $V_{jk} \to \exp[i(\omega_k - \theta_j)]V_{jk}$ leaving only 1 physical phase. Then, the CKM matrix can be parametrized with three angles and one phase as

$$V = \begin{pmatrix} c_{12}c_{13} & s_{12}c_{13} & s_{13}e^{-\delta_{13}} \\ -s_{12}c_{23} - c_{12}s_{23}s_{13}e^{i\delta_{13}} & c_{12}c_{23} - s_{12}s_{23}s_{13}e^{i\delta_{13}} & s_{23}c_{13} \\ c_{12}s_{23} - c_{12}c_{23}s_{13}e^{i\delta_{13}} & -c_{12}s_{23} - s_{12}c_{23}s_{13}e^{i\delta_{13}} & c_{23}c_{13} \end{pmatrix}, \tag{1.69}$$

following the Particle Data Group (PDG) advice [20]. Along this thesis, the Wolfenstein parametrization [33] that reads

$$V = \begin{pmatrix} 1 - \frac{\lambda^2}{2} & \lambda & A\lambda^3(\rho - i\eta) \\ -\lambda & 1 - \frac{\lambda^2}{2} & A\lambda^2 \\ A\lambda^3(1 - \rho - i\eta) & -A\lambda^2 & 1 \end{pmatrix} + \mathcal{O}(\lambda^4), \tag{1.70}$$

will also be used. The current experimental values for this parametrization can be found in table 1.3. These values are obtained by CKMfitter [34] and UTfit [35] performing a global fit to flavor observables. In this parametrization it is easy to notice that the CKM matrix has a very hierarchical structure since it is written as an expansion of a small parameter $\lambda \approx 0.23$. Furthermore, we can directly see that flavor changing transitions will be suppressed compared to the flavor conserving ones.

To sum up, when the three Yukawa matrices were introduced there were, in principle, 54 real parameters but we have seen that thanks to the WB invariance it is possible to reduce them to only 13 physical parameters coming from the nine fermion masses, the three angles and one phase from the CKM mixing matrix. It is important to notice as well that the complex CKM phase δ_{13} is the only complex phase in the Standard Model Lagrangian which means that it is the only possible source of $\mathcal{CP}$ violation. This fact was used to assume the existence of the third family [30], given that a CKM matrix for two families does not have a complex phase.

Finally, it is important to realize that there are no tree-level Flavor Changing Neutral Currents (FCNC) in the SM. Not only neutral currents coming from the

photon and Z boson preserve flavor but also higgs-mediated interactions do. This happens because once the mass matrices are diagonalized, there is no Yukawa term that mixes different fermion families. The CKM matrix, which is the quark mixing matrix, is only present in vertices mediated by the $W^{\pm}$ bosons. At one loop level, FCNC are very suppressed in the SM by the GlashowIliopoulosMaiani (GIM) mechanism [10]. This strong suppression is also observed experimentally. In following sections, we will see that this is a key feature when building NP models as the 2HDM.

Complete SM Lagrangian

In the previous sections, we have studied all the mechanisms that play a role in the SM as well as the full Lagrangian by parts. Combining all of them, the SM Lagrangian is obtained

$$\mathscr{L}_{\text{SM}} = \mathscr{L}_{\text{QCD}} + \mathscr{L}_{\text{EW}} + \mathscr{L}_{\text{S}} + \mathscr{L}_{\text{Y}} + \mathscr{L}_{\text{GF}} + \mathscr{L}_{\text{ghost}} \,. \tag{1.71}$$

The QCD Lagrangian can be found in eq. (1.6), the electroweak piece in eq. (1.17), the corresponding part from the scalar sector in eq. (1.48) and the Yukawa term in eq. (1.55). Here a gauge-fixing term has been added in order to avoid quadratic terms mixing scalar and gauge bosons as well as define the propagators

$$\begin{aligned} \mathscr{L}_{\text{GF}} = &- \frac{1}{2\xi_g} \left(\partial_\mu G_a^\mu\right)^2 - \frac{1}{2\xi_\gamma} \left(\partial_\mu A^\mu\right)^2 \\ &- \frac{1}{2\xi_Z} \left(\partial_\mu Z^\mu - \xi_Z M_Z \eta\right)^2 - \frac{1}{\xi_W} \left|\partial_\mu W^\mu + i\xi_W M_W \varphi^{+\dagger}\right|^2 \,. \end{aligned} \tag{1.72}$$

Moreover, the ghost Lagrangian, $\mathscr{L}_{\text{ghost}}$, must be included for consistency of the theory [36].

1.2 Going beyond the Standard Model

The SM has overcome almost every single experimental test to which it has been subjected. For this reason, it is said that it is the simplest and most successful theory that can explain the fundamental matter content and its interactions. However, the SM cannot be the ultimate theory since there are a few experimental and theoretical aspects that it cannot explain. In recent times, some small deviations

have also been found and even though they are not yet statistically significant, they could be an open gate for a best and a more complete model. In this section, all these hints will be briefly reviewed. There are some experimental measurements that cannot be accounted for in the SM:

- **Neutrino masses**

  As mentioned in section 1.1.3 neutrinos are massless particles in the SM. However, in 1968 The Homestake chlorine solar neutrino experiment claimed an deficit of electronic neutrinos (ν_e) coming from the Sun compared to the prediction of the standard solar model. Since then, several experiments have obtained a value below the expectations [37]. For example, the Sudbury Neutrino Observatory showed evidence of neutrinos changing flavor inside the sun core [38]. This has been also measured in more recent experiments as Super-Kamiokande [39], KamLAND [40] and Borexino experiments [41]. There is another evidence of neutrino oscillations coming from atmospheric neutrino experiments. In this case, there is a lack of muon-neutrinos (ν_μ) reported by Super-Kamiokande [42], K2K [43] and MINOS [44].

  The neutrino oscillations point to the existence of a unitary mixing matrix in the leptonic sector analogous to the CKM matrix for the quark sector, that is, the PMNS matrix [31, 32]. Moreover, neutrino oscillations also enforce non-zero and different neutrino masses of at least two families since the probability of oscillation is proportional to the squared-mass difference between neutrinos and oscillations mixing the three families have been observed.

  The SM can be enlarged with a right-handed singlet neutrino to build a Dirac mass term as done for the rest of the fermions. However, this singlet would not couple to the rest of the gauge sector, it is said to be *sterile*. If the right-handed neutrinos do exist and they interact in any way, it should be via some unknown dynamics. In addition to the Yukawa coupling, giving rise to the Dirac masses, it is also possible to write a Majorana mass term

$$\mathscr{L}_{\mathrm{M}} = -\frac{1}{2}\,\bar{\nu^c_{iR}}\,M_{ij}\,\nu_{jR} + \mathrm{h.c.}\,, \tag{1.73}$$

where $\bar{\nu}^c_{iR} \equiv \mathcal{C}\bar{\nu}^T_{iR}$ is the charged-conjugated neutrino field. This term violates lepton number by two units.

Either neutrinos are Dirac or Majorana fermions, the fact that they are massive and that there is no flavor conservation is outside the scope of the SM and for that reason neutrinos are one strong motivation for physics beyond the SM.

- **B Meson Anomalies**

  Some flavor oriented experiments such as LHCb, Babar and Belle have presented several experimental results in the B-meson decays that deviate from the SM prediction. Although they are not statistically significant enough to claim the discovery of physics beyond the SM there is a pattern among them that has drawn the attention of the High Energy Physics (HEP) community. The results points towards the possibility of large flavor universality violation. These observables will be presented with greater detail in chapter 7.

- **Electron and Muon g-2**

  After an improved determination of the fine structure constant [45], a new anomaly has emerged [46] concerning the anomalous magnetic moment of the electron $a_e = (g_e - 2)/2$: there is a discrepancy among the experimental determination and the Standard Model prediction [47–52],

$$\delta a_e \equiv a_e^{\text{Exp}} - a_e^{\text{SM}} = -(8.7 \pm 3.6) \times 10^{-13} \,. \tag{1.74}$$

  However, at the end of 2020, a new determination of the fine structure constant was presented [60] resulting on a different value for the electron g-2

$$\delta a_e \equiv a_e^{\text{Exp}} - a_e^{\text{SM}} = (4.8 \pm 3) \times 10^{-13} \,. \tag{1.75}$$

  consistent with the SM prediction.

  Another well-known and long standing anomaly concerns the anomalous magnetic moment of the muon [53–59],

$$\delta a_\mu \equiv a_\mu^{\text{Exp}} - a_\mu^{\text{SM}} = (2.7 \pm 0.9) \times 10^{-9} \,. \tag{1.76}$$

Moreover, during the writing of this thesis, the Muon g-2 collaboration at Fermilab, presented a new result for the muon anomalous magnetic moment [61]

$$\delta a_\mu \equiv a_\mu^{\text{Exp}} - a_\mu^{\text{SM}} = (2.51 \pm 0.59) \times 10^{-9} \,. \tag{1.77}$$

Again, the experimental deviations are not significant enough. The combination of both is close to the 4.1σ deviation what may point towards New Physics (NP). These observables together with a model that can explain both at the same time will be studied in chapter 9.

- **Matter-antimatter Asymmetry**

  The observed universe is almost entirely composed of matter that cannot be explained in the SM framework since it predicts that in the early universe matter and antimatter should be created approximately in the same amount. Moreover, even though CP violation could explain the present observations starting from a symmetric universe at its origin, CP is not violated enough in the SM. Furthermore, according to the Sakharov conditions [62] baryon number should also be violated in order to explain the observations. An explanation of this asymmetry thus requires an extension of the SM.

- **Dark sector**

  According to cosmological measurements, only 5% of the observable universe is made from regular matter, that is the one described by the SM in table 1.1. Around 26% must be what is called Dark Matter (DM) in order to explain astrophysical and cosmological observations such as galaxy velocities, gravitational lensing, cosmic microwave background and motion of galaxies within galaxy clusters among others. This matter would not interact neither electromagnetically nor strongly but rather gravitationally or weakly. Moreover, for the sake of understanding the acceleration rate of expansion of the universe there must be a 69% additional unknown component that is called dark energy.

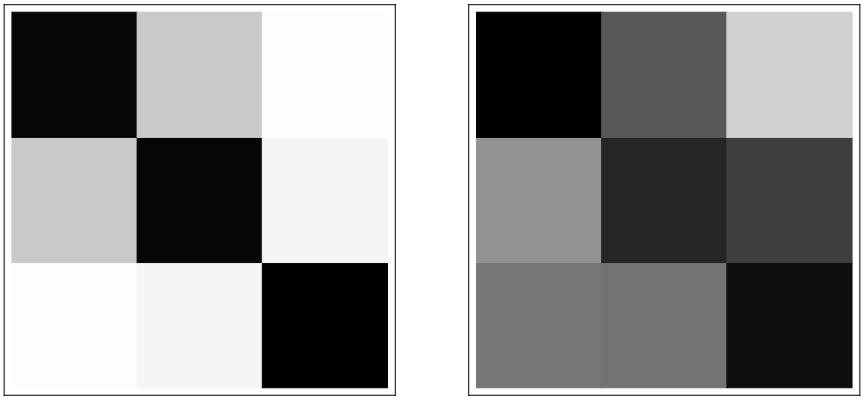

(a) CKM matrix pattern **(b)** PMNS matrix pattern

Figure 1.6: Measured hierarchical patterns of the CKM (1.6a) and PMNS (1.6b) matrices. Elements with lighter indicate that are more suppressed as compared with the darker ones. Figure from [63].

On the other hand, there are also some theoretical issues that motivate the extension of the SM:

- **Gravity**

  The SM does describe all fundamental interactions among particles but gravity. It would be desirable to have a theory that is capable of describing all the matter content and interactions, in order to do so, the SM should be extended in order to provide a quantum description of gravity.

- **The flavor puzzle**

  In the previous section, it was said that the third fermion family was predicted [30] as a necessary condition to include CP-violation but there is no fundamental reason to explain that there are only three families. There is also no theoretical explanation of why the mass matrices for the quarks and charged leptons and the CKM matrix follow hierarchical patterns but the PMNS matrix and neutrino masses do not (see figure 1.6).

- **The hierarchy problem**

  New physics may strongly contribute to radiative corrections to the Higgs boson mass since these corrections would be proportional to the new mass

scale. These huge corrections would be canceled by the mass parameter in the Lagrangian in order to achieve the experimental value for the mass, 125GeV which would lead to an uncomfortable fine tuning from the theoretical point of view.

- **The strong CP problem**

  The SM symmetry group allows the addition to the Lagrangian in eq. (1.6) of the following term:

$$\mathscr{L}_{\bar{\theta}} = -\frac{g_c^2}{16\pi^2}\bar{\theta}\mathrm{Tr}\left(G_\alpha^{\mu\nu}\tilde{G}_{\mu\nu}^{\alpha}\right) , \tag{1.78}$$

  where $\bar{\theta} = \theta + \mathrm{Arg}\left(\det \mathrm{M}_q\right)$ being M_q the quark mass matrix. Such a term is CP-violating but there is no experimental evidence of CP-violation in the strong sector. As there is no mechanism in the SM to forbid this term, the fact that this coupling needs to be so small leads to a fine tuning problem. Indeed, measurements of the neutron electric dipole moment set the bound $\bar{\theta} \lesssim 10^{-10}$ [64].

- **Grand Unification**

  The interaction couplings run with the energy, that is they vary depending on the energy scale at which they are measured. In the SM framework, the three couplings of the strong and electroweak forces become approximately equal at a very high energy. This feature may point to NP since it seems that they could unify in a single force at that scale, just as it happens with the electromagnetic and weak forces. The models that try to accommodate these features are known as Grand Unified Theories (GUT).

–Don't turn me into anything...unnatural.

— SAMwise Gamgee, *The Lord of the Rings*,
J. R. R. Tolkien

2 The Two Higgs Doublets Model

In 2012, ATLAS [27] and CMS [28] claimed the discovery of a scalar particle with a mass of 125 GeV. The properties of this particle were compatible with the SM Higgs. The Higgs boson was the last missing piece of the SM puzzle even though it was predicted by Higgs [22], Brout and Englert [23] in 1964. This fact could be seen as a closing door for New Physics, but it is not. Since the scalar sector is one of the less known ones, it might happen that NP manifests there.

There is no theoretical reason that forbids the enlargement of the minimal SM scalar sector. In fact there are plenty of NP models that require an enlarged scalar sector like Supersymmetric models [65] and spontaneous CP violation (SCPV) models [66–68]. Moreover, many extensions that solve the Baryon Asymmetry of the Universe [69–71], the Dark Matter [72, 73] or the Strong CP [74, 75] problems require a richer scalar sector than the SM one.

In particular, Two Higgs Doublet Models (2HDM) [66, 76, 77] are a simple and popular class of extensions of the Standard Model. Besides the original motivation, in particular the possibility of having spontaneous CP violation [66], extending the SM scalar sector with a second doublet allows a number of interesting phenomenological consequences. To name a few generic ones: the appearance of new fundamental scalar particles, non-standard properties of the "quite Higgs-like" scalar discovered at the LHC with a mass of 125 GeV [27, 78], and, related to them, a number of

potential deviations in low energy processes with respect to SM expectations. They have been the focus of intense scrutiny before and after the 2012 discovery [79–102]. Additional aspects, including DM candidates [72, 103] or sources of CP violation in addition to the Cabibbo-Kobayashi-Maskawa matrix [34, 104, 105], of interest for baryogenesis [69, 106, 107], provide further interest in 2HDM.

This chapter presents the general 2HDM, its Lagrangian as well as some well known 2HDM models. It is organized as follows. In the next section, the 2HDM scalar potential is presented. In section 2.2 the interactions among gauge bosons and the new scalar particles are studied. This is followed by a detailed review of the quark and lepton Yukawa sector in section 2.3. Finally, the most common solutions to the appearance of dangerous Scalar Flavor Changing Neutral Couplings (SFCNC) are presented in section 2.4 and section 2.5.

2.1 Scalar Potential

The scalar sector of the 2HDM consists of two SU(2) doublets with hypercharge $Y = 1/2$ defined as:

$$\Phi_j = \begin{pmatrix} \varphi_j^+ \\ \varphi_j^0 \end{pmatrix}, \tag{2.1}$$

and with two of these doublets, the most general renormalizable scalar potential invariant under $\mathrm{SU}(2) \times \mathrm{U}(1)$

$$\begin{aligned} V =& \mu_{11}^2 \Phi_1^\dagger \Phi_1 + \mu_{22}^2 \Phi_2^\dagger \Phi_2 - \left(\mu_{12}^2 \Phi_1^\dagger \Phi_2 + \text{h.c.}\right) \\ &+ \frac{1}{2}\lambda_1 \left(\Phi_1^\dagger \Phi_1\right)^2 + \frac{1}{2}\lambda_2 \left(\Phi_2^\dagger \Phi_2\right)^2 + \lambda_3 \left(\Phi_1^\dagger \Phi_1\right)\left(\Phi_2^\dagger \Phi_2\right) + \lambda_4 \left(\Phi_1^\dagger \Phi_2\right)\left(\Phi_2^\dagger \Phi_1\right) \\ &+ \left[\frac{1}{2}\lambda_5 \left(\Phi_1^\dagger \Phi_2\right)^2 + \lambda_6 \left(\Phi_1^\dagger \Phi_1\right)\left(\Phi_1^\dagger \Phi_2\right) + \lambda_7 \left(\Phi_2^\dagger \Phi_2\right)\left(\Phi_1^\dagger \Phi_2\right) + \text{h.c.}\right], \end{aligned} \tag{2.2}$$

where the parameters μ_{12} and $\lambda_{5,6,7}$ can be complex but μ_{11}^2, μ_{22}^2 and $\lambda_{1,2,3,4}$ must be real to preserve hermiticity. That is a total of fourteen real parameters, six from real ones and eight coming from the complex parameters. However, it can be proved [108, 109] that the freedom to redefine the basis leads to having only

eleven physical (real) parameters. The appropriate vacuum expectation values for Electroweak Symmetry Breaking (EWSB) read

$$\langle 0|\Phi_1|0\rangle = \frac{1}{\sqrt{2}}\begin{pmatrix}0\\ v_1 e^{i\theta_1}\end{pmatrix}, \quad \langle 0|\Phi_2|0\rangle = \frac{1}{\sqrt{2}}\begin{pmatrix}0\\ v_2 e^{i\theta_2}\end{pmatrix}, \tag{2.3}$$

where we can set one of the complex phases to zero by rephasing the scalars fields. These VEVs v_j of the scalar fields Φ_j are in general non-vanishing; expanding around the vacuum,

$$\Phi_j = e^{i\theta_j}\begin{pmatrix}\varphi_j^+\\ \frac{v_j+\rho_j+i\eta_j}{\sqrt{2}}\end{pmatrix}. \tag{2.4}$$

It is convenient to use the so-called Higgs basis [80, 110, 111] that is defined by

$$\begin{pmatrix}H_1\\ H_2\end{pmatrix} = \mathcal{R}_\beta \begin{pmatrix}e^{-i\theta_1}\Phi_1\\ e^{-i\theta_2}\Phi_2\end{pmatrix}, \quad \text{with} \quad \mathcal{R}_\beta = \begin{pmatrix}c_\beta & s_\beta\\ -s_\beta & c_\beta\end{pmatrix}, \ \mathcal{R}_\beta^T = \mathcal{R}_\beta^{-1}, \tag{2.5}$$

in such a way that only one of the scalar doublets has a non-vanishing vacuum expectation value: $\langle H_1\rangle = \frac{v}{\sqrt{2}}\binom{0}{1}$, $\langle H_2\rangle = \binom{0}{0}$ where we have defined $v_1^2 + v_2^2 = v^2 = \frac{1}{\sqrt{2}G_F}$. In eq. (2.5), we have used $c_\beta \equiv \cos\beta = v_1/v$ and $s_\beta \equiv \sin\beta = v_2/v$. Expanding around the vacuum, the doublets read

$$H_1 = \begin{pmatrix}G^+\\ \frac{v+H^0+iG^0}{\sqrt{2}}\end{pmatrix}, \quad H_2 = \begin{pmatrix}\mathrm{H}^+\\ \frac{R^0+iI^0}{\sqrt{2}}\end{pmatrix}, \tag{2.6}$$

where

$$\begin{pmatrix}G^+\\ \mathrm{H}^+\end{pmatrix} = \mathcal{R}_\beta\begin{pmatrix}\varphi_1^+\\ \varphi_2^+\end{pmatrix}, \quad \begin{pmatrix}G^0\\ I^0\end{pmatrix} = \mathcal{R}_\beta\begin{pmatrix}\eta_1\\ \eta_2\end{pmatrix}, \quad \begin{pmatrix}H^0\\ R^0\end{pmatrix} = \mathcal{R}_\beta\begin{pmatrix}\rho_1\\ \rho_2\end{pmatrix}. \tag{2.7}$$

The Electroweak Symmetry Breaking described in section 1.1.3 is then realized through the H_1 doublet where the would-be Goldstone bosons G^0, $G^\pm$ can already be identified. Each complex doublet has four degrees of freedom, associated with the real and imaginary part of each component, thus for two doublets it makes a total of eight. The three degrees of freedom from the charged and neutral Goldstone bosons are absorbed after EWSB to give mass to the $\mathrm{W}^\pm$ and Z gauge bosons. The five remaining degrees of freedom appear as five physical particles, two charged scalars ($\mathrm{H}^\pm$) that can be already identified in eq. (2.6), and three neutral scalars.

These neutral scalars $\{H^0, R^0, I^0\}$ are not, in general, the mass eigenstates. Thus, the potential in the Higgs Basis can be written as

$$\begin{aligned} V =& m_{11}^2 H_1^\dagger H_1 + m_{22}^2 H_2^\dagger H_2 - \left(m_{12}^2 H_1^\dagger H_2 + \text{h.c.}\right) \\ &+ \frac{1}{2}\bar{\lambda}_1 \left(H_1^\dagger H_1\right)^2 + \frac{1}{2}\bar{\lambda}_2 \left(H_2^\dagger H_2\right)^2 + \bar{\lambda}_3 \left(H_1^\dagger H_1\right)\left(H_2^\dagger H_2\right) + \bar{\lambda}_4 \left(H_1^\dagger H_2\right)\left(H_2^\dagger H_1\right) \\ &+ \left[\frac{1}{2}\bar{\lambda}_5 \left(H_1^\dagger H_2\right)^2 + \bar{\lambda}_6 \left(H_1^\dagger H_1\right)\left(H_1^\dagger H_2\right) + \bar{\lambda}_7 \left(H_2^\dagger H_2\right)\left(H_1^\dagger H_2\right) + \text{h.c.}\right]. \end{aligned} \tag{2.8}$$

The relation between different basis can be found in Ref. [108, 109]. For the vacuum state to be a stability point of the potential, the linear terms in the neutral scalars must vanish, what leads to

$$m_{11}^2 = -\frac{\bar{\lambda}_1 v^2}{2}, \quad m_{12}^2 = -\frac{\bar{\lambda}_6 v^2}{2}. \tag{2.9}$$

Applying these conditions (eq. (2.9)) to the potential and expanding in the fields it is possible to extract the mass terms from the terms quadratic in the fields.

$$V_2 = m_{\mathrm{H}^\pm}^2 \mathrm{H}^+\mathrm{H}^- + \frac{1}{2}\begin{pmatrix} H^0 & R^0 & I^0 \end{pmatrix} \mathcal{M}^2 \begin{pmatrix} H^0 \\ R^0 \\ I^0 \end{pmatrix}, \tag{2.10}$$

with $m_{\mathrm{H}^\pm}^2 = m_{22}^2 + \frac{v^2\lambda_3}{2}$ and the neutral mass matrix

$$\mathcal{M}^2 = \begin{pmatrix} v^2\,\bar{\lambda}_1 & v^2\,\mathrm{Re}\left(\bar{\lambda}_6\right) & -v^2\,\mathrm{Im}\left(\bar{\lambda}_6\right) \\ v^2\,\mathrm{Re}\left(\bar{\lambda}_6\right) & m_{\mathrm{H}^\pm}^2 + \frac{v^2}{2}[\bar{\lambda}_4 + \mathrm{Re}\left(\bar{\lambda}_5\right)] & -\frac{v^2}{2}\mathrm{Im}\left(\bar{\lambda}_5\right) \\ -v^2\,\mathrm{Im}\left(\bar{\lambda}_6\right) & -\frac{v^2}{2}\mathrm{Im}\left(\bar{\lambda}_5\right) & m_{\mathrm{H}^\pm}^2 + \frac{v^2}{2}[\bar{\lambda}_4 - \mathrm{Re}\left(\bar{\lambda}_5\right)] \end{pmatrix}, \tag{2.11}$$

and given that the $\mathcal{M}^2$ matrix is symmetric it is diagonalized by an orthogonal rotation

$$\mathcal{M}^2 = \mathcal{R}_{[3]}(\vec{\alpha})\mathrm{diag}\left(\mathrm{m}_\mathrm{h}^2, m_\mathrm{H}^2, m_\mathrm{A}^2\right)\mathcal{R}_{[3]}(\vec{\alpha})^T, \tag{2.12}$$

where $\mathcal{R}_{[3]}(\vec{\alpha})^T = \mathcal{R}_{[3]}(\vec{\alpha})^{-1}$. Thereby the transformation $\mathcal{R}_{[3]}(\vec{\alpha})$ relates the neutral scalar mass eigenstates $\{\mathrm{h}, \mathrm{H}, \mathrm{A}\}$ with the fields $\{H^0, R^0, I^0\}$ by

$$\begin{pmatrix} H^0 \\ R^0 \\ I^0 \end{pmatrix} = \mathcal{R}_{[3]}(\vec{\alpha}) \begin{pmatrix} \mathrm{h} \\ \mathrm{H} \\ \mathrm{A} \end{pmatrix}. \tag{2.13}$$

Being $\mathcal{R}_{[3]}(\vec{\alpha})$ a real orthogonal rotation it can be described by three real mixing angles, $\vec{\alpha} = \{\alpha_{12}, \alpha_{13}, \alpha_{23}\}$ ($c_x \equiv \cos x$, $s_x \equiv \sin x$),

$$\mathcal{R}_{[3]}(\vec{\alpha}) = \begin{pmatrix} c_{\alpha_{12}} & -s_{\alpha_{12}} & 0 \\ s_{\alpha_{12}} & c_{\alpha_{12}} & 0 \\ 0 & 0 & 1 \end{pmatrix} \begin{pmatrix} c_{\alpha_{13}} & 0 & -s_{\alpha_{13}} \\ 0 & 1 & 0 \\ s_{\alpha_{13}} & 0 & c_{\alpha_{13}} \end{pmatrix} \begin{pmatrix} 1 & 0 & 0 \\ 0 & c_{\alpha_{23}} & -s_{\alpha_{23}} \\ 0 & s_{\alpha_{23}} & c_{\alpha_{23}} \end{pmatrix} . \quad (2.14)$$

It is interesting to study the limit where there is no CP violation in the scalar potential, i.e. no mixing connecting the CP-even H^0, R^0, and the CP-odd I^0, so it is customary to introduce the mixing angle α

$$\begin{pmatrix} \mathrm{h} \\ \mathrm{H} \end{pmatrix} = \begin{pmatrix} s_\alpha & c_\alpha \\ -c_\alpha & s_\alpha \end{pmatrix} \begin{pmatrix} \rho_1 \\ \rho_2 \end{pmatrix} = \begin{pmatrix} s_{\alpha\beta} & c_{\alpha\beta} \\ -c_{\alpha\beta} & s_{\alpha\beta} \end{pmatrix} \begin{pmatrix} H^0 \\ R^0 \end{pmatrix} , \quad (2.15)$$

where $s_{\alpha\beta} = \sin(\alpha+\beta)$ and $c_{\alpha\beta} = \cos(\alpha+\beta)$ (that is, $\alpha_{13} = \alpha_{23} = 0$ and $\alpha_{12} = \pi/2 - (\alpha+\beta)$ in Eq. (2.14)). The field I^0 is now the mass eigenstate A. Since a ± sign can be included in the definition of the scalar fields without changing their kinetic terms, different conventions for Eqs. (2.14)–(2.15) are used in the literature, which may be relevant when comparing expressions. If the scalar potential does not add new sources of CP violation, that means that the parameters that in principle could be complex ($\bar{\lambda}_5$, $\bar{\lambda}_6$ and $\bar{\lambda}_7$) must be real $\left(\mathrm{Im}\left(\bar{\lambda}_5\right) = \mathrm{Im}\left(\bar{\lambda}_6\right) = \mathrm{Im}\left(\bar{\lambda}_7\right) = \mathrm{Im}\left(m_{12}^2\right) = 0\right)$.

2.2 Gauge Sector

As it was shown in section 1.1.3 once SSB is realized, interaction terms connecting the scalar and the gauge bosons arise. The Lagrangian involving the gauge bosons[1] reads

$$\mathscr{L}_{\mathrm{gauge}} = \underbrace{-\frac{1}{4} W^a_{\mu\nu} W_a^{\mu\nu} - \frac{1}{4} B_{\mu\nu} B^{\mu\nu}}_{\mathscr{L}_{\mathrm{kin}}} + \sum_{j=1}^{2} \left(D_\mu \Phi_j\right)^\dagger D^\mu \Phi_j + \mathscr{L}_{\mathrm{GF}} \quad (2.16)$$

$$= \mathscr{L}_{V^2} + \mathscr{L}_{S^2} + \mathscr{L}_{SV} + \mathscr{L}_{S^2V} + \mathscr{L}_{SV^2} + \mathscr{L}_{S^2V^2} , \quad (2.17)$$

where the covariant derivative in terms of the physical photon (A_μ) and EW gauge bosons (W_μ and Z_μ) is given by

$$D_\mu = \partial_\mu + ie\mathcal{Q}A_\mu + i\frac{g}{\cos\theta_W} Z_\mu \left(T_3 - \mathcal{Q}\sin^2\theta_W\right) + ig\left(T_+ W_\mu^\dagger + T_- W_\mu\right) , \quad (2.18)$$

[1] Here we are not including the terms connecting fermions and gauge bosons that generate neutral and charged currents (eq. 1.18) since they are the same as in the SM.

and

$$T_{\pm} \equiv \frac{1}{\sqrt{2}}\left(T_1 \pm T_2\right), \qquad T_j = \frac{\sigma_j}{2}. \tag{2.19}$$

As in the SM (section 1.1.3), it is convenient to add a gauge-fixing term in order to cancel quadratic terms mixing Goldstone and gauge bosons ($\mathscr{L}_{SV} = 0$) and provide the gauge boson masses. The gauge fixing term in the Feynman-'t Hooft gauge ($\xi = 1$) reads

$$\mathscr{L}_{\mathrm{GF}} = -\frac{1}{2}\left(\partial_\mu A^\mu\right)^2 - \frac{1}{2}\left(\partial_\mu Z^\mu - M_Z G^0\right)^2 - \left|\partial_\mu W^\mu - i M_W G^-\right|^2, \tag{2.20}$$

where we can see that $M^{\pm}_{\mathrm{G}} = m_{\mathrm{W}} = gv/2$ and $M^0_{\mathrm{G}} = m_{\mathrm{Z}} = M_W/\cos\theta_W$. The other quadratic terms do not vanish and they read

$$\mathscr{L}_{V^2} = -\frac{1}{2}\left(\partial_\mu A^\mu\right)^2 - \frac{1}{2}\left(\partial_\mu Z^\mu\right)^2 + \frac{1}{2}M_Z^2 Z_\mu Z^\mu - \partial^\mu W^\dagger_\mu\left(\partial_\nu W^\nu\right) + M_W^2 W^\dagger_\mu W^\mu, \tag{2.21}$$

and

$$\begin{aligned}\mathscr{L}_{S^2} =& \frac{1}{2}\left[\partial_\mu h \partial^\mu h + \partial_\mu H \partial^\mu H + \partial_\mu A \partial^\mu A\right] + \partial_\mu H^+ \partial^\mu H^- \\ &+\frac{1}{2}\partial_\mu G^0 \partial^\mu G^0 - \frac{1}{2}M_Z^2\left(G^0\right)^2 \\ &+\partial_\mu G^+ \partial^\mu G^- - M_W^2 G^+ G^-.\end{aligned} \tag{2.22}$$

Furthermore, the Lagrangian contains interaction terms that involve scalar and vector bosons

$$\begin{aligned}\mathscr{L}_{S^2V} =& ie\left[A^\mu + \cot(2\theta_w) Z^\mu\right]\left[\left(\mathrm{H}^+ \overleftrightarrow{\partial}_\mu \mathrm{H}^-\right) + \left(\mathrm{G}^+ \overleftrightarrow{\partial}_\mu \mathrm{G}^-\right)\right] \\ &+\frac{e}{\sin(2\theta_W)} Z^\mu\left[\left(\mathrm{G}^0 \overleftrightarrow{\partial}_\mu H^0\right) + \left(I^0 \overleftrightarrow{\partial}_\mu R^0\right)\right] \\ &+\frac{g}{2} W^{\mu\dagger}\left[\left(\mathrm{H}^- \overleftrightarrow{\partial}_\mu I^0\right) - i\left(\mathrm{H}^- \overleftrightarrow{\partial}_\mu R^0\right)\right. \\ &\left.\quad + \left(\mathrm{G}^- \overleftrightarrow{\partial}_\mu \mathrm{G}^0\right) - i\left(\mathrm{G}^- \overleftrightarrow{\partial}_\mu H^0\right)\right] \\ &+\frac{g}{2} W^{\mu}\left[\left(\mathrm{H}^+ \overleftrightarrow{\partial}_\mu I^0\right) + i\left(\mathrm{H}^+ \overleftrightarrow{\partial}_\mu R^0\right)\right. \\ &\left.\quad + \left(\mathrm{G}^+ \overleftrightarrow{\partial}_\mu \mathrm{G}^0\right) - i\left(\mathrm{G}^+ \overleftrightarrow{\partial}_\mu H^0\right)\right],\end{aligned} \tag{2.23}$$

$$\begin{aligned}\mathscr{L}_{SV^2} =& \frac{2}{v} H^0\left[\frac{1}{2}M_Z^2 Z_\mu Z^\mu + M_W^2 W^\dagger_\mu W^\mu\right] \\ &+\left(e M_W A^\mu - g M_Z \sin^2\theta_W\right)\left(\mathrm{G}^+ W_\mu + \mathrm{G}^- W^\dagger_\mu\right),\end{aligned} \tag{2.24}$$

$$\begin{aligned}\mathscr{L}_{S^2V^2} =& \frac{1}{v^2}\left[\frac{1}{2}M_Z^2 Z_\mu Z^\mu + M_W^2 W_\mu^\dagger W^\mu\right]\left[\mathrm{h}^2+\mathrm{H}^2+\mathrm{A}^2+(\mathrm{G}^0)^2\right]\\ &+\left\{e^2\left[A^\mu+\cot(2\theta_W)Z^\mu\right]^2+\frac{g^2}{2}W_\mu^\dagger W^\mu\right\}(\mathrm{G}^+\mathrm{G}^-+\mathrm{H}^+\mathrm{H}^-)\\ &+\frac{eg}{2}\left(A^\mu-\tan\theta_W Z^\mu\right)\left[H^0\left(\mathrm{G}^+W_\mu+\mathrm{G}^-W_\mu^\dagger\right)\right.\\ &+R^0\left(\mathrm{H}^+W_\mu+\mathrm{H}^-W_\mu^\dagger\right)+iI^0\left(\mathrm{H}^-W_\mu^\dagger-\mathrm{H}^+W_\mu\right)\\ &\left.+i\mathrm{G}^0\left(\mathrm{G}^-W_\mu^\dagger-\mathrm{G}^+W_\mu\right)\right],\end{aligned} \tag{2.25}$$

where for compactness we use the notation $A\overleftrightarrow{\partial}_\mu B \equiv A(\partial_\mu B)-(\partial_\mu A)B$.

2.3 Yukawa

The SM Yukawa sector, when a second scalar doublet is added, is extended to

$$\begin{aligned}\mathscr{L}_{\mathrm{Y}} =& -\bar{Q}_L^0\left(\Phi_1 Y_{d,1}+\Phi_2 Y_{d,2}\right)d_R^0-\bar{Q}_L^0\left(\tilde{\Phi}_1 Y_{u,1}+\tilde{\Phi}_2 Y_{u,2}\right)u_R^0\\ &-\bar{L}_L^0\left(\Phi_1 Y_{\ell,1}+\Phi_2 Y_{\ell,2}\right)\ell_R^0-\bar{L}_L^0\left(\tilde{\Phi}_1 Y_{\nu,1}+\tilde{\Phi}_2 Y_{\nu,2}\right)\nu_R^0+\mathrm{h.c.},\end{aligned} \tag{2.26}$$

where

$$\tilde{\Phi}_j \equiv i\sigma_2\Phi_j^* = \begin{pmatrix}\varphi_j^{0\dagger}\\ -\varphi_j^-\end{pmatrix}, \tag{2.27}$$

with hypercharge $Y=-1/2$. Here we have included a right-handed neutrino since its existence will be crucial in some models studied in this thesis, e.g. in chapter 5. In all of them we will focus on Dirac neutrinos and we will not include a Majorana mass term. To achieve this, total Leptonic number conservation will be applied. It is in the Higgs basis where the Yukawa couplings have the simplest interpretation:

$$\begin{aligned}\mathscr{L}_{\mathrm{Y}} =& -\frac{\sqrt{2}}{v}\bar{Q}_L^0\left(H_1\mathrm{M}_d^0+H_2\mathrm{N}_d^0\right)d_R^0-\frac{\sqrt{2}}{v}\bar{Q}_L^0\left(\tilde{H}_1\mathrm{M}_u^0+\tilde{H}_2\mathrm{N}_u^0\right)u_R^0\\ &-\frac{\sqrt{2}}{v}\bar{L}_L^0\left(H_1\mathrm{M}_\ell^0+H_2\mathrm{N}_\ell^0\right)\ell_R^0-\frac{\sqrt{2}}{v}\bar{L}_L^0\left(\tilde{H}_1\mathrm{M}_\nu^0+\tilde{H}_2\mathrm{N}_\nu^0\right)\nu_R^0+\mathrm{h.c.}\ .\end{aligned} \tag{2.28}$$

Since only the neutral component of H_1 has a non-vanishing vacuum expectation value, the Yukawa couplings M_f^0, for all the fermions $f=u,d,\ell,\nu$, will be the corresponding mass matrices. These together with N_f^0 will encode the flavor

structure of the 2HDM and are given by:

$$\begin{aligned}
\mathrm{M}_d^0 &= \frac{v\, e^{i\theta_1}}{\sqrt{2}}\left[c_\beta Y_{d,1} + e^{i\theta} s_\beta Y_{d,2}\right], \qquad \mathrm{N}_d^0 = \frac{v\, e^{i\theta_1}}{\sqrt{2}}\left[-s_\beta Y_{d,1} + e^{i\theta} c_\beta Y_{d,2}\right], \\
\mathrm{M}_u^0 &= \frac{v\, e^{-i\theta_1}}{\sqrt{2}}\left[c_\beta Y_{u,1} + e^{-i\theta} s_\beta Y_{u,2}\right], \quad \mathrm{N}_u^0 = \frac{v\, e^{-i\theta_1}}{\sqrt{2}}\left[-s_\beta Y_{u,1} + e^{-i\theta} c_\beta Y_{u,2}\right], \\
\mathrm{M}_\ell^0 &= \frac{v\, e^{i\theta_1}}{\sqrt{2}}\left[c_\beta Y_{\ell,1} + e^{i\theta} s_\beta Y_{\ell,2}\right], \qquad \mathrm{N}_\ell^0 = \frac{v\, e^{i\theta_1}}{\sqrt{2}}\left[-s_\beta Y_{\ell,1} + e^{i\theta} c_\beta Y_{\ell,2}\right], \\
\mathrm{M}_\nu^0 &= \frac{v\, e^{-i\theta_1}}{\sqrt{2}}\left[c_\beta Y_{\nu,1} + e^{-i\theta} s_\beta Y_{\nu,2}\right], \quad \mathrm{N}_\nu^0 = \frac{v\, e^{-i\theta_1}}{\sqrt{2}}\left[-s_\beta Y_{\nu,1} + e^{-i\theta} c_\beta Y_{\nu,2}\right],
\end{aligned} \tag{2.29}$$

where we have defined $\theta \equiv \theta_2 - \theta_1$. For later usage, it can be convenient to write N_f^0 in the following way

$$\begin{aligned}
\mathrm{N}_d^0 &= t_\beta^{-1}\mathrm{M}_d^0 - \left(t_\beta + t_\beta^{-1}\right)\frac{v_1\, e^{i\theta_1}}{\sqrt{2}} Y_{d,1}, \quad \mathrm{N}_u^0 = t_\beta^{-1}\mathrm{M}_u^0 - \left(t_\beta + t_\beta^{-1}\right)\frac{v_1\, e^{-i\theta_1}}{\sqrt{2}} Y_{u,1}, \\
\mathrm{N}_\ell^0 &= t_\beta^{-1}\mathrm{M}_\ell^0 - \left(t_\beta + t_\beta^{-1}\right)\frac{v_1\, e^{i\theta_1}}{\sqrt{2}} Y_{\ell,1}, \quad \mathrm{N}_\nu^0 = t_\beta^{-1}\mathrm{M}_\nu^0 - \left(t_\beta + t_\beta^{-1}\right)\frac{v_1\, e^{-i\theta_1}}{\sqrt{2}} Y_{\nu,1},
\end{aligned} \tag{2.30}$$

or analogously

$$\begin{aligned}
\mathrm{N}_d^0 &= -t_\beta\mathrm{M}_d^0 + \left(t_\beta + t_\beta^{-1}\right)\frac{v_2\, e^{i\theta_2}}{\sqrt{2}} Y_{d,2}, \quad \mathrm{N}_u^0 = -t_\beta\mathrm{M}_u^0 + \left(t_\beta + t_\beta^{-1}\right)\frac{v_2\, e^{-i\theta_2}}{\sqrt{2}} Y_{u,2}, \\
\mathrm{N}_\ell^0 &= -t_\beta\mathrm{M}_\ell^0 + \left(t_\beta + t_\beta^{-1}\right)\frac{v_2\, e^{i\theta_2}}{\sqrt{2}} Y_{\ell,2}, \quad \mathrm{N}_\nu^0 = -t_\beta\mathrm{M}_\nu^0 + \left(t_\beta + t_\beta^{-1}\right)\frac{v_2\, e^{-i\theta_2}}{\sqrt{2}} Y_{\nu,2}.
\end{aligned} \tag{2.31}$$

In this parametrization it is straightforward to see that if one of the Yukawa matrices ($Y_{f,1}$ or $Y_{f,2}$) equals zero, the M_f and N_f matrices are proportional and the SFCNC vanish. This scenario will be discussed in section 2.4.

2.3.1 Quark Sector

The mass matrices have have to be diagonalized in order to write the Lagrangian in the fermion mass basis. In order to do it, the usual bi-diagonalization of the mass matrices M_d^0, M_u^0 is performed. The quark weak interaction eigenstates get transformed into the mass eigenstates (without "0" superscript) as

$$d_L = \mathcal{U}_{d_L}^\dagger d_L^0,\ d_R = \mathcal{U}_{d_R}^\dagger d_R^0,\ u_L = \mathcal{U}_{u_L}^\dagger u_L^0,\ u_R = \mathcal{U}_{u_R}^\dagger u_R^0, \tag{2.32}$$

leading to the diagonal mass matrices

$$\begin{aligned}
\mathrm{M}_d &= \mathcal{U}_{d_L}^\dagger \mathrm{M}_d^0 \mathcal{U}_{d_R} = \mathrm{diag}(m_d, m_s, m_b), \\
\mathrm{M}_u &= \mathcal{U}_{u_L}^\dagger \mathrm{M}_u^0 \mathcal{U}_{u_R} = \mathrm{diag}(m_u, m_c, m_t),
\end{aligned} \tag{2.33}$$

and

$$\mathrm{N}_d = \mathcal{U}_{d_L}^{\dagger}\,\mathrm{N}_d^0\,\mathcal{U}_{d_R}\,,\ \ \mathrm{N}_u = \mathcal{U}_{u_L}^{\dagger}\,\mathrm{N}_u^0\,\mathcal{U}_{u_R}\,, \tag{2.34}$$

leading finally to the Lagrangian

$$\mathscr{L}_{\mathrm{Y}}^{[q]} = -\frac{\sqrt{2}}{v}\bar{Q}_L[\mathrm{M}_d H_1 + \mathrm{N}_d H_2]d_R - \frac{\sqrt{2}}{v}\bar{Q}_L[\mathrm{M}_u \tilde{H}_1 + \mathrm{N}_u \tilde{H}_2]u_R + \mathrm{h.c.}\,. \tag{2.35}$$

The CKM quark-mixing matrix is $V = \mathcal{U}_{u_L}^{\dagger}\mathcal{U}_{d_L}$ as usual. It is important to remark that, in general, the N_q are not diagonal, leading to Flavor Changing Neutral Couplings at tree level. When both N_d and N_u are diagonal, tree-level SFCNC in the quark sector are absent.

Expressing Eq. (2.35) in terms of quark and scalar mass eigenstates (as a shorthand we use $\mathcal{R}_{[3]}(\vec{\alpha})_{ij} = \mathcal{R}_{ij}$), and reversing the chiral projections of the spinors with

$$\psi_{R(L)} = P_{R(L)}\,\psi, \quad \bar{\psi}_{R(L)} = \bar{\psi}\,P_{L(R)}, \tag{2.36}$$

where $P_{R(L)}$ are the right-handed and left-handed chirality projector operators defined in eq. (1.21), we get the following Lagrangian

$$\mathscr{L}_{\mathrm{m}}^{[q]} = -\,\bar{d}\mathrm{M}_d P_R d - \bar{u}\mathrm{M}_u P_R u + \mathrm{h.c.}\,, \tag{2.37}$$

$$\begin{aligned}\mathscr{L}_{\mathrm{G}}^{[q]} = -\,\frac{\sqrt{2}}{v}\Big[&G^{+}\bar{u}V\mathrm{M}_d P_R d + iG^0\bar{d}\mathrm{M}_d P_R d \\ &+ G^{-}\bar{d}V^{\dagger}\mathrm{M}_u P_R u - iG^0\bar{u}\mathrm{M}_u P_R u\Big] + \mathrm{h.c.}\,,\end{aligned} \tag{2.38}$$

$$\mathscr{L}_{\mathrm{Ch}}^{[q]} = -\,\frac{\sqrt{2}}{v}\left\{\mathrm{H}^{+}\bar{u}\left[V\mathrm{N}_d P_R - \mathrm{N}_u^{\dagger}V P_L\right]d + \mathrm{H}^{-}\bar{d}\left[\mathrm{N}_d^{\dagger}V^{\dagger}P_L - V^{\dagger}\mathrm{N}_u P_R\right]u\right\}\,, \tag{2.39}$$

$$\begin{aligned}\mathscr{L}_{\mathrm{N}}^{[q]} = &-\frac{\mathrm{h}}{v}\left\{\bar{d}\left[\mathcal{R}_{11}\mathrm{M}_d + \mathcal{R}_{21}\mathcal{H}_{\mathrm{d}} + i\mathcal{R}_{31}\mathcal{A}_{\mathrm{d}}\right]d + \bar{d}\left[\mathcal{R}_{21}\mathcal{A}_{\mathrm{d}} + i\mathcal{R}_{31}\mathcal{H}_{\mathrm{d}}\right]\gamma_5 d\right\} \\ &-\frac{\mathrm{h}}{v}\left\{\bar{u}\left[\mathcal{R}_{11}\mathrm{M}_u + \mathcal{R}_{21}\mathcal{H}_{\mathrm{u}} - i\mathcal{R}_{31}\mathcal{A}_{\mathrm{u}}\right]u + \bar{u}\left[\mathcal{R}_{21}\mathcal{A}_{\mathrm{u}} - i\mathcal{R}_{31}\mathcal{H}_{\mathrm{u}}\right]\gamma_5 u\right\} \\ &-\frac{\mathrm{H}}{v}\left\{\bar{d}\left[\mathcal{R}_{12}\mathrm{M}_d + \mathcal{R}_{22}\mathcal{H}_{\mathrm{d}} + i\mathcal{R}_{32}\mathcal{A}_{\mathrm{d}}\right]d + \bar{d}\left[\mathcal{R}_{22}\mathcal{A}_{\mathrm{d}} + i\mathcal{R}_{32}\mathcal{H}_{\mathrm{d}}\right]\gamma_5 d\right\} \\ &-\frac{\mathrm{H}}{v}\left\{\bar{u}\left[\mathcal{R}_{12}\mathrm{M}_u + \mathcal{R}_{22}\mathcal{H}_{\mathrm{u}} - i\mathcal{R}_{32}\mathcal{A}_{\mathrm{u}}\right]u + \bar{u}\left[\mathcal{R}_{22}\mathcal{A}_{\mathrm{u}} - i\mathcal{R}_{32}\mathcal{H}_{\mathrm{u}}\right]\gamma_5 u\right\} \\ &-\frac{\mathrm{A}}{v}\left\{\bar{d}\left[\mathcal{R}_{13}\mathrm{M}_d + \mathcal{R}_{23}\mathcal{H}_{\mathrm{d}} + i\mathcal{R}_{33}\mathcal{A}_{\mathrm{d}}\right]d + \bar{d}\left[\mathcal{R}_{23}\mathcal{A}_{\mathrm{d}} + i\mathcal{R}_{33}\mathcal{H}_{\mathrm{d}}\right]\gamma_5 d\right\} \\ &-\frac{\mathrm{A}}{v}\left\{\bar{u}\left[\mathcal{R}_{13}\mathrm{M}_u + \mathcal{R}_{23}\mathcal{H}_{\mathrm{u}} - i\mathcal{R}_{33}\mathcal{A}_{\mathrm{u}}\right]u + \bar{u}\left[\mathcal{R}_{23}\mathcal{A}_{\mathrm{u}} - i\mathcal{R}_{33}\mathcal{H}_{\mathrm{u}}\right]\gamma_5 u\right\}\,,\end{aligned} \tag{2.40}$$

where

$$\mathcal{H}_{\rm q} \equiv \frac{{\rm N}_q + {\rm N}_q^\dagger}{2}, \quad \mathcal{A}_{\rm q} \equiv \frac{{\rm N}_q - {\rm N}_q^\dagger}{2}, \quad q = u, d\,, \tag{2.41}$$

are the hermitian and anti-hermitian combinations of N_q and $\mathrm{N}_q^\dagger$.

2.3.2 Lepton Sector

Analogously for the leptonic sector, the fields get transformed as

$$\ell_L = \mathcal{U}_{\ell_L}^\dagger \ell_L^0\,, \quad \ell_R = \mathcal{U}_{\ell_R}^\dagger \ell_R^0\,, \quad \nu_L = \mathcal{U}_{\nu_L}^\dagger \nu_L^0\,, \quad \nu_R = \mathcal{U}_{\nu_R}^\dagger \nu_R^0\,, \tag{2.42}$$

where again, the terms without "0" superscript, correspond to the mass eigenstates. These transformations leave the following mass matrices

$$\begin{aligned} {\rm M}_\ell &= \mathcal{U}_{\ell_L}^\dagger\, {\rm M}_\ell^0\, \mathcal{U}_{\ell_R} = {\rm diag}(m_e, m_\mu, m_\tau), \\ {\rm M}_\nu &= \mathcal{U}_{\nu_L}^\dagger\, {\rm M}_\nu^0\, \mathcal{U}_{\nu_R} = {\rm diag}(m_{\nu_1}, m_{\nu_2}, m_{\nu_3}), \end{aligned} \tag{2.43}$$

$$\mathrm{N}_\ell = \mathcal{U}_{\ell_L}^\dagger\, \mathrm{N}_\ell^0\, \mathcal{U}_{\ell_R}, \quad \mathrm{N}_\nu = \mathcal{U}_{\nu_L}^\dagger\, \mathrm{N}_\nu^0\, \mathcal{U}_{\nu_R}\,. \tag{2.44}$$

As in the quark sector, the N matrices, in general, are not diagonal, this implies the existence of SFCNC at tree level in this sector. The lepton-mixing PMNS matrix is defined now as $U = \mathcal{U}_{\ell_L}^\dagger \mathcal{U}_{\nu_L}$. With this rotation, the Lagrangian in the lepton mass eigenstates reads

$$\mathscr{L}_{\rm Y}^{[\ell]} = -\frac{\sqrt{2}}{v}\bar{L}_L[{\rm M}_\ell H_1 + {\rm N}_\ell H_2]\ell_R - \frac{\sqrt{2}}{v}\bar{L}_L[{\rm M}_\nu \tilde{H}_1 + {\rm N}_\nu \tilde{H}_2]\nu_R + {\rm h.c.}\,. \tag{2.45}$$

If we now rotate the scalar terms to the mass eigenstates, eq. (2.13) and using the shorthand $\mathcal{R}_{[3]}(\vec{\alpha})_{ij} = \mathcal{R}_{ij}$ again, we get

$$\mathscr{L}_{\rm Ch}^{[\ell]} = -\frac{\sqrt{2}}{v}\left\{{\rm H}^+\bar{\nu}\left[U^\dagger {\rm N}_\ell P_R - {\rm N}_\nu^\dagger U^\dagger P_L\right]\ell + {\rm H}^-\bar{\ell}\left[{\rm N}_\ell^\dagger U P_L - U{\rm N}_\nu P_R\right]\nu\right\}, \tag{2.46}$$

$$\begin{aligned} \mathscr{L}_{\rm N}^{[\ell]} = &-\frac{\rm h}{v}\left\{\bar{\ell}\left[\mathcal{R}_{11}{\rm M}_\ell + \mathcal{R}_{21}\mathcal{H}_\ell + i\mathcal{R}_{31}\mathcal{A}_\ell\right]\ell + \bar{\ell}\left[\mathcal{R}_{21}\mathcal{A}_\ell + i\mathcal{R}_{31}\mathcal{H}_\ell\right]\gamma_5\ell\right\} \\ &-\frac{\rm h}{v}\left\{\bar{\nu}\left[\mathcal{R}_{11}{\rm M}_\nu + \mathcal{R}_{21}\mathcal{H}_\nu - i\mathcal{R}_{31}\mathcal{A}_\nu\right]\nu + \bar{\nu}\left[\mathcal{R}_{21}\mathcal{A}_\nu - i\mathcal{R}_{31}\mathcal{H}_\nu\right]\gamma_5\nu\right\} \\ &-\frac{\rm H}{v}\left\{\bar{\ell}\left[\mathcal{R}_{12}{\rm M}_\ell + \mathcal{R}_{22}\mathcal{H}_\ell + i\mathcal{R}_{32}\mathcal{A}_\ell\right]\ell + \bar{\ell}\left[\mathcal{R}_{22}\mathcal{A}_\ell + i\mathcal{R}_{32}\mathcal{H}_\ell\right]\gamma_5\ell\right\} \\ &-\frac{\rm H}{v}\left\{\bar{\nu}\left[\mathcal{R}_{12}{\rm M}_\nu + \mathcal{R}_{22}\mathcal{H}_\nu - i\mathcal{R}_{32}\mathcal{A}_\nu\right]\nu + \bar{\nu}\left[\mathcal{R}_{22}\mathcal{A}_\nu - i\mathcal{R}_{32}\mathcal{H}_\nu\right]\gamma_5\nu\right\} \\ &-\frac{\rm A}{v}\left\{\bar{\ell}\left[\mathcal{R}_{13}{\rm M}_\ell + \mathcal{R}_{23}\mathcal{H}_\ell + i\mathcal{R}_{33}\mathcal{A}_\ell\right]\ell + \bar{\ell}\left[\mathcal{R}_{23}\mathcal{A}_\ell + i\mathcal{R}_{33}\mathcal{H}_\ell\right]\gamma_5\ell\right\} \\ &-\frac{\rm A}{v}\left\{\bar{\nu}\left[\mathcal{R}_{13}{\rm M}_\nu + \mathcal{R}_{23}\mathcal{H}_\nu - i\mathcal{R}_{33}\mathcal{A}_\nu\right]\nu + \bar{\nu}\left[\mathcal{R}_{23}\mathcal{A}_\nu - i\mathcal{R}_{33}\mathcal{H}_\nu\right]\gamma_5\nu\right\}, \end{aligned} \tag{2.47}$$

with

$$\mathcal{H}_\ell \equiv \frac{\mathrm{N}_\ell + \mathrm{N}_\ell^\dagger}{2}, \quad \mathcal{A}_\ell \equiv \frac{\mathrm{N}_\ell - \mathrm{N}_\ell^\dagger}{2}. \tag{2.48}$$

In order to work with the Lagrangian in a more compact form, along this thesis, the following notation will be used for eqs. (2.40)–(2.47)

$$\mathscr{L}_N = -\sum_{S=\mathrm{h,H,A}} \sum_{f=u,d,\ell,\nu} \sum_{j,k=1}^{3} \frac{m_{f_j}}{v}\, S\, \bar{f}_j (a_{jk}^{S,f} + i b_{jk}^{S,f}\gamma_5) f_k\,, \tag{2.49}$$

and analogously, eqs. (2.39)–(2.46)

$$\mathscr{L}_{Ch} = -\frac{1}{\sqrt{2}v} \sum_{f=q,l} \sum_{j,k=1}^{3} \left\{ \mathrm{H}^- \bar{f}_{-\frac{1}{2},j} (\alpha_{jk}^f + i\beta_{jk}^f \gamma_5) f_{\frac{1}{2},k} + \mathrm{H}^+ \bar{f}_{\frac{1}{2},k} (\alpha_{jk}^{f*} + i\beta_{jk}^{f*}\gamma_5) f_{-\frac{1}{2},j} \right\}. \tag{2.50}$$

2.4 Natural Flavor Conservation

In the SM the diagonalization of the mass matrices (eqs. (2.33)–(2.43)) automatically diagonalizes the Yukawa interactions. However, as it has been commented in the previous section, the addition of a second scalar doublet to the Lagrangian, leads to the appearance of tree-level Flavor Changing Neutral Couplings. This is potentially one of the biggest constraints to 2HDM since experimentally, SFCNC are very restricted. The flavor changing processes will be mediated by one of the new neutral scalars, H or A. For example, the coupling involving the d and s quarks will lead to K^0–$\bar{K^0}$ meson mixing through a tree level diagram. For generic couplings to the new scalars, the mass of the given scalar should be large in order to surpass the experimental constraints.

In order to completely avoid SFCNC, Glashow and Weinberg [112] proved that a sufficient condition is that all fermions with the same quantum numbers couple to one of the Higgs doublets and not the other. This is known as the Glashow-Weinberg theorem. In the Standard Model where the fermions are left-handed doublets and right-handed singlets, this theorem forces all right-handed quarks of a given charge to couple to a single Higgs multiplet. In the 2HDM, this can be realized by imposing a discrete or a continuous symmetry and it is known as Natural Flavor Conservation (NFC).

In the quark sector there are only two possibilities, the so-called Type-I and Type-II. In the Type-I all the quarks couple to the same scalar doublet, conventionally chosen to be Φ_2. However, in the Type-II model, the right-handed singlets of the up-quarks ($Q = 2/3$) couple to Φ_2 doublet (just a convention) and the down-quarks ($Q = -1/3$) to the remaining doublet (Φ_1 following the same convention).

Taking into account the leptonic sector, without right-handed neutrinos, two more models arise in addition to Type I and II, the so-called Lepton Specific and Flipped 2HDM. By convention in the Type I the right-handed lepton singlets are charged under the $\mathbb{Z}_2$ symmetry in the same way as the right-handed quarks, which means that they couple to Φ_2. The Lepton-Specific is like the Type-I for the quarks, but the leptons couple to Φ_1 instead. In the Type -II again by convention, the leptons couple to the same doublet as the down quarks, that is Φ_1. And again, the Flipped 2HDM is like the Type-II but now the leptons being coupled to Φ_2 (like the up-quarks). All these models are generated through a discrete $\mathbb{Z}_2$ symmetry. In the case of the Type-I 2HDM the fields transform as

$$\Phi_1 \to -\Phi_1\,, \tag{2.51}$$

whereas the Type-II 2HDM is enforced by

$$\Phi_1 \to -\Phi_1\,, \quad d_R \to -d_R\,, \quad \ell_R \to -\ell_R\,, \tag{2.52}$$

where the rest of the fields stay invariant under the transformation. Analogously for the lepton specific

$$\Phi_1 \to -\Phi_1\,, \quad \ell_R \to -\ell_R\,, \tag{2.53}$$

and for the Flipped 2HDM

$$\Phi_1 \to -\Phi_1\,, \quad d_R \to -d_R\,. \tag{2.54}$$

The charges of all the fields for the four different models are summarized in table 2.1

Model	Φ_1	Φ_2	u_R	d_R	ℓ_R
Type I	−	+	+	+	+
Type II	−	+	+	−	−
Lepton-Specific	−	+	+	+	−
Flipped	−	+	+	−	+

Table 2.1: Field charges under the $\mathbb{Z}_2$ of the NFC models

2.4.1 Type-I 2HDM

The Type-I 2HDM was firstly introduced in Ref. [79]. From eq. (2.29) it is easy to see that both M_q^0 and N_q^0 matrices can be diagonalized simultaneously since they are proportional

$$\mathrm{N}_f^0 = t_\beta^{-1}\mathrm{M}_f^0\,, \quad (Y_{u,1} = Y_{d,1} = Y_{\ell,1} = 0)\,. \tag{2.55}$$

There are three interesting limits of this model. The first one is when $\alpha = \pi/2$, where all the fermions completely decouple from the lightest Higgs (h); this limit is known as the fermiophobic limit [113–115]. This decoupling is only preserved at tree-level. In second place, if $s_{\alpha\beta}$ ($c_{\alpha\beta}$) vanishes, then the h (H) field is gaugephobic, i.e. it does not couple to WW and ZZ, radically changing the phenomenology of Higgs decays. The third is the known as Inert 2HDM. Here the $\mathbb{Z}_2$ is exactly realized in the scalar potential and the VEV of Φ_1 vanish [72, 103]. Now, the $\mathbb{Z}_2$ symmetry remains unbroken even after SSB and the SM-like Higgs does not mix with the extra scalars. In this scenario the DM problem can be explained with the lightest of the extra neutral scalars playing the role of a dark particle [72, 73].

2.4.2 Type-II 2HDM

Type-II is the most studied model of all four since it shares the Yukawa structure with all the supersymmetric models and with the original Peccei-Quinn model [74, 75] . It was firstly introduced in Ref. [79, 80]. Again, the mass matrices can be diagonalized simultaneously, given that for the down-type fermions $Y_{d,2}$ and $Y_{\ell,2}$ equal zero and

for the up-type one $Y_{u,1}$ is the one that vanishes. The mass matrices now read

$$\mathrm{N}_u^0 = t_\beta^{-1}\mathrm{M}_u^0 \quad (Y_{u,1} = 0)\,, \tag{2.56}$$

$$\mathrm{N}_d^0 = -t_\beta\mathrm{M}_d^0 \quad (Y_{d,2} = 0)\,, \tag{2.57}$$

$$\mathrm{N}_\ell^0 = -t_\beta\mathrm{M}_\ell^0 \quad (Y_{\ell,2} = 0)\,. \tag{2.58}$$

The couplings to the gauge sector are analogous to the Type-I model, so there is a gaugephobic limit as well but in this case, there is no possibility of having a fermiophobic limit. Still it is possible to make the couplings of h (H) to the up-quarks (down-quarks and leptons) vanish by setting $\alpha = \pi/2$ (0). A very deep analysis of the phenomenology of the Type-II model can be found in Refs. [76, 116, 117].

2.4.3 Lepton-Specific 2HDM

In this model, all the quarks couple to Φ_1 as in the Type I but now the leptons couple to Φ_1. It was firstly discussed in Ref. [118, 119] related to very light scalars. Given that there are a few recent anomalies concerning the leptonic sector such as $(g-2)_{e,\mu}$ and the semileptonic B anomalies, this model is receiving more attention in the literature [87, 120–123]. This model is also referred to as Type X.

2.4.4 Flipped 2HDM

The least studied of the previous four models is the Flipped 2HDM or Type Y, that was mentioned in the first place in Ref. [124]. Here the up-quarks and leptons couple to Φ_1 and the down-quarks do so with Φ_2.

2.4.5 Aligned 2HDM

The Aligned-2HDM (A2HDM) presented in Ref. [125] is a more general model that includes the previous four discussed in this section. As a consequence of introducing the symmetry that enforces NFC, the Yukawa couplings (in the Higgs basis) in each fermion sector become proportional to the corresponding mass matrices. The A2HDM starts with the assumption that the Yukawa couplings of each fermion sector is proportional to the corresponding mass matrix. This model is not generated

Model	ς_u	ς_d	ς_ℓ
Type I	t_β^{-1}	t_β^{-1}	t_β^{-1}
Type II	t_β^{-1}	$-t_\beta$	$-t_\beta$
Lepton-Specific (X)	t_β^{-1}	t_β^{-1}	$-t_\beta$
Flipped (Y)	t_β^{-1}	$-t_\beta$	t_β^{-1}
Inert	0	0	0

Table 2.2: Alignment parameters at the limit where the A2HDM recovers the NFC models.

by a symmetry so this proportionality of the mass matrices is not stable under RGE [126–129], but the misalignment is small enough to overcome the experimental constraints [125, 130–132]. The couplings N_f and the mass matrices M_f are related by the alignment parameters as

$$\mathrm{N}_u = \varsigma_u^\dagger \mathrm{M}_u\,, \quad \mathrm{N}_d = \varsigma_d \mathrm{M}_d\,, \quad \mathrm{N}_\ell = \varsigma_\ell \mathrm{M}_\ell\,, \tag{2.59}$$

where the alignment parameters are complex numbers. These quantities introduce new sources of CP violation. This model includes the previous four by choosing the appropriate values of the alignment parameters ς_f (see table 2.2).

2.5 Minimal Flavor Violation and BGL models

We have seen in the previous section that the simplest way of avoiding SFCNC in the scalar sector is by postulating that quarks of a given charge receive contributions to their mass only from one Higgs doublet. However, this is not the only possibility. A very interesting approach to controll SFCNC was suggested by Branco-Grimus-Lavoura (BGL) [133]. In BGL models there are SFCNC at tree level but their flavor structure is controlled by the elements of the CKM matrix V and the fermion masses, without the appearance of extra flavor parameters.

Models where the general structure of SFCNC processes is shared with the SM are known as Minimal Flavor Violation (MFV) models [134–136]. This hypothesis

imposes that all flavor violating and CP-violating transitions are governed by elements of the CKM matrix and the only relevant local operators are those that are relevant in the SM [137].

Although the BGL models predate the MFV hypothesis by a few years, they satisfy the requirement of having the whole New Physics' flavor structure controlled by V [133, 138]. This flavor structure is generated by an exact symmetry of the Lagrangian[2] which means that it is renormalizable.

As it has been explained in section 2.3, the quark sector of the general 2HDM contains SFCNC, with its flavor structure parametrized by two complex matrices N_d, N_u [139]. These matrices depend on a large number of parameters if nothing is done to avoid it, in particular on $\mathcal{U}_{d_L}$,$\mathcal{U}_{u_L}$,$\mathcal{U}_{d_R}$ and $\mathcal{U}_{u_R}$, the unitary matrices which enter in the diagonalization of the down and up quark mass matrices. Having N_d, N_u to depend only on $V = \mathcal{U}_{u_L}^\dagger \mathcal{U}_{d_L}$ in a natural way looks like an impossible task. Yet, this task is accomplished by BGL models, which were first constructed for the quark sector and then generalized to the lepton sector [140]. There are six types of BGL models in the quark sector and six (three) types in the lepton sector for Dirac (Majorana) neutrinos, which can be combined to have a total of 36 (18) BGL models, with different phenomenological implications, which were thoroughly analyzed [141–143]. An interesting feature of BGL models is the fact they contain SFCNC either in the up or the down sectors but not in both sectors.

2.5.1 BGL Yukawa Sector

Recovering the Lagrangian in eq. (2.26)

$$\begin{aligned}\mathscr{L}_{\mathrm{Y}} = &- \bar{Q}_L^0 \left(\Phi_1 Y_{d,1} + \Phi_2 Y_{d,2}\right) d_R^0 - \bar{Q}_L^0 \left(\tilde{\Phi}_1 Y_{u,1} + \tilde{\Phi}_2 Y_{u,2}\right) u_R^0 \\ &- \bar{L}_L^0 \left(\Phi_1 Y_{\ell,1} + \Phi_2 Y_{\ell,2}\right) \ell_R^0 - \bar{L}_L^0 \left(\Phi_1 Y_{\nu,1} + \Phi_2 Y_{\nu,2}\right) \nu_R^0 + \mathrm{h.c.}\,, \end{aligned} \tag{2.60}$$

and in order to obtain the desired flavor structure, that is controlled by the elements of the CKM matrix, Branco, Grimus and Lavoura [133] proposed the following

[2] If the Lagrangian contains operators with dimension higher than four it would be non-renormalizable regardless of the symmetry

symmetry for the quark and scalar sector of the Lagrangian:

$$\begin{aligned} Q^0_{L_j} &\mapsto e^{i\tau} Q^0_{L_j}\,, \\ d^0_R &\mapsto d^0_R\,, & \Phi_1 &\mapsto \Phi_1\,, \\ u^0_{R_j} &\mapsto e^{i2\tau} u^0_{R_j}\,, & \Phi_2 &\mapsto e^{i\tau}\Phi_2\,, \end{aligned} \tag{2.61}$$

for the up-type BGL models and

$$\begin{aligned} Q^0_{L_j} &\mapsto e^{i\tau} Q^0_{L_j}\,, \\ d^0_{R_j} &\mapsto e^{i2\tau} d^0_{R_j}\,, & \Phi_1 &\mapsto \Phi_1\,, \\ u^0_R &\mapsto u^0_R\,, & \Phi_2 &\mapsto e^{-i\tau}\Phi_2\,, \end{aligned} \tag{2.62}$$

for the down-type.

The transformation in Eq. (2.61) leads to Higgs SFCNC in the down sector, while the one in Eq. (2.62) cancels the SFCNC in the down sector by making them appear in the up sector. These two alternative choices of symmetry combined with the three possible choices of quark families (index j) lead to six different realizations of BGL-2HDM.

Taking now into account the leptonic sector, there is a perfect analogy with what we have just seen if neutrinos are Dirac. In this case, SFCNC at tree level are no longer controlled by CKM but by the PMNS matrix. These models are enforced by the following symmetries

$$\begin{aligned} L^0_{L_j} &\mapsto e^{i\tau} L^0_{L_j}\,, \\ \ell^0_R &\mapsto \ell^0_R\,, & \Phi_1 &\mapsto \Phi_1\,, \\ \nu^0_{R_j} &\mapsto e^{i2\tau} \nu^0_{R_j}\,, & \Phi_2 &\mapsto e^{i\tau}\Phi_2\,, \end{aligned} \tag{2.63}$$

or

$$\begin{aligned} L^0_{L_j} &\mapsto e^{i\tau} L^0_{L_j}\,, \\ \ell^0_R &\mapsto e^{i2\tau} \ell^0_R\,, & \Phi_1 &\mapsto \Phi_1\,, \\ \nu^0_{R_j} &\mapsto \nu^0_{R_j}\,, & \Phi_2 &\mapsto e^{-i\tau}\Phi_2\,. \end{aligned} \tag{2.64}$$

The combination of symmetries in Eqs. (2.61)–(2.62)–(2.63)–(2.64) gives rise to the 36 different BGL models. It is important to take into account that in order to combine, for example, Eq. (2.61) and Eq. (2.63) a global change of sign must be applied to one of the sectors.

In order to illustrate the behavior of the previous symmetry let us see the texture zeros of the Yukawa matrices for a top-BGL model, that is, applying the symmetry in Eq. (2.61) with the index $j = 3$. In this example, we are going to put our attention in the quark sector, forgetting, for a moment, the lepton sector. However, all the expressions are completely analogous to the ones in the case with Dirac neutrinos. The Yukawa matrices have the structure

$$Y_{d,1} = \begin{pmatrix} \times & \times & \times \\ \times & \times & \times \\ 0 & 0 & 0 \end{pmatrix}, \qquad Y_{d,2} = \begin{pmatrix} 0 & 0 & 0 \\ 0 & 0 & 0 \\ \times & \times & \times \end{pmatrix}, \tag{2.65}$$

$$Y_{u,1} = \begin{pmatrix} \times & \times & 0 \\ \times & \times & 0 \\ 0 & 0 & 0 \end{pmatrix}, \qquad Y_{u,2} = \begin{pmatrix} 0 & 0 & 0 \\ 0 & 0 & 0 \\ 0 & 0 & \times \end{pmatrix}, \tag{2.66}$$

where the elements denoted by × are arbitrary. Obviously, these zero texture structures are valid in a particular set of Weak Basis, the WB where the definition of the symmetry applies. Introducing now these textures into the flavor matrices definition in eq. (2.30), N_d^0 and N_u^0 take the form

$$\begin{aligned} \mathrm{N}_d^0 &= \left(-t_\beta \mathbf{1} + (t_\beta + t_\beta^{-1})\mathrm{P}_3\right)\mathrm{M}_d^0\,, \quad \mathrm{P}_3\mathrm{M}_d^0 = \frac{v_2\, e^{i\theta_2}}{\sqrt{2}} Y_{d,2}\,, \\ \mathrm{N}_u^0 &= \left(-t_\beta \mathbf{1} + (t_\beta + t_\beta^{-1})\mathrm{P}_3\right)\mathrm{M}_u^0\,, \quad \mathrm{P}_3\mathrm{M}_d^0 = \frac{v_2\, e^{-i\theta_2}}{\sqrt{2}} Y_{u,2}\,, \end{aligned} \tag{2.67}$$

where P_3 is the projector $\mathrm{P}_3 = \mathrm{diag}(0,0,1)$. Going into the quark mass basis (eq. (2.33)) where the mass matrices M_q are diagonal, the expressions in eq. (2.67) read

$$\begin{aligned} \mathrm{N}_d &= \mathcal{U}_{d_L}\, \mathrm{N}_d^0\, \mathcal{U}_{d_R}^\dagger = \left(-t_\beta \mathbf{1} + (t_\beta + t_\beta^{-1})\mathrm{P}_3^{[d_L]}\right)\mathrm{M}_d\,, \\ \mathrm{N}_u &= \mathcal{U}_{u_L}\, \mathrm{N}_u^0\, \mathcal{U}_{u_R}^\dagger = \left(-t_\beta \mathbf{1} + (t_\beta + t_\beta^{-1})\mathrm{P}_3^{[u_L]}\right)\mathrm{M}_u\,, \end{aligned} \tag{2.68}$$

where now $\mathrm{P}_3^{[d_L]} = \mathcal{U}_{d_L}^\dagger \mathrm{P}_3 \mathcal{U}_{d_L}$ and $\mathrm{P}_3^{[u_L]} = \mathcal{U}_{u_L}^\dagger \mathrm{P}_3 \mathcal{U}_{u_L}$ that can be related to each other by the CKM matrix

$$\mathrm{P}_3^{[d_L]} = \mathcal{U}_{d_L}^\dagger \underbrace{\left(\mathcal{U}_{u_L} \mathrm{P}_3^{[u_L]} \mathcal{U}_{u_L}^\dagger\right)}_{=\mathrm{P}_3} \mathcal{U}_{d_L} = V^\dagger \mathrm{P}_3^{[u_L]} V \,. \tag{2.69}$$

Then, we can introduce this relation into eq. (2.68) taking into account that in the case we are describing (top-BGL) $\mathrm{P}_3^{[u_L]} = \mathrm{P}_3$. This relation is satisfied because, as can be seen in eq. (2.66), the up-quarks Yukawa matrices are block diagonal. This condition makes $\mathcal{U}_{u_L}$ (and analogously $\mathcal{U}_{u_R}$) also block diagonal what simplify $\mathrm{P}_3^{[u_L]}$. Finally the quark matrices N_q read

$$\begin{aligned} \mathrm{N}_d &= \left(-t_\beta \mathbf{1} + (t_\beta + t_\beta^{-1}) V^\dagger \mathrm{P}_3 V\right) \mathrm{M}_d \,, \\ \mathrm{N}_u &= -t_\beta \,\mathrm{diag}\,(m_u, m_c, 0) + t_\beta^{-1} \,\mathrm{diag}\,(0, 0, m_t) \,. \end{aligned} \tag{2.70}$$

As we expected, in the top-BGL model N_u is diagonal, which means that there are no SFCNC at tree level in the up sector. In the down sector, the SFCNC do not vanish but they are controlled by entries of the CKM matrix, in particular by the elements of the third row

$$\left(V^\dagger \mathrm{P}_3 V\right)_{ij} = (V)^*_{3i} (V)_{3j} \,. \tag{2.71}$$

In this section we have seen that the two main features of BGL models are that, first, they only present SFCNC in one sector, up or down, and second that these SFCNC are controlled by both elements of CKM matrix and masses of the fermions. All the results and expressions presented in the previous lines are replicable to the ones from the leptonic sector when neutrinos are Dirac. These unique features allow BGL models to avoid the strong experimental constraints even in the scenarios with lighter new scalars. In fact, in the literature there are phenomenological analyses [141–144] covering these models that show that it is possible to have new scalars as light as 100 GeV. In Ref. [145, 146] it was proven that the symmetry in eqs. (2.61)–(2.62)–(2.64)–(2.63) developed by Branco, Grimus and Lavoura is the only possibility, using abelian symmetries, that can relate SFCNC with the elements of the CKM matrix in the 2HDM context. Furthermore, as the model is generated by a symmetry, this solution is stable under renormalization group equations.

Part II

Theoretical Research

–Do you remember the taste of strawberries? It'll be spring soon, and the orchards will be in blossom. And, they'll be sowing the summer barley in the lower fields... and eating the first of the strawberries and cream.

— SAMwise Gamgee, *The Lord of the Rings*, J. R. R. Tolkien

3

Generalizing Flavor Conservation

In Chapter 1 it was described that in the SM, concentrating on quarks, a single Yukawa structure in each sector – up and down – is both responsible for: (i) the generation of mass upon spontaneous breaking of $\mathrm{SU}(2)_L \times \mathrm{U}(1)_Y$ into $\mathrm{U}(1)_{\mathrm{EM}}$, and (ii) the couplings of the quarks to the only fundamental scalar leftover, the Higgs boson, after associating the three would-be Goldstone bosons to the longitudinal polarizations of the massive Z and $W^{\pm}$ gauge bosons. As a consequence, there are no tree level Flavor Changing Neutral Couplings of the Higgs to quarks. With two independent Yukawa structures available in each sector, the situation is dramatically changed in the general 2HDM (see chapter 2), and SFCNC couplings of quarks do arise at tree level. To which extent they appear in the couplings of the different physical neutral scalars depends then on the details of the scalar potential [110]: if the 125 GeV scalar is a mixture of the true-but-unphysical Higgs and the additional neutral scalars, SFCNC "leak" into its couplings through that mixing. At the end of the day, as with many New Physics avenues, the presence of SFCNC is a double edged feature: since the competing SM gauge mediated contributions to SFCNC processes are loop induced, those transitions pose severe constraints while, on the same grounds, provide immediate opportunities to discover deviations from the SM picture.

The study of different ways to dispense without problematic too large SFCNC couplings and the conditions for their appearance or absence, has drawn sustained attention over the years. As analysed in [112] and reviewed in Chapter 2, the absence of SFCNC is guaranteed by forcing each right-handed fermion type to couple to one and only one scalar doublet; this absence of SFCNC, backed by a $\mathbb{Z}_2$ symmetry, is a popular option, and several implementations of this Natural Flavor Conservation idea, namely 2HDM of types I, II, and of types X, Y (when the lepton sector is also considered) have been thoroughly explored (see section 2.4). Additional $U(1)$ gauge symmetries have also been considered, for example, in [147, 148]. The general conditions for the absence of SFCNC, that is, that the mass matrix and the remaining Yukawa coupling matrix can be diagonalised simultaneously, were identified early [149–152]. The interplay of how a symmetry requirement could enforce that *general* NFC and shed some light into the structure of the resulting CKM matrix was addressed in [149, 153–160] with interesting consequences.

In a more recent popular scenario, the Aligned 2HDM [125] (see section 2.4.5), the absence of SFCNC is a priori achieved (and parametrised) with simple requirements on the Yukawa couplings (for an early mention of this kind of possibility, although in the context of real Yukawa couplings and spontaneous CP violation, see also [161]). The possibility of having effective aligned scenarios has been studied in [162, 163]. Radiative effects and the interplay of tree level SFCNC with the Renormalization Group Evolution (RGE) have also been addressed by and large in the literature [82, 126, 128, 130, 132, 156, 164–167].

The aim of the work [2] presented in this chapter is to explore different facets of scenarios with general flavor conservation (gFC) in 2HDM; in other words, analysing relevant aspects of the most general 2HDM scenarios where tree level SFCNC are, a priori, absent. A partial analysis of SFCNC induced in this context by the RGE was presented in [129]. On a purely phenomenological basis, a scenario of this type restricted to the lepton sector was also considered in [130, 168].

The chapter is organized as follows. In section 3.1, we revisit some generalities of 2HDM, fix the notation for the discussion to follow, and recall the most relevant

aspects of the conditions leading to gFC. They are then analyzed attending to the Renormalization Group Evolution that they obey in section 3.2, leading to the full set of conditions required to have RGE-stable gFC. The well known type I and type II cases are briefly revisited in section 3.2.3; section 3.2.5 is devoted to a particular solution which arises when the CKM matrix is reduced to a single Cabibbo-like mixing. The gFC stability of the lepton sector is discussed in section 3.2.4. Appendix A provides details omitted in the discussion of section 3.2.

In chapter 9 this model will be presented as a possible solution for the electron and muon $g-2$ anomalies. There, we will discuss the most relevant experimental constraints on gFC arising from flavor conserving Higgs-related observables.

3.1 General Flavor Conserving Conditions

The Yukawa Lagrangian relevant in this sections reads

$$\begin{aligned}\mathscr{L}_{\rm Y} = &- \bar{Q}^0_L \left(\Phi_1 Y_{d,1} + \Phi_2 Y_{d,2}\right) d^0_R - \bar{Q}^0_L \left(\tilde{\Phi}_1 Y_{u,1} + \tilde{\Phi}_2 Y_{u,2}\right) u^0_R \\ &- \bar{L}^0_L \left(\Phi_1 Y_{\ell,1} + \Phi_2 Y_{\ell,2}\right) \ell^0_R + \text{h.c.}\,. \end{aligned} \tag{3.1}$$

Notice that we do not include right-handed neutrinos ν^0_R and thus, unlike in the quark sector, there is only one set of Yukawa coupling matrices and we work in the massless neutrino approximation.

The necessary and sufficient conditions obeyed by the quark Yukawa coupling matrices $Y_{d,\alpha}$ and $Y_{u,\alpha}$ with $\alpha = 1,2$, in order to have gFC [149–152], are that each of the sets

$$\{Y_{d,\alpha}Y^\dagger_{d,\beta}\}\,,\ \{Y^\dagger_{d,\alpha}Y_{d,\beta}\}\,,\ \{Y_{u,\alpha}Y^\dagger_{u,\beta}\}\,,\ \{Y^\dagger_{u,\alpha}Y_{u,\beta}\}\,,\quad \alpha,\beta = 1,2\,, \tag{3.2}$$

is *abelian*, that is, their elements commute:

$$\begin{aligned}&\left[Y_{d,\alpha}Y^\dagger_{d,\beta}\,,\, Y_{d,\gamma}Y^\dagger_{d,\delta}\right] = 0\,,\ \left[Y^\dagger_{d,\alpha}Y_{d,\beta}\,,\, Y^\dagger_{d,\gamma}Y_{d,\delta}\right] = 0\,,\\ &\left[Y_{u,\alpha}Y^\dagger_{u,\beta}\,,\, Y_{u,\gamma}Y^\dagger_{u,\delta}\right] = 0\,,\ \left[Y^\dagger_{u,\alpha}Y_{u,\beta}\,,\, Y^\dagger_{u,\gamma}Y_{u,\delta}\right] = 0\,,\end{aligned} \tag{3.3}$$

with $\alpha,\beta,\gamma,\delta = 1,2$. In that case, $Y_{d,1}\,, Y_{d,2}$ are simultaneously bi-diagonalyzed, and $Y_{u,1}\,, Y_{u,2}$ too. Being the Yukawa matrices diagonalizable at the same time automatically implies that the M^0_f and N^0_f can be diagonalyzed simultaneously.

A crucial corollary to these necessary and sufficient conditions is the fact that the simultaneous diagonalizability is intrinsic to the Yukawa coupling matrices themselves, independently of the spontaneous symmetry breaking vacuum characterised by the VEVs v_1, v_2. In other words, the property is independent of β in eq. (2.29); the simultaneous bi-diagonalizability of $\{\mathrm{M}_q^0, \mathrm{N}_q^0\}$ is equivalent to the simultaneous bi-diagonalizability of the Yukawa couplings matrices or of any other independent linear combinations of them. Of course, the actual values of the eigenvalues of both M_q^0 (the masses) and N_q^0 do depend on the particular linear combinations.
For leptons, similarly, $\{Y_{\ell,\alpha} Y_{\ell,\beta}^\dagger\}$ and $\{Y_{\ell,\alpha}^\dagger Y_{\ell,\beta}\}$ must be abelian in order to have gFC, and the previous corollary applies equally to them.

A very relevant consequence follows [149, 153–160]: if gFC is due to the Lagrangian in eq. (3.1) being invariant under a (symmetry) transformation of quarks and scalars, the CKM mixing matrix cannot be related to the values of the masses; for example, predictions being made at the time (late 70's)[1] for the Cabibbo angle, like $\tan\theta_c = m_d/m_s$ [169, 170], *could not lead simultaneously to gFC*. Moreover, the resulting mixings are unrealistic (for example, no mixing or a permutation times a complex phase) and radiative corrections cannot be invoked to yield realistic mixings [156].

The most general parametrization of tree level couplings of fermions to scalars obeying gFC is, quite trivially,

$$\mathrm{N}_d = \begin{pmatrix} n_d & 0 & 0 \\ 0 & n_s & 0 \\ 0 & 0 & n_b \end{pmatrix}, \; \mathrm{N}_u = \begin{pmatrix} n_u & 0 & 0 \\ 0 & n_c & 0 \\ 0 & 0 & n_t \end{pmatrix}, \; \mathrm{N}_\ell = \begin{pmatrix} n_e & 0 & 0 \\ 0 & n_\mu & 0 \\ 0 & 0 & n_\tau \end{pmatrix}, \quad n_j \in \mathbb{C}\,, \qquad (3.4)$$

which we use in the rest of the thesis: in section 3.2 for the study of the renormalization group evolution and in chapter 9 for a phenomenological analysis.

Notice that, while for the flavor changing couplings the simultaneous presence of scalar and pseudoscalar terms in fermion-scalar Yukawa interactions is not necessarily CP violating, in the diagonal, flavor conserving ones, on the contrary, it is CP violating (see for example [171]). With the flavor conserving matrices N_f in

[1] In the context of $\mathrm{SU}(2)_L \times \mathrm{U}(1)_Y$ gauge theories; the literature is richer in examples for $\mathrm{SU}(2)_L \otimes \mathrm{SU}(2)_R \otimes \mathrm{U}(1)_{B-L}$ scenarios.

eq. (3.4), the hermitian and antihermitian couplings in eqs. (2.40) and (2.47) are, respectively, their real and imaginary parts. For example, for a CP conserving scalar sector with non-zero mixing $c_{\alpha\beta} \neq 0$, if N_f are not real, they constitute new sources of CP violation in neutral couplings. For the couplings to the charged scalar, without entering into details, if $\mathrm{Im}\left(n_{u_i} n_{d_j}\right) \neq 0$, the combination of scalar and pseudoscalar terms in the coupling $\mathrm{H}^+ \bar{u}_i \, d_j$ is CP violating.

3.2 Renormalization Group Evolution and Flavor Conservation

3.2.1 Evolution of the Quark Yukawa Coupling Matrices

The one loop evolution of the Yukawa couplings under the renormalization group [126, 166, 167, 172] is (with $\mathcal{D} \equiv 16\pi^2 \frac{d}{d\ln\mu}$ and μ the energy scale):

$$\begin{aligned}
\mathcal{D} Y_{d,\alpha} &= a_d Y_{d,\alpha} + \sum_{\rho=1}^{n=2} T^d_{\alpha,\rho} Y_{d,\rho} \\
&+ \sum_{\rho=1}^{n=2} \left(-2 Y_{u,\rho} Y^\dagger_{u,\alpha} Y_{d,\rho} + Y_{d,\alpha} Y^\dagger_{d,\rho} Y_{d,\rho} + \frac{1}{2} Y_{u,\rho} Y^\dagger_{u,\rho} Y_{d,\alpha} + \frac{1}{2} Y_{d,\rho} Y^\dagger_{d,\rho} Y_{d,\alpha} \right) \qquad (3.5) \\
&\text{with } T^d_{\alpha,\rho} \equiv 3\,\mathrm{Tr}\left(Y_{d,\alpha} Y^\dagger_{d,\rho} + Y^\dagger_{u,\alpha} Y_{u,\rho} \right) + \mathrm{Tr}\left(Y_{\ell,\alpha} Y^\dagger_{\ell,\rho} \right),
\end{aligned}$$

$$\begin{aligned}
\mathcal{D} Y_{u,\alpha} &= a_u Y_{u,\alpha} + \sum_{\rho=1}^{n=2} T^u_{\alpha,\rho} Y_{u,\rho} \\
&+ \sum_{\rho=1}^{n=2} \left(-2 Y_{d,\rho} Y^\dagger_{d,\alpha} Y_{u,\rho} + Y_{u,\alpha} Y^\dagger_{u,\rho} Y_{u,\rho} + \frac{1}{2} Y_{d,\rho} Y^\dagger_{d,\rho} Y_{u,\alpha} + \frac{1}{2} Y_{u,\rho} Y^\dagger_{u,\rho} Y_{u,\alpha} \right) \qquad (3.6) \\
&\text{with } T^u_{\alpha,\rho} \equiv 3\,\mathrm{Tr}\left(Y_{u,\alpha} Y^\dagger_{u,\rho} + Y^\dagger_{d,\alpha} Y_{d,\rho} \right) + \mathrm{Tr}\left(Y^\dagger_{\ell,\alpha} Y_{\ell,\rho} \right) = T^{d\,*}_{\alpha,\rho},
\end{aligned}$$

where

$$a_d = -8 g_c^2 - \frac{9}{4} g^2 - \frac{5}{12} g'^2, \qquad a_u = a_d - g'^2, \qquad (3.7)$$

with g_c, g, g', as usual, the gauge coupling constants of $SU(3)_c$, $SU(2)_L$ and $U(1)_Y$, respectively. Introducing

$$Y^L_d = \sum_{\rho=1}^{n=2} Y_{d,\rho} Y^\dagger_{d,\rho}, \quad Y^R_d = \sum_{\rho=1}^{n=2} Y^\dagger_{d,\rho} Y_{d,\rho}, \quad Y^L_u = \sum_{\rho=1}^{n=2} Y_{u,\rho} Y^\dagger_{u,\rho}, \quad \text{and} \quad Y^R_u = \sum_{\rho=1}^{n=2} Y^\dagger_{u,\rho} Y_{u,\rho}, \qquad (3.8)$$

eqs. (3.5)–(3.6) read

$$\mathcal{D} Y_{d,\alpha} = a_d Y_{d,\alpha} + \sum_{\rho=1}^{n=2} T^d_{\alpha,\rho} Y_{d,\rho} + Y_{d,\alpha} Y^R_d + \frac{1}{2} Y^L_d Y_{d,\alpha} + \frac{1}{2} Y^L_u Y_{d,\alpha} - 2 \sum_{\rho=1}^{n=2} Y_{u,\rho} Y^\dagger_{u,\alpha} Y_{d,\rho}, \qquad (3.9)$$

$$\mathcal{D}Y_{u,\alpha} = a_u Y_{u,\alpha} + \sum_{\rho=1}^{n=2} T^u_{\alpha,\rho} Y_{u,\rho} + Y_{u,\alpha} Y_u^R + \frac{1}{2} Y_u^L Y_{u,\alpha} + \frac{1}{2} Y_d^L Y_{u,\alpha} - 2 \sum_{\rho=1}^{n=2} Y_{d,\rho} Y_{d,\alpha}^\dagger Y_{u,\rho} \,. \quad (3.10)$$

Equations (3.9)–(3.10) are the starting point to analyze the one loop stability of the necessary and sufficient conditions for gFC. For that, one needs to know

$$\begin{aligned} &\mathcal{D}\left(\left[Y_{d,\alpha} Y_{d,\beta}^\dagger \,,\, Y_{d,\gamma} Y_{d,\delta}^\dagger\right]\right), \mathcal{D}\left(\left[Y_{d,\alpha}^\dagger Y_{d,\beta} \,,\, Y_{d,\gamma}^\dagger Y_{d,\delta}\right]\right), \\ &\mathcal{D}\left(\left[Y_{u,\alpha} Y_{u,\beta}^\dagger \,,\, Y_{u,\gamma} Y_{u,\delta}^\dagger\right]\right), \mathcal{D}\left(\left[Y_{u,\alpha}^\dagger Y_{u,\beta} \,,\, Y_{u,\gamma}^\dagger Y_{u,\delta}\right]\right), \end{aligned} \quad (3.11)$$

under the assumption that eq. (3.3) holds. With that objective in mind, some simplifications are worth mentioning. Starting with $Y_{d,\alpha} Y_{d,\beta}^\dagger$, we first notice that

$$\mathcal{D}(Y_{d,\alpha} Y_{d,\beta}^\dagger) = (\mathcal{D}Y_{d,\alpha}) Y_{d,\beta}^\dagger + Y_{d,\alpha} (\mathcal{D}Y_{d,\beta})^\dagger = f_{\alpha\beta}^{[\mathrm{d_L}]}(Y_{d,}) + g_{\alpha\beta}^{[\mathrm{d_L}]}(Y_{d,}, Y_u) \,, \quad (3.12)$$

with[2]

$$\begin{aligned} f_{\alpha\beta}^{[\mathrm{d_L}]}(Y_d) = 2a_d Y_{d,\alpha} Y_{d,\beta}^\dagger + \sum_{\rho=1}^{n=2} \left[T^d_{\alpha,\rho} Y_{d,\rho} Y_{d,\beta}^\dagger + T^{d*}_{\beta,\rho} Y_{d,\alpha} Y_{d,\rho}^\dagger \right] \\ + 2 Y_{d,\alpha} Y_d^R Y_{d,\beta}^\dagger + \frac{1}{2} Y_d^L Y_{d,\alpha} Y_{d,\beta}^\dagger + \frac{1}{2} Y_{d,\alpha} Y_{d,\beta}^\dagger Y_d^L \,, \end{aligned} \quad (3.13)$$

and

$$g_{\alpha\beta}^{[\mathrm{d_L}]}(Y_d, Y_u) = \frac{1}{2} Y_u^L Y_{d,\alpha} Y_{d,\beta}^\dagger + \frac{1}{2} Y_{d,\alpha} Y_{d,\beta}^\dagger Y_u^L - 2 \sum_{\rho=1}^{n=2} \left[Y_{u,\rho} Y_{u,\alpha}^\dagger Y_{d,\rho} Y_{d,\beta}^\dagger + Y_{d,\alpha} Y_{d,\rho}^\dagger Y_{u,\beta} Y_{u,\rho}^\dagger \right]. \quad (3.14)$$

The relevant property of the decomposition in eq. (3.12) is that $f_{\alpha\beta}^{[\mathrm{d_L}]}$ depends only[3], in terms of matrices, on $Y_d Y_{d,}^\dagger$ and $Y_d Y_{d,}^\dagger Y_d Y_{d,}^\dagger$ terms, while $g_{\alpha\beta}^{[\mathrm{d_L}]}$ collects the remaining dependence on Y_u's, which has terms $Y_d Y_d^\dagger Y_u Y_u^\dagger$ and $Y_u Y_u^\dagger Y_d Y_d^\dagger$. Then,

$$\begin{aligned} &\mathcal{D}\left[Y_{d,\alpha} Y_{d,\beta}^\dagger \,,\, Y_{d,\gamma} Y_{d,\delta}^\dagger\right] = \left[\mathcal{D}(Y_{d,\alpha} Y_{d,\beta}^\dagger) \,,\, Y_{d,\gamma} Y_{d,\delta}^\dagger\right] + \left[Y_{d,\alpha} Y_{d,\beta}^\dagger \,,\, \mathcal{D}(Y_{d,\gamma} Y_{d,\delta}^\dagger)\right] = \\ &\left[f_{\alpha\beta}^{[\mathrm{d_L}]}(Y_d) + g_{\alpha\beta}^{[\mathrm{d_L}]}(Y_d, Y_u) \,,\, Y_{d,\gamma} Y_{d,\delta}^\dagger\right] + \left[Y_{d,\alpha} Y_{d,\beta}^\dagger \,,\, f_{\gamma\delta}^{[\mathrm{d_L}]}(Y_d) + g_{\gamma\delta}^{[\mathrm{d_L}]}(Y_d, Y_u)\right]. \end{aligned} \quad (3.15)$$

3.2.2 Evolution with gFC Matrices

It is clear that, if there is gFC, i.e. with eq. (3.3),

$$\left[f_{\alpha\beta}^{[\mathrm{d_L}]}(Y_d) \,,\, Y_{d,\gamma} Y_{d,\delta}^\dagger\right] = \left[Y_{d,\alpha} Y_{d,\beta}^\dagger \,,\, f_{\gamma\delta}^{[\mathrm{d_L}]}(Y_d)\right] = 0 \,, \quad (3.16)$$

[2]The superscript $[\mathrm{d_L}]$ is chosen in correspondence with the $Y_{d,\alpha} Y_{d,\beta}^\dagger$ matrix combinations; similarly $f_{\alpha\beta}^{[\mathrm{d_R}]}$ and $g_{\alpha\beta}^{[\mathrm{d_R}]}$ will appear in $\mathcal{D}(Y_{d,\alpha}^\dagger Y_{d,\beta})$, and $f_{\alpha\beta}^{[\mathrm{u_{L,R}}]}$ in $\mathcal{D}(Y_{u,\alpha} Y_{u,\beta}^\dagger)$ and $\mathcal{D}(Y_{u,\alpha}^\dagger Y_{u,\beta})$, but we concentrate for the moment on $\mathcal{D}(Y_{d,\alpha} Y_{d,\beta}^\dagger)$.

[3]Although $T^d_{\alpha,\rho}$ do depend on $Y_{u,\alpha}$'s, there is no matrix depence, only $\mathbb{C}$ numbers; this also applies to the leptonic Yukawa couplings $Y_{\ell,\alpha}$.

and thus

$$\mathcal{D}\left[Y_{d,\alpha}Y^{\dagger}_{d,\beta}\,,\,Y_{d,\gamma}Y^{\dagger}_{d,\delta}\right]=\left[g^{[\mathrm{d_L}]}_{\alpha\beta}(Y_d,Y_u)\,,\,Y_{d,\gamma}Y^{\dagger}_{d,\delta}\right]+\left[Y_{d,\alpha}Y^{\dagger}_{d,\beta}\,,\,g^{[\mathrm{d_L}]}_{\gamma\delta}(Y_d,Y_u)\right]. \quad (3.17)$$

After the simplication brought by eq. (3.16), the next step is to trade eq. (3.17) for conditions expressed in terms of the physical parameters entering in the matrices M^0_d, N^0_d, M^0_u, N^0_u. It is convenient to introduce the following notation

$$T^0_{[\mathrm{d}]1}=\mathrm{M}^0_d,\quad T^0_{[\mathrm{d}]2}=\mathrm{N}^0_d,\quad T^0_{[\mathrm{u}]1}=\mathrm{M}^0_u,\quad T^0_{[\mathrm{u}]2}=\mathrm{N}^0_u, \quad (3.18)$$

which allows us to rewrite eq. (2.29) compactly (with summation over repeated indices understood):

$$\begin{aligned}\frac{v}{\sqrt{2}}Y_{d,\alpha}&=\mathrm{W}_{\alpha i}T^0_{[\mathrm{d}]i}\,, & T^0_{[\mathrm{d}]i}&=\frac{v}{\sqrt{2}}Y_{d,\alpha}\mathrm{W}^{*}_{\alpha i}\,,\\ \frac{v}{\sqrt{2}}Y_{u,\alpha}&=\mathrm{W}^{*}_{\alpha i}T^0_{[\mathrm{u}]i}\,, & T^0_{[\mathrm{u}]i}&=\frac{v}{\sqrt{2}}Y_{u,\alpha}\mathrm{W}_{\alpha i}\,,\end{aligned} \quad (3.19)$$

where

$$\mathrm{W}=\begin{pmatrix}e^{-i\theta_1}&0\\0&e^{-i\theta_2}\end{pmatrix}\begin{pmatrix}c_\beta&-s_\beta\\s_\beta&c_\beta\end{pmatrix},\quad \mathrm{W}\mathrm{W}^{\dagger}=\mathrm{W}^{\dagger}\mathrm{W}=\mathbf{1}\,. \quad (3.20)$$

For completeness, notice that

$$\frac{v}{\sqrt{2}}Y^{\dagger}_{d,\alpha}=\mathrm{W}^{*}_{\alpha i}T^{0\dagger}_{[\mathrm{d}]i}\,,\ \frac{v}{\sqrt{2}}Y^{\dagger}_{u,\alpha}=\mathrm{W}_{\alpha i}T^{0\dagger}_{[\mathrm{u}]i}\,,\ T^{0\dagger}_{[\mathrm{d}]i}=\frac{v}{\sqrt{2}}Y^{\dagger}_{d,\alpha}\mathrm{W}_{\alpha i}\,,\ T^{0\dagger}_{[\mathrm{u}]i}=\frac{v}{\sqrt{2}}Y^{\dagger}_{u,\alpha}\mathrm{W}^{*}_{\alpha i}\,, \quad (3.21)$$

i.e. the hermitian conjugate † (in the space of flavor indices) only gives a complex conjugate in W. One can then write

$$\left[Y_{d,\alpha}Y^{\dagger}_{d,\beta}\,,\,Y_{d,\gamma}Y^{\dagger}_{d,\delta}\right]=\frac{4}{v^4}\mathrm{W}_{\alpha i}\mathrm{W}^{*}_{\beta j}\mathrm{W}_{\gamma k}\mathrm{W}^{*}_{\delta l}\left[T^0_{[\mathrm{d}]i}T^{0\dagger}_{[\mathrm{d}]j}\,,\,T^0_{[\mathrm{d}]k}T^{0\dagger}_{[\mathrm{d}]l}\right], \quad (3.22)$$

and thus

$$\begin{aligned}\mathcal{D}\left[Y_{d,\alpha}Y^{\dagger}_{d,\beta}\,,\,Y_{d,\gamma}Y^{\dagger}_{d,\delta}\right]=\mathcal{D}&\left(\frac{4}{v^4}\mathrm{W}_{\alpha i}\mathrm{W}^{*}_{\beta j}\mathrm{W}_{\gamma k}\mathrm{W}^{*}_{\delta l}\right)\left[T^0_{[\mathrm{d}]i}T^{0\dagger}_{[\mathrm{d}]j}\,,\,T^0_{[\mathrm{d}]k}T^{0\dagger}_{[\mathrm{d}]l}\right]\\&+\frac{4}{v^4}\mathrm{W}_{\alpha i}\mathrm{W}^{*}_{\beta j}\mathrm{W}_{\gamma k}\mathrm{W}^{*}_{\delta l}\,\mathcal{D}\left[T^0_{[\mathrm{d}]i}T^{0\dagger}_{[\mathrm{d}]j}\,,\,T^0_{[\mathrm{d}]k}T^{0\dagger}_{[\mathrm{d}]l}\right].\end{aligned} \quad (3.23)$$

With gFC, the first commutator vanishes, and we just have a linear combination of different $\mathcal{D}[T^0_{[\mathrm{d}]i}T^{0\dagger}_{[\mathrm{d}]j},T^0_{[\mathrm{d}]k}T^{0\dagger}_{[\mathrm{d}]l}]$. One can indeed invert eq. (3.23),

$$\frac{4}{v^4}\mathcal{D}\left[T^0_{[\mathrm{d}]i}T^{0\dagger}_{[\mathrm{d}]j}\,,\,T^0_{[\mathrm{d}]k}T^{0\dagger}_{[\mathrm{d}]l}\right]=\mathrm{W}^{*}_{\alpha i}\mathrm{W}_{\beta j}\mathrm{W}^{*}_{\gamma k}\mathrm{W}_{\delta l}\,\mathcal{D}\left[Y_{d,\alpha}Y^{\dagger}_{d,\beta}\,,\,Y_{d,\gamma}Y^{\dagger}_{d,\delta}\right] \quad (3.24)$$

and express the right-hand side of eq. (3.24) in terms of $T^0_{[\mathrm{d}]i}$, $T^0_{[\mathrm{u}]j}$:

$$\begin{aligned}
&\frac{v^2}{2}\mathcal{D}\left[T^0_{[\mathrm{d}]i}T^{0\dagger}_{[\mathrm{d}]j}\,,\,T^0_{[\mathrm{d}]k}T^{0\dagger}_{[\mathrm{d}]l}\right] = \\
&\quad T^0_{[\mathrm{d}]i}T^{0\dagger}_{[\mathrm{d}]j}T^0_{[\mathrm{u}]h}T^{0\dagger}_{[\mathrm{u}]h}T^0_{[\mathrm{d}]k}T^{0\dagger}_{[\mathrm{d}]l} - T^0_{[\mathrm{d}]k}T^{0\dagger}_{[\mathrm{d}]l}T^0_{[\mathrm{u}]h}T^{0\dagger}_{[\mathrm{u}]h}T^0_{[\mathrm{d}]i}T^{0\dagger}_{[\mathrm{d}]j} \\
&-2\left[T^0_{[\mathrm{u}]h}T^{0\dagger}_{[\mathrm{u}]i}\,,\,T^0_{[\mathrm{d}]k}T^{0\dagger}_{[\mathrm{d}]l}\right]T^0_{[\mathrm{d}]h}T^{0\dagger}_{[\mathrm{d}]j} - 2T^0_{[\mathrm{d}]i}T^{0\dagger}_{[\mathrm{d}]h}\left[T^0_{[\mathrm{u}]j}T^{0\dagger}_{[\mathrm{u}]h}\,,\,T^0_{[\mathrm{d}]k}T^{0\dagger}_{[\mathrm{d}]l}\right] \\
&+2\left[T^0_{[\mathrm{u}]h}T^{0\dagger}_{[\mathrm{u}]k}\,,\,T^0_{[\mathrm{d}]i}T^{0\dagger}_{[\mathrm{d}]j}\right]T^0_{[\mathrm{d}]h}T^{0\dagger}_{[\mathrm{d}]l} + 2T^0_{[\mathrm{d}]k}T^{0\dagger}_{[\mathrm{d}]h}\left[T^0_{[\mathrm{u}]l}T^{0\dagger}_{[\mathrm{u}]h}\,,\,T^0_{[\mathrm{d}]i}T^{0\dagger}_{[\mathrm{d}]j}\right].
\end{aligned} \tag{3.25}$$

As expected from the discussion in section 3.1, having a gFC scenario is related to the Yukawa coupling matrices themselves, it does not hinge on the particular EW vacuum configuration that determines which particular combinations of them are the mass matrices M^0_d, M^0_u and the matrices N^0_d, N^0_u (the vacuum configuration is "encoded" in W, which does not appear in eq. (3.25)). The last step is to transform into the mass eigenstate basis with $\mathcal{U}_{d_L}$ in eq. (2.32):

$$\begin{aligned}
&\frac{v^2}{2}\mathcal{U}^\dagger_{d_L}\left(\mathcal{D}\left[T^0_{[\mathrm{d}]i}T^{0\dagger}_{[\mathrm{d}]j}\,,\,T^0_{[\mathrm{d}]k}T^{0\dagger}_{[\mathrm{d}]l}\right]\right)\mathcal{U}_{d_L} = \\
&\quad T_{[\mathrm{d}]i}T^\dagger_{[\mathrm{d}]j}V^\dagger T_{[\mathrm{u}]h}T^\dagger_{[\mathrm{u}]h}V\,T_{[\mathrm{d}]k}T^\dagger_{[\mathrm{d}]l} - T_{[\mathrm{d}]k}T^\dagger_{[\mathrm{d}]l}V^\dagger T_{[\mathrm{u}]h}T^\dagger_{[\mathrm{u}]h}V\,T_{[\mathrm{d}]i}T^\dagger_{[\mathrm{d}]j} \\
&-2\left[V^\dagger T_{[\mathrm{u}]h}T^\dagger_{[\mathrm{u}]i}V\,,\,T_{[\mathrm{d}]k}T^\dagger_{[\mathrm{d}]l}\right]T_{[\mathrm{d}]h}T^\dagger_{[\mathrm{d}]j} - 2T_{[\mathrm{d}]i}T^\dagger_{[\mathrm{d}]h}\left[V^\dagger T_{[\mathrm{u}]j}T^\dagger_{[\mathrm{u}]h}V\,,\,T_{[\mathrm{d}]k}T^\dagger_{[\mathrm{d}]l}\right] \\
&+2\left[V^\dagger T_{[\mathrm{u}]h}T^\dagger_{[\mathrm{u}]k}V\,,\,T_{[\mathrm{d}]i}T^\dagger_{[\mathrm{d}]j}\right]T_{[\mathrm{d}]h}T^\dagger_{[\mathrm{d}]l} + 2T_{[\mathrm{d}]k}T^\dagger_{[\mathrm{d}]h}\left[V^\dagger T_{[\mathrm{u}]l}T^\dagger_{[\mathrm{u}]h}V\,,\,T_{[\mathrm{d}]i}T^\dagger_{[\mathrm{d}]j}\right],
\end{aligned} \tag{3.26}$$

where the CKM matrix $V = \mathcal{U}^\dagger_{u_L}\mathcal{U}_{d_L}$ appears together with the diagonal matrices

$$T_{[\mathrm{d}]1} = \mathrm{M}_d,\ T_{[\mathrm{d}]2} = \mathrm{N}_d,\ T_{[\mathrm{u}]1} = \mathrm{M}_u,\ T_{[\mathrm{u}]2} = \mathrm{N}_u\,. \tag{3.27}$$

In this generic notation – eq. (3.18) –,

$$\begin{aligned}
T_{[\mathrm{d}]i} = \mathrm{diag}(t^{\mathrm{d}}_{i,j}), \quad &\{t^{\mathrm{d}}_{1,1}, t^{\mathrm{d}}_{1,2}, t^{\mathrm{d}}_{1,3}\} = \{m_d, m_s, m_b\}, \\
&\{t^{\mathrm{d}}_{2,1}, t^{\mathrm{d}}_{2,2}, t^{\mathrm{d}}_{2,3}\} = \{n_d, n_s, n_b\}, \\
T_{[\mathrm{u}]i} = \mathrm{diag}(t^{\mathrm{u}}_{i,j}), \quad &\{t^{\mathrm{u}}_{1,1}, t^{\mathrm{u}}_{1,2}, t^{\mathrm{u}}_{1,3}\} = \{m_u, m_c, m_t\}, \\
&\{t^{\mathrm{u}}_{2,1}, t^{\mathrm{u}}_{2,2}, t^{\mathrm{u}}_{2,3}\} = \{n_u, n_c, n_t\}.
\end{aligned} \tag{3.28}$$

The previous derivation concerns the set $\{Y_{d,\alpha}Y^\dagger_{d,\beta}\}$; the evolution equations for $\{Y^\dagger_{d,\alpha}Y_{d,\beta}\}$, $\{Y_{u,\alpha}Y^\dagger_{u,\beta}\}$ and $\{Y^\dagger_{u,\alpha}Y_{u,\beta}\}$ are given in appendix A.

In order to have a gFC scenario stable under the one loop RGE, one needs that

the simultaneous diagonalizability of $\{T^0_{[\mathrm{q}]1}, T^0_{[\mathrm{q}]2}\}$ is preserved, that is

$$\begin{aligned} &\mathcal{D}\left[T^0_{[\mathrm{d}]i}T^{0\dagger}_{[\mathrm{d}]j}\,,\,T^0_{[\mathrm{d}]k}T^{0\dagger}_{[\mathrm{d}]l}\right]=0\,, \qquad \mathcal{D}\left[T^0_{[\mathrm{u}]i}T^{0\dagger}_{[\mathrm{u}]j}\,,\,T^0_{[\mathrm{u}]k}T^{0\dagger}_{[\mathrm{u}]l}\right]=0\,,\\ &\mathcal{D}\left[T^{0\dagger}_{[\mathrm{d}]i}T^0_{[\mathrm{d}]j}\,,\,T^{0\dagger}_{[\mathrm{d}]k}T^0_{[\mathrm{d}]l}\right]=0\,, \qquad \mathcal{D}\left[T^{0\dagger}_{[\mathrm{u}]i}T^0_{[\mathrm{u}]j}\,,\,T^{0\dagger}_{[\mathrm{u}]k}T^0_{[\mathrm{u}]l}\right]=0\,. \end{aligned} \tag{3.29}$$

With eqs. (3.26)–(3.28), the conditions expressed by the matrix equations in (3.29) are formulated in full generality, for fixed mass matrices M_d, M_u, and CKM mixings V, in terms of the 6 complex parameters n_j in eq. (3.4). For example, element (a,b) of the first stability condition in eq. (3.29), for $i=j$, $k=l$, $\mathcal{D}[T^0_{[\mathrm{d}]i}T^{0\dagger}_{[\mathrm{d}]i}, T^0_{[\mathrm{d}]k}T^{0\dagger}_{[\mathrm{d}]k}]=0$, reads

$$\begin{aligned} 0=\sum_{q=1}^{3}\sum_{h=1}^{2}V^*_{qa}V_{qb}\Big\{ &\left|t^{\mathrm{u}}_{h,q}\right|^2\left(\left|t^{\mathrm{d}}_{i,a}\right|^2\left|t^{\mathrm{d}}_{k,b}\right|^2-\left|t^{\mathrm{d}}_{i,b}\right|^2\left|t^{\mathrm{d}}_{k,a}\right|^2\right)\\ &-2\left(t^{\mathrm{u}}_{h,q}t^{\mathrm{u}*}_{i,q}t^{\mathrm{d}}_{h,b}t^{\mathrm{d}*}_{i,b}+t^{\mathrm{u}}_{i,q}t^{\mathrm{u}*}_{h,q}t^{\mathrm{d}}_{i,a}t^{\mathrm{d}*}_{h,a}\right)\left(\left|t^{\mathrm{d}}_{k,b}\right|^2-\left|t^{\mathrm{d}}_{k,a}\right|^2\right)\\ &+2\left(t^{\mathrm{u}}_{h,q}t^{\mathrm{u}*}_{k,q}t^{\mathrm{d}}_{h,b}t^{\mathrm{d}*}_{k,b}+t^{\mathrm{u}}_{k,q}t^{\mathrm{u}*}_{h,q}t^{\mathrm{d}}_{k,a}t^{\mathrm{d}*}_{h,a}\right)\left(\left|t^{\mathrm{d}}_{i,b}\right|^2-\left|t^{\mathrm{d}}_{i,a}\right|^2\right)\Big\}. \end{aligned} \tag{3.30}$$

The complete set of conditions is given in appendix A. For each set in eq. (3.29) there are six choices of $i,j,k,l=1,2$, in 2HDM, which give, at least, 3 independent complex equations each. It is clear that, in terms of the 6 complex parameters n_j, the system is largely overconstrained. In section 3.2.3 below, we check that the known stable solutions with $\mathrm{N}_f \propto \mathrm{M}_f$ are recovered. It is however beyond the scope of the work presented here to address if other solutions could a priori exist for the general one loop RGE stability conditions of gFC.

The lepton sector is discussed in section 3.2.4. Finally, in section 3.2.5, we present some particular solutions which arise when the CKM matrix reduces to a Cabibbo-like block diagonal mixing.

3.2.3 Stable gFC with $\mathrm{N}_f \propto \mathrm{M}_f$

When one substitutes $\mathrm{N}_q=\alpha_q\mathrm{M}_q$, $\alpha_q\in\mathbb{C}$, in the conditions for one loop RGE stability of gFC given in appendix A, solving them for α_u, α_d, reduces to finding solutions of

$$(1+\alpha_d\alpha_u)(\alpha_u^*-\alpha_d)=0\,, \tag{3.31}$$

that is $\alpha_u = -\alpha_d^{-1}$ or $\alpha_u^* = \alpha_d$. In both cases, there is a basis for the scalars [126]

$$\begin{pmatrix} H_1' \\ H_2' \end{pmatrix} = \frac{1}{\sqrt{1+|\alpha_d|^2}} \begin{pmatrix} 1 & \alpha_d \\ -\alpha_d^* & 1 \end{pmatrix} \begin{pmatrix} H_1 \\ H_2 \end{pmatrix}, \tag{3.32}$$

with H_1 and H_2 in eq. (2.5), such that in eq. (2.28) H_1' couples only to d_R^0 while H_2' couples only to u_R^0 for $\alpha_u = -\alpha_d^{-1}$; for $\alpha_u = \alpha_d^*$, H_1' couples to d_R^0 and u_R^0, while H_2' does not. These cases are none other than the 2HDM of type II and I respectively which where introduced in 2.4. For the particular case $\alpha_u = \alpha_d^* = 0$, the scalar doublet which has a zero vacuum expectation value has vanishing Yukawa couplings: this is the Inert 2HDM [103].

3.2.4 Stable gFC in the Lepton Sector

The one loop RGE of the lepton Yukawa couplings in eq. (3.1) reads [172, 173]

$$\mathcal{D}Y_{\ell,\alpha} = a_\ell Y_{\ell,\alpha} + \sum_{\rho=1}^{n=2} T^\ell_{\alpha,\rho} Y_{\ell,\rho} + \sum_{\rho=1}^{n=2} \left(Y_{\ell,\alpha} Y^\dagger_{\ell,\rho} Y_{\ell,\rho} + \frac{1}{2} Y_{\ell,\rho} Y^\dagger_{\ell,\rho} Y_{\ell,\alpha} \right) \quad \text{with } T^\ell_{\alpha,\rho} = T^d_{\alpha,\rho}\,, \tag{3.33}$$

where $a_\ell = -\frac{9}{4}g^2 - \frac{15}{4}g'^2$. With $Y^L_\ell = \sum_{\rho=1}^{n=2} Y_{\ell,\rho} Y^\dagger_{\ell,\rho}$, $Y^R_\ell = \sum_{\rho=1}^{n=2} Y^\dagger_{\ell,\rho} Y_{\ell,\rho}$,

$$\mathcal{D}Y_{\ell,\alpha} = a_\ell Y_{\ell,\alpha} + \sum_{\rho=1}^{n=2} T^\ell_{\alpha,\rho} Y_{\ell,\rho} + Y_{\ell,\alpha} Y^R_\ell + \frac{1}{2} Y^L_\ell Y_{\ell,\alpha}\,. \tag{3.34}$$

The crucial difference in the leptonic sector is that, following eq. (3.34),

$$\begin{aligned} \mathcal{D}(Y_{\ell,\alpha} Y^\dagger_{\ell,\beta}) = 2a_\ell Y_{\ell,\alpha} Y^\dagger_{\ell,\beta} + \sum_{\rho=1}^{n=2} \left(T^\ell_{\alpha,\rho} Y_{\ell,\rho} Y^\dagger_{\ell,\beta} + T^{\ell *}_{\beta,\rho} Y_{\ell,\alpha} Y^\dagger_{\ell,\rho} \right) + 2 Y_{\ell,\alpha} Y^R_\ell Y^\dagger_{\ell,\beta} \\ + \frac{1}{2} \left(Y^L_\ell Y_{\ell,\alpha} Y^\dagger_{\ell,\beta} + Y_{\ell,\alpha} Y^\dagger_{\ell,\beta} Y^L_\ell \right), \end{aligned} \tag{3.35}$$

and thus it is clear that, if $\{Y_{\ell,\alpha} Y^\dagger_{\ell,\beta}\}_{\alpha,\beta=1,2}$ is abelian, then

$$\mathcal{D}\left[Y_{\ell,\alpha} Y^\dagger_{\ell,\beta}\,,\, Y_{\ell,\gamma} Y^\dagger_{\ell,\delta} \right] = \left[\mathcal{D}(Y_{\ell,\alpha} Y^\dagger_{\ell,\beta})\,,\, Y_{\ell,\gamma} Y^\dagger_{\ell,\delta} \right] + \left[Y_{\ell,\alpha} Y^\dagger_{\ell,\beta}\,,\, \mathcal{D}(Y_{\ell,\gamma} Y^\dagger_{\ell,\delta}) \right] = 0\,. \tag{3.36}$$

Similarly,

$$\begin{aligned} \mathcal{D}(Y^\dagger_{\ell,\alpha} Y_{\ell,\beta}) = 2a_\ell Y^\dagger_{\ell,\alpha} Y_{\ell,\beta} + \sum_{\rho=1}^{n=2} \left(T^{\ell *}_{\alpha,\rho} Y^\dagger_{\ell,\rho} Y_{\ell,\beta} + T^\ell_{\beta,\rho} Y^\dagger_{\ell,\alpha} Y_{\ell,\rho} \right) \\ + Y^R_\ell Y^\dagger_{\ell,\alpha} Y^\dagger_{\ell,\beta} + Y^\dagger_{\ell,\alpha} Y^\dagger_{\ell,\beta} Y^R_\ell + Y^\dagger_{\ell,\alpha} Y^L_\ell Y_{\ell,\beta}\,, \end{aligned} \tag{3.37}$$

and thus, if $\{Y^\dagger_{\ell,\alpha} Y_{\ell,\beta}\}_{\alpha,\beta=1,2}$ is abelian, then

$$\mathcal{D}\left[Y^\dagger_{\ell,\alpha} Y_{\ell,\beta}\,,\, Y^\dagger_{\ell,\gamma} Y_{\ell,\delta} \right] = \left[\mathcal{D}(Y^\dagger_{\ell,\alpha} Y_{\ell,\beta})\,,\, Y^\dagger_{\ell,\gamma} Y_{\ell,\delta} \right] + \left[Y^\dagger_{\ell,\alpha} Y_{\ell,\beta}\,,\, \mathcal{D}(Y^\dagger_{\ell,\gamma} Y_{\ell,\delta}) \right] = 0\,. \tag{3.38}$$

That is, if the Yukawa couplings of leptons are gFC, as in eq. (3.4), this is not altered by the RGE: general flavor conservation is one-loop stable in the lepton sector. This can be directly traced back to the absence of right-handed neutrinos and Yukawa couplings involving them in eq. (2.45), in clear contrast with the quark sector. This result represents a generalization of previous results restricted to the so called aligned case and pointed out in [128], in agreement with the findings of [127, 130]: *at one loop level the charged lepton sector remains general Flavor Conserving in full generality without any additional constraint.* To be specific and going to the simplest aligned cases, type I, II, X and Y models are defined in the quark sector by

$$\text{Type I,X} \begin{cases} \mathrm{N}_d = \cot\beta\, \mathrm{M}_d, \\ \mathrm{N}_u = \cot\beta\, \mathrm{M}_u, \end{cases} \qquad \text{Type II,Y} \begin{cases} \mathrm{N}_d = -\tan\beta\, \mathrm{M}_d, \\ \mathrm{N}_u = \cot\beta\, \mathrm{M}_u. \end{cases} \tag{3.39}$$

The fact that the leptonic sector alignment was known to be stable under RGE implies that one could analyze the experimental data with previous equation together with the more general leptonic structure ($Y_{\ell,2} = \xi_\ell e^{-i\theta} Y_{\ell,1}$)

$$\mathrm{N}_\ell = \cot\beta \left(\frac{-\tan\beta + \xi_\ell}{\cot\beta + \xi_\ell} \right) \mathrm{M}_\ell \,, \tag{3.40}$$

in the framework of a model one loop stable under RGE. This would include in a single analysis both type I and X or type II and Y. Note that with the appropriate limits $\xi_\ell \to 0$ or $\xi_\ell \to \infty$ one recovers the four models. Equation (3.38) implies the new more general result that the models implemented by eq. (3.39) together with an *arbitrary* diagonal N_ℓ (not just with eq. (3.40)) are one loop stable under RGE. These models are going to be referred as I-gℓFC and II-gℓFC 2HDM models:

- Model I-gℓFC is defined by[4]

$$\mathrm{N}_u = t_\beta^{-1} \mathrm{M}_u, \quad \mathrm{N}_d = t_\beta^{-1} \mathrm{M}_d, \quad \mathrm{N}_\ell = \mathrm{diag}(n_e, n_\mu, n_\tau) \,. \tag{3.41}$$

  The couplings $\mathrm{N}_u, \mathrm{N}_d$ are the same as in 2HDMs of types I or X.

- Model II-gℓFC is defined by

$$\mathrm{N}_u = t_\beta^{-1} \mathrm{M}_u, \quad \mathrm{N}_d = -t_\beta \mathrm{M}_d, \quad \mathrm{N}_\ell = \mathrm{diag}(n_e, n_\mu, n_\tau) \,. \tag{3.42}$$

  The couplings $\mathrm{N}_u, \mathrm{N}_d$ are the same as in 2HDMs of types II or Y.

[4]Here and in the following, $t_\beta \equiv \tan\beta$ and $t_\beta^{-1} \equiv \cot\beta$.

In both models N_ℓ is diagonal, arbitrary and stable at one loop level under RGE, in the sense that it remains diagonal.

To complete the definition of the model, in accordance with the fact that the quark sector is a type I or type II 2HDM, we adopt a $\mathbb{Z}_2$ symmetric scalar potential

$$\begin{aligned} V(\Phi_1,\Phi_2) = {} & \mu_{11}^2\Phi_1^\dagger\Phi_1 + \mu_{22}^2\Phi_2^\dagger\Phi_2 + \left(\mu_{12}^2\Phi_1^\dagger\Phi_2 + \text{h.c.}\right) + \lambda_1(\Phi_1^\dagger\Phi_1)^2 + \lambda_2(\Phi_2^\dagger\Phi_2)^2 \\ & + 2\lambda_3(\Phi_1^\dagger\Phi_1)(\Phi_2^\dagger\Phi_2) + 2\lambda_4(\Phi_1^\dagger\Phi_2)(\Phi_2^\dagger\Phi_1) + \left(\lambda_5(\Phi_1^\dagger\Phi_2)^2 + \text{h.c.}\right). \end{aligned} \quad (3.43)$$

For $\mu_{12}^2 \neq 0$, the $\mathbb{Z}_2$ symmetry is softly broken.

In table 3.1 the Yukawa couplings, following the general notation introduced in eq. (2.49), of the neutral scalars can be found for both models I-gℓFC and II-gℓFC. The Yukawa couplings of the neutral scalars are flavor conserving. Here, we focus on a simplified case: we assume that (i) there is no CP violation in the scalar sector and (ii) the new Yukawa couplings are real, $\text{Im}\,(n_\ell) = 0$. In the scalar sector, this corresponds to

$$\mathcal{R} = \begin{pmatrix} s_{\alpha\beta} & -c_{\alpha\beta} & 0 \\ c_{\alpha\beta} & s_{\alpha\beta} & 0 \\ 0 & 0 & 1 \end{pmatrix}, \quad (3.44)$$

with $s_{\alpha\beta} \equiv \sin(\alpha-\beta)$ and $c_{\alpha\beta} \equiv \cos(\alpha-\beta)$. The alignment limit, in which h has the same couplings of the SM Higgs, corresponds to $s_{\alpha\beta} \to 1$. The absence of CP

		a_u^S	b_u^S	a_d^S	b_d^S	a_ℓ^S	b_ℓ^S
I-gℓFC	h	$s_{\alpha\beta} + c_{\alpha\beta}t_\beta^{-1}$	0	$s_{\alpha\beta} + c_{\alpha\beta}t_\beta^{-1}$	0	$s_{\alpha\beta} + c_{\alpha\beta}\frac{\text{Re}(n_\ell)}{m_\ell}$	0
	H	$-c_{\alpha\beta} + s_{\alpha\beta}t_\beta^{-1}$	0	$-c_{\alpha\beta} + s_{\alpha\beta}t_\beta^{-1}$	0	$-c_{\alpha\beta} + s_{\alpha\beta}\frac{\text{Re}(n_\ell)}{m_\ell}$	0
	A	0	$-t_\beta^{-1}$	0	$+t_\beta^{-1}$	0	$\frac{\text{Re}(n_\ell)}{m_\ell}$
II-gℓFC	h	$s_{\alpha\beta} + c_{\alpha\beta}t_\beta^{-1}$	0	$s_{\alpha\beta} - c_{\alpha\beta}t_\beta$	0	$s_{\alpha\beta} + c_{\alpha\beta}\frac{\text{Re}(n_\ell)}{m_\ell}$	0
	H	$-c_{\alpha\beta} + s_{\alpha\beta}t_\beta^{-1}$	0	$-c_{\alpha\beta} - s_{\alpha\beta}t_\beta$	0	$-c_{\alpha\beta} + s_{\alpha\beta}\frac{\text{Re}(n_\ell)}{m_\ell}$	0
	A	0	$-t_\beta^{-1}$	0	$-t_\beta$	0	$\frac{\text{Re}(n_\ell)}{m_\ell}$

Table 3.1: Fermion couplings to neutral scalars.

violation is clear from the exact relation $a_f^S b_f^S = 0$ [171]; one important consequence of this simplification is the absence of new contributions generating electric dipole moments (EDMs), in particular contributions to the electron EDM d_e, which is quite constrained: $|d_e| < 1.1 \times 10^{-29}$ e·cm [174, 175]. The Yukawa couplings of $H^\pm$ are

	α^q_{ij}	β^q_{ij}	α^l_{ij}	β^l_{ij}
I-gℓFC	$V^*_{ji}\, t_\beta^{-1}(m_{u_j} - m_{d_i})$	$V^*_{ji}\, t_\beta^{-1}(m_{u_j} + m_{d_i})$	$-\mathrm{Re}\,(n_{\ell_i})\,\delta_{ij}$	$\mathrm{Re}\,(n_{\ell_i})\,\delta_{ij}$
II-gℓFC	$V^*_{ji}\,(t_\beta^{-1} m_{u_j} + t_\beta m_{d_i})$	$V^*_{ji}\,(t_\beta^{-1} m_{u_j} - t_\beta m_{d_i})$	$-\mathrm{Re}\,(n_{\ell_i})\,\delta_{ij}$	$\mathrm{Re}\,(n_{\ell_i})\,\delta_{ij}$

Table 3.2: Fermion couplings to $H^\pm$.

given in Table 3.2. Note that the Yukawa couplings of the charged leptons in Tables 3.1 and 3.2 are the same in both models I-gℓFC and II-gℓFC. The phenomenology of these models will be studied in further detail in chapter 9.

3.2.5 Stable gFC with Cabibbo-like mixing

The CKM matrix has a hierarchical structure; keeping only the largest mixing, it has the form

$$V_{\theta_c} = \begin{pmatrix} \cos\theta_c & \sin\theta_c & 0 \\ -\sin\theta_c & \cos\theta_c & 0 \\ 0 & 0 & 1 \end{pmatrix}, \tag{3.45}$$

with $\theta_c \simeq 0.22$ the Cabibbo mixing angle. It is interesting to analyze the question of one loop RGE stability of gFC conditions with $V \to V_{\theta_c}$ in eq. (3.45). First, it is interesting on its own to know if this simplified mixing allows for some stable gFC scenario; second, if that is the case, in terms of those N_q matrices, the deviations of gFC produced by the RGE would be controlled by the initial deviations of the complete CKM matrix from V_{θ_c}, the subleading mixings.

One should first notice that, since V_{θ_c} decouples the third quark generation, n_b and n_t are expected to remain free parameters. Then, since the only remaining stability conditions concern elements $(a,b) = (1,2)$ or $(2,1)$, all the mixing combinations $V^*_{qa}V_{qb}$, $V_{aq}V^*_{bq}$ equal either $\cos\theta_c \sin\theta_c$ or $-\cos\theta_c \sin\theta_c$, and thus the dependence of the stability conditions on θ_c disappears.

Two classes of stable gFC scenarios follow from the discussion in section 3.2.3. The first, with

$$\mathrm{N}_d = \mathrm{diag}(\alpha\, m_d,\, \alpha\, m_s,\, n_b), \quad \mathrm{N}_u = \mathrm{diag}(\alpha^* m_u,\, \alpha^* m_c, n_t\,), \tag{3.46}$$

corresponds to a type I 2HDM for the first two generations, while n_b and n_t are free (and thus $\mathrm{M}_q^{-1}\mathrm{N}_q \neq \alpha_q \mathbf{1}$). Some particular limit – the extreme chiral limit – of

eq. (3.46) was already obtained in [128] to justify $V \simeq \mathbf{1}$. The second is

$$\mathrm{N}_d = \mathrm{diag}(\alpha\, m_d,\, \alpha\, m_s,\, n_b), \quad \mathrm{N}_u = \mathrm{diag}(-\alpha^{-1} m_u,\, -\alpha^{-1} m_c, n_t\,), \tag{3.47}$$

which corresponds instead to a type II 2HDM for the first two generations (with free n_b, n_t and $\mathrm{M}_q^{-1}\mathrm{N}_q \neq \alpha_q \mathbf{1}$ too). In addition to eqs. (3.46)–(3.47), one can check that

$$\mathrm{N}_d = \mathrm{diag}(e^{i\varphi_d} m_s,\, e^{i\varphi_d} m_d,\, n_b), \quad \mathrm{N}_u = \mathrm{diag}(e^{i\varphi_u} m_c,\, e^{i\varphi_u} m_u, n_t\,), \tag{3.48}$$

with arbitrary real φ_d, φ_u (and again, arbitrary complex n_b and n_t), gives indeed another stable gFC scenario where N_q and M_q are not even proportional in the first two generations sector.

–If I take one more step... It'll be the farthest away from home I've ever been.

— SAMwise Gamgee, *The Lord of the Rings*, J. R. R. Tolkien

4 Generalizing BGL Models

As it has been discussed, the general 2HDM has Flavor Changing Neutral Couplings at tree level which have to be suppressed in order to avoid the strong experimental constraints. Along the previous chapters, different ways of avoiding SFCNC have been presented. As it was introduced in section 2.5, there is a very interesting approach to solve this issue that is the control of SFCNC. One example is provided by Branco-Grimus-Lavoura models [133], where there are SFCNC at tree level but their intensity is controlled by the elements of the CKM matrix V. Although these models were proposed some years before the Minimal Flavor Violation hypothesis [134–136] was put forward, BGL models satisfy the MFV hypothesis of having all the flavor structure of New Physics controlled by V and masses [133, 138]. BGL models are renormalizable, since the flavor structure of the Yukawa couplings is generated by an exact symmetry of the Lagrangian.

The flavor structure of the general 2HDM, which contains SFCNC, is parametrized by two complex matrices N_d, N_u [139]. These matrices depend on several parameters, in particular on $\mathcal{U}_{d_L}$, $\mathcal{U}_{u_L}$, $\mathcal{U}_{d_R}$ and $\mathcal{U}_{u_R}$, the unitary matrices which diagonalize the quark mass matrices. BGL model achive the difficult task of making N_d, N_u depend only on $V = \mathcal{U}_{u_L}^\dagger \mathcal{U}_{d_L}$ and quark masses in a natural way. These models were first proposed for the quark sector and then generalized to the lepton sector [140]. As it was presented in section 2.5 there are six types of BGL models in the quark

sector and six (three) types in the lepton sector for Dirac (Majorana) neutrinos, which can be combined to have a total of 36 (18) BGL models, with different phenomenological implications, which were thoroughly analyzed [141–143]. An interesting feature of BGL models is the fact they contain FCNC either in the up or the down sectors but not in both sectors.

In this chapter, we analyze the possibility of generalizing BGL models, asking ourselves two questions. The first is if it is possible to find a renormalizable model which contains all the BGL models as special cases. And the second, if it is possible to have a renormalizable 2HDM with non-vanishing SFCNC in both the up and down quark sectors but controlled in some way.

The chapter is organized as follows. In the next section BGL models are briefly reviewed and then a more general framework denoted gBGL is proposed. The generalization contains BGL models as an special limit. In section 4.2 Yukawa textures corresponding to gBGL models are examined as well as how gBGL contain BGL models as special cases. In this section Weak Basis invariant conditions for having gBGL models are derived. In section 4.3, using WB covariant projectors, we introduce a convenient parametrization of gBGL models. In section 4.4 the scalar potential is briefly described. Section 4.5 includes the analysis of the intensity of SFCNC in gBGL models, with particular emphasis, in section 4.6, on models close to BGL models of types b and t. In section 4.7 the implications of gBGL models for the Baryon Asymmetry of the Universe are discussed.

4.1 Generalising BGL models: gBGL

From eq. (2.31) it is easy to realize that N_d^0, N_u^0 are complex matrices which contain a large number of new parameters. They also introduce SFCNC which, as we already know, have strong experimental constraints. As it was seen in section 2.5 BGL models are able to control the size of SFCNC, despite their appearance at tree level. They have some remarkable features which can be summarized in the following way.

(i) Being generated by a symmetry of the full Lagrangian, BGL models are renormalizable.

(ii) The only parameters in the couplings of the physical neutral scalars to the quark mass eigenstates are the elements of the CKM matrix, t_β and the quark masses.

(iii) In BGL models there are SFCNC either in the up or down sectors, but not in both. It has been shown [145] that if one imposes a flavor symmetry such that the SFCNC only depend on V and further assumes that the flavor symmetry is abelian, then BGL models are unique.

As it was introduced in section 2.5, the symmetries that generate the BGL models read

- For the up-type BGL models (uBGL):

$$\begin{aligned} Q_{L_3} &\mapsto e^{i\tau} Q_{L_3}\,, \\ d_R &\mapsto d_R\,, \qquad & \Phi_1 &\mapsto \Phi_1\,, \\ u_{R_3} &\mapsto e^{i2\tau} u_{R_3}\,, \qquad & \Phi_2 &\mapsto e^{i\tau}\Phi_2\,. \end{aligned} \tag{2.61}$$

- For the down-type BGL models (dBGL):

$$\begin{aligned} Q_{L_3} &\mapsto e^{i\tau} Q_{L_3}\,, \\ d_{R_3} &\mapsto e^{i2\tau} d_{R_3}\,, \qquad & \Phi_1 &\mapsto \Phi_1\,, \\ u_R &\mapsto u_R\,, \qquad & \Phi_2 &\mapsto e^{-i\tau}\Phi_2\,, \end{aligned} \tag{2.62}$$

  with $\tau \neq 0, \pi$. It was shown [140] that in order to extend a BGL model to the lepton sector, with Majorana neutrinos and a realistic seesaw mechanism, the phase τ must equal $\pi/2$ which leads to a $\mathbb{Z}_4$ symmetry.

In the work [1] presented in this chapter, we addressed the question whether it was possible to generalize BGL models so that the new class of models, called generalized BGL (gBGL), kept some of the interesting features of BGL models, like renormalizability, but allowing for SFCNC both in the up and the down sectors. The gBGL models are implemented through a $\mathbb{Z}_2$ symmetry, where u_R and d_R are even and only one of the scalar doublets and one of the left-handed quark doublets are odd:

$$\begin{aligned} Q_{L_3} &\mapsto -Q_{L_3}\,, \\ d_R &\mapsto d_R\,, \qquad & \Phi_1 &\mapsto \Phi_1\,, \\ u_R &\mapsto u_R\,, \qquad & \Phi_2 &\mapsto -\Phi_2\,. \end{aligned} \tag{4.1}$$

The gBGL model generated by the symmetry above includes all BGL models as special cases. Indeed when the new free parameters contained by gBGL models are set to zero, what corresponds to taking $e^{i}\tau$ in eqs. (2.61)–(2.62) equal −1, a BGL model is recovered and the Lagrangian acquires a larger symmetry, namely $\mathbb{Z}_4$ [1]. It is worth emphasizing that gBGL models are implemented through a $\mathbb{Z}_2$ symmetry, as it is also the case in the Glashow–Weinberg model with NFC. The only difference is that the left-handed quark families transform differently in the two models. In other words, one may say that *the principle leading to gBGL constrains the Yukawa couplings so that each line of* $Y_{d,j}$, $Y_{u,j}$ *couples only to one Higgs doublet.*

4.2 Yukawa Textures

Imposing the $\mathbb{Z}_2$ symmetry in eq. (4.1), the Yukawa matrices in these models have the general form

$$\begin{aligned} Y_{d,1} &= \begin{pmatrix} \times & \times & y^d_{13} \\ \times & \times & y^d_{23} \\ 0 & 0 & 0 \end{pmatrix}, \qquad Y_{d,2} = \begin{pmatrix} 0 & 0 & 0 \\ 0 & 0 & 0 \\ y^d_{31} & y^d_{32} & \times \end{pmatrix}, \\ Y_{u,1} &= \begin{pmatrix} \times & \times & y^u_{13} \\ \times & \times & y^u_{23} \\ 0 & 0 & 0 \end{pmatrix}, \qquad Y_{u,2} = \begin{pmatrix} 0 & 0 & 0 \\ 0 & 0 & 0 \\ y^u_{31} & y^u_{32} & \times \end{pmatrix}, \end{aligned} \tag{4.2}$$

where $\times$, y^d_{ij} and y^u_{ij} stand for arbitrary complex parameters. In eq. (4.2), the y^d_{ij} and y^u_{ij} entries have been singled out in order to show how gBGL contain BGL models as special cases: it is evident that taking $y^d_{ij} = 0$, we obtain dBGL models, where

$$\begin{aligned} Y_{d,1} &= \begin{pmatrix} \times & \times & 0 \\ \times & \times & 0 \\ 0 & 0 & 0 \end{pmatrix}, \qquad Y_{d,2} = \begin{pmatrix} 0 & 0 & 0 \\ 0 & 0 & 0 \\ 0 & 0 & \times \end{pmatrix}, \\ Y_{u,1} &= \begin{pmatrix} \times & \times & \times \\ \times & \times & \times \\ 0 & 0 & 0 \end{pmatrix}, \qquad Y_{u,2} = \begin{pmatrix} 0 & 0 & 0 \\ 0 & 0 & 0 \\ \times & \times & \times \end{pmatrix}, \end{aligned} \tag{4.3}$$

while taking $y^u_{ij} = 0$ we obtain uBGL models, with

[1] We focus on the generalization of BGL models in the quark sector and do not address in detail the inclusion of the leptonic sector.

$$
\begin{aligned}
Y_{d,1} &= \begin{pmatrix} \times & \times & \times \\ \times & \times & \times \\ 0 & 0 & 0 \end{pmatrix}, \qquad Y_{d,2} = \begin{pmatrix} 0 & 0 & 0 \\ 0 & 0 & 0 \\ \times & \times & \times \end{pmatrix}, \\
Y_{u,1} &= \begin{pmatrix} \times & \times & 0 \\ \times & \times & 0 \\ 0 & 0 & 0 \end{pmatrix}, \qquad Y_{u,2} = \begin{pmatrix} 0 & 0 & 0 \\ 0 & 0 & 0 \\ 0 & 0 & \times \end{pmatrix}.
\end{aligned} \tag{4.4}
$$

So our goal is achieved, that is, gBGL models include both up and down type BGL models, while being renormalizable. They also contain SFCNC in both quark sectors while in the BGL models the SCFCN are confined to one and only one sector. In the case of gBGL models this features is achieved because the appearance of SFCNC in one sector depends on the Yukawa couplings of that sector alone, without regard to the Yukawa couplings in the other sector.

4.2.1 Weak basis invariant conditions

As a summary of the previous discussion, gBGL models are defined by a $\mathbb{Z}_2$ symmetry or by the following matrix textures:

$$
\begin{aligned}
Y_{d,1} &= \begin{pmatrix} \times & \times & \times \\ \times & \times & \times \\ 0 & 0 & 0 \end{pmatrix}, \qquad Y_{d,2} = \begin{pmatrix} 0 & 0 & 0 \\ 0 & 0 & 0 \\ \times & \times & \times \end{pmatrix}, \\
Y_{u,1} &= \begin{pmatrix} \times & \times & \times \\ \times & \times & \times \\ 0 & 0 & 0 \end{pmatrix}, \qquad Y_{u,2} = \begin{pmatrix} 0 & 0 & 0 \\ 0 & 0 & 0 \\ \times & \times & \times \end{pmatrix}.
\end{aligned} \tag{4.5}
$$

Obviously, these zero texture structures are valid in a particular set of Weak Basis, the WB where the definition of the symmetry applies[2]. Introducing the projection operator P_3,

$$
\mathrm{P}_3 = \begin{pmatrix} 0 & 0 & 0 \\ 0 & 0 & 0 \\ 0 & 0 & 1 \end{pmatrix}, \qquad \mathrm{P}_3\mathrm{P}_3 = \mathrm{P}_3\,, \qquad (\mathbf{1} - \mathrm{P}_3)\mathrm{P}_3 = 0\,, \tag{4.6}
$$

it is straightforward to check that imposing the textures in eqs. (4.5) is equivalent to the following definition of gBGL models:

$$
\begin{aligned}
\mathrm{P}_3 Y_{d,1} &= 0\,, \qquad \mathrm{P}_3 Y_{d,2} = Y_{d,2}\,, \\
\mathrm{P}_3 Y_{u,1} &= 0\,, \qquad \mathrm{P}_3 Y_{u,2} = Y_{u,2}\,.
\end{aligned} \tag{4.7}
$$

[2]WB transformations are discussed in detail in section 4.3.1.

BGL models, are defined by more relations: in terms of P_3, uBGL models satisfy

$$\begin{aligned} \mathrm{P}_3 Y_{d,1} &= 0\,, \qquad \mathrm{P}_3 Y_{d,2} = Y_{d,2}\,, \\ \mathrm{P}_3 Y_{u,1} &= 0\,, \qquad \mathrm{P}_3 Y_{u,2} = Y_{u,2}\,, \\ Y_{u,1}\mathrm{P}_3 &= 0\,, \qquad Y_{u,2}\mathrm{P}_3 = Y_{u,2}\,, \end{aligned} \tag{4.8}$$

while dBGL models satisfy

$$\begin{aligned} \mathrm{P}_3 Y_{d,1} &= 0\,, \qquad \mathrm{P}_3 Y_{d,2} = Y_{d,2}\,, \\ \mathrm{P}_3 Y_{u,1} &= 0\,, \qquad \mathrm{P}_3 Y_{u,2} = Y_{u,2}\,, \\ Y_{d,1}\mathrm{P}_3 &= 0\,, \qquad Y_{d,2}\mathrm{P}_3 = Y_{d,2}\,. \end{aligned} \tag{4.9}$$

The last two conditions in eqs. (4.8) and (4.9) give the block diagonal form of the Yukawa matrices in the corresponding sector (up in uBGL and down in dBGL models), enforcing the absence of SFCNC in that sector. From these conditions valid in a set of WB, we can get WB independent matrix conditions for all three types of models. The conditions of interest for gBGL models are

$$\begin{aligned} Y_{d,2}^\dagger Y_{d,1} &= 0, \qquad Y_{d,2}^\dagger Y_{u,1} = 0, \\ Y_{u,2}^\dagger Y_{u,1} &= 0, \qquad Y_{u,2}^\dagger Y_{d,1} = 0. \end{aligned} \tag{4.10}$$

Notice that eqs. (4.10) are satisfied trivially in case $Y_{d,1} = Y_{u,1} = 0$ or in case $Y_{d,2} = Y_{u,2} = 0$, which correspond to 2HDM of types I or X; note, however, that this kind of models are not of the gBGL type. Coming back to eqs. (4.10), it is straightforward to show that they are necessary conditions for gBGL models since, from eq. (4.7),

$$Y_{d,2}^\dagger Y_{d,1} = (\mathrm{P}_3 Y_{d,2})^\dagger Y_{d,1} = (Y_{d,2}^\dagger \mathrm{P}_3) Y_{d,1} = Y_{d,2}^\dagger (\mathrm{P}_3 Y_{d,1}) = 0\,, \tag{4.11}$$

and similarly for the remaining conditions in eq. (4.10). The sufficiency of these conditions in order to have gBGL models is shown in appendix B, where the relation with 2HDM of type I is also analyzed.

4.3 Parametrization of gBGL models

The number of free parameters in the gBGL models is clearly lower than in the general 2HDM case. In this section, we are going to introduce a convenient parametrization based on projection operators.

4.3.1 Weak basis invariant projectors

Under a WB transformation we have

$$Q_L^0 \mapsto Q_L^{0\prime} = W_{\rm L} Q_L^0\,,\ d_R^0 \mapsto d_R^{0\prime} = W_{\rm d_R} d_R^0\,,\ u_R^0 \mapsto u_R^{0\prime} = W_{\rm u_R} u_R^0\,, \tag{4.12}$$

and

$$Y_{d,i} \mapsto Y'_{d,i} = W_{\rm L}^\dagger Y_{d,i} W_{\rm d_R}\,, \quad Y_{u,i} \mapsto Y'_{u,i} = W_{\rm L}^\dagger Y_{u,i} W_{\rm u_R}\,, \tag{4.13}$$

with $W_{\rm L}$, $W_{\rm d_R}$ and $W_{\rm u_R}$ unitary matrices.

If we now take the gBGL definition through projectors in eq. (4.7) for $Y_{d,i}$ and $Y_{u,i}$, and go to an arbitrary weak basis, we have

$$\begin{aligned} &W_{\rm L}^\dagger {\rm P}_3 W_{\rm L} W_{\rm L}^\dagger Y_{d,1} W_{\rm d_R} = 0\,, \qquad W_{\rm L}^\dagger {\rm P}_3 W_{\rm L} W_{\rm L}^\dagger Y_{d,2} W_{\rm d_R} = W_{\rm L}^\dagger Y_{d,2} W_{\rm d_R}\,, \\ &W_{\rm L}^\dagger {\rm P}_3 W_{\rm L} W_{\rm L}^\dagger Y_{u,1} W_{\rm u_R} = 0\,, \qquad W_{\rm L}^\dagger {\rm P}_3 W_{\rm L} W_{\rm L}^\dagger Y_{u,2} W_{\rm u_R} = W_{\rm L}^\dagger Y_{u,2} W_{\rm u_R}\,. \end{aligned} \tag{4.14}$$

These equations are valid for any weak basis. Introducing the projector

$$P_3^{[W_{\rm L}]} = W_{\rm L}^\dagger {\rm P}_3 W_{\rm L}\,, \tag{4.15}$$

we have

$$\begin{aligned} &P_3^{[W_{\rm L}]} Y'_{d,1} = 0\,, \qquad P_3^{[W_{\rm L}]} Y'_{d,2} = Y'_{d,2}\,, \\ &P_3^{[W_{\rm L}]} Y'_{u,1} = 0\,, \qquad P_3^{[W_{\rm L}]} Y'_{u,2} = Y'_{u,2}\,, \end{aligned} \tag{4.16}$$

for an arbitrary WB (from now on, we drop the primes). If we choose, for convenience,

$$W_{\rm L}^\dagger = \mathcal{U}_{u_L}^\dagger \mathcal{U}\,, \tag{4.17}$$

where $\mathcal{U}_{u_L}^\dagger$ appears in the usual bi-diagonalization $\mathcal{U}_{u_L}^\dagger {\rm M}_u^0 \mathcal{U}_{u_R} = {\rm M}_u$ (see section 4.3.3), then $\mathcal{U}$ is an arbitrary unitary matrix and we have a general WB invariant parametrization in terms of that arbitrary $\mathcal{U}$ and of $\mathcal{U}_{u_L}^\dagger$; eqs. (4.15) and (4.16) read

$$P_{\mathcal{U}3}^{[u_L]} = \mathcal{U}_{u_L} (\mathcal{U} {\rm P}_3 \mathcal{U}^\dagger) \mathcal{U}_{u_L}^\dagger\,, \tag{4.18}$$

and

$$\begin{aligned} &P_{\mathcal{U}3}^{[u_L]} Y_{d,1} = 0\,, \qquad P_{\mathcal{U}3}^{[u_L]} Y_{d,2} = Y_{d,2}\,, \\ &P_{\mathcal{U}3}^{[u_L]} Y_{u,1} = 0\,, \qquad P_{\mathcal{U}3}^{[u_L]} Y_{u,2} = Y_{u,2}\,. \end{aligned} \tag{4.19}$$

Notice that this $\mathcal{U}_{u_L}$ dependence reminds us of uBGL models. An alternative parametrization is obtained taking

$$W_{\rm L}^\dagger = \mathcal{U}_{d_L}\mathcal{U}' \,, \tag{4.20}$$

where in this case $\mathcal{U}_{d_L}^\dagger$ comes from the down mass matrix diagonalization $\mathcal{U}_{d_L}^\dagger \mathrm{M}_d^0 \mathcal{U}_{d_R} = \mathrm{M}_d$, with

$$P_{\mathcal{U}'3}^{[d_L]} = \mathcal{U}_{d_L}(\mathcal{U}'\mathrm{P}_3\mathcal{U}'^\dagger)\mathcal{U}_{d_L}^\dagger \,, \tag{4.21}$$

and

$$\begin{aligned} P_{\mathcal{U}'3}^{[d_L]} Y_{d,1} = 0 \,, \qquad P_{\mathcal{U}'3}^{[d_L]} Y_{d,2} = Y_{d,2} \,, \\ P_{\mathcal{U}'3}^{[d_L]} Y_{u,1} = 0 \,, \qquad P_{\mathcal{U}'3}^{[d_L]} Y_{u,2} = Y_{u,2} \,, \end{aligned} \tag{4.22}$$

where now the $\mathcal{U}_{d_L}$ dependence reminds us of dBGL models. Identifying eqs. (4.17) and (4.20),

$$W_{\rm L}^\dagger = \mathcal{U}_{u_L}\mathcal{U} = \mathcal{U}_{d_L}\mathcal{U}' \,, \tag{4.23}$$

and it is straightforward to conclude that one can use equivalently one or the other parametrization of the same model provided

$$V^\dagger = \mathcal{U}_{d_L}^\dagger \mathcal{U}_{u_L} = \mathcal{U}'\mathcal{U}^\dagger, \quad \text{i.e. } \mathcal{U}\mathcal{U}'^\dagger = V \,. \tag{4.24}$$

4.3.2 Weak basis covariant parametrization

We have in the general 2HDM[3]

$$\mathrm{N}_d^0 = -t_\beta \mathrm{M}_d^0 + (t_\beta + t_\beta^{-1})\frac{v}{\sqrt{2}} e^{i\theta} Y_{d,2} \,, \tag{4.25}$$

$$\mathrm{N}_u^0 = -t_\beta \mathrm{M}_u^0 + (t_\beta + t_\beta^{-1})\frac{v}{\sqrt{2}} e^{-i\theta} Y_{u,2} \,. \tag{4.26}$$

Assuming the existence of the projection operator $P_{X3}^{[q_L]}$ satisfying

$$P_{X3}^{[q_L]} Y_{d,1} = 0, \quad P_{X3}^{[q_L]} Y_{d,2} = Y_{d,2} \,, \tag{4.27}$$

$$P_{X3}^{[q_L]} Y_{u,1} = 0, \quad P_{X3}^{[q_L]} Y_{u,2} = Y_{u,2} \,, \tag{4.28}$$

[3]Note that eqs. (4.25)–(4.26) do not match with the expressions given in our paper [1]. The reason is that there is a difference of $\pi/2$ in the definition of the Higgs basis rotation in eq. (2.5).

with X and $P_{X3}^{[q_L]}$ to be specified later,

$$P_{X3}^{[q_L]}\mathrm{M}_d^0 = P_{X3}^{[q_L]}\frac{v}{\sqrt{2}}(c_\beta Y_{d,1} + e^{i\theta}s_\beta Y_{d,2}) = \frac{ve^{i\theta}}{\sqrt{2}}s_\beta P_{X3}^{[q_L]}Y_{d,2} = \frac{ve^{i\theta}}{\sqrt{2}}s_\beta Y_{d,2}\,, \tag{4.29}$$

$$P_{X3}^{[q_L]}\mathrm{M}_u^0 = P_{X3}^{[q_L]}\frac{v}{\sqrt{2}}(c_\beta Y_{u,1} + e^{-i\theta}s_\beta Y_{u,2}) = \frac{ve^{-i\theta}}{\sqrt{2}}s_\beta P_{X3}^{[q_L]}Y_{u,2} = \frac{ve^{-i\theta}}{\sqrt{2}}s_\beta Y_{u,2}\,. \tag{4.30}$$

Equations (4.25) and (4.26) can then be rewritten as the general WB covariant gBGL parametrization

$$\mathrm{N}_d^0 = \left[-t_\beta \mathbf{1} + (t_\beta + t_\beta^{-1})P_{X3}^{[q_L]}\right]\mathrm{M}_d^0\,, \tag{4.31}$$

$$\mathrm{N}_u^0 = \left[-t_\beta \mathbf{1} + (t_\beta + t_\beta^{-1})P_{X3}^{[q_L]}\right]\mathrm{M}_u^0\,. \tag{4.32}$$

We can choose the up parametrization for $P_{X3}^{[q_L]}$,

$$P_{X3}^{[q_L]} = P_{\mathcal{U}3}^{[u_L]} = \mathcal{U}_{u_L}(\mathcal{U}\mathrm{P}_3\mathcal{U}^\dagger)\mathcal{U}_{u_L}^\dagger\,, \tag{4.33}$$

or, equivalently, we can choose the down parametrization for $P_{X3}^{[q_L]}$,

$$P_{X3}^{[q_L]} = P_{\mathcal{U}'3}^{[d_L]} = \mathcal{U}_{d_L}(\mathcal{U}'\mathrm{P}_3\mathcal{U}'^\dagger)\mathcal{U}_{d_L}^\dagger\,, \tag{4.34}$$

with $V = \mathcal{U}\mathcal{U}'^\dagger$, to completely define the model. Let us analyze the details of these parametrizations, after we finally rotate the quark fields to the mass basis.

4.3.3 Parametrizations in the quark mass basis

Quark fields are rotated in the following manner

$$u_L^0 = \mathcal{U}_{u_L}u_L,\ u_R^0 = \mathcal{U}_{u_R}u_R,\ d_L^0 = \mathcal{U}_{d_L}d_L,\ d_R^0 = \mathcal{U}_{d_R}d_R, \tag{4.35}$$

with unitary $\mathcal{U}_{q_X}$ $(q = u, d,\ X = L, R)$, such that

$$\mathcal{U}_{u_L}^\dagger \mathrm{M}_u^0 \mathcal{U}_{u_R} = \mathrm{M}_u = \mathrm{diag}(m_u, m_c, m_t), \quad \mathcal{U}_{d_L}^\dagger \mathrm{M}_d^0 \mathcal{U}_{d_R} = \mathrm{M}_d = \mathrm{diag}(m_d, m_s, m_b). \tag{4.36}$$

The matrices N_u^0 and N_d^0 are transformed accordingly,

$$\mathrm{N}_u^0 \mapsto \mathrm{N}_u = \mathcal{U}_{u_L}^\dagger \mathrm{N}_u^0 \mathcal{U}_{u_R}, \quad \mathrm{N}_d^0 \mapsto \mathrm{N}_d = \mathcal{U}_{d_L}^\dagger \mathrm{N}_d^0 \mathcal{U}_{d_R}\,, \tag{4.37}$$

and, following eqs. (4.31)–(4.32) e ca write

$$\mathrm{N}_d = \left[-t_\beta \mathbf{1} + (t_\beta + t_\beta^{-1}) \mathcal{U}_{d_L}^\dagger P_{X3}^{[q_L]} \mathcal{U}_{d_L}\right] \mathrm{M}_d \,, \tag{4.38}$$

$$\mathrm{N}_u = \left[-t_\beta \mathbf{1} + (t_\beta + t_\beta^{-1}) \mathcal{U}_{u_L}^\dagger P_{X3}^{[q_L]} \mathcal{U}_{u_L}\right] \mathrm{M}_u \,. \tag{4.39}$$

If we choose the down parametrization in eq. (4.34), eqs. (4.38)–(4.39) give

$$\mathrm{N}_d = \left[-t_\beta \mathbf{1} + (t_\beta + t_\beta^{-1}) \mathcal{U}' \mathrm{P}_3 \mathcal{U}'^\dagger\right] \mathrm{M}_d \,, \tag{4.40}$$

$$\mathrm{N}_u = \left[-t_\beta \mathbf{1} + (t_\beta + t_\beta^{-1}) V \mathcal{U}' \mathrm{P}_3 \mathcal{U}'^\dagger V^\dagger\right] \mathrm{M}_u \,, \tag{4.41}$$

while, if we choose the up parametrization in eq. (4.33), eqs. (4.38)–(4.39) give

$$\mathrm{N}_d = \left[-t_\beta \mathbf{1} + (t_\beta + t_\beta^{-1}) V^\dagger \mathcal{U} \mathrm{P}_3 \mathcal{U}^\dagger V\right] \mathrm{M}_d \,, \tag{4.42}$$

$$\mathrm{N}_u = \left[-t_\beta \mathbf{1} + (t_\beta + t_\beta^{-1}) \mathcal{U} \mathrm{P}_3 \mathcal{U}^\dagger\right] \mathrm{M}_u \,. \tag{4.43}$$

Equations (4.40)–(4.41) and (4.42)–(4.43) are of course equivalent, since $V = \mathcal{U}\mathcal{U}'^\dagger$. At this point it is important to discuss a central question: it may appear that there is a large arbitrariness in the definition of the model since there is a completely arbitrary unitary matrix $\mathcal{U}$ involved in eqs. (4.42)–(4.43). Nevertheless, there is much less freedom since the quantities involving $\mathcal{U}$ are

$$[\mathcal{U} \mathrm{P}_3 \mathcal{U}^\dagger]_{ij} = \mathcal{U}_{i3} \mathcal{U}^*_{j3}, \tag{4.44}$$

that is, only the elements of the third column of $\mathcal{U}$, which form a unitary complex vector, are needed to define the model. To stress this fact, we introduce

$$\hat{n}_{[\mathrm{u}]i} \equiv \mathcal{U}_{i3}, \quad \text{and} \quad \hat{n}_{[\mathrm{d}]i} = \mathcal{U}'_{i3}, \quad \text{with} \quad \hat{n}_{[\mathrm{u}]j} = V_{ji} \hat{n}_{[\mathrm{d}]i} \,, \tag{4.45}$$

where the subindex $[u]$ or $[d]$ specifies the parametrization under consideration. The matrix elements of N_u and N_d in equations (4.38) and (4.39) can be written, explicitely,

$$[\mathrm{N}_d]_{ij} = -t_\beta \delta_{ij} m_{d_i} + (t_\beta + t_\beta^{-1}) \hat{n}_{[\mathrm{d}]i} \hat{n}^*_{[\mathrm{d}]j} m_{d_j} \,, \tag{4.46}$$

$$[\mathrm{N}_u]_{ij} = -t_\beta \delta_{ij} m_{u_i} + (t_\beta + t_\beta^{-1}) \hat{n}_{[\mathrm{u}]i} \hat{n}^*_{[\mathrm{u}]j} m_{u_j} \,. \tag{4.47}$$

Since $\hat{n}_{[\mathrm{u}]j} = V_{ji}\hat{n}_{[\mathrm{d}]i}$, one is free to rewrite eqs. (4.40)–(4.41) as

$$[\mathrm{N}_d]_{ij} = -t_\beta \delta_{ij} m_{d_i} + (t_\beta + t_\beta^{-1})\hat{n}_{[\mathrm{d}]i}\,\hat{n}^*_{[\mathrm{d}]j}\,m_{d_j}\,, \tag{4.48}$$

$$[\mathrm{N}_u]_{ij} = -t_\beta \delta_{ij} m_{u_i} + (t_\beta + t_\beta^{-1})V_{ia}V^*_{jb}\,\hat{n}_{[\mathrm{d}]a}\,\hat{n}^*_{[\mathrm{d}]b}\,m_{u_j}\,, \tag{4.49}$$

or eqs. (4.42)–(4.43) as

$$[\mathrm{N}_d]_{ij} = -t_\beta \delta_{ij} m_{d_i} + (t_\beta + t_\beta^{-1})\hat{n}_{[\mathrm{u}]a}\,\hat{n}^*_{[\mathrm{u}]b}V^*_{ai}V_{bj}\,m_{d_j}\,, \tag{4.50}$$

$$[\mathrm{N}_u]_{ij} = -t_\beta \delta_{ij} m_{u_i} + (t_\beta + t_\beta^{-1})\hat{n}_{[\mathrm{u}]i}\,\hat{n}^*_{[\mathrm{u}]j}\,m_{u_j}\,. \tag{4.51}$$

One can now identify easily all the usual BGL models with this parametrization. The notation is straightforward, for example, BGL model "s" corresponds to $\hat{s}$, and so on:

- dBGL models in the down parametrization,

$$\hat{d}_{[\mathrm{d}]} = \begin{pmatrix}1\\0\\0\end{pmatrix}, \quad \hat{s}_{[\mathrm{d}]} = \begin{pmatrix}0\\1\\0\end{pmatrix}, \quad \hat{b}_{[\mathrm{d}]} = \begin{pmatrix}0\\0\\1\end{pmatrix}. \tag{4.52}$$

- uBGL models in the up parametrization,

$$\hat{u}_{[\mathrm{u}]} = \begin{pmatrix}1\\0\\0\end{pmatrix}, \quad \hat{c}_{[\mathrm{u}]} = \begin{pmatrix}0\\1\\0\end{pmatrix}, \quad \hat{t}_{[\mathrm{u}]} = \begin{pmatrix}0\\0\\1\end{pmatrix}. \tag{4.53}$$

- dBGL models in the up parametrization,

$$\hat{d}_{[\mathrm{u}]} = \begin{pmatrix}V_{ud}\\V_{cd}\\V_{td}\end{pmatrix}, \quad \hat{s}_{[\mathrm{u}]} = \begin{pmatrix}V_{us}\\V_{cs}\\V_{ts}\end{pmatrix}, \quad \hat{b}_{[\mathrm{u}]} = \begin{pmatrix}V_{ub}\\V_{cb}\\V_{tb}\end{pmatrix}. \tag{4.54}$$

- uBGL models in the down parametrization,

$$\hat{u}_{[\mathrm{d}]} = \begin{pmatrix}V^*_{ud}\\V^*_{us}\\V^*_{ub}\end{pmatrix}, \quad \hat{c}_{[\mathrm{d}]} = \begin{pmatrix}V^*_{cd}\\V^*_{cs}\\V^*_{cb}\end{pmatrix}, \quad \hat{t}_{[\mathrm{d}]} = \begin{pmatrix}V^*_{td}\\V^*_{ts}\\V^*_{tb}\end{pmatrix}. \tag{4.55}$$

It is also possible to give a graphical description of the gBGL class of models, as shown in figure 4.1. Since a model is defined by a complex unitary vector $\hat{n}$, $|\hat{n}_1|^2 + |\hat{n}_2|^2 + |\hat{n}_3|^2 = 1$, and $(|\hat{n}_1|, |\hat{n}_2|, |\hat{n}_3|)$ is located on the sphere of unit radius (specifically, on an octant of that sphere). Furthermore, there are two

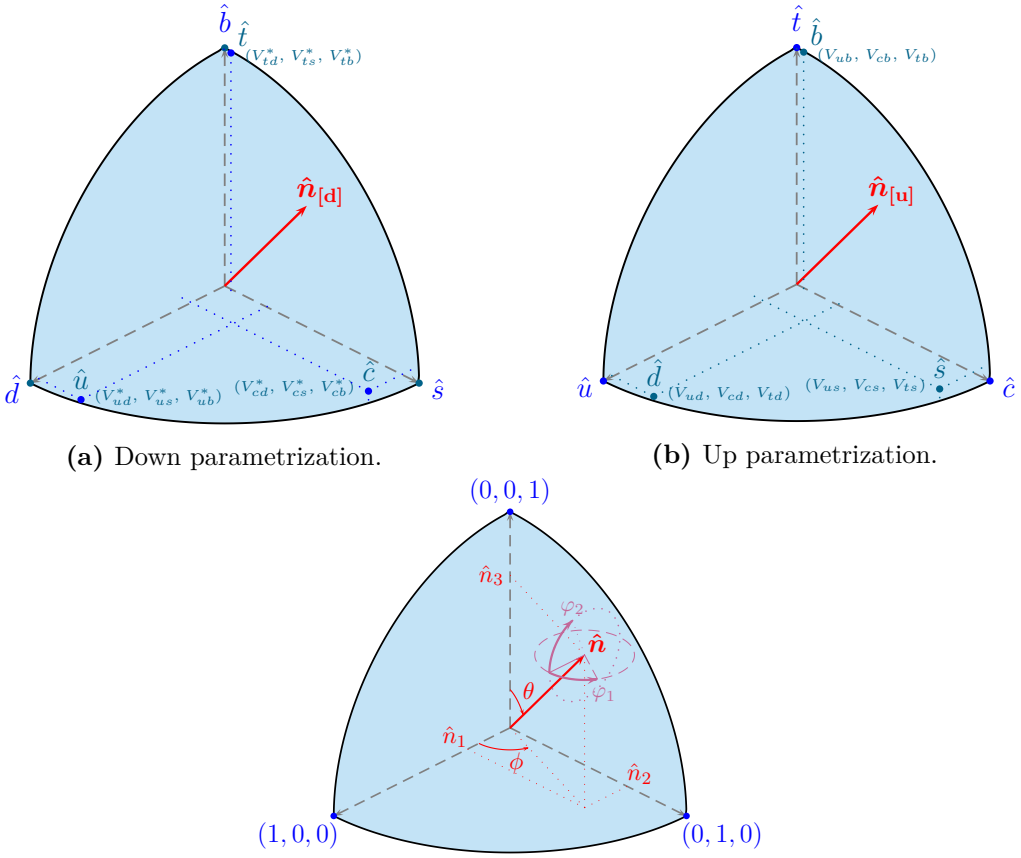

(a) Down parametrization.

(b) Up parametrization.

(c) Generic parametrization.

Figure 4.1: gBGL models.

physical complex phases, since one can readily see that $\hat{n}_i\,\hat{n}_j^*$ is unaffected by a global rephasing of $\hat{n}$, which can be used to remove one out of the three initial phases in the $\hat{n}$ components. This is illustrated in figure 4.1c, where no explicit reference to up, down or other parametrizations is made[4]. Figures 4.1a and 4.1b illustrate the situation for down and up parametrizations, including the usual BGL models in eqs. (4.52) to (4.55).

[4]Notice that one can trivially adopt spherical coordinates with, for example, $(|\hat{n}_1|, |\hat{n}_2|, |\hat{n}_3|) = (\sin\theta\cos\phi, \sin\theta\sin\phi, \cos\theta)$.

4.4 The scalar sector

The scalar potential, imposing invariance under $\Phi_2 \mapsto -\Phi_2$ in eq. (4.1), is

$$V(\Phi_1,\Phi_2) = \mu_{11}^2\Phi_1^\dagger\Phi_1 + \mu_{22}^2\Phi_2^\dagger\Phi_2 + \lambda_1(\Phi_1^\dagger\Phi_1)^2 + \lambda_2(\Phi_2^\dagger\Phi_2)^2 + 2\lambda_3(\Phi_1^\dagger\Phi_1)(\Phi_2^\dagger\Phi_2) + 2\lambda_4(\Phi_1^\dagger\Phi_2)(\Phi_2^\dagger\Phi_1) + [\lambda_5(\Phi_1^\dagger\Phi_2)^2 + \text{h.c.}]\,. \quad (4.56)$$

Obviously, this scalar potential coincides with the one in Glashow-Weinberg model [112], since in both cases a $\mathbb{Z}_2$ symmetry is introduced. In BGL models where instead of $\mathbb{Z}_2$ one uses a larger symmetry, namely $\mathbb{Z}_4$, the term in λ_5 is not $\mathbb{Z}_4$ invariant and therefore cannot be introduced. This leads to a global symmetry which upon spontaneous breaking would lead to a Golstone boson. This difficulty can be avoided by softly breaking the discrete symmetry through the addition of a term $(\mu_{12}^2\Phi_1^\dagger\Phi_2 + \text{h.c.})$. When this bilinear term is introduced, being $\lambda_5 \neq 0$, one can have either spontaneous [176] or explicit CP breaking in the scalar sector. This will become very important in chapter 5.

4.5 The intensity of SFCNC in gBGL

As it has been mentioned before, SFCNC are extremely constrained by experimental data, consequently we have to worry about their intensity in gBGL models. We also know that BGL models are Minimal Flavor Violating, which imply that SFCNC are controlled by the deviation of the CKM matrix V from $\mathbf{1}$, i.e. in the limit $V = \mathbf{1}$, there are no SFCNC in BGL models at tree level. However, gBGL models are no MFV and SFCNC are no longer controlled by the deviations of V from unity. The Yukawa couplings of gBGL models are given, following eq. (2.40), by

$$\mathscr{L}_{\text{h}\bar{\text{q}}\text{q}} = -\sum_{i,j=d,s,b} \text{h}\bar{d}_{L_i} a_{ij}^{h,d} d_{R_j} - \sum_{i,j=u,c,t} \text{h}\bar{u}_{L_i} a_{ij}^{h,u} u_{R_j}\,, \quad (4.57)$$

with

$$a_{ij}^{h,d} = \frac{1}{v}\left[s_{\alpha\beta}(\text{M}_d)_{ij} + c_{\alpha\beta}(\text{N}_d)_{ij}\right]\,,$$
$$a_{ij}^{h,u} = \frac{1}{v}\left[s_{\alpha\beta}(\text{M}_u)_{ij} + c_{\alpha\beta}(\text{N}_u)_{ij}\right]\,, \quad (4.58)$$

with N_q given in eqs. (4.46)–(4.47), that generically can be written

$$(\mathrm{N}_q)_{ij} = \left[-t_\beta \delta_{ij} + (t_\beta + t_\beta^{-1})\hat{n}_{[\mathrm{q}]i}\hat{n}^*_{[\mathrm{q}]j}\right] m_{q_j} \,. \tag{4.59}$$

So, the flavor changing intensities are controlled by N_q with the following factors.

- In an $q_{R_j} \to q_{L_i}$ and in $q_{L_i} \to q_{R_j}$ transitions there is a factor m_{q_j}/v. Notice that in $q_{R_i} \to q_{L_j}$ and in $q_{L_j} \to q_{R_i}$ transitions the factor is instead m_{q_i}/v. That is, in general, for a $q_j \to q_i$ vertex, there is a suppression factor given by the heaviest of the two quarks mass, $\max(m_{q_i}, m_{q_j})$. This suppression factor is a very relevant one except, obviously, for any transition where the top quark is present.

- A factor $c_{\alpha\beta}(t_\beta + t_\beta^{-1})$; from perturbative unitarity requirements on the scalar sector, is constrained to be at most one [143, 177–180]. Notice that in the limit $c_{\alpha\beta} \to 0$, the SFCNC associated to the standard Higgs h disappear, and the ones associated to the remaining scalars can be suppressed by making them heavier. Therefore, this is the quantity which, in a global approach, is bounded from above by Higgs mediated SFCNC processes.

- Finally, there is the factor $\hat{n}_{[\mathrm{q}]i}\hat{n}^*_{[\mathrm{q}]j}$, which ranges from 0 to 1/2 (which is only reached when only *one* transition is allowed). We remind that in BGL models, the analogous factor is $V_{iq}V^*_{jq}$. With the naive bounds on $c_{\alpha\beta}(t_\beta + t_\beta^{-1})$ from meson mixings in [143], one can compare and analyze how the suppression factors change in these new gBGL models. We collect the suppression factors for the different transitions in all BGL models in table 4.1 (with the corresponding power counting in Wolfenstein's parameter λ). One has to compare the maximum value of $|\hat{n}_{[\mathrm{q}]i}\hat{n}^*_{[\mathrm{q}]j}|_{\max} = 1/2$ with λ, which corresponds to the less suppressed transition in some BGL models. This means that the most stringent constraint on BGL models obtained in [143] for $|c_{\alpha\beta}(t_\beta + t_\beta^{-1})|$ should be reduced by a factor 2λ. In this way, taking into

Transition \ Model	d	s	b
$u \leftrightarrow c$	$V_{ud}V_{cd}^* \sim \lambda$	$V_{us}V_{cs}^* \sim \lambda$	$V_{ub}V_{cb}^* \sim \lambda^5$
$u \leftrightarrow t$	$V_{ud}V_{td}^* \sim \lambda^3$	$V_{us}V_{ts}^* \sim \lambda^3$	$V_{ub}V_{tb}^* \sim \lambda^3$
$c \leftrightarrow t$	$V_{cd}V_{td}^* \sim \lambda^4$	$V_{cs}V_{ts}^* \sim \lambda^2$	$V_{cb}V_{tb}^* \sim \lambda^2$
Transition \ Model	**u**	**c**	**t**
$d \leftrightarrow s$	$V_{ud}^*V_{us} \sim \lambda$	$V_{cd}^*V_{cs} \sim \lambda$	$V_{td}^*V_{ts} \sim \lambda^5$
$d \leftrightarrow b$	$V_{ud}^*V_{ub} \sim \lambda^3$	$V_{cd}^*V_{cb} \sim \lambda^3$	$V_{td}^*V_{tb} \sim \lambda^3$
$s \leftrightarrow b$	$V_{us}^*V_{ub} \sim \lambda^4$	$V_{cs}^*V_{cb} \sim \lambda^2$	$V_{ts}^*V_{tb} \sim \lambda^2$

Table 4.1: CKM suppression in SFCNC transitions in BGL models.

account the analysis of [143] and the constraints in [181], one can conclude that the gBGL models are safe, over the entire parameter space, provided

$$\left|c_{\alpha\beta}(t_\beta + t_\beta^{-1})\right| \leq 0.02\,. \tag{4.60}$$

This constraint arises from D^0–$\bar{D}^0$ mixing and it turns out to be more stringent than the K^0–$\bar{K}^0$ one. It is worth mentioning that in some regions of the parameter space, this constraint will be relaxed. For example, in all BGL models this constraint is much weaker as shown in reference [143], and in some of them $|c_{\alpha\beta}(t_\beta + t_\beta^{-1})|$ can span the entire theoretically allowed parameter space, arriving to values of order 1.

A final remark is related to the absence of the mass suppression factor on $t \leftrightarrow q$ transitions in gBGL models. In this case, the relevant bounds come from rare top decays $t \to \mathrm{h}u, \mathrm{h}c$, which give [143]

$$\mathrm{BR}(t \to \mathrm{h}q) = 0.13\,\frac{\left|\hat{n}_{[\mathrm{u}]q}\hat{n}^*_{[\mathrm{u}]t}\right|^2}{|V_{tb}|^2}\left(c_{\alpha\beta}(t_\beta + t_\beta^{-1})\right)^2\,. \tag{4.61}$$

The experimental data from ATLAS [182] and CMS [183] leads to the following constraint[5]

$$\left|c_{\alpha\beta}(t_\beta + t_\beta^{-1})\right| \leq 0.3\,, \tag{4.62}$$

[5]The experimental bounds, at the time when this model was presented, from ATLAS [184] and CMS [185, 186] yielded $\left|c_{\alpha\beta}(t_\beta + t_\beta^{-1})\right| \leq 0.4$

for the maximal value[6] $|\hat{n}_{[\mathrm{u}]q}\hat{n}^*_{[\mathrm{u}]t}| = 1/2$.

So we can conclude that SFCNC in the gBGL framework are not much larger that the ones produced by the BGL models. This is in spite of having simultaneously SFCNC in the up and in the down sectors. In the next sections we discuss other important differences.

4.6 Near the top and the bottom models

It is worth mention that BGL top and bottom models are the only renormalizable 2HDM that verify the MFV principle in any of the different versions one can find in the literature [138]. In this section we analyze in greater detail the properties of gBGL models that are "close" to these models, that is, that they depart from the top or bottom models by a "small amount". As we know, the SFCNC in the down and the up sectors of the top model arise from

$$(\mathrm{N}_d)_{ij} = (t_\beta + t_\beta^{-1})\,\hat{t}_{[\mathrm{d}]i}\hat{t}^*_{[\mathrm{d}]j}\,m_{d_j}\,, \qquad (\mathrm{N}_u)_{ij} = (t_\beta + t_\beta^{-1})\,\hat{t}_{[\mathrm{u}]i}\hat{t}^*_{[\mathrm{u}]j}\,m_{u_j}\,, \tag{4.63}$$

and, following eqs. (4.53)–(4.55), $\hat{t}_{[\mathrm{u}]}$ and $\hat{t}_{[\mathrm{d}]} = V^\dagger \hat{t}_{[\mathrm{u}]}$, are

$$\hat{t}_{[\mathrm{u}]} = \begin{pmatrix} 0 \\ 0 \\ 1 \end{pmatrix}, \quad \hat{t}_{[\mathrm{d}]} = \begin{pmatrix} V^*_{td} \\ V^*_{ts} \\ V^*_{tb} \end{pmatrix}. \tag{4.64}$$

It is clear that the BGL top model does not have SFCNC in the up sector. Let us now consider small deviations from $\hat{t}_{[\mathrm{d}]}$ near the top model parameterised in terms of a complex vector $\vec{\delta} = (\delta_d, \delta_s, \delta_b)$ (with the appropriate normalization):

$$\hat{t}_{[\mathrm{d}]} + \hat{\delta}t_{[\mathrm{d}]} \sim \begin{pmatrix} V^*_{td}(1+\delta_d) \\ V^*_{ts}(1+\delta_s) \\ V^*_{tb}(1+\delta_b) \end{pmatrix}. \tag{4.65}$$

The elements of $\hat{t}_{[\mathrm{d}]} + \hat{\delta}t_{[\mathrm{d}]}$ control the flavor structure of the New Physics contributions to K^0–$\bar{K}^0$, B^0_d–$\bar{B}^0_d$ and B^0_s–$\bar{B}^0_s$. In particular, the leading order contributions

[6] The maximal value of $|\hat{n}_{[\mathrm{u}]q}\hat{n}^*_{[\mathrm{u}]t}|$ cannot be obtained, obviously, for both $t \to \mathrm{h}u$ and $t \to \mathrm{h}c$ simultaneously.

to the different meson mixings M_{12} have the following form:

$$\begin{aligned} M_{12}[K^0] &\propto (V_{td}^* V_{ts})^2[1+2(\delta_s^*+\delta_d)]\,, \\ M_{12}[B_d^0] &\propto (V_{td}^* V_{tb})^2[1+2(\delta_b^*+\delta_d)]\,, \\ M_{12}[B_s^0] &\propto (V_{ts}^* V_{tb})^2[1+2(\delta_b^*+\delta_s)]\,. \end{aligned} \tag{4.66}$$

Therefore, taking into account the phases of the dominant terms $(V_{ti}^* V_{tj})^2$, we can conclude that these "near top" models will give the same contribution to meson mixings provided

$$\mathrm{Re}\,(\delta_d) \sim \mathrm{Re}\,(\delta_s) \sim \mathrm{Im}\,(\delta_s) \leq \mathcal{O}(\lambda^2), \text{ and } \mathrm{Im}\,(\delta_d) \sim \mathrm{Im}\,(\delta_b) \leq \mathcal{O}(\lambda^3)\,. \tag{4.67}$$

Notice that we are not stating that these models do not have any contribution to the meson mixings, the point is, rather, that these models are "like the top BGL" in the sense that they give the same contributions to K^0–$\bar{K}^0$, B_d^0–$\bar{B}_d^0$ and B_s^0–$\bar{B}_s^0$ mixings. The immediate question is then: do these models produce too strong SFCNC in the up sector, in particular in D^0–$\bar{D}^0$ or in top decays? SFCNC in the up sector are controlled by

$$\hat{t}_{[\mathrm{u}]} + \hat{\delta t}_{[\mathrm{u}]} = V^\dagger(\hat{t}_{[\mathrm{d}]} + \hat{\delta t}_{[\mathrm{d}]}) \sim \begin{pmatrix} \mathcal{O}(\lambda^5) \\ \delta_b V_{cb} V_{tb}^* \\ 1+\delta_b \end{pmatrix}. \tag{4.68}$$

It is clear that $M_{12}[D^0]$ will have a suppression given by

$$(\delta_b \lambda^5 V_{cb} V_{tb}^*)^2 \leq \lambda^{18}\,, \tag{4.69}$$

much smaller than any of the contributions in dBGL models.

To analyze $t \to \mathrm{h}c$ we have to compare the maximal value 1/4 of $\left|\hat{n}_{[\mathrm{u}]q}\hat{n}_{[\mathrm{u}]t}^*\right|^2$ in eq. (4.61) with the value obtained in the present case, $\left|(1+\delta_b)\delta_b V_{cb} V_{tb}^*\right|^2 \sim \mathcal{O}(\lambda^8)$. The conclusion is evident in the whole parameter space: these models will produce $t \to \mathrm{h}c$ still below the actual experimental bounds. The same conclusion applies to $t \to \mathrm{h}u$. In the next section we will see that these models can depart in a sizable way from the top BGL model in different physical observables.

The bottom dBGL model is specified by $\hat{b}$ (eqs. (4.52) and (4.54)):

$$\hat{b}_{[\mathrm{d}]} = \begin{pmatrix} 0 \\ 0 \\ 1 \end{pmatrix}, \quad \hat{b}_{[\mathrm{u}]} = \begin{pmatrix} V_{ub} \\ V_{cb} \\ V_{tb} \end{pmatrix}. \tag{4.70}$$

This model generates SFCNC in the up sector, and in particular it contributes to D^0–$\bar{D}^0$ mixing but not to K^0–$\bar{K}^0$, B_d^0–$\bar{B}_d^0$ and B_s^0–$\bar{B}_s^0$; gBGL models close to the $\hat{b}$ model that keep its essential properties are obtained with

$$\hat{b}_{[\mathrm{u}]} + \hat{\delta b}_{[\mathrm{u}]} \sim \begin{pmatrix} V_{ub}(1+\delta_u) \\ V_{cb}(1+\delta_c) \\ V_{tb}(1+\delta_t) \end{pmatrix}, \tag{4.71}$$

where

$$\delta_u \sim \delta_c \sim \delta_t \leq \mathcal{O}(\lambda^2), \tag{4.72}$$

as before. To see what happens with the important constraints in the down sector, we show, as before, that $\hat{b}_{[\mathrm{d}]} + \hat{\delta b}_{[\mathrm{d}]} = V(\hat{b}_{[\mathrm{u}]} + \hat{\delta b}_{[\mathrm{u}]})$,

$$\hat{b}_{[\mathrm{d}]} + \hat{\delta b}_{[\mathrm{d}]} \sim \begin{pmatrix} V_{td}^* V_{tb}(\delta_t - \delta_c) + V_{ud}^* V_{ub}(\delta_u - \delta_c) \\ V_{ts}^* V_{tb}(\delta_t - \delta_c) \\ |V_{tb}|^2(1+\delta_t) \end{pmatrix}, \tag{4.73}$$

is the relevant quantity. With values as in eq. (4.72), it turns out that the contributions to the mixing in the down sector are much smaller than in any uBGL model. Nevertheless, we will also see, in the next section, that there are important differences with respect to the bottom dBGL model in other observables while considering the same kind of parameter values close to the bottom model.

4.7 Baryon Asymmetry of the Universe

4.7.1 The leading gBGL contribution

The presence of additional sources of flavor and CP violation in the gBGL models can enhance the contribution to the Baryonic Asymmetry of the Universe (BAU) with respect to SM expectations. Having N_u and N_d in addition to M_u and M_d, a weak basis invariant with a non-zero imaginary part already arises [187] at the 4$^{\mathrm{th}}$ order[7][8]:

$$\mathrm{Im}\left(\mathrm{Tr}\left\{\mathrm{N}_d^0 \mathrm{M}_d^{0\dagger} \mathrm{M}_u^0 \mathrm{M}_u^{0\dagger}\right\}\right). \tag{4.74}$$

[7] To be compared with the 12$^{\mathrm{th}}$ order usual one, $-\frac{i}{6}\mathrm{Tr}\left\{[\mathrm{M}_u\mathrm{M}_u^\dagger, \mathrm{M}_d\mathrm{M}_d^\dagger]^3\right\}$ [188].

[8] The rephasing invariance in the Higgs sector [111] imposes that the complete invariant should include the $H_2^\dagger H_1$ coefficient in the Lagrangian: $(\mu_{11}^2 - \mu_{22}^2)s_\beta c_\beta$ [109]. This does not introduce new phases.

Considering N_d^0 in eq. (4.31),

$$\mathrm{Im}\left(\mathrm{Tr}\left\{\mathrm{N}_d^0\mathrm{M}_d^{0\dagger}\mathrm{M}_u^0\mathrm{M}_u^{0\dagger}\right\}\right) = (t_\beta + t_\beta^{-1})\mathrm{Im}\left(\mathrm{Tr}\left\{P_{X3}^{[q_L]}\mathrm{M}_d^0\mathrm{M}_d^{0\dagger}\mathrm{M}_u^0\mathrm{M}_u^{0\dagger}\right\}\right). \tag{4.75}$$

For $P_{X3}^{[q_L]} = P_{\mathcal{U}'3}^{[d_L]}$, that is, in the down parametrization, eq. (4.34),

$$(t_\beta + t_\beta^{-1})\mathrm{Im}\left(\mathrm{Tr}\left\{\mathcal{U}_{d_L}(\mathcal{U}'P_3\mathcal{U}'^\dagger)\mathcal{U}_{d_L}^\dagger\mathcal{U}_{d_L}\mathrm{M}_d\mathrm{M}_d^\dagger\mathcal{U}_{d_L}^\dagger\mathcal{U}_{u_L}\mathrm{M}_u\mathrm{M}_u^\dagger\mathcal{U}_{u_L}^\dagger\right\}\right) = (t_\beta + t_\beta^{-1})\mathrm{Im}\left(\mathrm{Tr}\left\{(\mathcal{U}'P_3\mathcal{U}'^\dagger)\mathrm{M}_d\mathrm{M}_d^\dagger V^\dagger\mathrm{M}_u\mathrm{M}_u^\dagger V\right\}\right). \tag{4.76}$$

Notice that, according to eq. (4.36), $\mathrm{M}_u\mathrm{M}_u^\dagger = \mathrm{diag}(m_{u_j}^2) = \mathrm{diag}(m_u^2, m_c^2, m_t^2)$, $\mathrm{M}_d\mathrm{M}_d^\dagger = \mathrm{diag}(m_{d_j}^2) = \mathrm{diag}(m_d^2, m_s^2, m_b^2)$. Following eq. (4.45),

$$(\mathcal{U}'P_3\mathcal{U}'^\dagger)_{ij} = \hat{n}_{[\mathrm{d}]i}\hat{n}_{[\mathrm{d}]j}^*, \tag{4.77}$$

and thus

$$\mathrm{Tr}\left\{(\mathcal{U}'P_3\mathcal{U}'^\dagger)\mathrm{M}_d\mathrm{M}_d^\dagger V^\dagger\mathrm{M}_u\mathrm{M}_u^\dagger V\right\} = \sum_{i,j,k} m_{d_j}^2 m_{u_k}^2 \hat{n}_{[\mathrm{d}]i}\hat{n}_{[\mathrm{d}]j}^* V_{ki}V_{kj}^*, \tag{4.78}$$

to obtain, finally

$$\mathrm{Im}\left(\mathrm{Tr}\left\{\mathrm{N}_d^0\mathrm{M}_d^{0\dagger}\mathrm{M}_u^0\mathrm{M}_u^{0\dagger}\right\}\right) = \frac{i}{2}(t_\beta + t_\beta^{-1})\sum_{i,j,k}(m_{d_i}^2 - m_{d_j}^2)m_{u_k}^2\hat{n}_{[\mathrm{d}]i}\hat{n}_{[\mathrm{d}]j}^* V_{ki}V_{kj}^*. \tag{4.79}$$

Although we have used the down parametrization (from eq. (4.76) onwards) for the later discussion the results obtained if the up parametrization is used instead are completely analogous. In eq. (4.79) we can see that the contributions to the BAU vanishes for $i = j$ what means that SFCNC must exist . This relation between the SFCNC and CP violation will be the center of the discussion in chapter 5.

In order to estimate the enhancement in the BAU due to $\mathrm{Im}\left(\mathrm{Tr}\left\{\mathrm{N}_d^0\mathrm{M}_d^{0\dagger}\mathrm{M}_u^0\mathrm{M}_u^{0\dagger}\right\}\right)$, let us first retain only potentially leading contributions in terms of masses and powers of the Wolfenstein parameter λ [33],

$$\begin{aligned}\mathrm{Im}\left(\mathrm{Tr}\left\{\mathrm{N}_d^0\mathrm{M}_d^{0\dagger}\mathrm{M}_u^0\mathrm{M}_u^{0\dagger}\right\}\right) \simeq \frac{i}{2}(t_\beta + t_\beta^{-1})\Big\{&\hat{n}_{[\mathrm{d}]2}\hat{n}_{[\mathrm{d}]1}^* m_s^2\left[m_c^2V_{cs}V_{cd}^* + m_t^2V_{ts}V_{td}^*\right] \\ &+ \hat{n}_{[\mathrm{d}]3}\hat{n}_{[\mathrm{d}]1}^* m_b^2\left[m_c^2V_{cb}V_{cd}^* + m_t^2V_{tb}V_{td}^*\right] + \hat{n}_{[\mathrm{d}]3}\hat{n}_{[\mathrm{d}]2}^* m_b^2\left[m_c^2V_{cb}V_{cs}^* + m_t^2V_{tb}V_{ts}^*\right]\Big\},\end{aligned} \tag{4.80}$$

that is,

$$\mathrm{Im}\left(\mathrm{Tr}\left\{\mathrm{N}_d^0\mathrm{M}_d^{0\dagger}\mathrm{M}_u^0\mathrm{M}_u^{0\dagger}\right\}\right) \sim i(t_\beta + t_\beta^{-1})\Big\{\hat{n}_{[\mathrm{d}]2}\hat{n}^*_{[\mathrm{d}]1} m_s^2\left[m_c^2\lambda + m_t^2\lambda^5\right] + \hat{n}_{[\mathrm{d}]3}\hat{n}^*_{[\mathrm{d}]1} m_b^2\left[m_c^2\lambda^3 + m_t^2\lambda^3\right] + \hat{n}_{[\mathrm{d}]3}\hat{n}^*_{[\mathrm{d}]2} m_b^2\left[m_c^2\lambda^2 + m_t^2\lambda^2\right]\Big\}. \quad (4.81)$$

In the SM, the BAU is proportional to [189, 190]

$$\mathrm{BAU}_{\mathrm{SM}} \sim \frac{m_t^4 m_b^4 m_c^2 m_s^2}{E^{12}}\, J\,, \quad (4.82)$$

where J is the rephasing invariant imaginary part of the CKM quartets [191], $J = \mathrm{Im}\left(V_{cs}^* V_{ts} V_{tb}^* V_{cb}\right) \simeq 3\times 10^{-5}$ and $E \sim 100$ GeV an energy of the order of the electroweak scale one. In eq. (4.81), we have contributions like the last one, giving

$$\mathrm{BAU}_{\mathrm{gBGL}} \sim (t_\beta + t_\beta^{-1})\frac{m_t^2 m_b^2}{E^4}\mathrm{Im}\left(\hat{n}_{[\mathrm{d}]3}\hat{n}^*_{[\mathrm{d}]2} V_{tb} V_{ts}^*\right). \quad (4.83)$$

This simple enhancement estimate with respect to eq. (4.82), in terms of $\alpha = \arg(\hat{n}_{[\mathrm{d}]3}\hat{n}^*_{[\mathrm{d}]2} V_{tb} V_{ts}^*)$ and $\left|\hat{n}_{[\mathrm{d}]3}\hat{n}^*_{[\mathrm{d}]2}\right|$ (which has a maximal value of 1/2), is:

$$\frac{\mathrm{BAU}_{\mathrm{gBGL}}}{\mathrm{BAU}_{\mathrm{SM}}} \sim (t_\beta + t_\beta^{-1})\left|\hat{n}_{[\mathrm{d}]3}\hat{n}^*_{[\mathrm{d}]2}\right|\sin\alpha\,\frac{|V_{ts}|}{J}\frac{E^8}{m_t^2 m_b^2 m_c^2 m_s^2} \sim 10^{16}(t_\beta + t_\beta^{-1})\left|\hat{n}_{[\mathrm{d}]3}\hat{n}^*_{[\mathrm{d}]2}\right|\sin\alpha\,, \quad (4.84)$$

showing that there is margin for substantial enhancement of the BAU with respect to the SM, and with respect to BGL models too [187].

4.7.2 The vanishing BGL limits

In BGL models, the previous contribution is vanishing: let us explicitely check this known result [187]. For dBGL models, with $\hat{n}_{\mathrm{d}}$ in eq. (4.52), only one component is non-vanishing and $\mathrm{Im}\left(\mathrm{Tr}\left\{\mathrm{N}_d^0\mathrm{M}_d^{0\dagger}\mathrm{M}_u^0\mathrm{M}_u^{0\dagger}\right\}\right) = 0$. The situation is slightly more involved for uBGL models. From eq. (4.55), for an uBGL model of type q, $\hat{n}_{[\mathrm{d}]i} = V_{qi}^*$. Then, going back to eq. (4.78),

$$\mathrm{Tr}\left\{(\mathcal{U}' P_3 \mathcal{U}'^\dagger)\mathrm{M}_d\mathrm{M}_d^\dagger V^\dagger \mathrm{M}_u\mathrm{M}_u^\dagger V\right\} = \sum_{i,j,k} m_{d_j}^2 m_{u_k}^2 V_{qi}^* V_{qj} V_{ki} V_{kj}^*\,, \quad (\text{uBGL } q)\,. \quad (4.85)$$

Since, from unitarity of V, $\sum_i V_{qi}^* V_{ki} = \delta_{qk}$, eq. (4.85) gives

$$\mathrm{Tr}\left\{(\mathcal{U}' P_3 \mathcal{U}'^\dagger)\mathrm{M}_d\mathrm{M}_d^\dagger V^\dagger \mathrm{M}_u\mathrm{M}_u^\dagger V\right\} = \sum_j m_{d_j}^2 m_{u_q}^2 |V_{qj}|^2\,, \quad (\text{uBGL } q)\,, \quad (4.86)$$

and thus $\mathrm{Im}\left(\mathrm{Tr}\left\{\mathrm{N}_d^0\mathrm{M}_d^{0\dagger}\mathrm{M}_u^0\mathrm{M}_u^{0\dagger}\right\}\right) = 0$.

4.7.3 Rephasing invariance

Although we have already mentioned that there are only two physical phases in $\hat{n}_{[\mathrm{d}]}$ or $\hat{n}_{[\mathrm{u}]}$, it is important to check that the invariant in eq. (4.79) is, at it should, invariant under individual rephasings of the different quark fields:

$$\begin{aligned} &d \mapsto e^{i\varphi_1} d, \qquad\qquad s \mapsto e^{i\varphi_2} s, \quad b \mapsto e^{i\varphi_3} b, \\ &V_{qd} \mapsto e^{i\varphi_1} V_{qd}, \quad V_{qs} \mapsto e^{i\varphi_2} V_{qs}, \quad V_{qb} \mapsto e^{i\varphi_3} V_{qb}\,. \end{aligned} \tag{4.87}$$

The origin of the rephasing of the CKM matrix is straightforward: since $V = \mathcal{U}_{u_L}^\dagger \mathcal{U}_{d_L}$, the rephasing of the down quarks corresponds to

$$\mathcal{U}_{d_L} \mapsto \mathcal{U}_{d_L} \begin{pmatrix} e^{i\varphi_1} & 0 & 0 \\ 0 & e^{i\varphi_2} & 0 \\ 0 & 0 & e^{i\varphi_3} \end{pmatrix}. \tag{4.88}$$

Then, since in eq. (4.76) $P_{\mathcal{U}'3}^{[d_L]} = \mathcal{U}_{d_L}(\mathcal{U}' P_3 \mathcal{U}'^\dagger)\mathcal{U}_{d_L}^\dagger$,

$$\mathcal{U}' \mapsto \begin{pmatrix} e^{-i\varphi_1} & 0 & 0 \\ 0 & e^{-i\varphi_2} & 0 \\ 0 & 0 & e^{-i\varphi_3} \end{pmatrix} \mathcal{U}', \tag{4.89}$$

to keep $\mathcal{U}_{d_L}\mathcal{U}'$ invariant; as a consequence, under the rephasing in eq. (4.87),

$$\hat{n}_{[\mathrm{d}]j} \mapsto e^{-i\varphi_j} \hat{n}_{[\mathrm{d}]j}\,, \tag{4.90}$$

and eq. (4.79) is clearly rephasing invariant.

4.7.4 Enhancements in models near the top and the bottom models

The BAU generated in the top BGL model is proportional to [187]

$$\begin{aligned} &\mathrm{Im}\left(\mathrm{Tr}\left\{\mathrm{M}_d \mathrm{N}_d^\dagger \mathrm{M}_d \mathrm{M}_d^\dagger \mathrm{M}_u \mathrm{M}_u^\dagger \mathrm{M}_d \mathrm{M}_d^\dagger\right\}\right) \\ &\quad = -(t_\beta + t_\beta^{-1})(m_b^2 - m_s^2)(m_b^2 - m_d^2)(m_s^2 - m_d^2)(m_c^2 - m_u^2)\mathrm{Im}\left(V_{cs}^* V_{ts} V_{tb}^* V_{cb}\right)\,, \end{aligned} \tag{4.91}$$

in such a way that the ratio to the SM BAU is, for $E \sim 100$ GeV,

$$\frac{\mathrm{BAU}_{\mathrm{BGL-t}}}{\mathrm{BAU}_{\mathrm{SM}}} = (t_\beta + t_\beta^{-1})\frac{E^4}{m_t^4} \sim 1\,. \tag{4.92}$$

Therefore, as far as CP violation is concerned, the top model suffers the same problem as the SM in not being able to generate sufficient BAU. There is no enhancement in the top BGL 2HDM. We can now consider a small departure from the top BGL model as in eq. (4.65) and apply it to eq. (4.84). With

$$\hat{n}^*_{[\mathrm{d}]3} \sim V^*_{tb}(1+\delta_b)\,, \quad \hat{n}^*_{[\mathrm{d}]2} \sim V_{ts}(1+\delta^*_s)\,, \tag{4.93}$$

$$\mathrm{Im}\left(\hat{n}^*_{[\mathrm{d}]2}\hat{n}^*_{[\mathrm{d}]3}V_{tb}V^*_{ts}\right) \sim |V_{ts}|^2\mathrm{Im}\left(\delta_b+\delta^*_s\right)\,, \tag{4.94}$$

and eq. (4.65) gives

$$\frac{\mathrm{BAU}_{\text{near t}}}{\mathrm{BAU}_{\mathrm{SM}}} = 10^{16}(t_\beta + t_\beta^{-1})|V_{ts}|\mathrm{Im}\left(\delta_b+\delta^*_s\right)\,, \tag{4.95}$$

that can produce an enhancement as large as 10^{12}. Even if we are close to a top BGL model we find that, contrary to what happens with top model itself, there can be enough CP violation in this class of models to generate the BAU. In an analogous way, the BAU generated in the bottom BGL model is proportional to

$$\begin{aligned}&\mathrm{Im}\left(\mathrm{Tr}\left\{\mathrm{M}_u\mathrm{N}_u^\dagger\mathrm{M}_u\mathrm{M}_u^\dagger\mathrm{M}_d\mathrm{M}_d^\dagger\mathrm{M}_u\mathrm{M}_u^\dagger\right\}\right)\\ &\quad = -(t_\beta+t_\beta^{-1})(m_t^2-m_c^2)(m_t^2-m_u^2)(m_c^2-m_u^2)(m_s^2-m_d^2)\mathrm{Im}\left(V^*_{cs}V_{ts}V^*_{tb}V_{cb}\right)\,,\end{aligned} \tag{4.96}$$

and the ratio to the SM BAU, for $E \sim 100$ GeV, is

$$\frac{\mathrm{BAU}_{\text{BGL-b}}}{\mathrm{BAU}_{\mathrm{SM}}} = (t_\beta + t_\beta^{-1})\frac{E^4}{m_b^4} \sim 10^5\,. \tag{4.97}$$

In a pure bottom model there is still not enough CP violation – coming from the Yukawa sector – to generate the BAU. But, if we depart from an exact bottom BGL model in the manner explained in eq. (4.71), with

$$\hat{n}_{[\mathrm{d}]3} \sim |V_{tb}|^2(1+\delta_t)\,, \quad \hat{n}^*_{[\mathrm{d}]2} \sim V_{ts}V^*_{tb}(\delta^*_t-\delta^*_c)\,, \tag{4.98}$$

then

$$\mathrm{Im}\left(\hat{n}_{[\mathrm{d}]3}\hat{n}^*_{[\mathrm{d}]2}V_{tb}V^*_{ts}\right) \sim |V_{tb}|^4|V_{ts}|^2\mathrm{Im}\left(\delta^*_t-\delta^*_c\right)\,, \tag{4.99}$$

and we obtain, for the models near the bottom BGL one,

$$\frac{\mathrm{BAU}_{\text{near b}}}{\mathrm{BAU}_{\mathrm{SM}}} = 10^{16}(t_\beta + t_\beta^{-1})|V_{ts}|\mathrm{Im}\left(\delta^*_t-\delta^*_c\right)\,, \tag{4.100}$$

that is, a potential enhancement of 10^{13} with respect to the SM.

–I feel like spring after winter, and sun on the leaves; and like trumpets and harps and all the songs I have ever heard!

— SAMwise Gamgee, *The Lord of the Rings*, J. R. R. Tolkien

5

The framework for a common origin of $\delta_{\rm CKM}$ and $\delta_{\rm PMNS}$

In this chapter we study the possibility of having a relation between CP violation in the quark and lepton sectors, parametrized by the phases $\delta_{\rm CKM}$ and $\delta_{\rm PMNS}$, respectively, of the CKM [29, 30] and PMNS [31, 32] mixing matrices. This question is specially important in view of the efforts to detect leptonic CP violation in neutrino experiments such as Dune, T2K and Nova [192–194]. At present, there is solid experimental evidence that CKM is complex, even if one allows for the presence of New Physics contributing to CP violation [105, 195].

The fact that CKM is complex does not imply that CP violation is violated at the Lagrangian level through complex Yukawa couplings. Indeed it has been pointed out [196] that one may have a vacuum induced CP violation generating a complex CKM matrix in agreement with experiment. If one considers an extension of the Standard Model with non-vanishing neutrino masses and assumes that the origin of CP violation is the presence of complex Yukawa couplings, then there is no relation between $\delta_{\rm CKM}$ and $\delta_{\rm PMNS}$. This just reflects the fact that in the SM the lepton and the quark Yukawa couplings are completely independent quantities. If one wants to obtain a relation between $\delta_{\rm CKM}$ and $\delta_{\rm PMNS}$, an interesting possibility is to assume that CP is spontaneously broken, with the vacuum phase generating both the phase

in the quark and in the lepton sectors. In this section, we consider the extension to the leptonic sector of a previously proposed viable minimal model [196] where the Lagrangian respects CP invariance but the vacuum is CP violating, with a complex phase which generates a complex CKM matrix. The model consists of a generalized Branco-Grimus-Lavoura model [1, 133, 138, 140] with a flavored $\mathbb{Z}_2$ symmetry.

It was shown in Ref. [196] that there is a profound connection between the possibility of generating a complex CKM matrix and the existence of tree level Scalar Flavor Changing Neutral Couplings both in the up and down quark sectors. The same correlation also occurs when one extends the model to the leptonic sector. In order for $\delta_{\rm PMNS} \neq 0$ to be generated one has to have SFCNC both in the charged lepton and neutrino sectors. The fact that SFCNC necessarily arise in the class of models which we are considering is both an obstacle and a blessing. It is an obstacle because one has to analyze which models are able to conform to the strict experimental limits on SFCNC in the quark and lepton sectors. It is a blessing because the class of models we are considering are falsifiable in the sense that they imply SFCNC at a level which can be probed at different experiments.

The chapter is organized as follows. In the next section we present the model, including the quark and lepton sectors. In section 5.2 we analyze how $\delta_{\rm CKM}$ and $\delta_{\rm PMNS}$ are generated. In section 5.3 we analyze how CP violation requires the presence of SFCNC. Section 5.4 is dedicated to a study of a general relation between $\delta_{\rm CKM}$ and $\delta_{\rm PMNS}$. In section 5.5 we present simplified models incorporating Minimal Flavor Violation [136, 197] and the connection to SFCNC; a specific model is analyzed in detail, including the prediction of $\delta_{\rm PMNS}$ arising in this subclass of models.

5.1 The model

The gBGL model studied in chapter 4 provides the required features in order to achieve our goal, i.e. to relate the CKM and PMNS complex phases. The fact that gBGL models contain SFCNC in both the up and the down sector plays a key role here. The only difference here with respect to what we have studied in the previous chapter resides in the scalar potential since we will require it to

spontaneously break CP while the scalar potential in eq. (4.56) is CP conserving. As we saw in chapter 2, the Yukawa sector of the most general 2HDM, in the case of Dirac neutrinos, can be written as

$$\begin{aligned}-\mathscr{L}_{\rm Y} = &-\bar{Q}^0_L\left(\Phi_1 Y_{d,1}+\Phi_2 Y_{d,2}\right)d^0_R-\bar{Q}^0_L\left(\tilde{\Phi}_1 Y_{u,1}+\tilde{\Phi}_2 Y_{u,2}\right)u^0_R\\ &-\bar{L}^0_L\left(\Phi_1 Y_{\ell,1}+\Phi_2 Y_{\ell,2}\right)\ell^0_R-\bar{L}^0_L\left(\Phi_1 Y_{\nu,1}+\Phi_2 Y_{\nu,2}\right)\nu^0_R+\text{h.c.}\,.\end{aligned} \tag{2.26}$$

Here, we extend the model presented in reference [196], where the CKM phase was generated from the vacuum phase, to the leptonic sector. The model is enforced by a $\mathbb{Z}_2$ symmetry, both in the quark and leptonic sectors. The fields Φ_2, $Q^0_{L_3}$ and $L^0_{L_3}$ are odd under $\mathbb{Z}_2$, the rest of the fields are even under $\mathbb{Z}_2$. This symmetry was presented in chapter 4 (see eq. (4.1)) since it gives rise to the so-called gBGL[1] textures [1] for the original Yukawa coupling matrices $Y_{f,i}$:

$$Y_{d,1}\sim Y_{u,1}\sim Y_{\ell,1}\sim Y_{\nu,1}\sim\begin{pmatrix}\times&\times&\times\\ \times&\times&\times\\ 0&0&0\end{pmatrix}, \tag{5.1}$$

$$Y_{d,2}\sim Y_{u,2}\sim Y_{\ell,2}\sim Y_{\nu,2}\sim\begin{pmatrix}0&0&0\\ 0&0&0\\ \times&\times&\times\end{pmatrix}, \tag{5.2}$$

with $\times$ denoting generic entries.

The structure of the matrices is such that $Y_{f,2}=\mathrm{P}_3 Y_{f,2}$ and $Y_{f,1}=(\mathbf{1}-\mathrm{P}_3)\,Y_{f,1}$ where P_3 is the projector in eq. (4.6) what leads to the most relevant property which is the following:

$$\mathrm{N}^0_f=\left[-t_\beta\mathbf{1}+\left(t_\beta+t_\beta^{-1}\right)\mathrm{P}_3\right]\mathrm{M}^0_f\,. \tag{5.3}$$

Note that even if N^0_f are proportional to M^0_f, this proportionality involves a diagonal matrix different from the identity. This means that in general it will not be possible to bi-diagonalize both matrices simultaneously. The matrices N^0_f control the scalar mediated flavor changing neutral couplings.

[1] In chapter 4 we limited ourselves to the quark sector, here the $\mathbb{Z}_2$ symmetry is also applied to the leptonic fields.

Regarding the scalar sector, the scalar potential[2] has the following form

$$V(\Phi_1,\Phi_2) = \mu_{11}^2\Phi_1^\dagger\Phi_1 + \mu_{22}^2\Phi_2^\dagger\Phi_2 + \left(\mu_{12}^2\Phi_1^\dagger\Phi_2 + \text{h.c.}\right) + \lambda_1(\Phi_1^\dagger\Phi_1)^2 + \lambda_2(\Phi_2^\dagger\Phi_2)^2 + 2\lambda_3(\Phi_1^\dagger\Phi_1)(\Phi_2^\dagger\Phi_2) + 2\lambda_4(\Phi_1^\dagger\Phi_2)(\Phi_2^\dagger\Phi_1) + \left(\lambda_5(\Phi_1^\dagger\Phi_2)^2 + \text{h.c.}\right). \quad (5.4)$$

As we discussed in section 4.4 when the bilinear term $\mu_{12}^2\left(\Phi_1^\dagger\Phi_2 + \Phi_2^\dagger\Phi_1\right)$ is introduced into scalar potential in eq. (4.56), and being $\lambda_5 \neq 0$, one can have either spontaneous [176] or explicit CP breaking in the scalar sector. This is going to play a key role in the following since the complex phase generated at the spontaneous symmetry breaking will be the responsible of generating the mixing matrices phases. Even with μ_{12}^2, $\lambda_5 \in \mathbb{R}$, which produces a CP invariant potential, CP can be violated through the vacuum phase. For further details concerning the scalar sector see Ref. [196].

5.2 Generation of CP violating CKM and PMNS matrices

It is clear that the global phase θ_1 in the M_f^0 and N_f^0 in eqs. (2.29)–(2.30) can be rephased away by redefining the phases of the H_i fields or of the right handed fermion fields, and thus we set $\theta_1 = 0$ from now on without loss of generality. Note also that invariance under CP of the entire Lagrangian implies that

$$Y_{f,i} = Y_{f,i}^* . \quad (5.5)$$

As shown in reference [196], taking into account the reality condition in eq. (5.5) and the position of the irremovable phase θ in the textures in eqs. (5.1)-(5.2), the mass matrices can be factorized as

$$\mathrm{M}_f^0 = \begin{pmatrix} 1 & 0 & 0 \\ 0 & 1 & 0 \\ 0 & 0 & e^{i\sigma_f} \end{pmatrix} \widehat{\mathrm{M}_f^0} = \varphi_3(\sigma_f)\,\widehat{\mathrm{M}_f^0}, \quad (5.6)$$

where $\widehat{\mathrm{M}_f^0}$ are arbitrary real mass matrices and $\sigma_d = \sigma_\ell = \theta$, $\sigma_u = \sigma_\nu = -\theta$. Note that the diagonal matrix of phases $\varphi_3(\sigma_f)$ can be written as

$$\varphi_3(\sigma_f) = \mathbf{1} + (e^{i\sigma_f} - 1)\mathrm{P}_3. \quad (5.7)$$

[2]Note that comparing to the gBGL scalar potential in eq. (4.56) here the symmetry is softly broken by the term $\mu_{12}^2\left(\Phi_1^\dagger\Phi_2 + \Phi_2^\dagger\Phi_1\right)$.

It is clear that θ, the relative phase among the vacuum expectation values of the original scalar fields, is the unique source of irremovable complexity in the mass matrices, and thus it is the candidate to generate the phases in the CKM and PMNS mixing matrices. To analyze the mixing matrices it is sufficient to diagonalize $\mathrm{M}_f^0\mathrm{M}_f^{0\dagger}$: following eq. (5.6),

$$\mathrm{M}_f^0\mathrm{M}_f^{0\dagger} = \varphi_3(\sigma_f)\widehat{\mathrm{M}_f^0}\widehat{\mathrm{M}_f^0}^T\varphi_3(-\sigma_f). \tag{5.8}$$

Since $\widehat{\mathrm{M}_f^0}\widehat{\mathrm{M}_f^0}^T$ is real, symmetric (and positive definite), it can be diagonalized with a real orthogonal (rotation) matrix O_{f_L}

$$O_{f_L}^T\widehat{\mathrm{M}_f^0}\widehat{\mathrm{M}_f^0}^T O_{f_L} = \mathrm{diag}(m_{f_1}^2, m_{f_2}^2, m_{f_3}^2). \tag{5.9}$$

One obtains trivially

$$\mathcal{U}_{f_L}^\dagger \mathrm{M}_f^0\mathrm{M}_f^{0\dagger}\mathcal{U}_{f_L} = \mathrm{diag}(m_{f_1}^2, m_{f_2}^2, m_{f_3}^2), \quad \mathcal{U}_{f_L} = \varphi_3(\sigma_f)O_{f_L}. \tag{5.10}$$

Since $\mathrm{M}_f^{0\dagger}\mathrm{M}_f^0 = \widehat{\mathrm{M}_f^0}^T\widehat{\mathrm{M}_f^0}$ is real and symmetric, we will also have

$$O_{f_R}^T\widehat{\mathrm{M}_f^0}^T\widehat{\mathrm{M}_f^0}O_{f_R} = \mathrm{diag}(m_{f_1}^2, m_{f_2}^2, m_{f_3}^2), \tag{5.11}$$

in such a way that the fermion mass matrix bi-diagonalization reads

$$\mathrm{M}_f = \mathcal{U}_{f_L}^\dagger \mathrm{M}_f^0 O_{f_R} = \begin{pmatrix} m_{f_1} & 0 & 0 \\ 0 & m_{f_2} & 0 \\ 0 & 0 & m_{f_3} \end{pmatrix}. \tag{5.12}$$

Correspondingly, the CKM mixing matrix $V = \mathcal{U}_{u_L}^\dagger\mathcal{U}_{d_L}$ and the PMNS mixing matrix $U = \mathcal{U}_{\ell_L}^\dagger\mathcal{U}_{\nu_L}$, defined with the usual conventions in the charged currents $W^\pm$ interactions, are:

$$V = O_{u_L}^T\,\varphi_3(2\theta)\,O_{d_L}, \quad U = O_{\ell_L}^T\,\varphi_3(-2\theta)\,O_{\nu_L}\,. \tag{5.13}$$

Since O_{f_L} are arbitrary real rotations, it is evident that there is enough freedom in eq. (5.13) to obtain arbitrary V and U, except for the fact that any CP violating observable in the quark sector and any CP violating observable in the lepton sector, must vanish with $\theta \to 0$. It is thus interesting to scrutinize in detail the relation that must exist among the CP violating phases in V and U, $\delta_{\rm CKM}$ and $\delta_{\rm PMNS}$ respectively. Anticipating the discussion in section 5.4, $\delta_{\rm CKM}$ and $\delta_{\rm PMNS}$ will simply correspond to the CP phases in a standard parametrization; notice that, a priori, the change of sign in θ entering V and U in eq. (5.13), does not imply in general that $\delta_{\rm CKM} = -\delta_{\rm PMNS}$.

5.3 CP violation and the presence of SFCNC

It was shown in [196] that in this class of 2HDMs with spontaneous CP violation, there is a deep connection between the complexity of the CKM matrix and the presence of SFCNC. Since there is no evidence yet of SFCNC beyond the SM, the simplest approach in the analysis of these models would be to impose that SFCNC are absent. As discussed in [196], this leads to a real CKM, contrary to evidence, and thus SFCNC are necessary. We recall here the essence of this connection.

The appearance of SFCNC is encoded in the N_f^0 matrices in eq. (2.29), which control the Yukawa couplings of H_2; in the fermion mass bases, $\mathrm{N}_f^0 \to \mathrm{N}_f$, and eq. (5.3) gives

$$\begin{aligned} \mathrm{N}_f = \mathcal{U}_{f_L}^\dagger \, \mathrm{N}_f^0 \, O_{f_R} &= \left[-t_\beta \mathbf{1} + \left(t_\beta + t_\beta^{-1} \right) P_3^{[f]} \right] \mathrm{M}_f \\ &= \left[-t_\beta \mathbf{1} + \left(t_\beta + t_\beta^{-1} \right) P_3^{[f]} \right] \mathrm{diag}(m_{f_1}, m_{f_2}, m_{f_3}), \end{aligned} \tag{5.14}$$

where we have introduced the projection operators

$$P_3^{[f]} \equiv \mathcal{U}_{f_L}^\dagger \, \mathrm{P}_3 \, \mathcal{U}_{f_L} = O_{f_L}^T \, \mathrm{P}_3 \, O_{f_L}. \tag{5.15}$$

In eqs. (5.14)-(5.15), SFCNC are controlled by the real projectors $P_3^{[f]}$, in particular the off-diagonal entries of $P_3^{[f]}$, which are controlled by the O_{f_L} matrices, which also give the CKM and PMNS mixing matrices.

It is important to notice that, by construction,

$$P_3^{[u]} = V \, P_3^{[d]} \, V^\dagger, \quad P_3^{[\ell]} = U \, P_3^{[\nu]} \, U^\dagger. \tag{5.16}$$

Equation (5.16) means that SFCNC in the up and down quark sectors are not independent, they are related through the CKM matrix. For example, if one fixes SFCNC in the up quark sector, SFCNC in the down quark sector are completely determined; this fact will be particularly relevant in order to address appropriately the count and the election of the independent parameters in the model. The situation in the lepton sector is analogous.

The elements of the matrices $P_3^{[f]}$ are

$$\left(P_3^{[f]} \right)_{ij} = \left(O_{f_L}^T \, \mathrm{P}_3 \, O_{f_L} \right)_{ij} = \left(O_{f_L} \right)_{3i} \left(O_{f_L} \right)_{3j} \equiv \hat{r}_{[\mathrm{f}]i} \hat{r}_{[\mathrm{f}]j} \,, \tag{5.17}$$

where $\hat{r}_{[\mathrm{f}]i} \equiv (O_{f_L})_{3i}$ are the components of real, unit vectors in three dimensions $\hat{r}_{[\mathrm{f}]}$, the third rows of the orthogonal matrices O_{f_L}. In principle each $\hat{r}_{[\mathrm{f}]}$ would require two independent parameters, but it follows from eq. (5.16) that $\hat{r}_{[\mathrm{u}]j} V_{jk} = e^{2i\theta} \hat{r}_{[\mathrm{d}]k}$ and $\hat{r}_{[\ell]j} U_{jk} = e^{-2i\theta} \hat{r}_{[\nu]k}$ in such a way that $\hat{r}_{[\mathrm{d}]k}$ is fixed once $\hat{r}_{[\mathrm{u}]j}$ and V_{jk} are known, and similarly for $\hat{r}_{[\nu]k}$ with respect to $\hat{r}_{[\ell]j}$ and U_{jk}. The only way to avoid SFCNC in $P_3^{[f]}$ is to set one component $\hat{r}_{[\mathrm{f}]k} = 1$ and the others $\hat{r}_{[\mathrm{f}]j} = 0$, $j \neq k$. In that case

$$\left(P_3^{[f]}\right)_{ij} = \delta_{ik}\delta_{jk} \equiv (P_k)_{ij} \ , \tag{5.18}$$

for a fixed k, i.e. $P_3^{[f]} = P_k$ for that given f. Consider, for example, the absence of SFCNC in the neutrino sector, that is $P_3^{[\nu]} = P_k$. Using eq. (5.7) in eq. (5.13),

$$\begin{aligned} U &= O_{\ell_L}^T \varphi_3(-2\theta) O_{\nu_L} = O_{\ell_L}^T O_{\nu_L} \left[\mathbf{1} + (e^{-2i\theta} - 1) O_{\nu_L}^T \mathrm{P}_3 O_{\nu_L}\right] \\ &= O_{\ell_L}^T O_{\nu_L} \left[\mathbf{1} + (e^{-2i\theta} - 1) P_3^{[\nu]}\right] = O_{\ell_L}^T O_{\nu_L} \left[\mathbf{1} + (e^{-2i\theta} - 1) P_k\right]. \end{aligned} \tag{5.19}$$

Then the PMNS matrix U is written as a real rotation times a diagonal matrix of phases (with $e^{-2i\theta}$ in position k and the rest of them 1), and thus there is no CP violation. Similarly, if one starts with the absence of SFCNC in the charged lepton sector, $P_3^{[\ell]} = P_k$ and

$$\begin{aligned} U &= O_{\ell_L}^T \varphi_3(-2\theta) O_{\nu_L} = \left[\mathbf{1} + (e^{-2i\theta} - 1) O_{\ell_L}^T \mathrm{P}_3 O_{\ell_L}\right] O_{\ell_L}^T O_{\nu_L} \\ &= \left[\mathbf{1} + (e^{-2i\theta} - 1) P_3^{[\ell]}\right] O_{\ell_L}^T O_{\nu_L} = \left[\mathbf{1} + (e^{-2i\theta} - 1) P_k\right] O_{\ell_L}^T O_{\nu_L}, \end{aligned} \tag{5.20}$$

giving again a CP conserving mixing matrix. Therefore, in this model, in order to have a non-vanishing CP violating phase in the CKM matrix, there must be tree level SFCNC both in the up and in the down quark sectors and, mutatis mutandis, in order to have a non-vanishing CP violating phase in the PMNS matrix, there must be tree level SFCNC both in the neutrino and in the charged lepton sectors.

5.4 The general relation between $\delta_{\rm CKM}$ and $\delta_{\rm PMNS}$

From the discussion in the previous sections, it is important to recall that

(i) $\theta \neq 0$ arising from the vacuum is the only possible source of CP violation in the CKM and in the PMNS mixing matrices,

(ii) if SFCNC are removed in one fermion sector, CP violation in the corresponding mixing matrix disappears even if $\theta \neq 0$.

The CKM and PMNS matrices can be parametrized, up to rephasing of fields, in terms of 4 quantities each; in the usual PDG parametrizations [20], the parameters are $\{\theta^q_{12}, \theta^q_{13}, \theta^q_{23}, \delta_q\}$ and $\{\theta^\ell_{12}, \theta^\ell_{13}, \theta^\ell_{23}, \delta_\ell\}$ respectively. In the quark sector, experimental information allows the extraction of θ^q_{12}, θ^q_{13}, θ^q_{23}, and of the CP violating phase δ_q, which is neatly different from zero. In the lepton sector, experimental information allows to extract θ^ℓ_{12}, θ^ℓ_{13}, θ^ℓ_{23}, but the phase δ_ℓ remains 'the last frontier', where some sensitivity is emerging in current analyses [198, 199], but still far from a neat determination.

Although the form of the CKM and PMNS matrices in eq. (5.13) is different from the PDG parametrization, one can impose in an invariant manner that V and U agree with the experimental information encoded in $\{\theta^q_{12}, \theta^q_{13}, \theta^q_{23}, \delta_q\}$ and $\{\theta^\ell_{12}, \theta^\ell_{13}, \theta^\ell_{23}, \delta_\ell\}$ (see appendix C for a detailed explanation). In particular, $\delta_{\rm CKM}$, the CP violating phase in V, is the model prediction for δ_q and similarly $\delta_{\rm PMNS}$, the CP violating phase in U, is the model prediction for δ_ℓ. We already know that if $\theta = 0$, then $\delta_{\rm CKM} = \delta_{\rm PMNS} = 0$, but $\theta \neq 0 \not\Rightarrow \delta_{\rm CKM} \neq 0$, $\delta_{\rm PMNS} \neq 0$.

At this point, we need to discuss the independent parameters in the model. We start with the quark sector, keeping in mind that an important goal is to analyze how information on CP violation in the quark sector, i.e. the constraint $\delta_q = \delta_{\rm CKM}$, can translate into some prediction on $\delta_{\rm PMNS}$.

The CKM matrix in eq. (5.13) involves 7 real parameters: 3 in the rotation O_{u_L}, 3 in the rotation O_{d_L}, and θ. It should match the four independent quantities measured in the CKM matrix, equivalent to $\{\theta^q_{12}, \theta^q_{13}, \theta^q_{23}, \delta_q\}$. Besides the CKM matrix, the parameters in O_{u_L} and O_{d_L}, in particular the ones in $(O_{u_L})_{3j} = \hat{r}_{[{\rm u}]j}$, $(O_{d_L})_{3j} = \hat{r}_{[{\rm d}]j}$ (see eq. (5.17)) also control the SFCNC which, we recall, must be present: they involve 2 of the parameters in O_{u_L}, O_{d_L}. This means that measurements of CKM and SFCNC processes (e.g. ${\rm h} \to u\bar{c}, \bar{u}c$, $t \to {\rm h}c$, $t \to {\rm h}u$, ${\rm h} \to b\bar{s}, \bar{b}s$, etc), that is measurements of $\{\theta^q_{12}, \theta^q_{13}, \theta^q_{23}, \delta_q\}$ and of $\{\hat{r}_{[{\rm u}]1}, \hat{r}_{[{\rm u}]2}\}$ (or, equivalently, of 2 independent $\hat{r}_{[{\rm u}]j}, \hat{r}_{[{\rm d}]k}$), can provide sufficient constraints to fix the parameters

of the model. Although there are in principle 7 parameters, one can reduce this number to 6 in a simple manner, as we now discuss. Each rotation can be written as the product of three two-dimensional rotations controlled by one parameter each,

$$O_{u_L} = \mathcal{R}_1(p_1^u)\mathcal{R}_2(p_2^u)\mathcal{R}_3(p_3^u), \quad O_{d_L} = \mathcal{R}_1(p_1^d)\mathcal{R}_2(p_2^d)\mathcal{R}_3(p_3^d), \tag{5.21}$$

where each $\mathcal{R}_j(x)$ can be one of the following (with $\mathcal{R}_1(p) \neq \mathcal{R}_2(p)$, $\mathcal{R}_2(p) \neq \mathcal{R}_3(p)$)

$$\mathcal{R}_{12}(x) = \begin{pmatrix} c_x & s_x & 0 \\ -s_x & c_x & 0 \\ 0 & 0 & 1 \end{pmatrix}, \quad \mathcal{R}_{13}(x) = \begin{pmatrix} c_x & 0 & s_x \\ 0 & 1 & 0 \\ -s_x & 0 & c_x \end{pmatrix}, \quad \mathcal{R}_{23}(x) = \begin{pmatrix} 1 & 0 & 0 \\ 0 & c_x & s_x \\ 0 & -s_x & c_x \end{pmatrix}, \tag{5.22}$$

and $c_x = \cos x$, $s_c = \sin x$.

If one chooses a parametrization with $\mathcal{R}_1(p_1^f) = \mathcal{R}_{12}(p_1^f)$ in both O_{u_L} and O_{d_L} (i.e. the leftmost rotation only acts in the 1-2 plane), for example

$$V = O_{u_L}^T \varphi_3(2\theta) O_{d_L}, \tag{5.23}$$

$$O_{u_L} = \mathcal{R}_{12}(p_1^u)\mathcal{R}_{23}(p_2^u)\mathcal{R}_{13}(p_3^u), \tag{5.24}$$

$$O_{d_L} = \mathcal{R}_{12}(p_1^d)\mathcal{R}_{23}(p_2^d)\mathcal{R}_{13}(p_3^d), \tag{5.25}$$

it is clear (note the $\varphi_3(2\theta)$ diagonal structure in eqs. (5.6)-(5.7)) that, rather than p_1^u and p_1^d separately, only $p_1^u - p_1^d$ enters V and we can eliminate one parameter at once (we simply set $p_1^d = 0$ without loss of generality). In summary, the experimental information constrains $\{\theta_{12}^q, \theta_{13}^q, \theta_{23}^q, \delta_q, \hat{r}_{[\mathrm{u}]1}, \hat{r}_{[\mathrm{u}]2}\}$, and could fix the model parameters $\{p_1^u, p_2^u, p_3^u, p_2^d, p_3^d, \theta\}$ (a full analysis along these lines was presented in [196]). The most important aspect here, in which we are interested, is the fact that, ideally, one can fix θ with this procedure, since CP violation is well established in the quark sector. One can address the lepton sector similarly with

$$U = O_{\ell_L}^T \varphi_3(-2\theta) O_{\nu_L}, \tag{5.26}$$

$$O_{\nu_L} = \mathcal{R}_{12}(p_1^\nu)\mathcal{R}_{23}(p_2^\nu)\mathcal{R}_{13}(p_3^\nu), \tag{5.27}$$

$$O_{\ell_L} = \mathcal{R}_{12}(p_1^\ell)\mathcal{R}_{23}(p_2^\ell)\mathcal{R}_{13}(p_3^\ell). \tag{5.28}$$

Again, one can set $p_1^\nu = 0$ without loss of generality, ending up with $\{p_1^\ell, p_2^\ell, p_3^\ell, p_2^\nu, p_3^\nu, \theta\}$ as parameters in the lepton flavor sector. The experimental information on PMNS

strongly constrains $\{\theta_{12}^{\ell}, \theta_{13}^{\ell}, \theta_{23}^{\ell}\}$; additional information from SFCNC sensitive processes like $h \to \ell_i \bar{\ell}_j$, $i \neq j$, is needed in order to constrain or fix the parameters in eq. (5.26). The crucial point is that θ can be a priori fixed in the quark sector and thus, with one less experimental input in the leptonic sector, one could in principle predict the value of the CP violating Dirac phase δ_ℓ in PMNS prior to its measurement. It is in this sense that we can ideally relate the PMNS phase to the CKM phase in this class of generalized BGL-2HDM with spontaneous CP violation.

5.5 Simplified models incorporating MFV and their connections to SFCNC

In the full analysis of the quark sector presented in [196], it was shown that the model was viable after surmounting a large set of constraints related to flavor transitions, Higgs signals, electroweak precision and requirements on the scalar potential. In particular, the right amount of CP violation in the CKM matrix could be accommodated, together with the presence of SFCNC. Surprisingly, this could be achieved with significant freedom in the values of θ and SFCNC. Therefore, direct generalization of the full analysis to include the lepton flavor sector does not appear to be the most promising avenue to explore the connection among CP violation in the CKM and PMNS mixing matrices in this kind of model, since this connection is blurred by this remaining freedom in θ and SFCNC.

An interesting possibility is to restrict the model by making simplifying assumptions about SFCNC, with these assumptions guided by – and thus compatible with – experimental data. In the following we focus on that kind of restricted scenario. We will first address the quark sector and then discuss the extension to the lepton sector.

5.5.1 Quark sector

As explained in section 5.3, eliminating SFCNC either in the up or in the down quark sector, definitely simplifies SFCNC but eliminates altogether a CP violating CKM matrix. The next level of simplification would be to impose the absence of some SFCNC. Considering the general structure of SFCNC, proportional to $\hat{r}_{[\mathrm{f}]j}\hat{r}_{[\mathrm{f}]k}$, the

only simplified alternative between the most general possibility and the absence of SFCNC is to assume only one vanishing component $\hat{r}_{[\mathrm{f}]i} = 0$ for a given $i = 1, 2$ or 3; in that case only one SFCNC transition $j \leftrightarrows k$ is present (i, j, k all different). Notice that, a priori, one can make this kind of assumption simultaneously in both the up and the down sectors: that is, for given i and l, one can in principle impose $\hat{r}_{[\mathrm{u}]i} = 0$ and $\hat{r}_{[\mathrm{d}]l} = 0$. According to the discussion in section 5.4, we have 6 parameters that need to satisfy the 4 constraints to obtain a realistic CKM matrix, to which we are now adding these 2 new requirements on SFCNC. One can indeed implement these 2 SFCNC conditions directly with a reduction from 6 to 4 parameters in our CKM matrix in eq. (5.23). Notice, in that case, that the models incorporate the MFV ansatz [136, 197], since they have exactly as many parameters in the flavor sector as the CKM matrix requires. Furthermore, the only non-vanishing SFCNC coupling in each sector will be controlled by one of the mixing angles of CKM.

Regarding the quark sector, one can consider, in principle, 9 different models of this type, out of which only one appears to satisfy the requirements to be viable. In the following we analyze how there is only one model which satisfies some basic requirements. We use the following notation to identify the different models: model $(ud) = (jk)$, $j, k = 1, 2, 3$, is the model in which $\hat{r}_{[\mathrm{u}]j} = 0$ and $\hat{r}_{[\mathrm{d}]k} = 0$: j identifies which generation does not have SFCNC in the up quark sector and similarly for k in the down quark sector. The extension of the notation to the lepton sector is straightforward: with $\hat{r}_{[\nu]}$, $\hat{r}_{[\ell]}$ in eq. (5.38), the complete label of the model is $(ud, \nu\ell) = (12, 32)$.

In principle, one would need to perform an analysis of each model similar to the one in [196], extended to the lepton sector (what would lead to 81 different analysis), a task which is beyond the scope of the work [5] presented in this chapter. It is nevertheless possible to consider simpler analyses and a few requirements to understand how all but one model have to be discarded.

The first requirement in the quark sector is that a CKM matrix in agreement with data can be obtained. All 9 models $(ud) = (jk)$, $j, k = 1, 2, 3$, can give a good CKM matrix. The next requirement concerns SFCNC: if one sorts the absolute

value of the components of $\hat{r}_{[\mathrm{f}]}$, $\left|\hat{r}_{[\mathrm{f}]Max}\right| \geq \left|\hat{r}_{[\mathrm{f}]Mid}\right| \geq \left|\hat{r}_{[\mathrm{f}]Min}\right|$, the presence of SFCNC is necessary in order to obtain a complex CKM matrix, which means $\left|\hat{r}_{[\mathrm{f}]Mid}\right| > 0$. Notice that in the class of models under consideration, $\hat{r}_{[\mathrm{f}]Min} = 0$. In the analysis of [196], rather restrictive ranges for $\left|\hat{r}_{[\mathrm{u}]Mid}\right|$ and $\left|\hat{r}_{[\mathrm{d}]Mid}\right|$ were obtained. We impose that constraint as a proxy for more involved analyses, explicitely we require

$$\left|\hat{r}_{[\mathrm{u}]Mid}\right| \in [0.04; 0.25], \quad \left|\hat{r}_{[\mathrm{d}]Mid}\right| \in [0.003; 0.10]. \tag{5.29}$$

Models $(ud) = (13)$, (21), (22), (23), (33), violate grossly that requirement when a good CKM matrix is obtained. Although model $(ud) = (11)$ can give values close to the ranges in eq. (5.29), it cannot produce a good CKM matrix while satisfying eq. (5.29). Models $(ud) = (31)$ and (32) can produce a good CKM matrix and also fulfill eq. (5.29) with $\left|\hat{r}_{[\mathrm{u}]1}\hat{r}_{[\mathrm{u}]2}\right| \simeq 0.22$. The corresponding h-SFCNC interaction is of the form $\mathscr{L}_{huc} = C^{\mathrm{h}}_{ud}\overline{c_L}u_R\mathrm{h}$. It gives rise, at tree level, to an effective operator $\frac{(C^{\mathrm{h}}_{ud})^2}{\mathrm{m}^2_{\mathrm{h}}}(\overline{c_L}u_R)$ contributing to D^0–$\bar{D}^0$ mixing. Omitting the possibility of significant cancellations with similar contributions mediated by H and A, D^0–$\bar{D}^0$ mixing sets strong bounds on C^{h}_{ud} (see for example [181]), which cannot be satisfied within models $(ud) = (31)$ and (32).

The only model left in the quark sector is $(ud) = (12)$ which is the specific example that we consider now, step by step, in order to illustrate the central idea.

1. We start imposing the following form of the $\hat{r}_{[\mathrm{f}]}$ vectors controlling SFCNC:

$$\begin{aligned} \hat{r}_{[\mathrm{u}]} &= \left(0, -\sin p^u_2, \cos p^u_2\right), \\ \hat{r}_{[\mathrm{d}]} &= \left(-\sin p^d_2, 0, \cos p^d_2\right), \end{aligned} \tag{5.30}$$

   with parameters p^u_2, p^d_2. The assumption in eq. (5.30) is that $t \leftrightarrows c$ and $b \leftrightarrows d$ SFCNC are present while $u \leftrightarrows c$, $u \leftrightarrows t$, $d \leftrightarrows s$, $b \leftrightarrows s$ SFCNC are absent.

2. Concerning CKM, since $\hat{r}_{[\mathrm{f}]i} = (O_{f_L})_{3i}$, we must have

$$O_{u_L} = \mathcal{R}_{12}(p^u_1)\mathcal{R}_{23}(p^u_2), \quad O_{d_L} = \mathcal{R}_{13}(p^d_2)\,. \tag{5.31}$$

One can add a factor $\mathcal{R}_{12}(p_1^d)$ to the left of $\mathcal{R}_{13}(p_2^d)$ in O_{d_L} but, as discussed previously, this would just amount to a redefinition $p_1^u \mapsto p_1^u - p_1^d$. The main point is that the CKM matrix is

$$V = \mathcal{R}_{23}(p_2^u)^T \mathcal{R}_{12}(p_1^u)^T \varphi_3(2\theta) \mathcal{R}_{13}(p_2^d)\,. \tag{5.32}$$

3. Performing a fit of eq. (5.32) to the measured CKM matrix (see appendix C), one obtains

$$\begin{aligned} &2\theta = 1.077^{+0.039}_{-0.031}, && p_1^u = 0.22694 \pm 0.00052, \\ &p_2^u = (4.235 \pm 0.059) \times 10^{-2}, && p_2^d = (3.774 \pm 0.098) \times 10^{-3}\,. \end{aligned} \tag{5.33}$$

In order to relate $\delta_{\rm CKM}$ and $\delta_{\rm PMNS}$ it is specially relevant that the quark sector fixes θ.

4. In addition, eq. (5.33) fixes SFCNC with

$$\hat{r}_{[\rm u]} = (0, -0.0423, 0.9991)\,, \quad \hat{r}_{[\rm d]} = (-0.0038, 0, 0.9999)\,. \tag{5.34}$$

A non-trivial result is that the values in eq. (5.34) are within the allowed regions arising in the analysis of [196] (for example in figures 6(b) and 6(c)). Even if eq. (5.34) fixes the intensity of SFCNC, the precise effects in specific processes depend on parameters such as t_β and elements $\mathcal{R}_{jk}$ of the mixing matrix of neutral scalars in eq. (2.14). With $2\theta = 1.077$, $|\sin 2\theta| = 0.88$ and one can read in figure 9 of [196]

$$\mathcal{R}_{11} \in [0.82;\, 0.90], \quad t_\beta \in [0.5, 1.8]. \tag{5.35}$$

5. Then, the most relevant prediction of this model in terms of SFCNC concerns $t \to {\rm h}c$ decays, where

$$\mathrm{Br}(t \to c{\rm h}) = \frac{1}{2}\left(1 - \mathcal{R}_{11}^2\right)\left(t_\beta + t_\beta^{-1}\right)^2 (\hat{r}_{[\rm u]2}\hat{r}_{[\rm u]3})^2 f(x_h, x_W), \tag{5.36}$$

$f(x_{\rm h}, x_W) = 0.2612$. With eqs. (5.34) and (5.36), one obtains

$$1.8 \times 10^{-4} \leq \mathrm{Br}(t \to c{\rm h}) \leq 4.3 \times 10^{-4}\,. \tag{5.37}$$

Notice that the range predicted in eq. (5.37) is rather reduced and indeed not far from current LHC bounds [200, 201].

6. In the down sector, with $(\hat{r}_{[\mathrm{d}]1}\hat{r}_{[\mathrm{d}]3})^2 \sim 10^{-2}(\hat{r}_{[\mathrm{u}]2}\hat{r}_{[\mathrm{u}]3})^2 \sim 1.6\times10^{-5}$, $b \leftrightarrows d$ SFCNC have a negligible effect in B_d^0–$\bar{B}_d^0$ oscillations, while $\mathrm{h} \to \bar{b}d, b\bar{d}$ are beyond the LHC capabilities.

5.5.2 Lepton sector

We address now the lepton sector, applying analogous requirements on SFCNC to the ones considered for the quark sector in the previous subsection. In the lepton sector, the most stringent constraint comes from bounds on $\mu \to e + \gamma$. If we only allowed $\mu \leftrightarrows e$ SFCNC, the coupling would be controlled by $\left|U_{ei}U_{\mu i}\right|^2$ with $i = 1, 2$ or 3. Since PMNS is rather non-hierarchical, one can estimate [143] that avoiding the current bound $\mathrm{Br}(\mu \to e + \gamma) < 4.2\times10^{-13}$ [202] requires a cancellation or fine-tuning at the 10^{-4}–10^{-5} level among scalar and pseudoscalar contributions in 2-loop Barr-Zee contributions [203, 204].

1. It is mandatory to eliminate $\mu \leftrightarrows e$ SFCNC: this can be achieved either with $\hat{r}_{[\ell]1} = 0$ or $\hat{r}_{[\ell]2} = 0$. In the neutrino sector all three choices $\hat{r}_{[\nu]k} = 0$, $k = 1, 2, 3$ are in principle available. The problem of exploring the viable models is then reduced to analyze the requirements on the lepton sector of the 6 models $(ud, \nu\ell) = (12, jk)$, $j = 1, 2, 3$, $k = 1, 2$. Models $(\nu\ell) = (11)$, (21), (31), can produce a realistic PMNS matrix, but then $\left|\hat{r}_{[\ell]2}\hat{r}_{[\ell]3}\right|$ is close to its maximal value, 1/2, yielding too large $\mathrm{Br}(\mathrm{h} \to \mu\tau)$ predictions. On the other hand, models $(\nu\ell) = (12)$, (22), cannot produce a realistic PMNS matrix; model $(\nu\ell) = (32)$, on the contrary, can produce a good PMNS matrix. We are left with $(ud, \nu\ell) = (12, 32)$, the model considered next, as the only viable candidate:

$$\begin{aligned} \hat{r}_{[\nu]} &= \left(-\sin p_2^{\nu}, \cos p_2^{\nu}, 0\right), \\ \hat{r}_{[\ell]} &= \left(-\sin p_2^{\ell}, 0, \cos p_2^{\ell}\right). \end{aligned} \tag{5.38}$$

2. With $\hat{r}_{[\ell]i} = (O_{\ell_L})_{3i}$, we must have

$$O_{\ell_L} = \mathcal{R}_{12}(p_1^{\ell})\mathcal{R}_{13}(p_2^{\ell}), \tag{5.39}$$

and

$$O_{\nu_L} = P_{23}\mathcal{R}_{12}(p_2^\nu)\,, \tag{5.40}$$

where the permutation P_{23} interchanges the third and second rows of $\mathcal{R}_{12}(p_2^\nu)$:

$$P_{23} = \begin{pmatrix} 1 & 0 & 0 \\ 0 & 0 & 1 \\ 0 & 1 & 0 \end{pmatrix}. \tag{5.41}$$

The inclusion of P_{23} deviates, apparently, from the general parametrization introduced in eq. (5.21). While $\mathcal{R}_{13}(p)$ and $\mathcal{R}_{23}(p)$ naturally have one vanishing component in the third row (the one controlling SFCNC) in position 2 and 1 respectively, parametrizing the MFV models in which the vanishing component is in position 3 requires an additional consideration. This permutation P_{23} is introduced in order to properly implement that case. One can indeed rewrite

$$P_{23} = \begin{pmatrix} 1 & 0 & 0 \\ 0 & -1 & 0 \\ 0 & 0 & 1 \end{pmatrix}\begin{pmatrix} 1 & 0 & 0 \\ 0 & 0 & -1 \\ 0 & 1 & 0 \end{pmatrix} = \begin{pmatrix} 1 & 0 & 0 \\ 0 & 0 & -1 \\ 0 & 1 & 0 \end{pmatrix}\begin{pmatrix} 1 & 0 & 0 \\ 0 & 1 & 0 \\ 0 & 0 & -1 \end{pmatrix} = \\ \mathrm{diag}(1,-1,1)\,\mathcal{R}_{23}(\pi/2) = \mathcal{R}_{23}(\pi/2)\,\mathrm{diag}(1,1-,1), \tag{5.42}$$

that is, P_{23} can be simply viewed as a product of a fixed rephasing and a 2-3 rotation with fixed angle $\pi/2$ and thus there is nothing essentially different with respect to the other cases.

As discussed previously, we do not include a left factor $\mathcal{R}_{12}(p_1^\nu)$ in O_{ν_L}, since it amounts to a redefinition of $p_1^\ell \to p_1^\ell - p_1^\nu$.

3. The PMNS matrix is

$$U = \mathcal{R}_{13}(p_2^\ell)^T\mathcal{R}_{12}(p_1^\ell)^T\varphi_3(-2\theta)P_{23}\mathcal{R}_{12}(p_2^\nu)\,. \tag{5.43}$$

It is fully fixed by 3 mixing angles and the CP violating phase θ already obtained in the quark sector.

4. We can fit now eq. (5.43) to the experimental information on PMNS encoded in $\{\theta_{12}^\ell, \theta_{13}^\ell, \theta_{23}^\ell\}$ (see appendix C). In this fit, θ is already set to the value obtained from the fit to the CKM matrix in eq. (5.33). Although different

PMNS analyses [198, 199] show some sensitivity to the phase δ_ℓ, we do not include that information in the fit since we are precisely interested in its prediction. The fit gives the following two solutions,

$$\text{Solution 1}: \quad p_1^\ell = 0.7496, \quad p_2^\ell = 1.3541, \quad p_2^\nu = 0.8974\,, \tag{5.44}$$

$$\text{Solution 2}: \quad p_1^\ell = 2.3889, \quad p_2^\ell = 1.3541, \quad p_2^\nu = 1.0542\,. \tag{5.45}$$

SFCNC are controlled in both cases by

$$\hat{r}_{[\ell]} = (-0.9765,\, 0,\, 0.2156)\,. \tag{5.46}$$

5. Most importantly, the solutions differ in the values of the (unique) CP violating imaginary part of an invariant quartet

$$J_{\text{PMNS}} = \text{Im}\left(U_{e1}U_{\mu 2}U_{e2}^* U_{\mu 1}^*\right)\,, \tag{5.47}$$

and of the phase δ_{PMNS},

Case	J_{PMNS}	δ_{PMNS}	$\Delta\chi^2_{\text{NO}}(\delta_{\text{PMNS}})$	$\Delta\chi^2_{\text{IO}}(\delta_{\text{PMNS}})$
Solution 1	-0.0316	$1.629\pi\,(293°)$	5	0
Solution 2	0.0282	$0.679\pi\,(126°)$	13	> 20

(5.48)

$\Delta\chi^2_{\text{NO}}(\delta_{\text{PMNS}})$ and $\Delta\chi^2_{\text{IO}}(\delta_{\text{PMNS}})$ show the values that correspond to δ_{PMNS} attending to the $\Delta\chi^2$ profiles for δ_ℓ obtained for normal and inverted neutrino mass orderings in [198].

We stress that using the information on CP violation in the quark sector, we have been able to predict the phase in PMNS using the connection that SCPV provides in this model; in particular, Solution 1 has $\delta_{\text{PMNS}} = 1.629\pi$, which is in good agreement with the most likely values in PMNS analyses.

6. With the values of $e \leftrightarrows \tau$ SFCNC in eq. (5.46), we have predictions such as

$$\text{Br}(\text{h} \to e\bar{\tau} + \bar{e}\tau) = \left(1 - \mathcal{R}_{11}^2\right)\left(t_\beta + t_\beta^{-1}\right)^2 (\hat{r}_{[\ell]1}\hat{r}_{[\ell]3})^2\, \text{Br}(\text{h}_{\text{SM}} \to \tau\bar{\tau})\, \frac{\Gamma(\text{h}_{\text{SM}})}{\Gamma(\text{h})}\,. \tag{5.49}$$

Using eq. (5.35), we have the sharp range

$$2.0 \times 10^{-3} \leq \text{Br}(\text{h} \to e\bar{\tau} + \bar{e}\tau)\frac{\Gamma(\text{h})}{\Gamma(\text{h}_{\text{SM}})} \leq 5.0 \times 10^{-3}, \tag{5.50}$$

which should be seen or disproved in the near future since the current bound is[3] $\mathrm{Br}(\mathrm{h} \to e\bar{\tau} + \bar{e}\tau)_{\rm Exp} \leq 4.7 \times 10^{-3}$ [206–208] (although there is some freedom in $\Gamma(\mathrm{h})/\Gamma(\mathrm{h}_{\rm SM})$, it does not modify substantially this conclusion).

[3]Recent work [205] might lower this bound closer to 2×10^{-3}.

–Potatoes. Boil em, mash em, stick em in a stew.

— SAMwise Gamgee, *The Lord of the Rings*,
J. R. R. Tolkien

6

Symmetries and $N_f \propto M_f$

Inspired by BGL and generalized BGL models where the coupling matrices N_d, N_u (see Eqs. (2.67)–(4.31)–(4.32)) can be written in terms of the quark mass matrices and projection operators, in the work [3] presented in this chapter we study in a systematic way scenarios arising from different implementations of Abelian symmetries in the context of 2HDM. This can lead to a natural reduction in the number of parameters in these models. Regarding symmetries, Ferreira and Silva [145] classified all possible implementations of Abelian symmetries in 2HDM with fermions which lead to non-vanishing quark masses and a CKM matrix which is not block diagonal (see also [146]).

In the search for the mentioned scenarios, we classify the different models according to the structures of N_d, N_u. We identify the symmetry leading to each of the models and the corresponding flavor textures of the Yukawa couplings. These textures are stable under renormalization, since they result from symmetries of the Lagrangian.

The organization of the chapter is the following. The notation is set up in section 6.1. We then present our main results in sections 6.2 and 6.3, obeying what we denote the *Left* and *Right conditions* introduced in eqs. (6.2) and (6.5), respectively. We show that, besides BGL and gBGL there is a new type of model obeying *Left conditions* and that there are six classes of models obeying *Right*

conditions which are presented in full generality. For definiteness, we concentrate on the quark sector. We defer some technical details to appendix D.1. In particular, we present in appendix D.1.4 conditions for the identification of the various models which are invariant under basis transformations in the spaces of left-handed doublets and of up-type and down-type right-handed singlets.

6.1 Generalities and notation

While the quark masses M_d and M_u in eq. (2.33) are characterised by $3 + 3 = 6$ physical parameters, in a general 2HDM the complex matrices

$$\mathcal{U}_{d_L}^\dagger \mathrm{N}_d^0 \mathcal{U}_{d_R} = \mathrm{N}_d, \quad \mathcal{U}_{u_L}^\dagger \mathrm{N}_u^0 \mathcal{U}_{u_R} = \mathrm{N}_u, \tag{2.34}$$

are free. This introduces in principle $2 \times 3 \times 3 \times 2 = 36$ new real parameters[1]. This large freedom is certainly a source of concern since, for example, SFCNC can put significant constraints on N_d and N_u.

Invariance under some (symmetry) transformation is the best motivated requirement which can limit this inflation of parameters. Following [145], we consider in particular Abelian symmetry transformations

$$\Phi_1 \mapsto \Phi_1, \ \Phi_2 \mapsto e^{i\theta}\Phi_2, \ Q_{Lj}^0 \mapsto e^{i\alpha_j\theta} Q_{Lj}^0, \ d_{Rj}^0 \mapsto e^{i\beta_j\theta} d_{Rj}^0, \ u_{Rj}^0 \mapsto e^{i\gamma_j\theta} u_{Rj}^0 \,, \tag{6.1}$$

where α_j, β_j, γ_j, are the charges of the different fermion doublets and singlets normalized to the charge of the second scalar doublet Φ_2. As already mentioned, all possible realistic implementations of eq. (6.1) were classified in [145]. In BGL models and their generalization in [1], the symmetry properties had an interesting translation into relations among the N_q^0 and M_q^0 matrices (very useful for example in the study of the renormalization group evolution of the Yukawa matrices). Having such a connection between a symmetry and matrix relations is not always possible. Inspired by the existence of that property in those two interesting classes of models, we focus on 2HDMs which obey an Abelian symmetry, eq. (6.1), and which fulfill an additional requirement; either (a) or (b) below:

[1]Notice however that the bidiagonalization of the mass matrices still leaves the freedom to rephase individual quark fields. Together with the CKM matrix, the N_d, N_u matrices should enter physical observables in rephasing invariant combinations [111].

(a) The Yukawa coupling matrices are required to obey *Left conditions*

$$N_d^0 = L_d^0 M_d^0, \quad N_u^0 = L_u^0 M_u^0, \tag{6.2}$$

with

$$L_q^0 = \ell_1^{[q]} P_1 + \ell_2^{[q]} P_2 + \ell_3^{[q]} P_3, \tag{6.3}$$

where $\ell_j^{[q]}$ are, *a priori*, arbitrary numbers. Here and henceforth we shall often use the index q to refer to matrices in the up ($q = u$) or down ($q = d$) sectors. We have used the projection operators P_i defined by $[P_i]_{jk} = \delta_{ij}\delta_{jk}$ (no sum in j). In matrix form:

$$P_1 = \begin{pmatrix} 1 & 0 & 0 \\ 0 & 0 & 0 \\ 0 & 0 & 0 \end{pmatrix}, \quad P_2 = \begin{pmatrix} 0 & 0 & 0 \\ 0 & 1 & 0 \\ 0 & 0 & 0 \end{pmatrix}, \quad P_3 = \begin{pmatrix} 0 & 0 & 0 \\ 0 & 0 & 0 \\ 0 & 0 & 1 \end{pmatrix}. \tag{6.4}$$

These projection operators satisfy $P_i P_j = \delta_{ij} P_i$ (no sum in i) and $\sum_i P_i = \mathbf{1}$.

(b) The Yukawa coupling matrices are instead required to obey *Right conditions*

$$N_d^0 = M_d^0 R_d^0, \quad N_u^0 = M_u^0 R_u^0, \tag{6.5}$$

with

$$R_q^0 = r_1^{[q]} P_1 + r_2^{[q]} P_2 + r_3^{[q]} P_3, \tag{6.6}$$

where $r_j^{[q]}$ are, again *a priori*, arbitrary numbers and, as in eq. (6.3), P_i are the projection operators in eqs. (6.4).

Upper (and lower) case L's and R's are used in correspondence with the matrices (and parameters) acting on the left or the right of M_q^0 in Eqs. (6.2) and (6.5). Although it is not required *a priori*, the matrices L_q^0 and R_q^0 are non-singular.

All the resulting models, that is all 2HDMs obeying eq. (6.1) and either *Left* or *Right conditions* are analyzed in section 6.2 and section 6.3, respectively.

We emphasize that our aim is to reduce the number of parameters. As shown in ref. [145], imposing Abelian symmetries leaves only a reduced set of possible models, each with a significantly reduced number of independent parameters. Here, we consider only those Abelian models which can in some sense be seen as generalizations

of the BGL models, by imposing, in addition, the *Left conditions* in eq. (6.2), or the *Right conditions* in eq. (6.5). As anticipated, the number of independent parameters of the models is significantly reduced with respect to the most general 2HDM. It is to be noticed that, as shown in sections 6.2.2 and 6.3.2, $\ell_j^{[q]}$ or $r_j^{[q]}$, which are a priori arbitrary, turn out to be unavoidably fixed in terms of t_β. Quite significantly, as analyzed in appendix D.1.1, Eqs. (6.2) and (6.5) have an elegant interpretation. In the popular 2HDMs of types I, II, X and Y [79, 80, 82, 83], a $\mathbb{Z}_2$ symmetry is incorporated and it eliminates the possibility of SFCNC. But, in those cases, the $\mathbb{Z}_2$ assignment is universal for the different fermion families; all fermions of a given charge couple to the *same* scalar doublet. Here, Eqs. (6.2) and (6.5) have a different non-universal interpretation which leads to controlled SFCNC:

- in the models of section 6.2, obtained by imposing the *Left conditions* in eq. (6.2), each left-handed doublet Q_{Li}^0 couples exclusively, i.e. to one and only one, of the scalar doublets Φ_k,
- in the models of section 6.3, obtained by imposing the *Right conditions* in eq. (6.5), each right-handed singlet d_{Ri}^0, u_{Rj}^0, couples exclusively to one scalar doublet Φ_k.

In particular, we stress that here, and in contrast to type I, II, X, and Y models, fermions of a given electric charge but different families need not couple all to the same scalar doublet. In this sense, conditions (6.2) and (6.5) - applied in the context of models with Abelian symmetries - can also be seen as a generalization of the Glashow, Weinberg conditions [112] for Natural Flavor Conservation. In the present approach, having L_d^0 and L_u^0 proportional to the identity (or R_d^0 and R_u^0 proportional to the identity) enforces the NFC type I and type II 2HDM.

6.2 Symmetry Controlled Models with "Left" Conditions

We present in this section the different models arising from an Abelian symmetry and for which there are matrices $\mathrm{L_d^0}$ and $\mathrm{L_u^0}$ such that eq. (6.2) is verified. We

studied systematically all models satisfying the Abelian symmetries in eq. (6.1), and which lead to non-vanishing quark masses and a CKM matrix which is not block diagonal, thus verifying the results in ref. [145]. Those models were then required to satisfy in addition eq. (6.2). Before addressing the models themselves, it is convenient to make some observations on the effect of rotating into mass bases of the up and down quarks.

6.2.1 Conditions in the mass basis

In the mass bases, given by the unitary transformations in eq. (2.33), eq. (6.2) reads

$$\mathrm{N}_d = \mathrm{L_d}\,\mathrm{M}_d\,, \quad \mathrm{N}_u = \mathrm{L_u}\,\mathrm{M}_u\,, \tag{6.7}$$

with the transformed matrices

$$\mathrm{L_d} = \mathcal{U}_{d_L}^{\dagger}\,\mathrm{L_d^0}\,\mathcal{U}_{d_L}, \quad \mathrm{L_u} = \mathcal{U}_{u_L}^{\dagger}\,\mathrm{L_u^0}\,\mathcal{U}_{u_L}\,. \tag{6.8}$$

Introducing transformed projection operators

$$P_j^{[d_L]} \equiv \mathcal{U}_{d_L}^{\dagger}\,\mathrm{P}_j\,\mathcal{U}_{d_L}, \quad P_j^{[u_L]} \equiv \mathcal{U}_{u_L}^{\dagger}\,\mathrm{P}_j\,\mathcal{U}_{u_L}\,, \tag{6.9}$$

one simply has

$$\mathrm{L_d} = \ell_1^{[d]} P_1^{[d_L]} + \ell_2^{[d]} P_2^{[d_L]} + \ell_3^{[d]} P_3^{[d_L]}\,, \quad \mathrm{L_u} = \ell_1^{[u]} P_1^{[u_L]} + \ell_2^{[u]} P_2^{[u_L]} + \ell_3^{[u]} P_3^{[u_L]}\,. \tag{6.10}$$

Furthermore, since the CKM matrix is $V = \mathcal{U}_{u_L}^{\dagger}\mathcal{U}_{d_L}$, one has the straightforward relation

$$P_k^{[u_L]} = V\,P_k^{[d_L]}\,V^{\dagger}\,, \tag{6.11}$$

which is relevant for the parametrization of the SFCNC couplings in the discussion to follow.

6.2.2 How to determine ℓ_i

Here we show how one determines the coefficients ℓ_i $(i = 1, 2, 3)$ just by examining the form of the Yukawa matrices $Y_{d,1}$ and $Y_{d,2}$. For definiteness, we concentrate

on the down sector. The reasoning for the up sector follows similar lines and yields the same conclusions.

As a first step, we notice that, under the assumption of an Abelian symmetry [145],

$$(Y_{d,1})_{ia} \neq 0 \quad \Rightarrow \quad (Y_{d,2})_{ia} = 0, \tag{6.12}$$

(and the converse $1 \leftrightarrow 2$ also holds); notice that this implication involves the *same* matrix element of $Y_{d,1}$ and $Y_{d,2}$.

As a second step, consider $(Y_{d,1})_{ia} \neq 0$. We already know that this implies $(Y_{d,2})_{ia} = 0$. But then, the (ia) entries in eq. (2.29) yield

$$\left(\mathrm{M}_d^0\right)_{ia} = \frac{v e^{i\theta_1}}{\sqrt{2}}\, c_\beta\, (Y_{d,1})_{ia}\ , \quad \left(\mathrm{N}_d^0\right)_{ia} = -\frac{v e^{i\theta_1}}{\sqrt{2}}\, s_\beta\, (Y_{d,1})_{ia}\ , \tag{6.13}$$

and we obtain

$$\left(\mathrm{N}_d^0\right)_{ia} = -t_\beta \left(\mathrm{M}_d^0\right)_{ia}\ . \tag{6.14}$$

Now we use the *Left conditions* in eqs. (6.2)-(6.4):

$$\left(\mathrm{N}_d^0\right)_{ia} = \ell_i^{[d]} \left(\mathrm{M}_d^0\right)_{ia}\ . \tag{6.15}$$

Combining eqs. (6.14) and (6.15), we find that

$$(Y_{d,1})_{ia} \neq 0 \quad \Rightarrow \quad \ell_i^{[d]} = -t_\beta\,. \tag{6.16}$$

As a third step, we consider the possibility that $(Y_{d,2})_{ib} \neq 0$. A similar argument entails

$$(Y_{d,2})_{ib} \neq 0 \quad \Rightarrow \quad \ell_i^{[d]} = t_\beta^{-1}\,. \tag{6.17}$$

Comparing eq. (6.16) and (6.17), we conclude that the combination of an Abelian symmetry, *c.f.* eq. (6.1), with the *Left conditions* of eq. (6.2) implies that one cannot have simultaneously $(Y_{d,1})_{ia} \neq 0$ and $(Y_{d,2})_{ib} \neq 0$, for *any* choices of a and b. So, for the *Left condition*, $Y_{d,1}$ and $Y_{d,2}$ cannot both have nonzero matrix elements in the same row. This has the physical consequence that each doublet Q_{Li}^0 couples to one and only one doublet Φ_k.

Moreover, we find the rule book for the assignment of $\ell_i^{[d]}$ in our models with *Left conditions*:

$$\begin{aligned} &\text{if } \left(Y_{d,1}\right)_{ia} \text{ exists, then } \ \ell_i^{[d]} = -t_\beta\,, \\ &\text{if } \left(Y_{d,2}\right)_{ia} \text{ exists, then } \ \ell_i^{[d]} = t_\beta^{-1}\,. \end{aligned} \tag{6.18}$$

One can easily see that the up sector matrices $Y_{u,1}$ and $Y_{u,2}$, and the corresponding $\ell_i^{[u]}$ follow exactly the same rule.

6.2.3 Left Models

Omitting the trivial cases of type I or type II 2HDMs, for which the transformation properties in eq. (6.1) have no flavor dependence (both $\mathrm{L_d}$ and $\mathrm{L_u}$ are in that case proportional to the identity matrix **1**), we now address the different possible models which obey *Left conditions*.

BGL models

We recover the well known case of BGL models [133]. The symmetry transformation is

$$\Phi_2 \mapsto e^{i\theta}\Phi_2, \quad Q^0_{L3} \mapsto e^{-i\theta}Q^0_{L3}, \quad d^0_{R3} \mapsto e^{-i2\theta}d^0_{R3}, \quad \theta \neq 0, \pi. \tag{6.19}$$

The corresponding Yukawa coupling matrices are

$$\begin{aligned} Y_{d,1} &= \begin{pmatrix} \times & \times & 0 \\ \times & \times & 0 \\ 0 & 0 & 0 \end{pmatrix}, \qquad Y_{d,2} = \begin{pmatrix} 0 & 0 & 0 \\ 0 & 0 & 0 \\ 0 & 0 & \times \end{pmatrix}, \\ Y_{u,1} &= \begin{pmatrix} \times & \times & \times \\ \times & \times & \times \\ 0 & 0 & 0 \end{pmatrix}, \qquad Y_{u,2} = \begin{pmatrix} 0 & 0 & 0 \\ 0 & 0 & 0 \\ \times & \times & \times \end{pmatrix}, \end{aligned} \tag{6.20}$$

where × denote arbitrary, independent, and (in general) non-vanishing matrix entries. Following the rule book in eq. (6.18) for the *Left conditions*, we find immediately

$$\mathrm{N}^0_d = \left(-t_\beta \mathrm{P}_1 - t_\beta \mathrm{P}_2 + t_\beta^{-1}\mathrm{P}_3\right)\mathrm{M}^0_d\,, \quad \mathrm{N}^0_u = \left(-t_\beta \mathrm{P}_1 - t_\beta \mathrm{P}_2 + t_\beta^{-1}\mathrm{P}_3\right)\mathrm{M}^0_u\,. \tag{6.21}$$

Here, the right-handed singlet transforming non-trivially in eq. (6.19) is a down quark leading to a down-type BGL model. In the particular implementation shown

in eq. (6.19), it is the third generation down quark which is involved; this is known as a "bottom-BGL model". We could equally well have substituted the $d^0_{R3} \mapsto e^{-i2\theta} d^0_{R3}$ transformation in eq. (6.19) by $d^0_{R1} \mapsto e^{-i2\theta} d^0_{R1}$, or by $d^0_{R2} \mapsto e^{-i2\theta} d^0_{R2}$ obtaining a "down-BGL model" and "strange-BGL model", respectively.

Parametrization

Following Eqs. (6.21) and (6.9), one can write

$$\mathrm{N}_d = (-t_\beta \mathbf{1} + (t_\beta + t_\beta^{-1}) P_3^{[d_L]}) \mathrm{M}_d \,, \quad \mathrm{N}_u = (-t_\beta \mathbf{1} + (t_\beta + t_\beta^{-1}) P_3^{[u_L]}) \mathrm{M}_u \,. \tag{6.22}$$

Since $Y_{d,1}$ and $Y_{d,2}$ are block diagonal, M_d^0 is block-diagonal too and then

$$P_3^{[d_L]} = \begin{pmatrix} 0 & 0 & 0 \\ 0 & 0 & 0 \\ 0 & 0 & 1 \end{pmatrix} . \tag{6.23}$$

Using eq. (6.11),

$$P_3^{[u_L]} = V P_3^{[d_L]} V^\dagger, \quad \text{i.e.} \quad \left(P_3^{[u_L]}\right)_{ij} = V_{i3} V_{j3}^* = V_{ib} V_{jb}^* \,, \tag{6.24}$$

and one obtains the final parametrization for the physical couplings

$$(\mathrm{N}_d)_{ij} = \delta_{ij}(-t_\beta + (t_\beta + t_\beta^{-1})\delta_{j3}) m_{d_j} \,, \quad (\mathrm{N}_u)_{ij} = (-t_\beta \delta_{ij} + (t_\beta + t_\beta^{-1}) V_{ib} V_{jb}^*) m_{u_j} \,. \tag{6.25}$$

Equation (6.25) involves quarks masses, CKM mixings and t_β, but *no new parameters*.

The transformation properties in eq. (6.19) give a block diagonal form for the down Yukawa coupling matrices: this corresponds to the fact that some matrix conditions of the *Right* type are also fulfilled for BGL models (this is not the case for the models in the next subsections).

Generalized BGL: gBGL

This second class of models is a generalization of BGL models, introduced in 4(see also [1, 209]); the defining transformation properties are

$$\Phi_2 \mapsto -\Phi_2, \quad Q^0_{L3} \mapsto -Q^0_{L3}, \tag{6.26}$$

and the symmetry group is just $\mathbb{Z}_2$. The corresponding Yukawa matrices are

$$\begin{aligned} Y_{d,1} &= \begin{pmatrix} \times & \times & \times \\ \times & \times & \times \\ 0 & 0 & 0 \end{pmatrix}, \qquad Y_{d,2} = \begin{pmatrix} 0 & 0 & 0 \\ 0 & 0 & 0 \\ \times & \times & \times \end{pmatrix}, \\ Y_{u,1} &= \begin{pmatrix} \times & \times & \times \\ \times & \times & \times \\ 0 & 0 & 0 \end{pmatrix}, \qquad Y_{u,2} = \begin{pmatrix} 0 & 0 & 0 \\ 0 & 0 & 0 \\ \times & \times & \times \end{pmatrix}. \end{aligned} \tag{6.27}$$

Following the rule book in eq. (6.18) for the *Left conditions*, we find immediately

$$\mathrm{N}_d^0 = (-t_\beta \mathrm{P}_1 - t_\beta \mathrm{P}_2 + t_\beta^{-1}\mathrm{P}_3)\,\mathrm{M}_d^0\,, \quad \mathrm{N}_u^0 = (-t_\beta \mathrm{P}_1 - t_\beta \mathrm{P}_2 + t_\beta^{-1}\mathrm{P}_3)\mathrm{M}_u^0\,. \tag{6.28}$$

Parametrization

While in the BGL model (of section 6.2.3) $Y_{d,1}$ and $Y_{d,2}$ are block-diagonal, this is not the case here. However, eqs. (6.21) and (6.28) are identical[2], giving again

$$\mathrm{N}_d = (-t_\beta \mathbf{1} + (t_\beta + t_\beta^{-1})P_3^{[d_L]})\mathrm{M}_d\,, \quad \mathrm{N}_u = (-t_\beta \mathbf{1} + (t_\beta + t_\beta^{-1})P_3^{[u_L]})\mathrm{M}_u\,. \tag{6.29}$$

Recalling eq. (6.9), one can introduce complex unitary vectors $\hat{n}_{[\mathrm{d}]}$ and $\hat{n}_{[\mathrm{u}]}$ by

$$\hat{n}_{[\mathrm{d}]j} \equiv (\mathrm{P}_3 \mathcal{U}_{d_L})_{3j}\,, \quad \hat{n}_{[\mathrm{u}]j} \equiv (\mathrm{P}_3 \mathcal{U}_{u_L})_{3j}\,, \tag{6.30}$$

in terms of which

$$\left(P_3^{[d_L]}\right)_{ij} = \hat{n}^*_{[\mathrm{d}]i}\hat{n}_{[\mathrm{d}]j}, \quad \left(P_3^{[u_L]}\right)_{ij} = \hat{n}^*_{[\mathrm{u}]i}\hat{n}_{[\mathrm{u}]j}. \tag{6.31}$$

The N_d and N_u matrices are then given by

$$(\mathrm{N}_d)_{ij} = (-t_\beta\delta_{ij} + (t_\beta + t_\beta^{-1})\hat{n}^*_{[\mathrm{d}]i}\hat{n}_{[\mathrm{d}]j})m_{d_j}, \quad (\mathrm{N}_u)_{ij} = (-t_\beta\delta_{ij} + (t_\beta + t_\beta^{-1})\hat{n}^*_{[\mathrm{u}]i}\hat{n}_{[\mathrm{u}]j})m_{u_j}\,. \tag{6.32}$$

It is important to stress that $\hat{n}_{[\mathrm{d}]}$ and $\hat{n}_{[\mathrm{u}]}$ are not independent. From eq. (6.11),

$$\hat{n}_{[\mathrm{u}]i} V_{ij} = \hat{n}_{[\mathrm{d}]j}\,, \tag{6.33}$$

and thus only four new independent parameters (besides quark masses, CKM mixings and t_β) appear in eq. (6.32): two moduli, the third being fixed by normalization, and two relative phases, since the products $\hat{n}^*_{[\mathrm{q}]i}\hat{n}_{[\mathrm{q}]j}$ are insensitive to an overall phase.

[2]This is consistent with the fact that BGL can be recovered as a particular limit of generalized BGL models.

jBGL

The last case in this section is a new model presented here for the first time (see also [210]). It is a sort of "Flipped" generalized BGL, which follows from

$$\Phi_2 \mapsto e^{i\theta}\Phi_2, \quad Q^0_{L3} \mapsto e^{-i\theta}Q^0_{L3}, \quad d^0_{Rj} \mapsto e^{-i\theta}d^0_{Rj},\ j = 1,2,3\,. \tag{6.34}$$

The corresponding Yukawa coupling matrices are

$$\begin{aligned} Y_{d,1} &= \begin{pmatrix} 0 & 0 & 0 \\ 0 & 0 & 0 \\ \times & \times & \times \end{pmatrix}, \qquad Y_{d,2} = \begin{pmatrix} \times & \times & \times \\ \times & \times & \times \\ 0 & 0 & 0 \end{pmatrix}, \\ Y_{u,1} &= \begin{pmatrix} \times & \times & \times \\ \times & \times & \times \\ 0 & 0 & 0 \end{pmatrix}, \qquad Y_{u,2} = \begin{pmatrix} 0 & 0 & 0 \\ 0 & 0 & 0 \\ \times & \times & \times \end{pmatrix}. \end{aligned} \tag{6.35}$$

The *Left conditions* read in this case

$$\mathrm{N}^0_d = (t_\beta^{-1}\mathrm{P}_1 + t_\beta^{-1}\mathrm{P}_2 - t_\beta\mathrm{P}_3)\,\mathrm{M}^0_d\,, \quad \mathrm{N}^0_u = (-t_\beta\mathrm{P}_1 - t_\beta\mathrm{P}_2 + t_\beta^{-1}\mathrm{P}_3)\mathrm{M}^0_u\,. \tag{6.36}$$

Notice how, with respect to eq. (6.27), the structures of the down Yukawa matrices $Y_{d,1}$ and $Y_{d,2}$ are interchanged (while the Δ matrices remain the same).

Parametrization

Benefiting from the details given in the parametrization of the gBGL models of section 6.2.3, it is now straightforward to obtain

$$\begin{aligned} (\mathrm{N}_d)_{ij} &= (t_\beta^{-1}\delta_{ij} - (t_\beta + t_\beta^{-1})\hat{n}^*_{[\mathrm{d}]i}\hat{n}_{[\mathrm{d}]j})m_{d_j}\,, \\ (\mathrm{N}_u)_{ij} &= (-t_\beta\delta_{ij} + (t_\beta + t_\beta^{-1})\hat{n}^*_{[\mathrm{u}]i}\hat{n}_{[\mathrm{u}]j})m_{u_j}\,, \end{aligned} \tag{6.37}$$

where, again, $\hat{n}_{[\mathrm{u}]i}V_{ij} = \hat{n}_{[\mathrm{d}]j}$. Notice the difference in the t_β dependence of N_d in eq. (6.37), with respect to the gBGL case in eq. (6.32).

One can see that BGL is *not* a particular case of jBGL. Also, BGL is a particular limit of gBGL, and jBGL is a sort of "Flipped" gBGL. One might wonder whether there is some sort of "Flipped" BGL, *obtainable from an Abelian symmetry*, which arises as a suitable limit of jBGL. It is possible to see by inspection of the symmetry transformations in eq. (6.1) that such a case is not allowed.

6.2.4 Summary of models with *Left conditions*

We summarize in Table 6.1 the main properties of the different models discussed in the previous subsections, which obey *Left conditions*. For the BGL models of subsection 6.2.3 we display separately up and down type models (uBGL and dBGL respectively). Since we have started from *all* Abelian models consistent with

Model \ Properties	Sym.	Tree SFCNC	Parameters
G-W	$\mathbb{Z}_2$	$(\mathrm{N}_u)_{ij} \propto \delta_{ij} m_{u_j}$ $(\mathrm{N}_d)_{ij} \propto \delta_{ij} m_{d_j}$	t_β, m_{q_k}
uBGL (t)	$\mathbb{Z}_{n\geq 4}$	$(\mathrm{N}_u)_{ij} = \delta_{ij}(-t_\beta + (t_\beta + t_\beta^{-1})\delta_{j3}) m_{u_j}$ $(\mathrm{N}_d)_{ij} = (-t_\beta \delta_{ij} + (t_\beta + t_\beta^{-1}) V_{ti}^* V_{tj}) m_{d_j}$	V, t_β, m_{q_k}
dBGL (b)	$\mathbb{Z}_{n\geq 4}$	$(\mathrm{N}_u)_{ij} = (-t_\beta \delta_{ij} + (t_\beta + t_\beta^{-1}) V_{ib} V_{jb}^*) m_{u_j}$ $(\mathrm{N}_d)_{ij} = \delta_{ij}(-t_\beta + (t_\beta + t_\beta^{-1})\delta_{j3}) m_{d_j}$	V, t_β, m_{q_k}
gBGL	$\mathbb{Z}_2$	$(\mathrm{N}_u)_{ij} = (-t_\beta \delta_{ij} + (t_\beta + t_\beta^{-1}) \hat{n}^*_{[\mathrm{u}]i} \hat{n}_{[\mathrm{u}]j}) m_{u_j}$ $(\mathrm{N}_d)_{ij} = (-t_\beta \delta_{ij} + (t_\beta + t_\beta^{-1}) \hat{n}^*_{[\mathrm{d}]i} \hat{n}_{[\mathrm{d}]j}) m_{d_j}$	V, t_β, m_{q_k} $\hat{n}_{[\mathrm{q}]}(+4)$
jBGL	$\mathbb{Z}_{n\geq 2}$	$(\mathrm{N}_u)_{ij} = (-t_\beta \delta_{ij} + (t_\beta + t_\beta^{-1}) \hat{n}^*_{[\mathrm{u}]i} \hat{n}_{[\mathrm{u}]j}) m_{u_j}$ $(\mathrm{N}_d)_{ij} = (t_\beta^{-1} \delta_{ij} - (t_\beta + t_\beta^{-1}) \hat{n}^*_{[\mathrm{d}]i} \hat{n}_{[\mathrm{d}]j}) m_{d_j}$	V, t_β, m_{q_k} $\hat{n}_{[\mathrm{q}]}(+4)$

Table 6.1: Models obeying the *Left conditions* of eq. (6.7). For the uBGL and dBGL models we only show the SFCNC corresponding to one case, the *top* and *bottom* models, respectively. The first row shows Glashow-Weinberg models without tree level SFCNC for comparison.

non-zero masses and a CKM matrix not block diagonal [145], we are certain that Table 6.1 contains all models satisfying the *Left condition*. We recovered the BGL [133] and gBGL [1] models already present in the literature, and proved that there exists only one such new class of models, which we dubbed "jBGL".

6.3 Symmetry Controlled Models with Right Conditions

In the previous section we have explored 2HDM whose symmetry under the Abelian transformations in eq. (6.1) is supplemented by the requirement that the M_q^0 and

N_q^0 obey the relations in eq. (6.2), where L_q^0 in eq. (6.3) acts *on the left*. In this section we analyze symmetry based models where we impose the conditions of eq. (6.5), $\mathrm{N}_q^0 = \mathrm{M}_q^0 \mathrm{R}_\mathrm{q}^0$, where R_q^0 in eq. (6.6) acts *on the right*, that is, models which obey *Right conditions*.

6.3.1 Conditions in the mass basis

In the mass basis, eq. (6.5) reads

$$\mathrm{N}_d = \mathrm{M}_d \mathrm{R}_\mathrm{d} , \quad \mathrm{N}_u = \mathrm{M}_u \mathrm{R}_\mathrm{u} , \tag{6.38}$$

with the transformed matrices

$$\mathrm{R}_\mathrm{d} = \mathcal{U}_{d_R}^\dagger \mathrm{R}_\mathrm{d}^0 \mathcal{U}_{d_R}, \quad \mathrm{R}_\mathrm{u} = \mathcal{U}_{u_R}^\dagger \mathrm{R}_\mathrm{u}^0 \mathcal{U}_{u_R} , \tag{6.39}$$

and

$$\mathrm{R}_\mathrm{d} = r_1^{[d]} P_1^{[d_R]} + r_2^{[d]} P_2^{[d_R]} + r_3^{[d]} P_3^{[d_R]} , \quad \mathrm{R}_\mathrm{u} = r_1^{[u]} P_1^{[u_R]} + r_2^{[u]} P_2^{[u_R]} + r_3^{[u]} P_3^{[u_R]} . \tag{6.40}$$

The transformed projection operators are now

$$P_j^{[d_R]} \equiv \mathcal{U}_{d_R}^\dagger \mathrm{P}_j \mathcal{U}_{d_R}, \quad P_j^{[u_R]} \equiv \mathcal{U}_{u_R}^\dagger \mathrm{P}_j \mathcal{U}_{u_R} . \tag{6.41}$$

$P_j^{[d_R]}$ and $P_j^{[u_R]}$ are related via $\mathcal{U}_{u_R}^\dagger \mathcal{U}_{d_R}$, but, contrary to section 6.2.1, this right-handed analog of the CKM matrix is completely arbitrary. This straightforward yet crucial difference among models with *Left* and *Right conditions* will ultimately be responsible for the wider parametric freedom of the latter.

6.3.2 How to determine r_i

Repeating the steps in section 6.2.2, one can easily establish here the following rule book for the assignment of r_i in our models with *Right conditions*:

$$\begin{aligned} &\text{if } \left(Y_{d,1}\right)_{ai} \text{ exists, then } \; r_i^{[d]} = -t_\beta , \\ &\text{if } \left(Y_{d,2}\right)_{ai} \text{ exists, then } \; r_i^{[d]} = t_\beta^{-1} . \end{aligned} \tag{6.42}$$

One can also see that the up sector matrices $Y_{u,1}$ and $Y_{u,2}$, and the corresponding $r_i^{[u]}$ follow exactly the same rule.

6.3.3 Right Models

It is obvious that cases in which both R_d and R_u are proportional to the identity matrix have been discarded automatically by the discussion of models with *Left conditions*. But, for *Right conditions* it is still possible to have either $R_d \propto \mathbf{1}$ or $R_u \propto \mathbf{1}$ (but not both). Among the six different types of models which obey *Right conditions*, the first four have that property.

Type A

The first model follows from symmetry under

$$\Phi_2 \mapsto e^{i\theta}\Phi_2, \quad u^0_{R3} \mapsto e^{i\theta}u^0_{R3}\,. \tag{6.43}$$

The Yukawa coupling matrices in this case are

$$\begin{aligned} Y_{d,1} &= \begin{pmatrix} \times & \times & \times \\ \times & \times & \times \\ \times & \times & \times \end{pmatrix}, \qquad Y_{d,2} = \begin{pmatrix} 0 & 0 & 0 \\ 0 & 0 & 0 \\ 0 & 0 & 0 \end{pmatrix}, \\ Y_{u,1} &= \begin{pmatrix} \times & \times & 0 \\ \times & \times & 0 \\ \times & \times & 0 \end{pmatrix}, \qquad Y_{u,2} = \begin{pmatrix} 0 & 0 & \times \\ 0 & 0 & \times \\ 0 & 0 & \times \end{pmatrix}. \end{aligned} \tag{6.44}$$

We should mention that, as explained in appendix D.1.3, it is immaterial whether $Y_{u,1}$ contains the first two columns and $Y_{u,2}$ the third, or some other permutation is chosen.

Following the rule book in eq. (6.42) for the *Right conditions*, we find immediately

$$N^0_d = -t_\beta M^0_d, \quad N^0_u = M^0_u(-t_\beta P_1 - t_\beta P_2 + t_\beta^{-1} P_3)\,. \tag{6.45}$$

Parametrization

Since only $Y_{d,1}$ is non-zero, the down sector is trivial: $N_d = -t_\beta M_d$. For the up sector, however,

$$N_u = M_u(-t_\beta \mathbf{1} + (t_\beta + t_\beta^{-1}) P_3^{[u_R]})\,. \tag{6.46}$$

Similarly to the models in section 6.2, one can introduce a complex unitary vector $\hat{r}_{[u]}$

$$\hat{r}_{[u]j} \equiv (P_3 \mathcal{U}_{u_R})_{3j}\,, \tag{6.47}$$

in terms of which

$$\left(P_3^{[u_R]}\right)_{ij} = \hat{r}^*_{[\mathrm{u}]i}\hat{r}_{[\mathrm{u}]j}, \tag{6.48}$$

and thus

$$(\mathrm{N}_d)_{ij} = -m_{d_i}t_\beta\delta_{ij}, \quad (\mathrm{N}_u)_{ij} = m_{u_i}\left(-t_\beta\delta_{ij} + (t_\beta + t_\beta^{-1})\hat{r}^*_{[\mathrm{u}]i}\hat{r}_{[\mathrm{u}]j}\right). \tag{6.49}$$

Therefore, besides quark masses and t_β, only four new independent parameters appear in eq. (6.49).

Type B

The second model follows from the symmetry

$$\Phi_2 \mapsto e^{i\theta}\Phi_2, \quad u^0_{R1} \mapsto e^{i\theta}u^0_{R1}, \quad u^0_{R2} \mapsto e^{i\theta}u^0_{R2}. \tag{6.50}$$

The corresponding Yukawa coupling matrices are

$$\begin{aligned} Y_{d,1} &= \begin{pmatrix} \times & \times & \times \\ \times & \times & \times \\ \times & \times & \times \end{pmatrix}, \qquad Y_{d,2} = \begin{pmatrix} 0 & 0 & 0 \\ 0 & 0 & 0 \\ 0 & 0 & 0 \end{pmatrix}, \\ Y_{u,1} &= \begin{pmatrix} 0 & 0 & \times \\ 0 & 0 & \times \\ 0 & 0 & \times \end{pmatrix}, \qquad Y_{u,2} = \begin{pmatrix} \times & \times & 0 \\ \times & \times & 0 \\ \times & \times & 0 \end{pmatrix}. \end{aligned} \tag{6.51}$$

Notice how, with respect to the previous model in eq. (6.44), the forms of $Y_{u,1}$ and $Y_{u,2}$ are interchanged in eq. (6.51). Thus, our Type B model is a sort of Flipped Type A model. The *Right conditions* become

$$\mathrm{N}^0_d = -\mathrm{M}^0_d t_\beta \mathbf{1}, \quad \mathrm{N}^0_u = \mathrm{M}^0_u\left(+t_\beta^{-1}\mathrm{P}_1 + t_\beta^{-1}\mathrm{P}_2 - t_\beta\mathrm{P}_3\right). \tag{6.52}$$

Parametrization

Given the parametrization of the previous case, it follows immediately that in this case:

$$(\mathrm{N}_d)_{ij} = -m_{d_i}t_\beta\delta_{ij}, \quad (\mathrm{N}_u)_{ij} = m_{u_i}\left(+t_\beta^{-1}\delta_{ij} - (t_\beta + t_\beta^{-1})\hat{r}^*_{[\mathrm{u}]i}\hat{r}_{[\mathrm{u}]j}\right). \tag{6.53}$$

Notice the different t_β dependence in eq. (6.53) with respect to eq. (6.49).

Type C

The transformation properties for this model are

$$\Phi_2 \mapsto e^{i\theta}\Phi_2, \quad d^0_{R3} \mapsto e^{-i\theta} d^0_{R3}, \tag{6.54}$$

and the *Right conditions* read

$$\mathrm{N}^0_d = \mathrm{M}^0_d(-t_\beta \mathrm{P}_1 - t_\beta \mathrm{P}_2 + t_\beta^{-1}\mathrm{P}_3), \quad \mathrm{N}^0_u = -t_\beta \mathrm{M}^0_u\,. \tag{6.55}$$

The Yukawa coupling matrices are in this case

$$\begin{aligned} Y_{d,1} &= \begin{pmatrix} \times & \times & 0 \\ \times & \times & 0 \\ \times & \times & 0 \end{pmatrix}, \qquad Y_{d,2} = \begin{pmatrix} 0 & 0 & \times \\ 0 & 0 & \times \\ 0 & 0 & \times \end{pmatrix}, \\ Y_{u,1} &= \begin{pmatrix} \times & \times & \times \\ \times & \times & \times \\ \times & \times & \times \end{pmatrix}, \qquad Y_{u,2} = \begin{pmatrix} 0 & 0 & 0 \\ 0 & 0 & 0 \\ 0 & 0 & 0 \end{pmatrix}. \end{aligned} \tag{6.56}$$

Parametrization

Since

$$\mathrm{N}_d = \mathrm{M}_d(-t_\beta \mathbf{1} + (t_\beta + t_\beta^{-1})P_3^{[d_R]}), \quad \mathrm{N}_u = -t_\beta \mathrm{M}_u\,, \tag{6.57}$$

defining

$$\hat{r}_{[\mathrm{d}]j} \equiv (\mathrm{P}_3 \mathcal{U}_{d_R})_{3j}\,, \tag{6.58}$$

and

$$\left(P_3^{[d_R]}\right)_{ij} = \hat{r}^*_{[\mathrm{d}]i}\hat{r}_{[\mathrm{d}]j}, \tag{6.59}$$

we find

$$(\mathrm{N}_d)_{ij} = m_{d_i}(-t_\beta \delta_{ij} + (t_\beta + t_\beta^{-1})\hat{r}^*_{[\mathrm{d}]i}\hat{r}_{[\mathrm{d}]j}), \quad (\mathrm{N}_u)_{ij} = -t_\beta m_{u_i}\delta_{ij}\,, \tag{6.60}$$

implying that, besides quark masses and t_β, only four new independent parameters appear in eq. (6.60). A particular case of these models appears in ref. [139], with all coefficients taken as real in order to have an exclusive spontaneous origin for CP violation (no CKM CP violation). As such, there are in ref. [139] only two instead of four parameters arising from $\hat{r}_{[\mathrm{d}]j}$.

Type D

The transformation properties for this model are

$$\Phi_2 \mapsto e^{i\theta}\Phi_2, \quad d^0_{R1} \mapsto e^{-i\theta}d^0_{R1}, \quad d^0_{R2} \mapsto e^{-i\theta}d^0_{R2}, \tag{6.61}$$

and the *Right conditions* read

$$\mathrm{N}^0_d = \mathrm{M}^0_d(+t_\beta^{-1}\mathrm{P}_1 + t_\beta^{-1}\mathrm{P}_2 - t_\beta\mathrm{P}_3), \quad \mathrm{N}^0_u = -t_\beta\mathrm{M}^0_u\,. \tag{6.62}$$

The Yukawa coupling matrices are in this case

$$\begin{aligned} Y_{d,1} &= \begin{pmatrix} 0 & 0 & \times \\ 0 & 0 & \times \\ 0 & 0 & \times \end{pmatrix}, \qquad Y_{d,2} = \begin{pmatrix} \times & \times & 0 \\ \times & \times & 0 \\ \times & \times & 0 \end{pmatrix}, \\ Y_{u,1} &= \begin{pmatrix} \times & \times & \times \\ \times & \times & \times \\ \times & \times & \times \end{pmatrix}, \qquad Y_{u,2} = \begin{pmatrix} 0 & 0 & 0 \\ 0 & 0 & 0 \\ 0 & 0 & 0 \end{pmatrix}. \end{aligned} \tag{6.63}$$

Parametrization

Here

$$\mathrm{N}_d = \mathrm{M}_d(t_\beta^{-1}\mathbf{1} - (t_\beta + t_\beta^{-1})P_3^{[d_R]}), \quad \mathrm{N}_u = -t_\beta\mathrm{M}_u\,, \tag{6.64}$$

from which

$$(\mathrm{N}_d)_{ij} = m_{d_i}(t_\beta^{-1}\delta_{ij} - (t_\beta + t_\beta^{-1})\hat{r}^*_{[\mathrm{d}]i}\hat{r}_{[\mathrm{d}]j}), \quad (\mathrm{N}_u)_{ij} = -t_\beta m_{u_i}\delta_{ij}\,. \tag{6.65}$$

Therefore, besides quark masses and t_β, only four new independent parameters appear in eq. (6.65).

Type E

The transformation properties for this model are

$$\Phi_2 \mapsto e^{i\theta}\Phi_2, \quad d^0_{R3} \mapsto e^{-i\theta}d^0_{R3}, \quad u^0_{R3} \mapsto e^{i\theta}u^0_{R3}, \tag{6.66}$$

and the corresponding Yukawa coupling matrices are

$$\begin{aligned} Y_{d,1} &= \begin{pmatrix} \times & \times & 0 \\ \times & \times & 0 \\ \times & \times & 0 \end{pmatrix}, \qquad Y_{d,2} = \begin{pmatrix} 0 & 0 & \times \\ 0 & 0 & \times \\ 0 & 0 & \times \end{pmatrix}, \\ Y_{u,1} &= \begin{pmatrix} \times & \times & 0 \\ \times & \times & 0 \\ \times & \times & 0 \end{pmatrix}, \qquad Y_{u,2} = \begin{pmatrix} 0 & 0 & \times \\ 0 & 0 & \times \\ 0 & 0 & \times \end{pmatrix}, \end{aligned} \tag{6.67}$$

leading to the *Right conditions*

$$\mathrm{N}_d^0 = \mathrm{M}_d^0(-t_\beta \mathrm{P}_1 - t_\beta \mathrm{P}_2 + t_\beta^{-1}\mathrm{P}_3), \quad \mathrm{N}_u^0 = \mathrm{M}_u^0(-t_\beta \mathrm{P}_1 - t_\beta \mathrm{P}_2 + t_\beta^{-1}\mathrm{P}_3)\,. \tag{6.68}$$

Parametrization

While in the previous models one quark sector had a trivial structure (since $\Gamma_2 = 0$ in types A and B, while $\Delta_2 = 0$ in types C and D), that is not the case in eq. (6.67), and one naturally expects an increase in the number of parameters. An appropriate parametrization is obtained along the same lines as before. With

$$\mathrm{N}_d = \mathrm{M}_d(-t_\beta \mathbf{1} + (t_\beta + t_\beta^{-1})P_3^{[d_R]})\,, \quad \mathrm{N}_u = \mathrm{M}_u(-t_\beta \mathbf{1} + (t_\beta + t_\beta^{-1})P_3^{[u_R]})\,, \tag{6.69}$$

but *two* complex unitary vectors are now necessary, $\hat{r}_{[\mathrm{d}]}$ and $\hat{r}_{[\mathrm{u}]}$, defined by

$$\hat{r}_{[\mathrm{d}]j} \equiv (\mathrm{P}_3 \mathcal{U}_{d_R})_{3j}\,, \quad \hat{r}_{[\mathrm{u}]j} \equiv (\mathrm{P}_3 \mathcal{U}_{u_R})_{3j}\,, \tag{6.70}$$

and in terms of which

$$\left(P_3^{[d_R]}\right)_{ij} = \hat{r}^*_{[\mathrm{d}]i}\hat{r}_{[\mathrm{d}]j}\,, \quad \left(P_3^{[u_R]}\right)_{ij} = \hat{r}^*_{[\mathrm{u}]i}\hat{r}_{[\mathrm{u}]j}\,. \tag{6.71}$$

The parametrization of this model is then

$$(\mathrm{N}_d)_{ij} = m_{d_i}(-t_\beta \delta_{ij} + (t_\beta + t_\beta^{-1})\hat{r}^*_{[\mathrm{d}]i}\hat{r}_{[\mathrm{d}]j}), \quad (\mathrm{N}_u)_{ij} = m_{u_i}(-t_\beta \delta_{ij} + (t_\beta + t_\beta^{-1})\hat{r}^*_{[\mathrm{u}]i}\hat{r}_{[\mathrm{u}]j})\,. \tag{6.72}$$

It is important to notice that now, besides the quark masses and t_β, four new independent real parameters enter eq. (6.72) via $\hat{r}_{[\mathrm{d}]j}$ and another four via $\hat{r}_{[\mathrm{u}]j}$. Contrary to the situation in models with *Left conditions* in section 6.2, where the CKM matrix ties $\hat{n}_{[\mathrm{u}]}$ and $\hat{n}_{[\mathrm{d}]}$, and it is fixed or given by another sector of the complete model (the couplings of quarks to the W gauge boson), in models with *Right conditions* there is no analog of the CKM matrix to connect $\hat{r}_{[\mathrm{u}]}$ and $\hat{r}_{[\mathrm{d}]}$ in a fixed manner[3].

[3]Interpreting the situation the other way around, eq. (6.72) would provide a window of sensitivity to the right-handed analog of CKM (for example, in extensions to models with a gauged $SU(2)_L \otimes SU(2)_R$ symmetry).

Type F

The transformation properties of this last model are

$$\Phi_2 \mapsto e^{i\theta}\Phi_2, \quad d^0_{R3} \mapsto e^{-i\theta} d^0_{R3}, \quad u^0_{R1} \mapsto e^{i\theta} u^0_{R1}, \quad u^0_{R2} \mapsto e^{i\theta} u^0_{R2}, \tag{6.73}$$

and the corresponding Yukawa coupling matrices have the following form:

$$\begin{aligned} Y_{d,1} &= \begin{pmatrix} \times & \times & 0 \\ \times & \times & 0 \\ \times & \times & 0 \end{pmatrix}, \qquad Y_{d,2} = \begin{pmatrix} 0 & 0 & \times \\ 0 & 0 & \times \\ 0 & 0 & \times \end{pmatrix}, \\ Y_{u,1} &= \begin{pmatrix} 0 & 0 & \times \\ 0 & 0 & \times \\ 0 & 0 & \times \end{pmatrix}, \qquad Y_{u,2} = \begin{pmatrix} \times & \times & 0 \\ \times & \times & 0 \\ \times & \times & 0 \end{pmatrix}. \end{aligned} \tag{6.74}$$

Notice how, with respect to the previous model in eq. (6.67), the forms of $Y_{u,1}$ and $Y_{u,2}$ are interchanged in eq. (6.74). Thus, our Type F model is a sort of Flipped Type E model. The *Right conditions* become

$$\mathrm{N}^0_d = \mathrm{M}^0_d(-t_\beta \mathrm{P}_1 - t_\beta \mathrm{P}_2 + t_\beta^{-1}\mathrm{P}_3), \quad \mathrm{N}^0_u = \mathrm{M}^0_u(t_\beta^{-1}\mathrm{P}_1 + t_\beta^{-1}\mathrm{P}_2 - t_\beta \mathrm{P}_3)\,. \tag{6.75}$$

Parametrization

Parametrising this last model follows trivially from the previous one:

$$(\mathrm{N}_d)_{ij} = m_{d_i}(-t_\beta \delta_{ij} + (t_\beta + t_\beta^{-1})\hat{r}^*_{[\mathrm{d}]i}\hat{r}_{[\mathrm{d}]j}), \quad (\mathrm{N}_u)_{ij} = m_{u_i}(t_\beta^{-1}\delta_{ij} - (t_\beta + t_\beta^{-1})\hat{r}^*_{[\mathrm{u}]i}\hat{r}_{[\mathrm{u}]j})\,. \tag{6.76}$$

The same comments made in Type E apply to the parameter count in Type F models: besides the quark masses and t_β, as in eq. (6.72), four new independent real parameters enter eq. (6.76) via $\hat{r}_{[\mathrm{d}]j}$ and another four via $\hat{r}_{[\mathrm{u}]j}$.

6.3.4 Summary of models with *Right conditions*

We summarize in Table 6.2 the main properties of the different models discussed in the previous subsections, which obey *Right conditions*.

Properties / Model	Sym.	Tree SFCNC	Parameters
G-W	$\mathbb{Z}_2$	$(\mathrm{N}_u)_{ij} \propto m_{u_i}\delta_{ij}$ $(\mathrm{N}_d)_{ij} \propto m_{d_i}\delta_{ij}$	t_β, m_{q_k}
Type A	$\mathbb{Z}_{n\geq 2}$	$(\mathrm{N}_u)_{ij} = m_{u_i}(-t_\beta\delta_{ij} + (t_\beta + t_\beta^{-1})\hat{r}^*_{[\mathrm{u}]i}\hat{r}_{[\mathrm{u}]j})$ $(\mathrm{N}_d)_{ij} = -m_{d_i}t_\beta\delta_{ij}$	t_β, m_{q_k} $\hat{r}_{[\mathrm{u}]}(+4)$
Type B	$\mathbb{Z}_{n\geq 2}$	$(\mathrm{N}_u)_{ij} = m_{u_i}(t_\beta^{-1}\delta_{ij} - (t_\beta + t_\beta^{-1})\hat{r}^*_{[\mathrm{u}]i}\hat{r}_{[\mathrm{u}]j})$ $(\mathrm{N}_d)_{ij} = -m_{d_i}t_\beta\delta_{ij}$	t_β, m_{q_k} $\hat{r}_{[\mathrm{u}]}(+4)$
Type C	$\mathbb{Z}_{n\geq 2}$	$(\mathrm{N}_u)_{ij} = -m_{u_i}t_\beta\delta_{ij}$ $(\mathrm{N}_d)_{ij} = m_{d_i}(-t_\beta\delta_{ij} + (t_\beta + t_\beta^{-1})\hat{r}^*_{[\mathrm{d}]i}\hat{r}_{[\mathrm{d}]j})$	t_β, m_{q_k} $\hat{r}_{[\mathrm{d}]}(+4)$
Type D	$\mathbb{Z}_{n\geq 2}$	$(\mathrm{N}_u)_{ij} = -m_{u_i}t_\beta\delta_{ij}$ $(\mathrm{N}_d)_{ij} = m_{d_i}(t_\beta^{-1}\delta_{ij} - (t_\beta + t_\beta^{-1})\hat{r}^*_{[\mathrm{d}]i}\hat{r}_{[\mathrm{d}]j})$	t_β, m_{q_k} $\hat{r}_{[\mathrm{d}]}(+4)$
Type E	$\mathbb{Z}_{n\geq 2}$	$(\mathrm{N}_u)_{ij} = m_{u_i}(-t_\beta\delta_{ij} + (t_\beta + t_\beta^{-1})\hat{r}^*_{[\mathrm{u}]i}\hat{r}_{[\mathrm{u}]j})$ $(\mathrm{N}_d)_{ij} = m_{d_i}(-t_\beta\delta_{ij} + (t_\beta + t_\beta^{-1})\hat{r}^*_{[\mathrm{d}]i}\hat{r}_{[\mathrm{d}]j})$	t_β, m_{q_k} $\hat{r}_{[\mathrm{u}]}$,$\hat{r}_{[\mathrm{d}]}(+8)$
Type F	$\mathbb{Z}_{n\geq 2}$	$(\mathrm{N}_u)_{ij} = m_{u_i}(t_\beta^{-1}\delta_{ij} - (t_\beta + t_\beta^{-1})\hat{r}^*_{[\mathrm{u}]i}\hat{r}_{[\mathrm{u}]j})$ $(\mathrm{N}_d)_{ij} = m_{d_i}(-t_\beta\delta_{ij} + (t_\beta + t_\beta^{-1})\hat{r}^*_{[\mathrm{d}]i}\hat{r}_{[\mathrm{d}]j})$	t_β, m_{q_k} $\hat{r}_{[\mathrm{u}]}$,$\hat{r}_{[\mathrm{d}]}(+8)$

Table 6.2: Models obeying *Right conditions*, eq. (6.38). As in Table 6.1, the first row shows Glashow-Weinberg models without tree level SFCNC for comparison.

Part III

Phenomenology

–Come, Mr. Frodo!– he cried– I can't carry it for you, but I can carry you.

— SAMwise Gamgee, *The Lord of the Rings*, J. R. R. Tolkien

7 Constraints

In this section we discuss the different constraints that can play a relevant role in the detailed analyses that are going to be presented in this part of the thesis. In order to study the allowed parameters space for a given model one has to build a likelihood or a χ^2 function with the model's theoretical predictions and the corresponding experimental observations. In our case, each constraint is implemented as a χ^2 function and then a global χ^2 function, the sum of all separate contributions, is used to drive the analyses and represent the relevant regions for different parameters and observables. For an efficient exploration of parameter space we employ Markov chain Monte Carlo techniques.

The usual form $\chi^2_{\mathcal{O}} = \left(\frac{\mathcal{O}_{\rm Th}-\mathcal{O}_{\rm Exp}}{\sigma_{\rm Exp}}\right)^2$ is adopted for the constraint corresponding to an observable $\mathcal{O}$, where the experimental input is a measurement $\mathcal{O}_{\rm Exp}$ with uncertainty $\sigma_{\rm Exp}$ and the theoretical prediction is $\mathcal{O}_{\rm Th}$ (for correlated measurements or asymmetric uncertainties, appropriate modifications are incorporated). Not all constraints are implemented through the usual χ^2 form: it is not adequate to incorporate the bounds for perturbativity requirements of the Yukawa couplings in subsection 7.2 and the bounds obtained in LHC searches in subsection 9.2.3. In those cases, instead of sharp bounds or cuts, the bounds are implemented as described in the respective subsections.

7.1 Scalar sector

For the scalar sector, given the fact that in the two analyses presented in chapters 8 and 9 the CP-conserving limit is adopted, we use the set of independent parameters $\{v, \mathrm{m_h}, m_{\mathrm{H}}, m_{\mathrm{A}}, m_{\mathrm{H}^\pm}, t_\beta, \alpha - \beta, \mu_{12}^2\}$ (from which the quartic parameters λ_j are obtained) with $v = 246$ GeV and $\mathrm{m_h} = 125$ GeV. We require the potential to be bounded from below following the method in [211], we also require the quartic parameters to respect perturbativity and perturbative unitarity in $2 \to 2$ scattering [177, 178, 212, 213] (see also [179, 214, 215]).

Regarding perturbativity, we require the absolute value of quartic parameters to be small enough to remain perturbative, in particular, we impose $|\lambda_j| < 4\pi$. For the perturbative unitarity one has to impose the eigenvalues of the $2 \to 2$ scattering matrices (see appendix A from Ref. [215]) to be smaller than one. In the CP-conserving scalar potential we get:

$$
\begin{aligned}
&|\lambda_3 + \lambda_4| < 8\pi\,, && |\lambda_3 - \lambda_4| < 8\pi\,,\\
&\left|\lambda_3 + 2\lambda_4 - 3\lambda_5^2\right| < 8\pi\,, && \left|\lambda_3 + 2\lambda_4 + 3\lambda_5^2\right| < 8\pi\,,\\
&\left|\lambda_1 + \lambda_2 - \sqrt{(\lambda_1 - \lambda_2)^2 + 4\lambda_5^2}\right| < 16\pi\,, && \left|\lambda_1 + \lambda_2 + \sqrt{(\lambda_1 - \lambda_2)^2 + 4\lambda_5^2}\right| < 16\pi\,,\\
&\left|\lambda_1 + \lambda_2 - \sqrt{(\lambda_1 - \lambda_2)^2 + 4\lambda_4^2}\right| < 16\pi\,, && \left|\lambda_1 + \lambda_2 + \sqrt{(\lambda_1 - \lambda_2)^2 + 4\lambda_4^2}\right| < 16\pi\,,\\
&\left|3\lambda_1 + 3\lambda_2 - \sqrt{9(\lambda_1 - \lambda_2)^2 + 4(2\lambda_3 + \lambda_4)^2}\right| < 16\pi\,,\\
&\left|3\lambda_1 + 3\lambda_2 + \sqrt{9(\lambda_1 - \lambda_2)^2 + 4(2\lambda_3 + \lambda_4)^2}\right| < 16\pi\,.
\end{aligned}
\tag{7.1}
$$

Finally the corrections to the oblique parameters in the CP-conserving limit read

$$
\begin{aligned}
\Delta T = \frac{1}{16\,\pi\, m_{\mathrm{W}}^2\, s_{\mathrm{W}}^2} \Big\{ & c_{\alpha\beta}^2 \mathcal{F}\left(m_{\mathrm{H}^\pm}^2, \mathrm{m_h}^2\right) + s_{\alpha\beta}^2 \mathcal{F}\left(m_{\mathrm{H}^\pm}^2, m_{\mathrm{H}}^2\right) + \mathcal{F}\left(m_{\mathrm{H}^\pm}^2, m_{\mathrm{A}}^2\right)\\
& - c_{\alpha\beta}^2 \mathcal{F}\left(\mathrm{m_h}^2, m_{\mathrm{A}}^2\right) - s_{\alpha\beta}^2 \mathcal{F}\left(m_{\mathrm{A}}^2, m_{\mathrm{H}}^2\right)\\
& + 3 c_{\alpha\beta}^2 \Big[\mathcal{F}\left(m_{\mathrm{Z}}^2, m_{\mathrm{H}}^2\right) - \mathcal{F}\left(m_{\mathrm{W}}^2, m_{\mathrm{H}}^2\right)\\
& \qquad - \mathcal{F}\left(m_{\mathrm{Z}}^2, \mathrm{m_h}^2\right) + \mathcal{F}\left(m_{\mathrm{W}}^2, \mathrm{m_h}^2\right) \Big] \Big\}\,,
\end{aligned}
\tag{7.2}
$$

and

$$\begin{aligned}\Delta S = \frac{1}{24\,\pi}\Bigg\{ &\log\left(\frac{m_{\mathrm{H}}^2 m_{\mathrm{A}}^2}{m_{\mathrm{H}^\pm}^4}\right) + \left(2\sin^2(\theta_{\mathrm{W}}) - 1\right)^2 \mathcal{G}\left(m_{\mathrm{H}^\pm}^2, m_{\mathrm{H}^\pm}^2\right) \\ &+ c_{\alpha\beta}^2 \mathcal{G}\left(\mathrm{m}_{\mathrm{h}}^2, m_{\mathrm{A}}^2\right) + s_{\alpha\beta}^2 \mathcal{G}\left(m_{\mathrm{H}}^2, m_{\mathrm{A}}^2\right) \\ &+ c_{\alpha\beta}^2 \left[\hat{\mathcal{G}}\left(\mathrm{m}_{\mathrm{h}}^2\right) + \hat{\mathcal{G}}\left(m_{\mathrm{H}}^2\right)\right]\Bigg\}.\end{aligned} \tag{7.3}$$

The oblique functions $\mathcal{F}$, $\mathcal{G}$ and $\hat{\mathcal{G}}$ are defined as [216, 217]

$$\begin{aligned}\mathcal{F}(x,y) &= \begin{cases} \frac{x+y}{2} - \frac{xy}{x-y}\log\frac{x}{y} & \text{if} \quad x \neq y \\ 0 & \text{if} \quad x = y \end{cases}, \\ \mathcal{G}(x,y) &= -\frac{16}{3} + \frac{5(x+y)}{m_{\mathrm{Z}}^2} - \frac{2(x+y)^2}{m_{\mathrm{Z}}^4} \\ &\quad + \frac{3}{m_{\mathrm{Z}}^2}\left[\frac{x^2+y^2}{x-y} - \frac{x^2-y^2}{m_{\mathrm{Z}}^2} + \frac{(x-y)^3}{3m_{\mathrm{Z}}^4}\right]\log\frac{x}{y} + \frac{r}{m_{\mathrm{Z}}^6} f(t,r)\,, \\ \hat{\mathcal{G}}(x) &= \mathcal{G}(x, m_{\mathrm{Z}}^2) + 12\,\tilde{\mathcal{G}}(x, m_{\mathrm{Z}}^2)\,,\end{aligned} \tag{7.4}$$

with

$$\tilde{\mathcal{G}}(x,y) = -2 + \left(\frac{x-y}{m_{\mathrm{Z}}^2} - \frac{x+y}{x-y}\right)\log\frac{x}{y} + \frac{f(t,r)}{m_{\mathrm{Z}}^2}\,, \tag{7.5}$$

where $t \equiv x + y - m_{\mathrm{Z}}^2$ and $r \equiv m_{\mathrm{Z}}^4 - 2m_{\mathrm{Z}}^2(x+y) + (x-y)^2$ and for compactness the function $f(t,r)$ has been defined as

$$f(t,r) = \begin{cases} \sqrt{r}\log\left|\frac{t-\sqrt{r}}{t+\sqrt{r}}\right| & , \quad r > 0\,, \\ 0 & , \quad r = 0\,, \\ 2\sqrt{-r}\arctan\frac{\sqrt{-r}}{t} & , \quad r < 0\,. \end{cases} \tag{7.6}$$

The oblique parameters S and T only depend on the scalar masses and on the scalar rotation matrix $\mathcal{R} \equiv \mathcal{R}_{[3]}(\vec{\alpha})$ in eq. (2.14). In the CP-conserving limit the only parameter besides the scalar masses is $\alpha - \beta$. The oblique parameters have to be in agreement with electroweak precision data [217], leading to the experimental values $\Delta S = 0.05 \pm 0.09$ and $\Delta T = 0.09 \pm 0.07$ with a correlation facotr of $\rho_{S,T} = 0.91$.

7.2 Fermion sector

In the fermion sector, the new couplings n_ℓ arise from the dimensionless Yukawa couplings $y_{jk}^f = (Y_f)_{jk}$ in eq. (2.26). If one required that Yukawa couplings remain perturbative, for example not exceeding $\mathcal{O}(1)$ values, this would translate into y_{jk}^f's smaller than $v/\sqrt{2} \simeq 174$ GeV. We adopt a more conservative approach, and

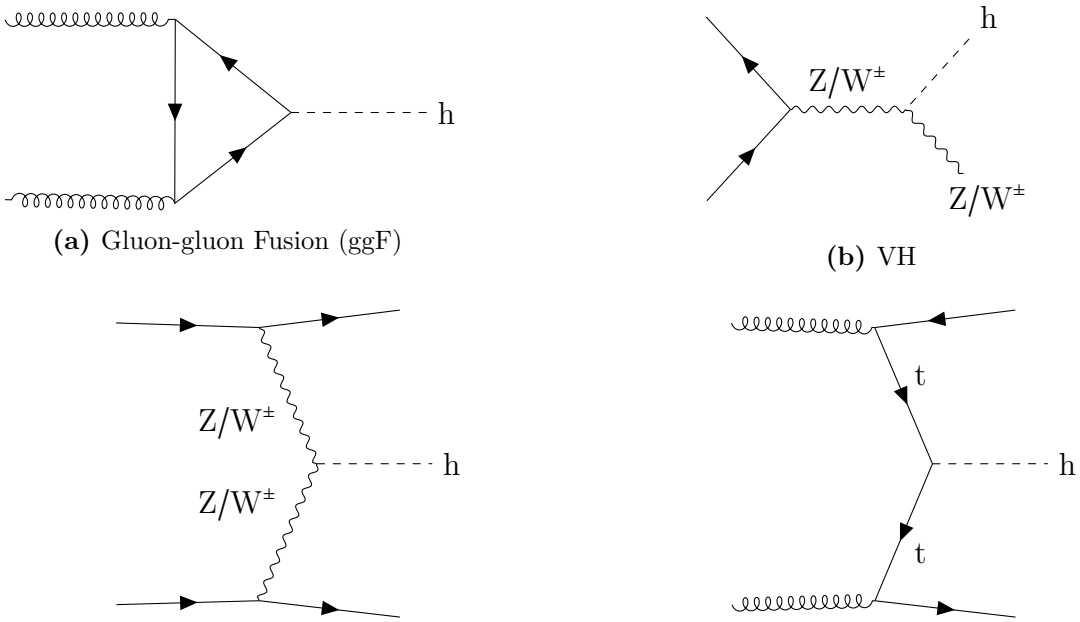

(a) Gluon-gluon Fusion (ggF)

(b) VH

(c) Vector Boson Fusion (VBF)

(d) ttH

Figure 7.1: Higgs production mechanisms included in the signal strengths constraints.

include a contribution of the following form to the global χ^2 function driving the numerical analyses

$$\chi^2_{\text{Pert}}(y^f_{jk}) = \begin{cases} 0, \text{ for } \left|y^f_{jk}\right| \leq y_0, \\ \left(\frac{\left|y^f_{jk}\right| - y_0}{\sigma_{y_0}}\right)^2, \text{ for } \left|y^f_{jk}\right| > y_0. \end{cases} \tag{7.7}$$

We choose $y_0 = 95$ GeV and $\sigma_{y_0} = 1$ GeV. One could have adopted a crude requirement such as imposing for example $\left|y^f_{jk}\right| \leq 100$ GeV with a sharp cut: eq. (7.7) is simply a smooth version (more convenient for numerical purposes) of that kind of requirement.

7.3 Higgs signal strengths

Concerning the 125 GeV Higgs-like scalar, agreement with the observed signal strengths, that is production cross section × decay branching ratio of the usual channels should also be imposed. These observables impose constraints on n_j [1] and $c_{\alpha\beta}$. The dominant Higgs production mechanisms, gluon-gluon Fusion (ggF), Vector Boson Fusion (VBF), Z and W$^\pm$ bremsstrahlung (VH) and top-top Fusion (ttH) are

[1] In the case of I-gℓFC and II-gℓFC the parameter n_j will be $t_\beta^{-1} m_j$ or $t_\beta m_j$ depending on the model and the sector.

Channel	ggF	VBF	VH	ttH
$b\bar{b}$	×	$0.99^{+0.36}_{-0.34}$[218]	$1.02^{+0.18}_{-0.17}$[219] $WH \to 0.95^{+0.27}_{-0.25}$[219] $ZH \to 1.08^{+0.25}_{-0.23}$[219]	$0.43^{+0.36}_{-0.33}$[220]
$\gamma\gamma$	1.02 ± 0.12[221]	$1.34^{+0.26}_{-0.24}$[221]	$WH \to 2.33^{+0.55}_{-0.50}$[221] $ZH \to -0.64^{+0.61}_{-0.57}$[221]	$0.92^{+0.27}_{-0.24}$[221]
$\mu^+\mu^-$	0.5 ± 2.3 [222]	1.8 ± 1.0[222]	VH+ttH 5.0 ± 3.5 [222]	
$\tau^+\tau^-$	$1.02^{+0.60}_{-0.55}$[223]	$1.15^{+0.57}_{-0.53}$[223]	×	$1.20^{+1.07}_{-0.93}$[223]
WW	$1.08^{+0.19}_{-0.18}$[223]	$0.60^{+0.36}_{-0.34}$[223]	$WH \to 2.3^{+1.2}_{-1.0}$[224] $ZH \to 2.9^{+1.9}_{-1.3}$[224]	$1.72^{+0.56}_{-0.53}$[223]
ZZ	0.96 ± 0.11[225]	$1.21^{+0.50}_{-0.41}$[225]	$1.44^{+1.17}_{-0.92}$[225]	$1.7^{+1.7}_{-1.2}$[225]

Table 7.1: Higgs signal strengths for different production ($\sqrt{s}$ = 13TeV) and decay channels measured by ATLAS.

included (see figure 7.1). The signal strength of a given production channel ($p = ggF, VBF, VH, ttH$) and a given decay mode ($d = b\bar{b}, \gamma\gamma, \tau^+\tau^-, \mu^+\mu^-, WW, ZZ$) is defined as

$$\mu_p^d = \frac{\left[\sigma_p \times \mathrm{Br}\left(\mathrm{h} \to d\right)\right]_{\mathrm{Exp}}}{\left[\sigma_p \times \mathrm{Br}\left(\mathrm{h} \to d\right)\right]_{\mathrm{SM}}} . \tag{7.8}$$

Here the cross section and the branching ratio can be factorized since the narrow width approximation (NWA) is being used. The experimental information used to constraint the parameter space is provided by ATLAS and CMS. The most recent data from LHC can be found in tables 7.1 and 7.2. All the experimental values are compatible with the SM ($\mu_p^d = 1$).

In connection to them, additional attention should be paid to the decays of h into light fermions since enhanced decays into light fermions can increase the total width and modify the precise SM pattern of branching ratios. For the different couplings to fermions $\mathscr{L}_{\mathrm{h}} = -\frac{m_f}{v}\mathrm{h}\bar{f}(a_f^{\mathrm{h}} + ib_f^{\mathrm{h}}\gamma_5)f$ in eq. (2.49), we have a scalar term a_f^{h}, straightforward to compare with the SM one,

$$a_f^{\mathrm{h}}: \qquad \mathrm{SM}: 1 \;\mapsto\; \mathrm{gFC\text{-}2HDM}: \left(s_{\alpha\beta} + c_{\alpha\beta}\,\frac{\mathrm{Re}\,(n_f)}{m_f}\right), \tag{7.9}$$

and a pseudoscalar term b_f^{h} absent in the SM,

$$b_f^{\mathrm{h}}: \qquad \mathrm{SM}: 0 \;\mapsto\; \mathrm{gFC\text{-}2HDM}: c_{\alpha\beta}\frac{\mathrm{Im}\,(n_f)}{m_f} . \tag{7.10}$$

Channel	ggF	VBF	VH	ttH
$b\bar{b}$	$2.45^{+2.53}_{-2.35}$[226]	$1.3^{+1.2}_{-1.1}$[227]	$WH \to 1.27^{+0.42}_{-0.40}$[226] $ZH \to 0.93^{+0.33}_{-0.31}$[226]	$1.13^{+0.33}_{-0.30}$[226]
$\gamma\gamma$	$1.07^{+0.12}_{-0.11}$[228]	$1.04^{+0.34}_{-0.31}$[228]	$1.34^{+0.36}_{-0.33}$[228] $WH \to 1.35^{+0.55}_{-0.49}$[228] $ZH \to 1.32^{+0.76}_{-0.65}$[228]	$1.00^{+0.37}_{-0.35}$[228]
$\mu^+\mu^-$	$0.63^{+0.65}_{-0.64}$[229]	$1.36^{+0.69}_{-0.61}$ [229]	$5.48^{+3.10}_{-2.83}$[229]	$2.32^{+2.27.}_{-1.95}$[229]
$\tau^+\tau^-$	$0.39^{+0.38}_{-0.39}$[226]	$1.05^{+0.30}_{-0.29}$[226]	$WH \to 3.01^{+1.65}_{-1.51}$[226] $ZH \to 1.53^{+1.60}_{-1.37}$[226]	$0.81^{+0.74}_{-0.67}$[226]
WW	$1.28^{+0.20}_{-0.19}$[226]	$0.63^{+0.65}_{-0.61}$[226]	$WH \to 2.85^{+2.11}_{-1.87}$[226] $ZH \to 0.90^{+1.77}_{-1.43}$[226]	$0.93^{+0.48}_{-0.45}$[226]
ZZ	$0.98^{+0.12}_{-0.11}$[226]	$0.57^{+0.46}_{-0.36}$[226]	$WH \to 1.66^{+1.74}_{-1.66}$[230] $ZH \to 0.00^{+5.44}_{-0.00}$[230]	$0.25^{+1.03}_{-0.25}$[226]

Table 7.2: Higgs signal strengths for different production ($\sqrt{s}$ = 13TeV) and decay channels measured by CMS.

However, the Yukawa couplings of the neutral light Higgs are not the only ones which are affected with respect to the SM. For example, owing to the mixing in the scalar sector, the couplings hVV ($V = W, Z$) are also modified. This term afects both in the production, via VBF or VH (see section 7.3), and in decay trough the ZZ and WW decay channels. In particular the SM and gFC couplings read

$$\mathrm{h}VV, \qquad \mathrm{SM}: m_V \;\mapsto\; \text{gFC-2HDM}: s_{\alpha\beta}\, m_V\,. \tag{7.11}$$

Constraints on the total width Γ_h, arising from off-shell (ggF+VBF)$\to \mathrm{h}^{(*)} \to WW^{(*)}$ [231], are also included [232, 233], even if in the models considered in this thesis their effect is negligible in the alignment limit. For additional details, see [2, 143, 196]. In the following we review how the decay channels and productions mechanisms are affected in the gFC with respect to the SM.

Decay channels

The light Higgs decay width into fermions has the general form

$$\Gamma(\mathrm{h} \to \bar{f}f) = N_c(f)\frac{m_f^2}{v^2}\frac{m_\mathrm{h}}{8\pi}\sqrt{1-4\frac{m_f^2}{m_\mathrm{h}^2}}\left[\left(1-4\frac{m_f^2}{m_\mathrm{h}^2}\right)\left|a_f^\mathrm{h}\right|^2 + \left|b_f^\mathrm{h}\right|^2\right], \tag{7.12}$$

with $N_c = 3$ for quarks and $N_c = 1$ for leptons; substituting the gFC couplings in eqs. (7.9)–(7.10) and neglecting $4m_f^2/m_\mathrm{h}^2 \ll 1$,

$$\Gamma(\mathrm{h} \to \bar{f}f)_\mathrm{gFC} = \Gamma(\mathrm{h} \to \bar{f}f)_\mathrm{SM}\left|s_{\alpha\beta} + c_{\alpha\beta}\, n_f\right|^2\,, \tag{7.13}$$

where the SM decay width reads

$$\Gamma(\mathrm{h} \to \bar{f} f)_{\mathrm{SM}} = \frac{N_c(f)}{8\pi} \frac{m_{\mathrm{h}}}{v^2} m_f^2 \,. \tag{7.14}$$

On the other hand, it is mandatory to study the decay $\mathrm{h} \to \gamma\gamma$, which played a central role in the discovery of the Higgs. It has an amplitude controlled in the SM by two interfering contributions, the one loop triangle diagrams with virtual W's and top quarks. The former is modified according to eq. (7.11). The later is the only relevant one involving quarks in the SM because of the large $\mathrm{h}\bar{t}t$ coupling: m_t/v; this amplitude is modified according to eq. (7.9). With a pseudoscalar coupling now present, eq. (7.10), there is an additional contribution which, however, does not interfere with the SM-like top(scalar coupling)+W. Furthermore, there are other contributions that one may consider: one due to diagrams with virtual $\mathrm{H}^\pm$'s, and the ones due to other fermions with enhanced couplings to h due to sizable n_j. For the charged scalar, they cannot be neglected if $\mathrm{H}^\pm$ is relatively light, and thus, barring that possibility, we do not consider them. For the remaining fermions, the values of $c_{\alpha\beta}$ that $\mathrm{h} \leftrightarrows WW$ decay and production require are typically small ($|c_{\alpha\beta}| \leq 0.1$), and thus the values of n_j that one would need for their contributions to be relevant would be at least $n_j \sim m_t$: they would produce huge contributions to the width $\Gamma(\mathrm{h})$ or to $\bar{q}q \to \mathrm{h}$ production cross sections, in addition to the perturbativity and fine tuning concerns on the Yukawa couplings already mentioned: we thus ignore them altogether, since they will be rendered negligible once other constraints are considered. The width of $\mathrm{h} \to \gamma\gamma$ reads

$$\begin{aligned}\Gamma(\mathrm{h} \to \gamma\gamma)_{\mathrm{gFC}} = \frac{\alpha^2}{256\pi^3} \frac{m_{\mathrm{h}}^3}{v^2} \times \\ \left(\left| \sum_f N_c(f) Q_f^2 a_f^{\mathrm{h}} A_F(x_f) + s_{\alpha\beta} A_V(x_W) + g_{\mathrm{H}^\pm} A_S(x_{\mathrm{H}^\pm}) \right|^2 \right. \\ \left. + \left| \sum_f N_c(f) Q_f^2 b_f^{\mathrm{h}} \hat{A}_F(x_f) \right|^2 \right),\end{aligned} \tag{7.15}$$

with $x_X = 4m_X^2/m_{\mathrm{h}}^2$. The sum over fermions f includes up and down type quarks, with $Q_f = 2/3$ and $-1/3$ respectively, and charged leptons with $Q_f = -1$. The contribution of the charged scalar $\mathrm{H}^\pm$ can be safely neglected for $m_{\mathrm{H}^\pm} > v$.

The decay into gluons $h \to gg$ proceeds through similar diagrams, with the ones mediated by leptons and by W and $H^\pm$ bosons absent:

$$\Gamma(h \to gg)_{\rm gFC} = \frac{\alpha_S^2}{128\pi^3}\frac{m_h^3}{v^2}\left(\left|\sum_f a_f^h A_F(x_f)\right|^2 + \left|\sum_f b_f^h \hat{A}_F(x_f)\right|^2\right). \tag{7.16}$$

The loop functions are [234]

$$\begin{aligned} A_F(x) &= -2x\left[1+(1-x)f(x)\right], \quad \hat{A}_F(x) = -2xf(x), \\ A_V(x) &= 2+3x+3x(2-x)f(x), \quad A_S(x) = x(1-xf(x)), \end{aligned} \tag{7.17}$$

where

$$f(x) = \begin{cases} \arcsin^2(1/\sqrt{x}), & x \geq 1, \\ -\frac{1}{4}\left[\ln\left(\frac{1+\sqrt{1-x}}{1-\sqrt{1-x}}\right) - i\pi\right]^2, & x < 1. \end{cases} \tag{7.18}$$

Here we follow the definitions in where the A_F and $\hat{A}_F$ functions are defined including the mass factor of the SM $h\bar{f}f$ vertex and which differ in a global sign from the ones in, for example, [235]. The dominant contribution in $h \to \gamma\gamma$ comes from $A_V(x_W) = -8.339$. Other representative values of the functions are shown in Table 7.3. It is important to stress that, while QCD corrections to eq. (7.15) are small, that is not the case for eq. (7.16) (see for example [236]): we account for them by using

$$\Gamma(h \to gg)_{\rm gFC} \to \frac{\Gamma(h \to gg)_{\rm gFC}}{\Gamma(h \to gg)_{\rm SM}} \times \Gamma(h \to gg)_{\text{SM ref.}}, \tag{7.19}$$

with $\Gamma(h \to gg)_{\text{SM ref.}} = 0.351$ MeV the SM reference value from Table 7.4, and $\Gamma(h \to gg)_{\rm gFC}/\Gamma(h \to gg)_{\rm SM}$ computed according to eq. (7.16) (for the SM denominator $a_f^h v/m_f = 1$, $b_f^h = 0$). For completeness, reference values of the SM Higgs decays [237–240] are reproduced in Table 7.4.

Production mechanisms

In addition to the decay widths, production mechanisms are also modified. Besides VBF and VH, already commented (eq. (7.11)), the most relevant one is gluon-gluon fusion $gg \to h$ [242]. The elementary process is the reverse of the decay $h \to gg$, which is then convoluted with the gluon distribution functions in the proton (in the narrow

f	t	b	τ
$A_F(x_f)$	1.3796	$-(4.37+4.75i)10^{-2}$	$-(2.30+2.09i)10^{-2}$
$\hat{A}_F(x_f)$	2.1010	$-(4.78+4.76i)10^{-2}$	$-(2.46+2.09i)10^{-2}$
f	c	s	μ
$A_F(x_f)$	$-(4.87+3.29i)10^{-3}$	$-(8.99+3.89i)10^{-5}$	$-(2.53+1.20i)10^{-4}$
$\hat{A}_F(x_f)$	$-(5.07+3.29i)10^{-3}$	$-(9.15+3.89i)10^{-5}$	$-(2.59+1.20i)10^{-4}$

Table 7.3: Values of A_F and $\hat{A}_F$ for charged fermions of the 2nd and 3rd generations; running masses at $\mu = m_{\rm h}$ [241] are used.

Channels $\bar{f}f$	$\bar{b}b$	$\bar{\tau}\tau$	$\bar{c}c$	$\bar{\mu}\mu$	$\bar{s}s$
BR	0.577	$6.32\cdot10^{-2}$	$2.91\cdot10^{-2}$	$2.19\cdot10^{-4}$	$2.46\cdot10^{-4}$
Channels VV	gg	$WW^{(*)}$	$ZZ^{(*)}$	$\gamma\gamma$	γZ
BR	$8.57\cdot10^{-2}$	0.215	$2.64\cdot10^{-2}$	$2.28\cdot10^{-3}$	$1.54\cdot10^{-3}$

Table 7.4: Reference SM Higgs decay branching ratios for $m_{\rm h} = 125$ GeV; the total width is $\Gamma(\rm h) = 4.1$ MeV.

width approximation production and decay are related straightforwardly). As in the case of the decay, eq. (7.19), we incorporate QCD corrections by normalizing the SM prediction to the reference value in Table 7.5, which shows reference cross sections for different production mechanisms [237–240]. For generic interaction terms

$$\mathscr{L}_{S\bar{q}q} = -\frac{m_t}{v} S\bar{t}(a_t^S + ib_t^S\gamma_5)t - \frac{m_b}{v} S\bar{b}(a_b^S + ib_b^S\gamma_5)b\,, \tag{7.20}$$

the gluon-gluon fusion production cross section reads

$$\sigma[pp\to S]_{\rm ggF} = \sigma[pp\to S]^{\text{SM-like}}_{[\rm ggF]} \times \frac{\left|a_t^S A_F(x_t) + a_b^S A_F(x_b)\right|^2 + \left|b_t^S \hat{A}_F(x_t) + b_b^S \hat{A}_F(x_b)\right|^2}{\left|A_F(x_t) + A_F(x_b)\right|^2}, \tag{7.21}$$

with $x_q \equiv 4(m_q/m_S)^2$, and $A_F(x)$ and $\hat{A}_F(x)$ the loop functions defined in eq. (7.17) corresponding to scalar or pseudoscalar couplings, respectively; $\sigma[pp\to S]^{\text{SM-like}}_{[\rm ggF]}$ can be found in [240, 243–245]. It is worth mentioning that the scalar and pseudoscalar terms do not mix what produces the appearance of the function $\hat{A}_F$. This simple recipe also gives sufficiently good agreement with results for a SM-Higgs-like neutral pseudoscalar, which can be found in [245–248]. The couplings in eq. (7.20) for $S = \rm H, A$ in each model can be read in Table 3.1.

	ggF	VBF	WH	ZH	ttH	bbH
8 TeV	19.27	1.578	0.7046	0.4153	0.1293	0.2035
13 TeV	43.92	3.748	1.380	0.8696	0.5085	0.5116
14 TeV	49.47	4.233	1.522	0.9690	0.6113	0.5805

Table 7.5: Reference SM production cross sections for $m_{\rm h} = 125$ GeV (in pb).

7.4 H± mediated contributions

Flavor transitions mediated by $W^\pm$ can receive new contributions where the charged scalar, H±, plays the role of the $W^\pm$ boson. For tree level processes involving leptons, one refers to "Lepton Flavor Universality" constraints; we also consider constraints at the loop level in the quark sector.

One may also worry about too large H±-mediated contributions to processes like $\ell_j \to \ell_k \gamma$: since in the models that are going to be studied (flavor conserving ones) we are considering massless neutrinos, lepton family numbers are conserved – i.e. there is a $[U(1)]^3$ symmetry –, and such processes are absent.

Lepton Flavor Universality

Pure leptonic decays $\ell_j \to \ell_k \nu \bar{\nu}$ described by the following Lagrangian

$$\mathscr{L}_{\rm eff} = -\frac{4G_F}{\sqrt{2}} \sum_{\ell_j \ell_k = e,\mu,\tau} \sum_{\alpha,\beta=1}^{3} U^*_{\ell_j \nu_\alpha} U_{\ell_k \nu_\beta} \left\{ \left[\bar{\nu}_\alpha \gamma^\mu P_L \ell_j\right] \left[\bar{\ell}_k \gamma^\mu P_L \nu_\beta\right] + g^{\rm S,RR}_{j\to k} \left[\bar{\nu}_\alpha P_R \ell_j\right] \left[\bar{\ell}_k P_L \nu_\beta\right] \right\} , \tag{7.22}$$

with $g^{\rm S,RR}_{j\to k} = \frac{n_{\ell_j} n_{ell_k}}{m^2_{\rm H^\pm}}$ include contributions mediated by H± that modify the SM leptonic decays as:

$$\Gamma(\ell_j \to \ell_k \nu \bar{\nu}) = \frac{G_F^2}{192\pi^3} m^5_{\ell_j} \, {\rm f}(x_{kj}) \left(1 + \frac{1}{4} \left| g^{\rm S,RR}_{j\to k} \right|^2 + 2{\rm Re}\left(g^{\rm S,RR}_{j\to k} \right) \frac{m_{\ell_k}}{m_{\ell_j}} \frac{{\rm g}(x_{kj})}{{\rm f}(x_{kj})} \right) \times (1 + \Delta^{\ell_j \ell_k}_{\rm RC}), \tag{7.23}$$

where ${\rm f}(x)$ and ${\rm g}(x)$ are the usual phase space integrals[2] [249], $x_{kj} \equiv (m_{\ell_k}/m_{\ell_j})^2$ and $\Delta^{\ell_j \ell_k}_{\rm RC}$ correspond to QED radiative corrections.The notation $g^{\rm S,RR}_{j\to k}$ reflects the

[2] ${\rm f}(x) = 1 - 8x + 8x^3 - x^4 - 12x^2 \ln x$, and ${\rm g}(x) = 1 + 9x - 9x^2 - x^3 + 6x(1+x)\ln x$.

fact that in the present models the new contributions only affect, in an effective description, the operator $\bar{\nu}_L \ell_{jR} \bar{\ell}_{kR} \nu_L$. The ratios

$$R\left[\frac{\ell_a\to\ell_b}{\ell_\alpha\to\ell_\beta}\right] \equiv \frac{\Gamma(\ell_a\to\ell_b\nu\bar{\nu})}{\Gamma(\ell_a\to\ell_b\nu\bar{\nu})_{\rm SM}} \frac{\Gamma(\ell_\alpha\to\ell_\beta\nu\bar{\nu})_{\rm SM}}{\Gamma(\ell_\alpha\to\ell_\beta\nu\bar{\nu})}\,, \tag{7.24}$$

give the following constraints [250]:

$$R[\tfrac{\tau\to\mu}{\tau\to e}] = 1 + (3.8 \pm 3.2)\times 10^{-3}\,, \qquad R\left[\tfrac{\tau\to e}{\mu\to e}\right] = 1 + (2.4 \pm 2.3)\times 10^{-3}\,. \tag{7.25}$$

In addition, measurements of decay spectra with polarized leptons [251] impose

$$\left|g^{\rm S,RR}_{\mu\to e}\right| < 0.035 \text{ at } 90\% \text{ CL}, \quad \left|g^{\rm S,RR}_{\tau\to\mu}\right| < 0.72 \text{ at } 95\% \text{ CL}, \quad \left|g^{\rm S,RR}_{\tau\to e}\right| < 0.7 \text{ at } 95\% \text{ CL}. \tag{7.26}$$

Besides purely leptonic decays $\ell_j \to \ell_k \bar{\nu}\nu$, semileptonic decay modes like $K, \pi \to e\nu, \mu\nu$ and $\tau \to K\nu, \pi\nu$, provide additional constraints on the different n_ℓ (together with the t_β dependence of the quark couplings with $H^\pm$). The relevant effective Lagrangian for these processes, assuming massless neutrinos $\alpha^\ell_{ab} = \beta^\ell_{ab}$, reads:

$$\begin{aligned}\mathscr{L}_{\rm eff} = -\frac{G_F}{\sqrt{2}} \sum_{u_j=u,c,t} \sum_{d_k=d,s,b} \sum_{\ell_a=e,\mu,\tau} \sum_{b=1}^{3} V_{u_j d_k} U_{\ell_a \nu_b} \\ \Bigg\{ \left[\bar{u}_j \gamma^\mu (1-\gamma_5) d_k\right] \left[\bar{\ell}_a \gamma^\mu (1-\gamma_5) \nu_b\right] \\ - \frac{1}{m^2_{H^\pm} V_{u_j d_k} U_{\ell_a \nu_b}} \left[\bar{u}_j \left(\alpha^{q*}_{jk} + i\beta^{q*}_{jk}\gamma_5\right) d_k\right] \left[\bar{\ell}_a \alpha^\ell_{ab} \left(1+\gamma_5\right) \nu_b\right] \Bigg\} + \text{h.c.}\,.\end{aligned} \tag{7.27}$$

In particular, we consider ratios

$$R^P_{\ell_1\ell_2} = \frac{\Gamma(P^+\to\ell_1^+\nu)}{\Gamma(P^+\to\ell_1^+\nu)_{\rm SM}} \frac{\Gamma(P^+\to\ell_2^+\nu)_{\rm SM}}{\Gamma(P^+\to\ell_2^+\nu)} = \frac{\left|1-\Delta^P_{\ell_1}\right|^2}{\left|1-\Delta^P_{\ell_2}\right|^2}\,, \tag{7.28}$$

where the quark content of P^+ is $u_j \bar{d}_k$ and

$$\Delta^P_{\ell_a} = -\frac{M_P^2}{m^2_{H^\pm}} \frac{\alpha^\ell_a}{m_{\ell_a}} \frac{i\beta^q_{jk}}{m_{u_j} + m_{d_k}}\,. \tag{7.29}$$

For ratios involving $\tau^+ \to P^+\nu$ decays, the expressions are unchanged. The actual constraints [250, 252, 253] read

$$\begin{aligned} R^\pi_{\mu e} &= 1 + (4.1 \pm 3.3)\times 10^{-3}, \qquad R^\pi_{\tau\mu} = 1 - (5.9 \pm 5.9)\times 10^{-3}, \\ R^K_{\mu e} &= 1 - (4.8 \pm 4.7)\times 10^{-3}, \qquad R^K_{\tau\mu} = 1 - (2.2 \pm 1.4)\times 10^{-2}. \end{aligned} \tag{7.30}$$

All these LFU violating effects scale with $1/m^2_{\mathrm{H}^\pm}$ and therefore one expects that the effects for large $m_{\mathrm{H}^\pm}$ are much more suppressed. This is quite clear in the pure leptonic decays, where the most relevant constraints, eq. (7.25) and $\left|g^{\mathrm{S,RR}}_{\mu\to e}\right|$ in eq. (7.26), can be comfortably satisfied, giving a contribution to the corresponding χ^2 at a level similar to the SM.

$b \to s\gamma$ **and** B^0_q–$\bar{B}^0_q$

As loop level transitions mediated by the charged scalar, we consider contributions to the mixing in B_d and B_s meson systems (in particular to the dispersive part of the mixing, which controls the mass differences) and contributions to the radiative decay $b \to s\gamma$. Contributions to the mentioned mass differences in B_d and B_s are required to not exceed the 2-3% level (that is already below the current level of theoretical uncertainty in the relevant matrix elements obtained from lattice QCD computations). For $b \to s\gamma$, we impose that the correction to the usual $\Gamma(B \to X_s\gamma)_{E_\gamma>1.6\mathrm{GeV}}$ is below the experimental uncertainty. We refer to [90, 141, 254] for further details.

7.5 SFCNC

The Yukawa couplings of the neutral scalars S to fermions, following section 2.3, read

$$\mathscr{L}_N = -\sum_{S=\mathrm{h,H,A}}\sum_{f=u,d,\ell}\sum_{j,k=1}^{3}\frac{m_{f_j}}{v}\,S\,\bar{f}_j(a^{S,f}_{jk}+ib^{S,f}_{jk}\gamma_5)f_k\,. \tag{2.49}$$

Here we will put our attention in the flavor changing neutral decays. In the first place, the SM like Higgs decay rate to a τ and a light lepton (e or μ) read

$$\Gamma(\mathrm{h}\to\ell_j\bar{\tau})+\Gamma(\mathrm{h}\to\bar{\ell}_j\tau)=\Gamma_{\mathrm{SM}}(\mathrm{h}\to\tau\bar{\tau})\times 2\left(\left|(a^{\mathrm{h},\ell}_{j\tau}\right|^2+\left|(b^{\mathrm{h},\ell}_{j\tau}\right|^2\right). \tag{7.31}$$

In the SM, the coupling of h_{SM} to $\bar{\tau}\tau$ is simply $-\frac{m_\tau}{v}\mathrm{h}_{\mathrm{SM}}\bar{\tau}\tau$ leading to $\Gamma_{\mathrm{SM}}(\mathrm{h}\to\tau\bar{\tau}) = \frac{\mathrm{m_h}}{8\pi}\frac{m_\tau^2}{v^2}$.

Similarly, for $t\to \mathrm{h}q\,(q=u,\ c)$ decays, the branching ratio reads:

$$\mathrm{Br}\,(t\to\mathrm{h}q_j)=\frac{\Gamma(t\to\mathrm{h}q_j)}{\Gamma(t\to Wb)}=f(x_\mathrm{h},x_W)\left(\left|(a^{\mathrm{h},q}_{jt}\right|^2+\left|(b^{\mathrm{h},q}_{jt}\right|^2\right), \tag{7.32}$$

considering that the top quark width is dominated by $t \to Wb$, i.e. $\Gamma(t) = \Gamma(t \to Wb)$ with $\left|V_{tb}\right| \simeq 1$; $f(x_{\mathrm{h}}, x_W)$ collects the differences among both decays due to (i) scalar h vs. vector W in the final state and (ii) hc vs. Wb phase space and reads

$$f(x_{\mathrm{h}}, x_W) = \frac{(1 - x_{\mathrm{h}})^2}{1 - 3x_W^2 + 2x_W^3}, \quad x_y = \frac{m_y^2}{m_t^2}\,. \tag{7.33}$$

It's like in the great stories Mr. Frodo. The ones that really mattered. Full of darkness and danger they were, and sometimes you didn't want to know the end. Because how could the end be happy? How could the world go back to the way it was when so much bad happened? But in the end, it's only a passing thing, this shadow. Even darkness must pass.

— SAMwise Gamgee, *The Lord of the Rings*, J. R. R. Tolkien

8

Phenomenology of the gFC

Chapter 3 describes a study of the stability under RGE of the condition that both Yukawa matrices can be diagonalized at the same time. The resulting models conserve flavor in tree level neutral transitions that, as has been mentioned before, it is not a general feature of the 2HDM. The models, being more general than the flavor alignment 2HDM, were denoted as gFC models. In this chapter we discuss the most relevant experimental constraints on gFC arising from flavor conserving Higgs-related observables.

The neutral yukawa interactions described by the Lagrangian in eq. (2.49), together with the absence of tree level SFCNC, provoked by the diagonal interaction matrices in eq. (2.15), have interesting phenomenological consequences in different observables, since they may produce deviations from SM expectations. The only new parameters with respect to the SM that control these observables are n_j in eq. (3.4), the values of the masses $m_{\mathrm{H}^\pm}$, m_{H}, m_{A}, and the mixing angle in the scalar sector $\alpha + \beta$, since here we adopt the CP conserving limit (see eq. (2.15)). Our interest is focused on the parameters n_j in eq. (3.4).

This chapter has the following distribution: in the following section the constraints from chapter 7 that apply in this case are enumerated and, when needed, particularized to the gFC parametrization and in section 8.2 the results of our analysis are presented.

8.1 Constraints

In this analysis we have focused on the flavor conserving observables related to h. Besides probing the gFC matrices in eq. (3.4), the bounds imposed by these observables also apply to the same flavor conserving couplings of a general 2HDM. Among the observables of interest, those that (i) involve the lowest number of new non-SM parameters and (ii) provide direct constraints from existing measurements, are preferred.

In the following we enumerate the applied constraints from chapter 7 while particularizing them to the gFC model. In section 8.1.1 we give a detailed explanation of the gFC contribution to the electric dipole moments (EDMs) which was not included in chapter 7 since this observable is only studied in this analysis.

- As usual we require that the Yukawa couplings remain perturbative, which in the gFC scenario means

$$\frac{|n_j|}{v} \leq \mathcal{O}(1)\,. \tag{8.1}$$

  The precise value adopted in eq. (8.1), for example $\mathcal{O}(1) \to 1$ or $\sqrt{4\pi}$, is not expected to be specially relevant: other phenomenological requirements will be, typically, more restrictive. There is, however, an exception: the "decoupling limit" [255] of the 2HDM, in which $s_{\alpha\beta} \to 1$ ($c_{\alpha\beta} \to 0$) removes the non-SM effects from the h couplings (while $m_{\mathrm{H}^\pm} \gg v$ suppresses $\mathrm{H}^\pm$ mediated non-SM effects), leaving the perturbativity requirement as the only effective constraint. One may further argue that having either $m_j \ll |n_j|$ or $m_j \gg |n_j|$, involves fine tuning between quantities of very different nature: both m_j and n_j are linear combinations, controlled by β, of Yukawa couplings (times v), but β originates in the scalar potential, meaning that very disparate values of m_j and n_j involve significant cancellations in one or the other, unless $\beta \to 0$ or $\beta \to \pi/2$. For the sake of clarity, we will only consider eq. (8.1) and ignore the previous concerns about eventual fine tuning.

- We also included the signal strengths that were available when this analysis was performed. Besided the usual production channels described in section 7.3 since here $|n_j|$ could be much larger than m_j we have to be careful with the $q\bar{q} \to h$ cross section since it may become inappropriately large. For a generic Yukawa interaction, the tree level cross section for direct production $pp(\bar{q}q) \to \mathrm{h}$ is, in the narrow width approximation,

$$\sigma[pp(\bar{q}q) \to \mathrm{h}] = \left(\left|a_q^{\mathrm{h}}\right|^2 + \left|b_q^{\mathrm{h}}\right|^2\right) \sigma_0(E)\, \mathcal{L}_{\bar{q}q}(E)\,, \tag{8.2}$$

where

$$\begin{aligned} \sigma_0(E) &\equiv 2\frac{\pi}{8N_c E^2} = \left(\frac{\mathrm{TeV}}{E}\right)^2 101.8 \text{ pb}\,, \\ \mathcal{L}_{\bar{q}q}(E) &\equiv \int_{x_0}^1 dx\, f_{\bar{q}}^p(x,Q^2) f_q^p(x_0/x,Q^2)\frac{1}{x}\,, \end{aligned} \tag{8.3}$$

with E the center of mass proton energy, f_y^p the distribution function of parton y in the proton, $x_0 = \frac{m_{\mathrm{h}}^2}{4E^2}$ and Q is the factorization scale.

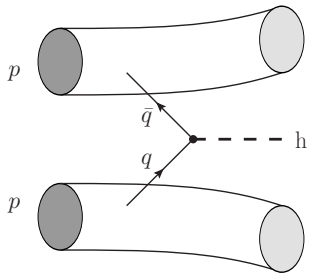

Figure 8.1: $\bar{q}q \to \mathrm{h}$ process.

In Table 8.1 we collect the values of $\sigma[pp(\bar{q}q) \to \mathrm{h}]$ and $\mathcal{L}_{\bar{q}q}$ computed [256] for different quarks[1] and setting $\left|a_q^{\mathrm{h}}\right|^2 + \left|b_q^{\mathrm{h}}\right|^2 = 1$ in eq. (8.2): this value of the couplings is obviously too large since it effectively corresponds, with respect to the SM, to the change $m_j/v \mapsto v/v$, but it allows for easy use. Consider,

[1] Eq. (8.2) is obtained using the tree level partonic cross section; furthermore, the results in table 8.1 are obtained multiplying these simple predictions by a common $\mathcal{O}(1)$ factor (one for each LHC energy case), chosen such that $\sigma[pp(\bar{b}b) \to \mathrm{h}]$ in eq. (8.2) reproduces the improved reference values in [237–240]. We also take $Q = E/2$.

	$\bar{d}d$		$\bar{u}u$		$\bar{s}s$		$\bar{c}c$	
	$\mathcal{L}_{\bar{d}d}$	σ	$\mathcal{L}_{\bar{u}u}$	σ	$\mathcal{L}_{\bar{s}s}$	σ	$\mathcal{L}_{\bar{c}c}$	σ
8 TeV	14.56	16.60	21.53	24.53	4.41	5.02	2.65	3.01
13 TeV	74.57	29.17	105.28	41.18	27.70	10.84	17.92	7.01
14 TeV	95.49	31.53	133.90	44.21	36.46	12.04	23.83	7.87

Table 8.1: $\sigma[pp(\bar{q}q) \to \mathrm{h}]$ ($\times 10^3$) in pb and $\mathcal{L}_{\bar{q}q}(E^2)$ ($\times 10^3$) for different $\bar{q}q$.

for illustration, that for the LHC at 8 TeV $\sigma[pp(\bar{u}u) \to \mathrm{h}] \sim 10$ pb: one can readily obtain

$$\sigma[pp(\bar{u}u) \to \mathrm{h}] \sim 10 \text{ pb} \;\Leftrightarrow\; \left|a_q^{\mathrm{h}}\right|^2 + \left|b_q^{\mathrm{h}}\right|^2 \sim 7.3 \times 10^{-5} \,. \tag{8.4}$$

Although considering $\sigma[pp(\bar{u}u) \to \mathrm{h}] \sim 10$ pb may be unrealistic (the *total* production cross section in Table 7.5 for 8 TeV is ~ 22 pb), from eq. (8.4), $\Gamma(\mathrm{h} \to u\bar{u}) \sim 1$ MeV: even if it is a significant contribution to the width $\Gamma(\mathrm{h})$, it might still be compatible with the overall pattern of Higgs signal strengths. To our knowledge, there are no dedicated analyses of $\bar{q}q \to \mathrm{h}$ ($q \neq b, t$) from which experimental input can be used in this manner. However, it is reasonable to expect that this kind of production potentially "contaminates" the analyses of gluon-gluon fusion: in that case, one should add all $\sigma[pp(\bar{q}q) \to \mathrm{h}]$ contributions for light q to the gluon-gluon fusion cross section when analysing Higgs signal strengths. It is then clear that bounds more stringent than eq. (8.4) would follow for the sum over all the different channels involved. The simple connection among the decays $\mathrm{h} \to \bar{q}q$ and the $\bar{q}q \to \mathrm{h}$ production mechanism – in the narrow width approximation – that follows from eqs. (7.13) and (8.2), is

$$\frac{\sigma[pp(\bar{q}q) \to \mathrm{h}] \,/\, 1\mathrm{pb}}{\Gamma(\mathrm{h} \to \bar{q}q) \,/\, 1\mathrm{MeV}} = 6.825 \left(\frac{\mathrm{TeV}}{E}\right)^2 \left(\frac{\mathcal{L}_{\bar{q}q}(E)}{10^3}\right) , \tag{8.5}$$

which allows for easy comparison of the relative strengths of the constraints imposed by $\bar{q}q \to \mathrm{h}$ production and $\mathrm{h} \to \bar{q}q$ decay for light quarks q.

8.1.1 Electric dipole moments

Non-real N_f matrices are a source of CP violation in scalar-fermion interactions, which can induce electric dipole moments. This constraint was not discussed in chapter 7 since it only applies to the analysis presented in this chapter but not the one from chapter 9. Let us consider for example an electron-Higgs coupling $\mathscr{L}_{\mathrm{hee}} = -\mathrm{h}\,\bar{e}(a_e^{\mathrm{h}} + ib_e^{\mathrm{h}}\gamma_5)e$; the one loop diagram in Figure 8.2 gives a contribution to the electron EDM d_e:

$$d_e = \frac{3m_e a_e^{\mathrm{h}} b_e^{\mathrm{h}}}{16\pi^2 m_{\mathrm{h}}^2}\left(1 + \mathcal{O}\left(\frac{m_e^2}{m_{\mathrm{h}}^2}\right)\right). \tag{8.6}$$

It is to be noticed that, for $a_e^{\mathrm{h}} \sim b_e^{\mathrm{h}} \sim m_e/v$, eq. (8.6) gives $d_e \sim 10^{-34}$e·cm. When $|a_e^{\mathrm{h}}|$, $|b_e^{\mathrm{h}}| \gg m_e/v$ are a priori allowed, up to the effect of other constraints, a significant enhancement in d_e can be expected. For an experimental bounds $|d_e| < 10^{-27}$e ·cm, considering only this contribution gives

$$a_e^{\mathrm{h}} b_e^{\mathrm{h}} < 8 \times 10^{-5}, \tag{8.7}$$

or, with eqs. (7.9)–(7.10) and neglecting m_e with respect to $c_{\alpha\beta}n_e$,

$$c_{\alpha\beta}^2 \mathrm{Re}\,(n_e)\,\mathrm{Im}\,(n_e) < 5\ \mathrm{GeV}^2. \tag{8.8}$$

Anticipating results from section 8.2, in particular Figure 8.4g, it is clear that the bounds imposed by the LHC results are more stringent than eq. (8.8). It should also be noticed that including contributions analog to Figure 8.2 with $\mathrm{h} \to \mathrm{H}, \mathrm{A}$, gives

$$\mathrm{Re}\,(n_e)\,\mathrm{Im}\,(n_e)\left(c_{\alpha\beta}^2 + s_{\alpha\beta}^2\frac{m_{\mathrm{h}}^2}{m_{\mathrm{H}}^2} + \frac{m_{\mathrm{h}}^2}{m_{\mathrm{A}}^2}\right) < 5\ \mathrm{GeV}^2, \tag{8.9}$$

and does not change this conclusion. Furthermore, one loop contributions with virtual $\mathrm{H}^{\pm}$ and neutrinos are suppressed.

It is well known that two loop "Barr-Zee" [203, 257–261] contributions can be significant: studies such as [262, 263] address such constraints on CP violating Higgs-fermion couplings. However, those contributions involve different n_f couplings simultaneously, together with the masses of the different scalars, preventing a

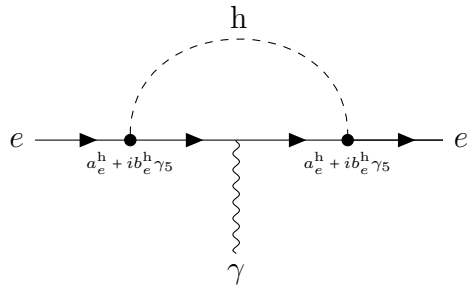

Figure 8.2: h mediated contribution to d_e at one loop.

simple translation into bounds on a single parameter. It is to be noticed too that cancellations among different diagrams in that class may occur [143, 264]. Including such kind of analysis was beyond the scope of the work presented here; in any case one should keep in mind that the analysis of EDMs may have some impact on the results of section 8.2. The previous discussion also applies to the EDMs of the u and d quarks and the experimental constraints that the neutron EDM bounds impose, including, in addition, the impact of QCD effects [265].

8.2 Results

With the deviations with respect to the SM of the couplings of h and their implications for decays and production mechanisms, one can impose the experimental constraints of section 8.1 and explore the allowed values of $c_{\alpha\beta}$ and the gFC parameters n_f in eq. (3.4). For the results presented in the following we consider the most conservative situation, i.e. all parameters are free to vary simultaneously. Compared to restricted situations where not all parameters are considered simultaneously, this offers a safer interpretation of excluded regions (they are excluded whatever the values of the parameters not displayed) at the price, of course, of larger allowed regions.

Figure 8.3 shows n_f vs. $c_{\alpha\beta}$ for all quarks and leptons. Some comments are in order.

- As expected, for $c_{\alpha\beta} \to 0$, the constraints on n_f disappear.
- For u, c, d and s quarks, the allowed regions are almost identical, as one could anticipate from their irrelevant role, within the SM, in the available

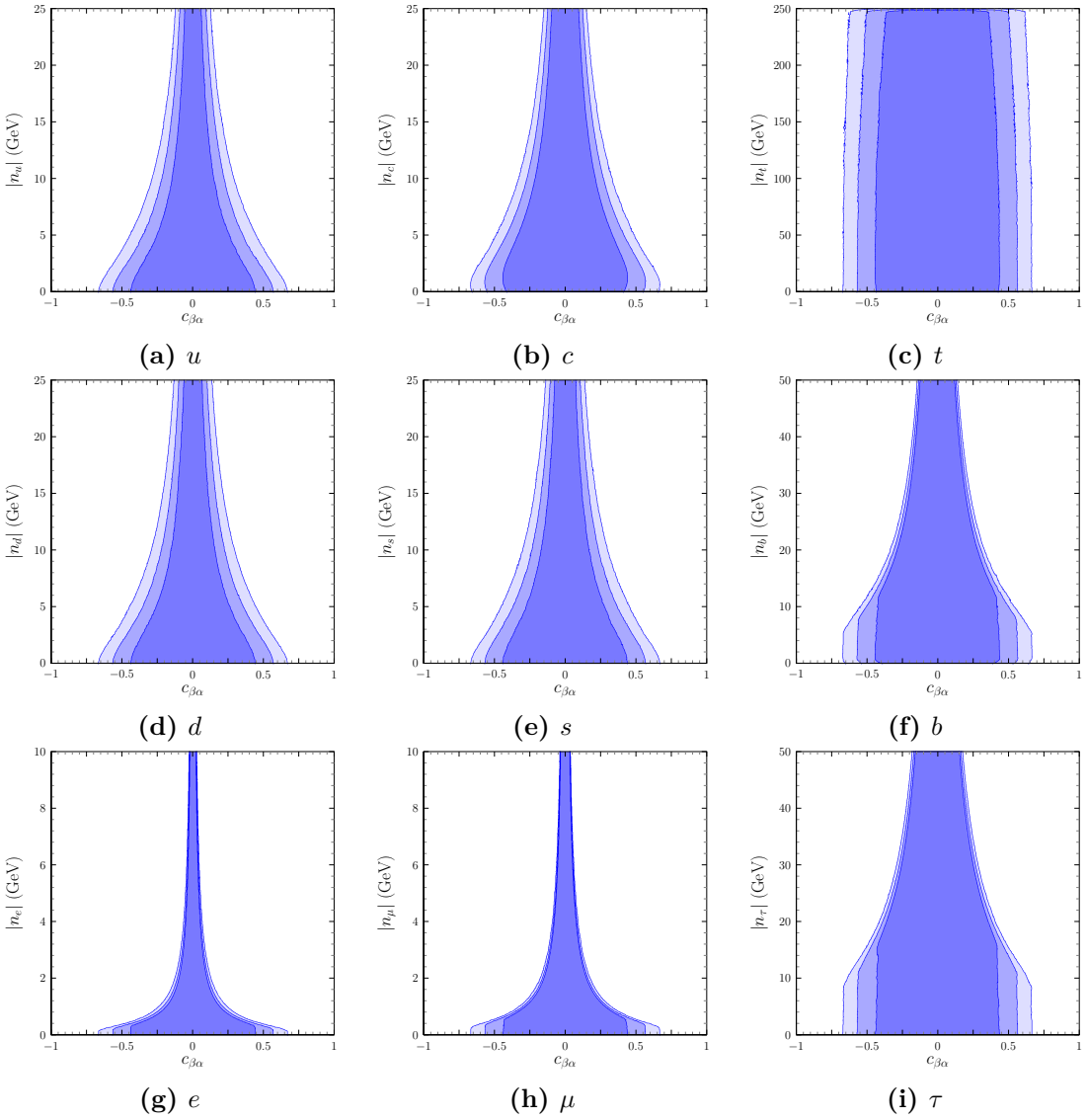

Figure 8.3: $|n_f|$ vs. $c_{\alpha\beta}$ for the different fermions f; darker to lighter regions correspond to 68, 95 and 99% CL.

production × decay Higgs signal strengths. The corresponding n_f's appear to be effectively limited by the contributions to the Higgs width.

- Surprisingly, the allowed size of $|n_t|$ appears to be independent of $c_{\alpha\beta}$: this will be discussed in connection with figure 8.4c below.

- The n_b and n_τ cases are also similar, with allowed regions differing from the u, c, d, s cases for $|n_q|$'s below 10-15 GeV and not small $c_{\alpha\beta}$.

- For n_e and n_μ, the allowed regions are much more constrained owing to the bounds set by dedicated $pp \to \mathrm{h} \to e^+e^-$, $\mu^+\mu^-$ analyses such as [266, 267].

Although figure 8.3 shows absolute bounds on $|n_f|$'s, it does not give information on $\arg(n_f)$'s and cannot be directly read in terms of the scalar and pseudoscalar couplings of h in eqs. (7.9)–(7.10). Considering that, Figure 8.4 shows $\bar{b}_f$ vs $\bar{a}_f$ with

$$\bar{a}_f \equiv s_{\alpha\beta} m_f + c_{\alpha\beta} \mathrm{Re}\,(n_f)\,, \quad \bar{b}_f = c_{\alpha\beta} \mathrm{Im}\,(n_f)\,. \tag{8.10}$$

Furthermore, to maintain some information on $c_{\alpha\beta}$, allowed regions corresponding to $|c_{\alpha\beta}| < 0.01$, to $0.01 < |c_{\alpha\beta}| < 0.1$ and to $0.1 < |c_{\alpha\beta}|$ are displayed. One can notice that

- for the first and second fermion generations, there is no dependence on $\arg(n_f)$, since only decays, with rates proportional to $|\bar{a}_f|^2 + |\bar{b}_f|^2$, are relevant. For quarks, the allowed region for $|c_{\alpha\beta}| < 0.01$ is smaller: this is simply due to the perturbativity requirement in eq. (8.1).

- For the top quark, two separate regions are allowed: this is also expected since independent sign changes in both $\bar{a}_t$ and $\bar{b}_t$ (together with sign changes in $c_{\alpha\beta}$, $s_{\alpha\beta}$) do not alter the predictions. For $|c_{\alpha\beta}| < 0.01$ the allowed regions are quite reduced and placed around $(\bar{a}_t, \bar{b}_t) = (\pm m_t, 0)$; with $0.01 < |c_{\alpha\beta}| < 0.1$ their size increases and only for $|c_{\alpha\beta}| > 0.1$ the interplay of (i) pseudoscalar contributions to $gg \to \mathrm{h}$ and $\mathrm{h} \to \gamma\gamma$, and (ii) W-top(scalar) interference in $\mathrm{h} \to \gamma\gamma$ gives rise to larger regions.

- For b and τ, the regions for not too small mixing, $|c_{\alpha\beta}| > 0.01$, are ring-shaped; m_b and m_τ set the radii of such regions, as could be expected from the agreement of $\mathrm{h} \to b\bar{b}$ and $\mathrm{h} \to \tau\bar{\tau}$ signal strengths with SM expectations. For small mixing, $|c_{\alpha\beta}| < 0.01$, the perturbativity requirement on $|n_b|$, $|n_\tau|$ limits the allowed departure from $(\bar{a}_f, \bar{b}_f) = (\pm m_f, 0)$, giving in fact, for the b case, two disjoint patches.

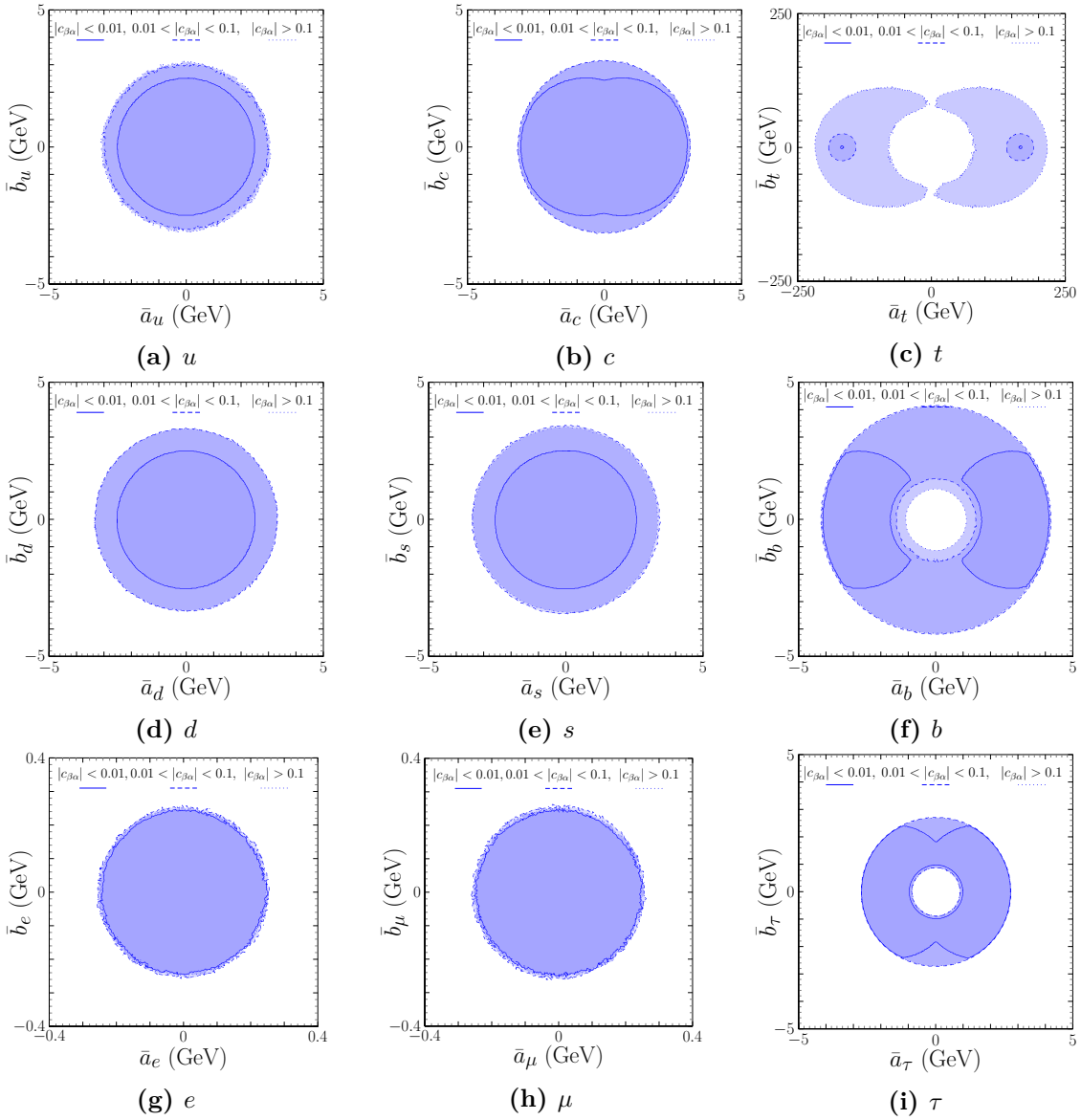

Figure 8.4: Allowed regions at 99% CL for pseudoscalar vs. scalar couplings for the different fermions f with $\mathscr{L}_{\mathrm{h}\bar{f}f} = -\frac{\mathrm{h}}{v}\bar{f}(\bar{a}_f + i\bar{b}_f\gamma_5)f$.

To close this section we recall the discussion on $\bar{q}q \to \mathrm{h}$ production in section 7.3: as commented there, values of n_f in agreement with the SM-like Higgs signal strengths could potentially give production cross sections not far from the dominating SM ones. Figure 8.5 shows

$$\frac{\sigma[q\bar{q}\mathrm{h}]}{\sigma[pp(gg)\to \mathrm{h}]_{\mathrm{SM}}} \equiv \left(\sum_{q=u,c,d,s} \sigma[pp(q\bar{q})\to \mathrm{h}]\right) \Big/ \sigma[pp(gg)\to \mathrm{h}]_{\mathrm{SM}}, \tag{8.11}$$

vs. the total Higgs width and vs. the gluon-gluon fusion production cross section

in two different analyses: in Figures 8.5a and 8.5b, $\sigma[q\bar{q}\mathrm{h}]$ is added to the ggF production cross section, while in Figures 8.5c and 8.5d it is not (and therefore, in the analysis, it does not affect directly observables constrained by experiment). Comparing 8.5a-8.5b with 8.5c-8.5d, one can notice that the constraints from Higgs signal strengths are able to bound the size of $\sigma[q\bar{q}\mathrm{h}]$, even if there is room for an overall $q\bar{q} \to \mathrm{h}$ cross section which is quite sizable, not far from the complete SM Higgs production cross section. Furthermore, when $\sigma[q\bar{q}\mathrm{h}]$ is added to the ggF production cross section, the agreement with the observed Higgs signal strengths allows for a smaller amount of $q\bar{q} \to \mathrm{h}$, and, for sizable $q\bar{q} \to \mathrm{h}$, it is achieved at the cost of (i) reducing the ggF production cross section and (ii) increasing the total width $\Gamma(\mathrm{h})$, as the shape of the allowed regions in Figures 8.5a and 8.5b shows. For the results in Figures 8.3 and 8.4, the bounds on the different $\bar{a}_f$, $\bar{b}_f$ do not differ in both analyses. It should be finally mentioned that, in connection with the previous comments and the size of $\sigma[pp(q\bar{q}) \to \mathrm{h}]$, it might be interesting to analyze, for the remaining neutral scalars H and A, the cross sections for $pp(q\bar{q}) \to \mathrm{H}, \mathrm{A}$ at the LHC.

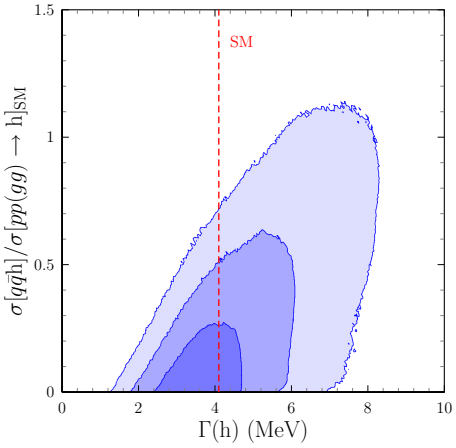

(a) $\sigma[q\bar{q}\mathrm{h}]$ vs. $\Gamma(\mathrm{h})$, $\sigma[q\bar{q}\mathrm{h}] \subset$ ggF.

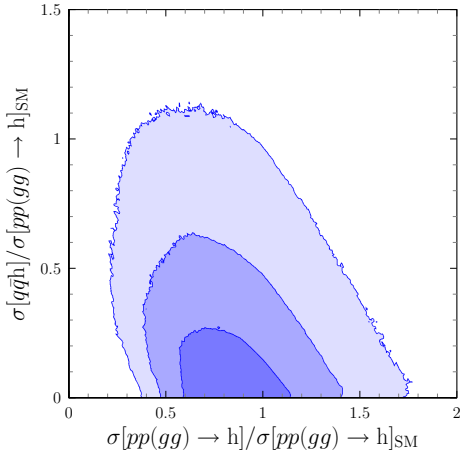

(b) $\sigma[q\bar{q}\mathrm{h}]$ vs. $\sigma[pp(gg) \to \mathrm{h}]$, $\sigma[q\bar{q}\mathrm{h}] \subset$ ggF

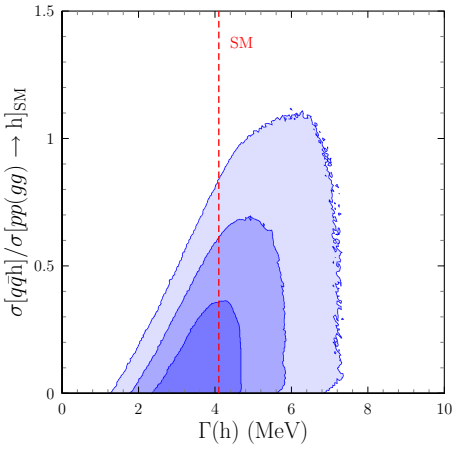

(c) $\sigma[q\bar{q}\mathrm{h}]$ vs. $\Gamma(\mathrm{h})$, $\sigma[q\bar{q}\mathrm{h}] \not\subset$ ggF

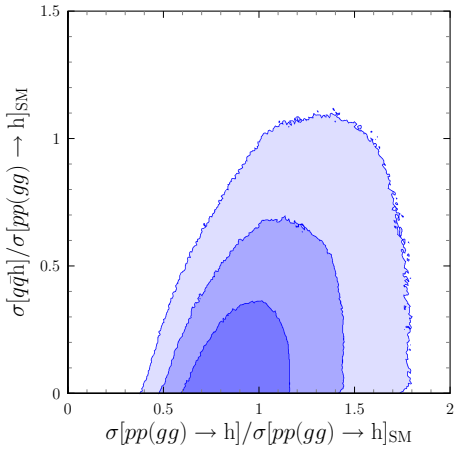

(d) $\sigma[q\bar{q}\mathrm{h}]$ vs. $\sigma[pp(gg) \to \mathrm{h}]$, $\sigma[q\bar{q}\mathrm{h}] \not\subset$ ggF

Figure 8.5: Effect of including $q\bar{q} \to \mathrm{h}$ production in ggF in analyses of Higgs signal strengths; darker to lighter regions correspond to 68, 95 and 99% CL.

A new day will come. And when the sun shines it will shine out the clearer. Those were the stories that stayed with you. That meant something. Even if you were too small to understand why. But I think, Mr. Frodo, I do understand. I know now. Folk in those stories had lots of chances of turning back only they didn't. They kept going. Because they were holding on to something.

— SAMwise Gamgee, *The Lord of the Rings*, J. R. R. Tolkien

9 Electron and Muon $(g-2)$

As it was seen in the SM chapter (section 1.2), the recent improved determination of the fine structure constant [45], has caused the appearance of a new anomaly [46] concerning the anomalous magnetic moment of the electron $a_e = (g_e - 2)/2$. There is a 2.4σ tension between the experimental determination [1] and the SM prediction [47–52],

$$\delta a_e \equiv a_e^{\text{Exp}} - a_e^{\text{SM}} = -(8.7 \pm 3.6) \times 10^{-13} \,. \tag{1.74}$$

In the anomalous magnetic moment of the muon [53–59] there is also another well known and long standing $\approx 3.7\sigma$ discrepancy between experiment and theory,

$$\delta a_\mu \equiv a_\mu^{\text{Exp}} - a_\mu^{\text{SM}} = (2.7 \pm 0.9) \times 10^{-9} \,. \tag{1.76}$$

It is to be noticed that the anomalies in eqs. (1.74) and (1.76) have opposite sign. Because of this difference of sign, several New Physics solutions addressing eq. (1.76) tend to be eliminated as solutions to both eqs. (1.76) and (1.74). In particular, many popular models in which the anomaly scales with the square of the lepton mass [268] tend to generate too large δa_e with the wrong sign. Some authors [269] argue that if the origin of both anomalies is beyond the SM, the corresponding model must

[1] After the work [4] that is presented in this chapter was published, the g-2 measurements for the electron [60] and for the muon [61] were updated (see section 1.2).

incorporate some sort of effective decoupling between μ and e. Recent beyond-SM explanations of both anomalies can be found in [122, 270–285]. Regarding the new measurement in eq. (1.77), of the muon (g-2) by the Muon g-2 collaboration at Fermilab [61] several explanations with extra Higgs doublets have already been proposed [286–291].

The two Higgs doublets model which introduces, in general, a new set of flavor structures in the Yukawa sector could implement the decoupling between μ and e required to explain δa_μ and δa_e. Of course, the most popular 2HDMs shaped by symmetries [76, 77], the so-called 2HDMs of types I, II, Lepton-Specific and Flipped [79, 83, 112], do not implement in a straightforward way this decoupling between μ and e, since the new Yukawa couplings in the lepton sector are proportional to the charged lepton mass matrix.

Going one step further in generality, the A2HDM [125] gives up stability of the model under the renormalization group evolution (RGE) [126] (the model is not shaped by a symmetry). The A2HDM cannot, however, incorporate some effective decoupling between μ and e since the new Yukawa structures are still proportional to the fermion mass matrices. It is nevertheless interesting to note that, as was mentioned in section 3.2.4, the lepton sector of the A2HDM is stable under one loop RGE[2] [127, 128, 130]: scalar flavor changing neutral couplings, absent at tree level, do not appear at one loop.

In the gFC-2HDM, at tree level, all Yukawa couplings are diagonal in the fermion mass basis [2, 129, 292]. It has been shown that the charged lepton sector of the gFC-2HDM is one loop stable under RGE, in the sense that SFCNC, absent at tree level, are not generated at one loop [2]. This implies that a well behaved and minimal 2HDM that can implement the effective decoupling among μ and e is a gFC-2HDM in the leptonic sector. Since this is all what is required to address the two anomalies in eqs. (1.74)–(1.76), we consider two minimal models in which the quark sector is a 2HDM of either type I or type II, while the lepton

[2]As in the SM, one is assuming massless neutrinos.

sector corresponds to a gFC-2HDM. We refer to them as models I-gℓFC and II-gℓFC respectively (see section 3.2.4). Note that these models do not have SFCNC at tree level neither in the quark nor in the lepton sectors. Additionally, the new Yukawa couplings in the lepton sector are independent of the charged lepton mass matrix. In the appropriate limits, model I-gℓFC can reproduce 2HDMs of types I and X while, similarly, model II-gℓFC can reproduce 2HDMs of types II and Y. In this sense model I-gℓFC is a generalization of 2HDMs of types I and X, while model II-gℓFC is instead a generalization of 2HDMs of types II and Y. The convenience of adopting this kind of generalized flavor conserving 2HDMs for phenomenological analyses was advocated in [2].

This chapter is organised as follows. In section 9.1, the one and two loop contributions to a_ℓ are revisited. In a simplified analysis it is shown that, with dominating two loop contributions, a new simple scaling law follows:

$$\frac{\delta a_e}{\delta a_\mu} = \frac{m_e \,\mathrm{Re}\,(n_e)}{m_\mu \,\mathrm{Re}\,(n_\mu)}\,, \tag{9.1}$$

with n_e, n_μ, the new Yukawa couplings of the charged leptons, in the lepton mass basis. In order to solve the discrepancies in eqs. (1.74)–(1.76) through the two loop contributions, the scaling in eq. (9.1) requires

$$\mathrm{Re}\,(n_\mu) = -\left(15.11^{+15.11}_{-7.56}\right) \mathrm{Re}\,(n_e)\ , \tag{9.2}$$

in the framework of models I-gℓFC and II-gℓFC. Besides solutions with dominating two loop contributions, an additional possibility with relevant one loop contributions is also analysed (similarly to [46]). In section 9.2, a number of constraints, relevant for a full analysis, is addressed. In section 9.3, the main results of such a full analysis are presented and discussed.

9.1 The new contributions to δa_ℓ

The full prediction a_ℓ^{Th} of the anomalous magnetic moments of $\ell = e, \mu$ has the form

$$a_\ell^{\mathrm{Th}} = a_\ell^{\mathrm{SM}} + \delta a_\ell\,, \tag{9.3}$$

with $a_\ell^{\rm SM}$ the SM contribution and δa_ℓ the corrections due to the model. To solve the discrepancies in eqs. (1.74)–(1.76), the aim is to obtain $\delta a_e \simeq \delta a_e^{\rm Exp}$ and $\delta a_\mu \simeq \delta a_\mu^{\rm Exp}$ within models I-gℓFC and II-gℓFC. It is convenient to introduce Δ_ℓ following

$$\delta a_\ell = K_\ell \, \Delta_\ell, \qquad K_\ell = \frac{1}{8\pi^2}\left(\frac{m_\ell}{v}\right)^2 = \frac{1}{8\pi^2}\left(\frac{g m_\ell}{2M_W}\right)^2 . \tag{9.4}$$

The quantities K_ℓ collect the typical factors arising in one loop contributions; since $K_e \simeq 5.5 \times 10^{-14}$ and $K_\mu \simeq 2.3 \times 10^{-9}$, in order to reproduce the anomalies we roughly need

$$\Delta_e \simeq -16\,, \qquad \Delta_\mu \simeq 1\,. \tag{9.5}$$

It is well known that in the type of models considered here, both one loop [293] or two loop Barr-Zee contributions [203, 259, 261, 294–296] can be dominant. Complete expressions used in the full analyses of section 9.3, can be found in appendix E. For the moment, we consider in this section two approximations: we only keep leading terms in a $(m_\ell/m_{\rm S})^2$ expansion (for the different scalars ${\rm S} = {\rm h}, {\rm H}, {\rm A}$), and the alignment limit $s_{\alpha\beta} \to 1$. With these approximations, the one loop contribution to Δ_ℓ in eq. (9.4) is

$$\Delta_\ell^{(1)} \simeq n_\ell^2 \left(\frac{I_{\ell {\rm H}}}{m_{\rm H}^2} - \frac{I_{\ell {\rm A}} - 2/3}{m_{\rm A}^2} - \frac{1}{6 m_{{\rm H}^\pm}{}^2} \right), \tag{9.6}$$

where

$$I_{\ell {\rm S}} = -\frac{7}{6} - 2\ln\left(\frac{m_\ell}{m_{\rm S}}\right). \tag{9.7}$$

Equation (9.6) applies to both model I-gℓFC and II-gℓFC. We do not consider light scalars or pseudoscalars (see reference [280]): in the different analyses it is assumed that h is the lightest scalar, i.e. ${\rm m_h} < m_{\rm H}, m_{\rm A}$. For a typical range $m_{\rm S} \in [0.2; 2.0]$ TeV, the loop functions $I_{\ell {\rm S}}$ obey

$$I_{e {\rm S}} \in [24.6; 29.2]\,, \qquad I_{\mu {\rm S}} \in [13.9; 18.5]\,, \tag{9.8}$$

and thus the dominant contributions to $\Delta_\ell^{(1)}$ in eq. (9.6) are the logarithmically enhanced contributions from H and A. Then, $\Delta_e \simeq -16$ can only arise from the negative sign of the A pseudoscalar contribution: $\Delta_e \simeq -[{\rm Re}\,(n_e)]^2 I_{e {\rm A}}/m_{\rm A}^2$. Taking

into account the $I_{e\mathrm{A}}$ value in eq. (9.8), it would require $[\mathrm{Re}\,(n_e)]^2 \sim m_{\mathrm{A}}^2$, which can easily violate perturbativity requirements in the Yukawa sector or constraints from resonant dilepton searches. Consequently, we do not expect an explanation of δa_e in terms of one loop contributions. For δa_μ, any relevant one loop contribution in eq. (9.6) should arise from the H contribution attending, again, to the required sign and the logarithmically enhanced value of $I_{\mu\mathrm{H}}$ in eq. (9.8): $\Delta_\mu \simeq [\mathrm{Re}\,(n_\mu)]^2 I_{\mu\mathrm{H}}/m_{\mathrm{H}}^2$. For $I_{\mu\mathrm{H}} \simeq 16$ such a contribution needs $[\mathrm{Re}\,(n_\mu)]^2 \sim [m_{\mathrm{H}}/4]^2$, that is a not too heavy H (in order to have reasonably perturbative n_μ) and $m_{\mathrm{A}} > m_{\mathrm{H}}$ in order to avoid cancellations with wrong sign contributions. In the same approximation (leading m_ℓ/m_{S} terms and $s_{\alpha\beta} \to 1$), the two loop contributions are dominated by Barr-Zee diagrams in which the internal fermion loop is connected with the external lepton via one virtual photon and one virtual neutral scalar H or A. The leading contribution to Δ_ℓ in eq. (9.4) is (for detailed expressions, see appendix E)

$$\Delta_\ell^{(2)} = -\left(\frac{2\alpha}{\pi}\right)\left(\frac{n_\ell}{m_\ell}\right) F\,. \tag{9.9}$$

The factor F depends on the masses of the fermions in the closed loop, on the couplings of those fermions to H and A, and, of course, on m_{H} and m_{A}; it is consequently different in models I-gℓFC and II-gℓFC:

$$\begin{aligned} F_{\mathrm{I}} &= \frac{\cot\beta}{3}\left[4(f_{t\mathrm{H}} + g_{t\mathrm{A}}) + (f_{b\mathrm{H}} - g_{b\mathrm{A}})\right] + \frac{\mathrm{Re}\,(n_\tau)}{m_\tau}(f_{\tau\mathrm{H}} - g_{\tau\mathrm{A}})\,, \\ F_{\mathrm{II}} &= \frac{\cot\beta}{3}\left[4(f_{t\mathrm{H}} + g_{t\mathrm{A}}) - \tan^2\beta(f_{b\mathrm{H}} - g_{b\mathrm{A}})\right] + \frac{\mathrm{Re}\,(n_\tau)}{m_\tau}(f_{\tau\mathrm{H}} - g_{\tau\mathrm{A}})\,, \end{aligned} \tag{9.10}$$

where

$$f_{f\mathrm{S}} \equiv f\left(\frac{m_f^2}{m_{\mathrm{S}}^2}\right), \quad g_{f\mathrm{S}} \equiv g\left(\frac{m_f^2}{m_{\mathrm{S}}^2}\right). \tag{9.11}$$

The functions $f(z)$ and $g(z)$ are defined in appendix E; they are represented in Figure 9.1. Their main features are: (i) $f(z) \simeq g(z)$ in the whole range of interest, (ii) the largest values correspond to the heavier fermion (the top quark), (iii) the values of f and g for the top quark contributions vary between 0.1 and 1 in the relevant range of scalar masses. Considering the dominant top quark terms, for $t_\beta \simeq 1$ and $m_{\mathrm{H}} \simeq m_{\mathrm{A}}$, it is easy to realize that for $m_{\mathrm{H}} \sim 1-2$ TeV, δa_e can be explained with Yukawa couplings $\mathrm{Re}\,(n_e) \sim 3-7$ GeV ($\mathrm{Re}\,(n_e) > 0$ gives the right

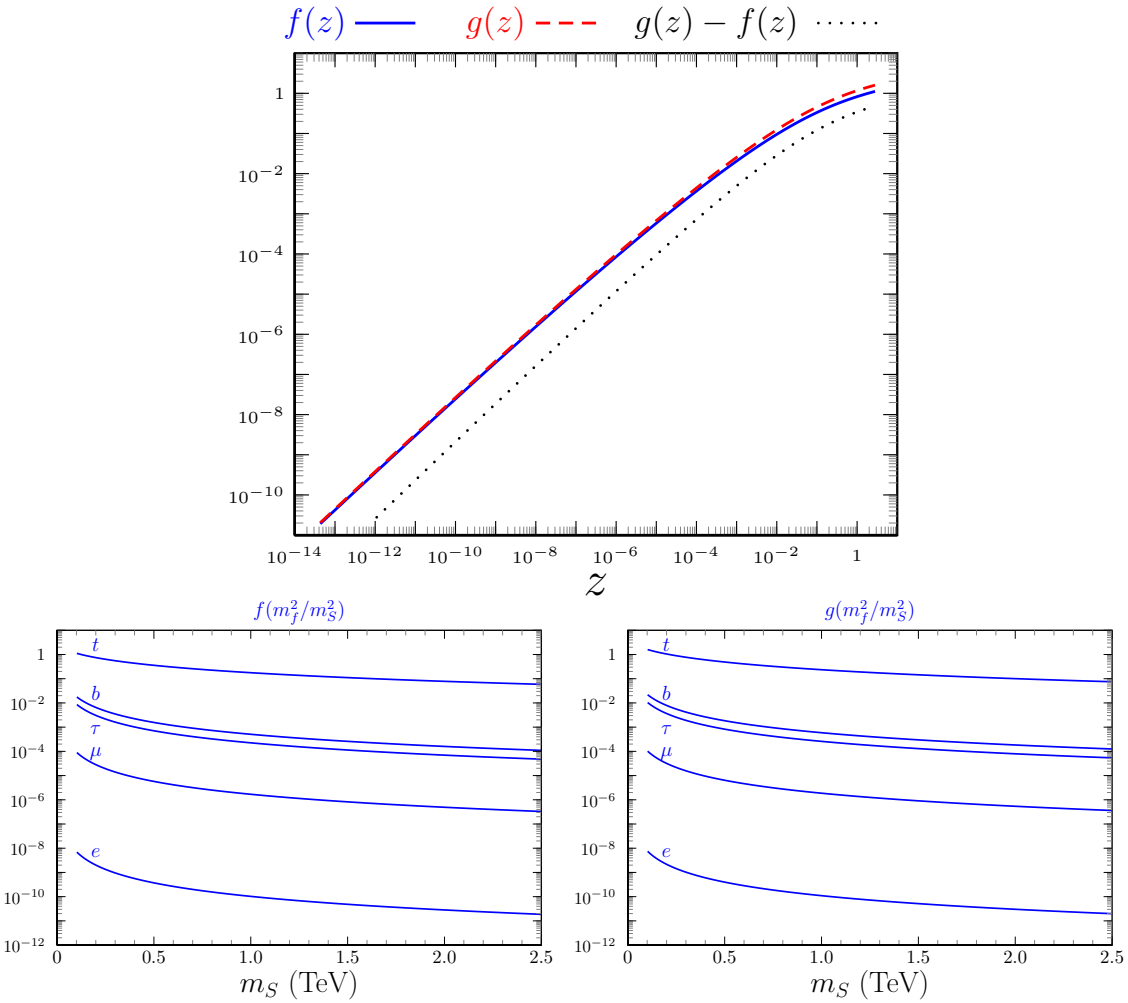

Figure 9.1: Loop functions.

sign of δa_e). If we assume that δa_μ must also be explained by the same kind of dominant Barr-Zee two loop contributions, which are independent of the specific charged lepton, it is straightforward that

$$\delta a_\mu = \frac{m_\mu \,\mathrm{Re}\,(n_\mu)}{m_e \,\mathrm{Re}\,(n_e)} \delta a_e \,. \tag{9.12}$$

With this relation, the origin of the different signs of δa_e and δa_μ relies on the freedom to have $\mathrm{Re}\,(n_e)$ and $\mathrm{Re}\,(n_\mu)$ with opposite signs, $\mathrm{Re}\,(n_\mu) \simeq -15\mathrm{Re}\,(n_e)$, as anticipated in eq. (9.1). In terms of $\mathrm{Re}\,(n_\mu)$, with the same assumptions ($t_\beta \sim 1$, $m_\mathrm{A} \sim m_\mathrm{H} \sim 1-2$ TeV), $\mathrm{Re}\,(n_\mu) \in -[45;105]$ GeV. The previous arguments apply to both models, I-gℓFC and II-gℓFC, since $4(f_{t\mathrm{H}} + g_{t\mathrm{A}})$ is the dominant term in both F_I and F_II.

Attending to the flavor constraints discussed in section 9.2 (B_d and B_s meson mixings, $b \to s\gamma$ radiative decays), $t_\beta \ll 1$ are excluded in 2HDMs of types I and II, and thus also in I-gℓFC and II-gℓFC models, there is no need to discuss the $t_\beta \ll 1$ regime.

Let us now analyse the two loop Barr-Zee contributions in eq. (9.10) for large values of t_β. As a reference, consider the analysis above with $t_\beta \sim 1$ and $m_{\rm A} \sim m_{\rm H} \sim 1-2$ TeV; for definiteness we now take $t_\beta = 50$. For large t_β, it is clear that these contributions in models I-gℓFC and II-gℓFC are quite different. Starting with model I-gℓFC, in order to maintain the right value of δa_e, the t_β suppression in $\mathrm{Re}\,(n_e)\, t_\beta^{-1}(f_{t\rm H} + g_{t\rm A})$ can be compensated with smaller $m_{\rm H}$, $m_{\rm A}$, and larger $\mathrm{Re}\,(n_e)$. For example, $m_{\rm A} \sim m_{\rm H} \sim 200$ GeV gives an increase of the loop functions by a factor of 10 with respect to $m_{\rm A} \sim m_{\rm H} \sim 1-2$ TeV; increasing then $\mathrm{Re}\,(n_e)$ by a factor of 5, the suppression $t_\beta^{-1} = 1/50$ is compensated. Therefore, the discrepancy in δa_e can be explained in the I-gℓFC model through two loop contributions, for large values of t_β and $\mathrm{Re}\,(n_e) \sim 15-35$ GeV. The question now is if one can explain, with the two loop contributions, the muon anomaly δa_μ. Attending to eq. (9.12), one would need $\mathrm{Re}\,(n_\mu) \in -[225; 505]$ GeV, which would be in conflict with perturbativity requirements in the Yukawa sector. However, as the discussion on one loop contributions after eq. (9.6) shows, for light $m_{\rm H}$, e.g. $m_{\rm H} \in [200; 400]$ GeV, δa_μ can be obtained with H-mediated one loop contributions, and $m_{\rm A} > m_{\rm H}$ to avoid cancellations. One needs $|\mathrm{Re}\,(n_\mu)| \sim m_{\rm H}/4$, in which case $|\mathrm{Re}\,(n_\mu)| \in [50; 100]$ GeV is acceptable from the perturbativity point of view.

Summarizing the previous discussion, we envisage, at least, two kinds of solutions:

- The first is realized with scalars having masses in the 1–2 TeV range, $t_\beta \sim 1$, and both anomalies produced by two loop Barr-Zee contributions. The coupling of electrons to the new scalar and pseudoscalar, $\mathrm{Re}\,(n_e)$, should be in the few GeV range. Following eq. (9.12), the corresponding muon coupling is larger. This first solution can appear, a priori, in both I-gℓFC and II-gℓFC models. In section 9.3 we refer to this first type of solution as "solution [A]".

- The second solution corresponds to a lighter H, $m_{\rm H} \in [200; 400]$ GeV and a heavier A; the required values of t_β are larger, $t_\beta \gg 1$. In this second solution, the electron anomaly is obtained with two loop contributions while the muon anomaly is one loop controlled; contrary to the first solution, there is no linear relation among $\mathrm{Re}\,(n_\mu)$ and $\mathrm{Re}\,(n_e)$. This second kind of solution can clearly appear in the I-gℓFC model, but in this simplified analysis it cannot be elucidated if this possibility is also open in the II-gℓFC model. Anticipating the results of the complete numerical analyses of section 9.3, this will not be the case: within the II-gℓFC model there is no solution with large t_β and relatively light H. In section 9.3 we refer to this second type of solution as "solution [B]". Notice also that, a priori, this second kind of solution might be obtained with both signs of $\mathrm{Re}\,(n_\mu)$.

9.2 Constraints

In this section we enumerate the different constraints from chapter 7 that are applied in analyses of section 9.3. Furthermore, since our purpose here is to explain simultaneously the anomalies present on the electron and muon $g-2$, we review in detail these constraints. Since δa_e and δa_μ have a role much more important than the rest of constraints, they are also incorporated in a different manner (as described in detail below) to ensure that the analysis focuses on the ability of the model to reproduce values which are clearly non-SM.

9.2.1 General constraints for the numerical analysis

In the analysis performed in section 9.3 the following constraints from chapter 7 are applied:

- The potential is required to be bounded from below as well as the quartic parameter to respect perturbativity and unitarity in $2 \to 2$ scattering. The oblique parameters S and T have to be in agreement with electroweak precision data.

- In the models studied there, the new couplings n_ℓ are dimensionless free parameters, so in principle they could be arbitrarily large. As in the previous chapters we require them to remain perturbative, in particular we apply $|n_\ell| \leq 95$ GeV.

- Concerning the 125 GeV Higgs-like scalar, agreement with the signal strengths is also imposed [297–300]. The measured signal strengths, with uncertainties reaching the 10% level, tend to favour the alignment limit in the scalar sector; it is to be noticed that since the models require $|\mathrm{Re}\,(n_e)| \gg m_e$ and $|\mathrm{Re}\,(n_\mu)| \gg m_\mu$, the Higgs measurements in the $\mu^+\mu^-$ channel such as [266] and [267] are even more effective in forcing that alignment limit. Constraints on the total width Γ_h, arising from off-shell (ggF+VBF)$\to \mathrm{h}^{(*)} \to WW^{(*)}$ [231], are also included.

- We also impose lepton flavor universality contrains. In particular pure leptonic decays and leptonic decays modes like $K, \pi \to e\nu, \mu\nu$ and $\tau \to K\nu, \pi\nu$, which provide additional constraints on the different n_ℓ (together with the t_β dependence of the quark couplings with $\mathrm{H}^\pm$). In the gFC case, eq. (7.29) reads

$$\Delta^P_{\ell_a} \equiv 1 - \frac{M_P^2}{M^2_{H^\pm}} \frac{k_u m_{u_i} + k_d^* m_{d_j}}{m_{u_i} + m_{d_j}} \frac{n_{\ell_a}}{m_{\ell_a}}, \tag{9.13}$$

  with $k_u = k_d = t_\beta^{-1}$ in model I-gℓFC and $k_u = -k_d^{-1} = t_\beta^{-1}$ in model II-gℓFC. Notice the enhanced sensitivity of these observables due to the $\frac{n_{\ell_a}}{m_{\ell_a}}$ factor: unlike the SM amplitude, the new $\mathrm{H}^\pm$-mediated amplitude is not helicity suppressed. For ratios involving $\tau^+ \to P^+\nu$ decays, the expressions are unchanged. All these LFU violating effects scale with $1/m^2_{\mathrm{H}^\pm}$ and therefore one expects that in both models, I-gℓFC and II-gℓFC, the effects for large $m_{\mathrm{H}^\pm}$ are much more suppressed, including in particular the solution [A] region introduced in section 9.1. This is quite clear in the pure leptonic decays, where the most relevant constraints, eq. (7.25) and $\left|g^{\mathrm{S,RR}}_{\mu\to e}\right|$ in eq. (7.26), can be comfortably satisfied, giving a contribution to the corresponding χ^2 at a level similar to the SM. Since solution [A] corresponds to $t_\beta \sim 1$, the effects in semileptonic

processes are similar in both models, with the effects in kaons larger by a factor of 10 than the effects in pions. The leading contribution to $R^K_{\mu e} - 1$ is of the order of the uncertainty: since in that channel there is essentially a change of sign between the contributions in models I-gℓFC and II-gℓFC, it turns out that in the II-gℓFC case the corresponding χ^2 value can improve over the SM one, while in the I-gℓFC case it is the other way around. In any case, for solution [A], these differences are small. For solution [B], the situation is different since we have:

$$\text{solution [B], model I-g}\ell\text{FC,} \qquad \Delta^K_\ell \sim \frac{M_K^2}{m_\ell}\frac{n_\ell}{M^2_{H^\pm}\, t_\beta}, \tag{9.14}$$

$$\text{solution [B], model II-g}\ell\text{FC,} \qquad \Delta^K_\ell \sim -\frac{M_K^2}{m_\ell}\frac{n_\ell\, t_\beta}{M^2_{H^\pm}}, \tag{9.15}$$

considering that it requires $t_\beta \gg 1$ and smaller $m_{\mathrm{H}^\pm}$. Clearly, lower values of $m_{\mathrm{H}^\pm}$ can be compensated by large values of t_β in model I-gℓFC , and solution [B] is similar to [A] concerning this constraint. On the contrary, in model II-gℓFC, lower values of $m_{\mathrm{H}^\pm}$ and larger values of t_β enhance the new contributions: this observable is highly relevant to eliminate solution [B] in model II-gℓFC.

The new scalars can also give one loop corrections to $Z \to \ell^+\ell^-$ decays. In the parameter space region corresponding to solution [A], one can easily check that these new contributions are at least a factor of 30 smaller than the experimental uncertainties (in the limit $m_{\mathrm{A}} = m_{\mathrm{H}} = m_{\mathrm{H}^\pm} \gg M_Z$ they decouple, see [301]); in the parameter space of solution [B], the new contributions are larger, but still below uncertainties.

- Contributions to the mixing in B_d and B_s meson systems as well as to the radiative decay $b \to s\gamma$ are also included. Both observables are insensitive to scalar-lepton couplings, they can only constrain $m_{\mathrm{H}^\pm}$ and t_β. For $m_{\mathrm{H}^\pm}$ the effect is straightforward: for large values of $m_{\mathrm{H}^\pm}$, the new contributions are suppressed. Concerning t_β, dominant new contributions with virtual top quarks are further enhanced or suppressed by the t_β^{-1} dependence in Table 3.1.

In the following some constraints that where not included in chapter 7 since they are only applied to the analysis in this chapter are reviewed.

9.2.2 $e^+e^- \to \mu^+\mu^-, \tau^+\tau^-$ at LEP

LEP measured $e^+e^- \to \mu^+\mu^-, \tau^+\tau^-$ with center-of-mass energies up to $\sqrt{s} = 208$ GeV: although s-channel contributions with virtual H and A do not interfere with SM γ and Z mediated contributions, for light H, A, the resonant enhancement together with the large couplings to leptons might give predictions in conflict with data (e.g. [302]). The effect of these LEP constraints is, essentially, to forbid values of m_{H}, m_{A} below $210 - 215$ GeV.

9.2.3 LHC searches

We consider constraints from LHC searches of scalars, in particular

- searches of dilepton resonances [303–308] which give constraints on $\sigma(pp \to S)_{[\mathrm{ggF}]} \times \mathrm{Br}\,(S \to \ell^+\ell^-)$, $S = \mathrm{H}, \mathrm{A}$ and $\ell = \mu, \tau$, where the production cross section $\sigma(pp \to S)_{[\mathrm{ggF}]}$ corresponds to gluon-gluon fusion,

- and searches of charged scalars [309–313] which give constraints on $\sigma(pp \to \mathrm{H}^\pm tb) \times \mathrm{Br}\,(\mathrm{H}^\pm \to f)$, $f = \tau\nu, tb$.

For production, the narrow width approximation is considered; the widths of H, A and $\mathrm{H}^\pm$ can reach $\sim 10\%$ of their respective masses: if one incorporates finite width effects through the convolution of the cross section computed in the NWA with a (relativistic) Breit-Wigner distribution for the scalars, the computed signal would be partially "diluted". In this sense, using the NWA is conservative since it gives stronger pointwise bounds. The constraints are incorporated as contributions of the following form in the global χ^2: for each "production × decay" channel with experimental bound $[\sigma \times \mathrm{Br}]_{\mathrm{Exp}}$ and theoretical prediction $[\sigma \times \mathrm{Br}]_{\mathrm{Th}}$, the contribution is given by

$$\chi^2([\sigma \times \mathrm{Br}]_{\mathrm{Th}}) = \begin{cases} 0, & \text{if } [\sigma \times \mathrm{Br}]_{\mathrm{Th}} \leq 0.9 \times [\sigma \times \mathrm{Br}]_{\mathrm{Exp}}, \\ 10^3 \times \left(\frac{[\sigma \times \mathrm{Br}]_{\mathrm{Th}}}{[\sigma \times \mathrm{Br}]_{\mathrm{Exp}}} - 0.9 \right), & \text{if } [\sigma \times \mathrm{Br}]_{\mathrm{Th}} > 0.9 \times [\sigma \times \mathrm{Br}]_{\mathrm{Exp}}. \end{cases} \tag{9.16}$$

Equation (9.16) is a convenient smooth approximation of a "sharp" bound/cut. Production cross sections incorporate corrections associated to the modified fermion-scalar vertices as shown in eq. (7.21).

Moreover, for the production cross sections $pp \to H^{\pm}tb$ (i.e. $H^{\pm}$ in association with tb), we refer to [314, 315], which provide results, labeled here $\sigma_{[\mathrm{Ref}]}$, for a type II 2HDM with $t_\beta = 1$. For arbitrary values of t_β, we use

$$\begin{aligned}
&\text{Model I-g}\ell\text{FC: } \sigma_{\mathrm{I}}(t_\beta) = \frac{(m_t/t_\beta)^2 + (m_b/t_\beta)^2}{m_t^2 + m_b^2} \times \sigma_{[\mathrm{Ref}]} = \frac{1}{t_\beta^2}\sigma_{[\mathrm{Ref}]},\\
&\text{Model II-g}\ell\text{FC: } \sigma_{\mathrm{II}}(t_\beta) = \frac{(m_t/t_\beta)^2 + (m_b t_\beta)^2}{m_t^2 + m_b^2} \times \sigma_{[\mathrm{Ref}]} = \frac{1}{t_\beta^2}\frac{1 + t_\beta^4 m_b^2/m_t^2}{1 + m_b^2/m_t^2}\sigma_{[\mathrm{Ref}]}.
\end{aligned} \tag{9.17}$$

As an additional check, (i) the previous cross sections and (ii) the computations of the decay branching ratios of the scalars, have been compared with the results of MadGraph5_aMC@NLO[316] at leading order. With FeynRules [317] and NLOCT [318, 319], the needed universal Feynrules Output at NLO of the I-gℓFC and II-gℓFC models is produced. A good agreement in the gluon-gluon fusion production cross section is found, given the fact that the MadGraph5_aMC@NLO calculation is at leading order (one loop in this case). For the branching ratios, there is complete agreement.

9.2.4 δa_ℓ constraints for the numerical analyses

The main motivation of this work [4] was to accommodate the departures from SM expectations in the anomalous magnetic moments of both electron and muon. We now discuss how these departures are implemented as constraints in the analyses presented in section 9.3. The $g-2$ anomalies $\delta a_\ell^{\mathrm{Exp}} = a_\ell^{\mathrm{Exp}} - a_\ell^{\mathrm{SM}}$ in eqs. (1.74)–(1.76) are

$$\delta a_e^{\mathrm{Exp}} = -(8.7 \pm 3.6) \times 10^{-13}\,, \quad \delta a_\mu^{\mathrm{Exp}} = (2.7 \pm 0.9) \times 10^{-9}\,. \tag{9.18}$$

The theoretical prediction in the present models is $a_\ell^{\mathrm{Th}} = \delta a_\ell + a_\ell^{\mathrm{SM}}$ and thus a simple and natural measure of their ability to accommodate the experimental

results is a χ^2 function

$$\chi^2_0(\delta a_e, \delta a_\mu) = \left(\frac{\delta a_e - c_e}{\sigma_e}\right)^2 + \left(\frac{\delta a_\mu - c_\mu}{\sigma_\mu}\right)^2 , \tag{9.19}$$

where $\delta a_\ell^{\rm Exp} = c_\ell \pm \sigma_\ell$ in eq. (9.18).

The interest in explanations of the experimental results in terms of non-SM contributions is due to the $3-4\sigma$ deviation $\chi^2_0(0,0) \simeq 15$. For the numerical exploration of the regions in parameter space which could provide such an explanation, rather than including a contribution $\chi^2_0(\delta a_e, \delta a_\mu)$ in the global χ^2, we impose a stronger requirement: instead of $\chi^2_0(\delta a_e, \delta a_\mu)$ we include

$$\chi^2(\delta a_e, \delta a_\mu) = \begin{cases} 0, & \text{if } \chi^2_0(\delta a_e, \delta a_\mu) \leq \frac{1}{4}, \\ 10^6 \times (\chi^2_0(\delta a_e, \delta a_\mu) - \frac{1}{4}), & \text{if } \chi^2_0(\delta a_e, \delta a_\mu) > \frac{1}{4}, \end{cases} \tag{9.20}$$

in order to guarantee that the models reproduce both anomalies simultaneously within less than $\frac{1}{2}\sigma_\ell$ of the central values (in the regions of interest, eq. (9.20) approximates a "sharp" box function). This approach is adopted in order to ensure that, when representing allowed regions at a given confidence level in the next section, they do not include regions where one or both anomalies are only partially reproduced. For illustration, Figure 9.2 shows the allowed region obtained in the complete numerical analyses (which is identical in both models); that is, in the results of section 9.3, within all the represented allowed regions, the values of δa_e and δa_μ belong to the allowed region of Figure 9.2. Notice, finally, that the SM

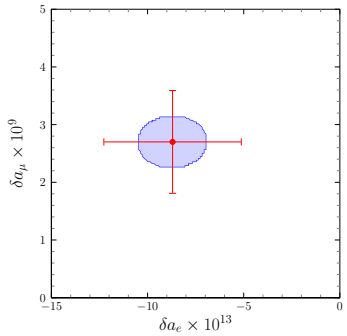

Figure 9.2: Allowed δa_μ vs. δa_e region.

prediction $a_\ell^{\rm SM}$ includes Higgs-mediated contributions: since these are just the h mediated contributions for exact alignment $s_{\alpha\beta} = 1$, they have to be subtracted

from the New Physics contributions to δa_ℓ mediated by h (quantitatively, however, this subtlety is rather irrelevant).

9.3 Results

As discussed in section 9.1, we expect, at least, two different types of solution to the δa_ℓ anomalies. In the following we refer to them, as anticipated, as solutions [A] and [B]. Solution [A] corresponds to $t_\beta \sim 1$, heavy neutral new scalars (with masses in the 1–2 TeV range), and both anomalies explained by two loop Barr-Zee contributions. Solution [B] corresponds instead to large t_β, lighter new scalars, with δa_e obtained through two loop Barr-Zee contributions while in δa_μ the most important contributions are one loop and H-mediated. Note that in general one would expect a set of intermediate solutions between [A] and [B], at least in model I-gℓFC, where we have a priori identified the presence of both solutions. For model II-gℓFC we can only anticipate with some certainty the presence of solution [A].
It is therefore very important to find out which constraints, if any, can distinguish among both types of solutions. One should also remember that quite large couplings of the new scalars to leptons are required to explain the anomalies. This fact confers a special role to dilepton resonance and charged scalar searches at the LHC. Consequently the analyses are separated in two stages: (i) one, labelled "No LHC", which includes all constraints discussed in section 9.2 except for the LHC searches which are not imposed as constraints, and (ii) the complete analysis with all constraints, including these LHC searches.
One should also remark, before presenting results, that solutions [A] and [B] as discussed above, cannot be realized when the scalar potential in eq. (3.43) is exactly $\mathbb{Z}_2$ symmetric, i.e. when $\mu_{12}^2 = 0$. This was to be expected. The reason to have difficulties obtaining solution [A] with the exactly $\mathbb{Z}_2$ symmetric potential is simple: it does not allow a "decoupling regime" [215, 255, 320], i.e. in that case one cannot have scalars heavier than ~ 1 TeV (without violating requirements such as perturbativity). On the other hand, concerning solution [B], the exact $\mathbb{Z}_2$ symmetry does not allow large t_β. Introducing $\mu_{12}^2 \neq 0$ removes both obstacles.

In the plots to follow, the results from the "No LHC" analysis correspond to lighter red regions while the results from the full analysis correspond to darker blue regions. The regions represented are allowed at 2σ (for a $2D-\chi^2$ distribution); the χ^2 or likelihood function used in the numerical analysis implements the constraints of section 9.2.

In Figure 9.3 we have $\mathrm{Re}\,(n_\mu)$ versus $\mathrm{Re}\,(n_e)$; the full analysis shows, clearly, three disjoint regions. As indicated in the figure, the bottom left small region corresponds to solution [A], and reproduces the linear relation of eq. (9.12), arising from the explanation of both anomalies through two loop Barr-Zee contributions. The largest blue region to the bottom right corresponds to solution [B] with $\mathrm{Re}\,(n_\mu)<0$, where δa_e is two loop dominated while δa_μ also receives significant one loop contributions. In this region there is no linear relation among $\mathrm{Re}\,(n_e)$ and $\mathrm{Re}\,(n_\mu)$. For $\mathrm{Re}\,(n_\mu)>0$, solution [B] corresponds to the top blue region (the subindex $\pm$ in $[\mathrm{B}_\pm]$ refers to the sign of $\mathrm{Re}\,(n_\mu)$). It is clear, from the underlying red region, that excluding LHC searches, there is a smooth transition between solutions [A] and $[\mathrm{B}_-]$ where all kinds of contributions must be considered: we recall that the numerical analyses incorporate the complete expressions of appendix E, which consider one and two loop contributions with all possible fermions in the fermion loop of Barr-Zee terms. It is important to stress that, since the lepton couplings to H and A can be quite large, it is mandatory to include all leptons in the computation of Barr-Zee terms.

Figure 9.4 shows results for $\mathrm{Re}\,(n_\ell)$ versus t_β and m_{H}. From previous discussions,

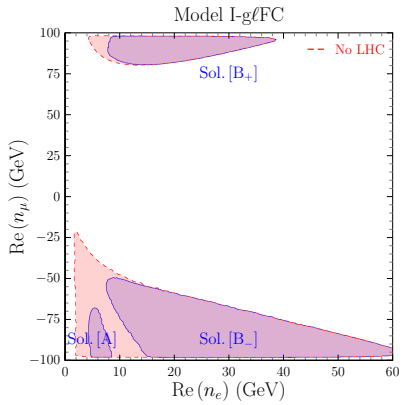

Figure 9.3: $\mathrm{Re}\,(n_\mu)$ vs. $\mathrm{Re}\,(n_e)$.

the regions corresponding to solutions [A] and [B] can be easily identified. For example, in Figure 9.4a, the blue region reaching larger values of $\mathrm{Re}\,(n_e)$, with $t_\beta \geq 13$ and 200 GeV $\leq m_{\mathrm{H}} \leq$ 370 GeV is clearly associated to solution [B]. Figures 9.4b and 9.4e illustrate the same aspects regarding now $\mathrm{Re}\,(n_\mu)$. For $\mathrm{Re}\,(n_\tau)$ it also follows from Figures 9.4c and 9.4f that $\mathrm{Re}\,(n_\tau) > 0$ is required in solution [B] (one can indeed check that it gives a subdominant but necessary two loop contribution to obtain the appropriate value of δa_μ).

To characterize more precisely solutions [A] and [B], Figure 9.5 shows correlations

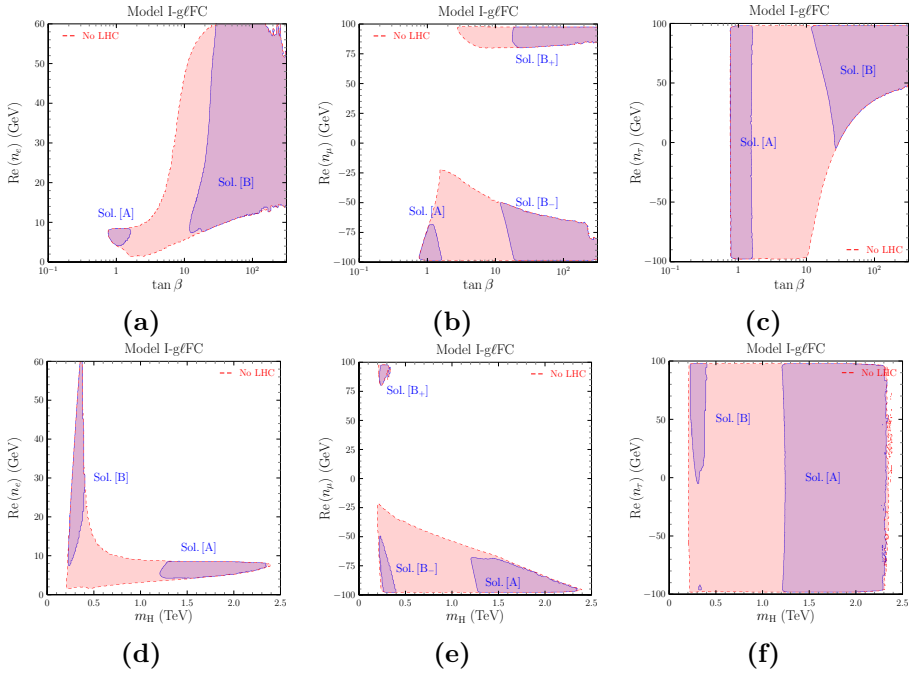

Figure 9.4: n_ℓ couplings versus t_β, m_{H}.

among scalar masses and with t_β. In particular, it is clear that in solution [A] all new scalars are heavy, with masses in the 1.2 – 2.3 TeV range, and mass differences not exceeding ±200 GeV. For solution [B], some important results can be observed: (i) in addition to the existence of separate regions [B$_+$] and [B$_-$] for both signs of $\mathrm{Re}\,(n_\mu)$, there are two separate manners in which solution [B] can arise, one region where $m_{\mathrm{H}^\pm} \in [0.4; 0.9]$ TeV and $m_{\mathrm{A}} = m_{\mathrm{H}^\pm}$ to a high degree of accuracy and another smaller region where $m_{\mathrm{H}^\pm} \in [0.25; 0.35]$ TeV and $m_{\mathrm{H}} = m_{\mathrm{H}^\pm}$ to a high degree of accuracy; (ii) in all cases, $m_{\mathrm{H}} < m_{\mathrm{A}}$. This last inequality, as analysed later, must

allow the decay $A \to HZ$ (additionally, either $H^\pm \to HW^\pm$ or $A \to H^\pm W^\mp$ would also be allowed); together with the electroweak precision constraints (in particular the oblique parameter T), this forces either $m_A = m_{H^\pm}$ or $m_H = m_{H^\pm}$. These two results match nicely with the need for H to be as light as possible (LEP constraints will force in any case $m_H \geq 210$ GeV) in order to produce the main contribution (at one loop) to δa_μ.

Figure 9.6 shows the resonant $[pp]_{ggF} \to S \to \mu^+\mu^-$ cross sections with respect

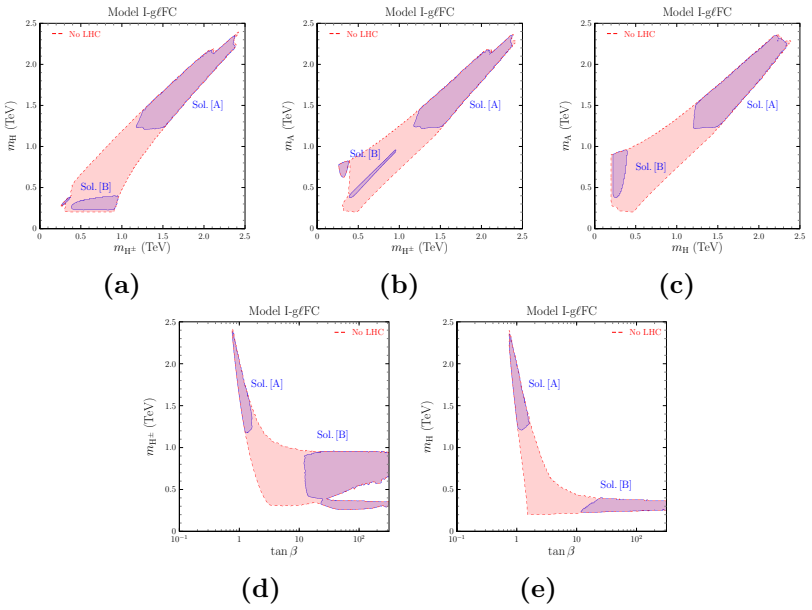

Figure 9.5: Scalar sector.

to m_S for $S = H, A$. The black line shows the LHC bounds included in the full analysis. In gluon-gluon fusion production, for the same scalar mass, the gluon-gluon-pseudoscalar amplitude is 2–6 times larger than the corresponding gluon-gluon-scalar amplitude (that is $2^2 - 6^2$ larger pseudoscalar vs. scalar production cross sections). One could have expected, attending to this fact, that the constraints from LHC searches on $\sigma(pp \to A)_{ggF} \times \mathrm{Br}(A \to \mu^+\mu^-)$ versus m_A would be responsible for the separation among solutions [A] and [B]. Figure 9.6a disproves this naive expectation; as Figure 9.6b shows it is rather $\sigma(pp \to H)_{ggF} \times \mathrm{Br}(H \to \mu^+\mu^-)$ which shows how the bounds from LHC searches separate the solutions by excluding $m_H \in [380; 1200]$ GeV (i.e. eliminating the red region "bridge" connecting the blue regions). Comparing

the shape of the allowed regions in Figures 9.6a and 9.6b it is also clear that, besides the production cross section, the branching ratios $\mathrm{Br}\,(\mathrm{H}, \mathrm{A} \to \mu^+\mu^-)$ may play an important role.

On this respect, let us start by observing that, since values of $|\mathrm{Re}\,(n_\mu)|$ larger

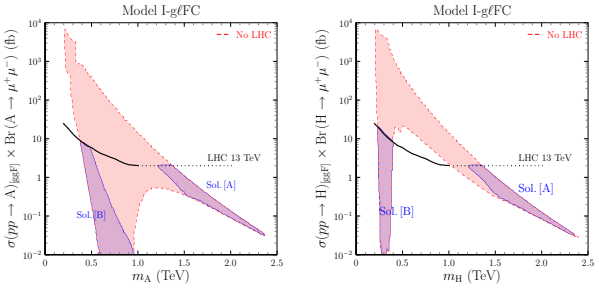

(a) **(b)**

Figure 9.6: $[pp]_{\mathrm{ggF}} \to \mathrm{S} \to \mu^+\mu^-$ versus m_{S}.

than some minimal $|\mathrm{Re}\,(n_\mu)|_{\mathrm{Min}}$ are required to explain δa_μ, both $\mathrm{Br}\,(\mathrm{H} \to \mu^+\mu^-)$ and $\mathrm{Br}\,(\mathrm{A} \to \mu^+\mu^-)$ are bounded from below. The dominant decay channels of the new scalars are shown in Figure 9.8; Figures 9.8b and 9.8f show that $\mathrm{Br}\,(\mathrm{H} \to \mu^+\mu^-)$ and $\mathrm{Br}\,(\mathrm{A} \to \mu^+\mu^-)$ are indeed bounded from below, but in the case of $\mathrm{H} \to \mu^+\mu^-$ the lower bound is larger than that of $\mathrm{A} \to \mu^+\mu^-$ (it can even saturate the decay width of H). This explains the narrowness of the red and blue regions in Figure 9.6b for $m_{\mathrm{H}} > 400$ GeV. One should keep in mind that solutions [A] and [B] also differ quite substantially in the values of t_β: in Figure 9.5e it is clear that large $m_{\mathrm{H}} > 1$ TeV requires $t_\beta \sim 1$, while $m_{\mathrm{H}} < 500$ GeV is compatible with a broad range $t_\beta \in [1; 10^2]$. This is the last ingredient necessary to interpret the shape of Figure 9.6b. For $m_{\mathrm{H}} < 500$ GeV, without constraints from LHC searches, the broad range of t_β values gives a broad range for $\sigma(pp \to \mathrm{H})_{\mathrm{ggF}}$: since the gluon-gluon fusion production cross section is proportional to t_β^{-2}, and thus for solution [B] there is a substantial suppression of $\sigma(pp \to \mathrm{H})_{\mathrm{ggF}}$ due to $t_\beta \gg 1$. Due to the larger production cross section of a pseudoscalar, despite the t_β^{-2} suppression, LHC searches might rule out $pp \to \mathrm{A} \to \mu^+\mu^-$ predictions for solution [B]: as Figure 9.6a shows, that is not the case. This is clearly achieved through a reduction of $\mathrm{Br}\,(\mathrm{A} \to \mu^+\mu^-)$; Figures 9.8f and 9.8e show that $\mathrm{A} \to \mathrm{H}Z$ contributes decisively to reduce $\mathrm{Br}\,(\mathrm{A} \to \mu^+\mu^-)$,

evade LHC bounds and obtain a viable solution [B]. For this reason, as anticipated, $m_{\rm A} > m_{\rm H} + M_Z$. For the charged scalar $\rm H^\pm$, the behaviour of the most relevant decay channels $\rm H^+ \to \mu^+\nu$, $\tau^+\nu$, $t\bar{b}$, $HW^\pm$ mirrors the corresponding $\rm A \to \mu^+\mu^-$, $\tau^+\tau^-$, $t\bar{t}$, HZ, as Figures 9.8j–9.8i show. The only minor difference arises for solution [B] in the small region where $m_{\rm H^\pm} \simeq m_{\rm H}$: in that region, (i) $\rm H^\pm \to HW^\pm$ is forbidden and (ii) in addition to $\rm A \to HZ$, also $\rm A \to H^\pm W^\mp$ (not shown) has a large branching ratio.

Figure 9.7 shows that resonant $\tau^+\tau^-$ searches are less constraining than the corresponding $\mu^+\mu^-$ searches in Figure 9.6. Concerning production of $\rm H^\pm$, Figure

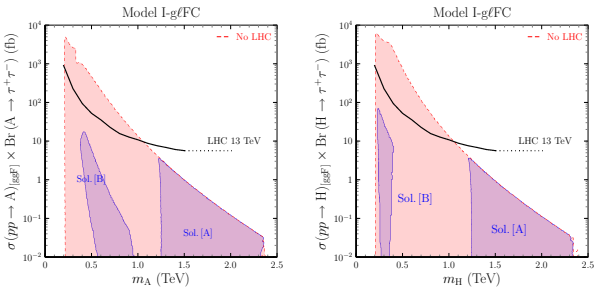

(a) **(b)**

Figure 9.7: $[pp]_{\rm ggF} \to {\rm S} \to \tau^+\tau^-$ versus $m_{\rm S}$.

9.9 shows that current results from searches at the LHC are much less constraining than the results from resonant dilepton searches in Figures 9.7 and 9.6. Results in the previous figures concern model I-gℓFC, where, in addition to solution [A] in which both δa_e and δa_μ arise from 2 loop contributions, a second set of solutions [B] exists in which 1 loop contributions are dominant in δa_μ. For model II-gℓFC this second possibility is not available, and only solution [A] is obtained. Furthermore, since $t_\beta \sim 1$ in solution [A], the corresponding allowed regions do not differ much in both models I-gℓFC and II-gℓFC. We do not show figures corresponding to model II-gℓFC since the allowed regions in that case very approximately coincide with "Sol. [A]" regions in model I-gℓFC plots.

Finally, Figure 9.10 illustrates with some examples the kind of clear signal that solution [B] in model I-gℓFC gives in $e^+e^- \to \mu^+\mu^-$ scattering at energies beyond the range explored at LEP.

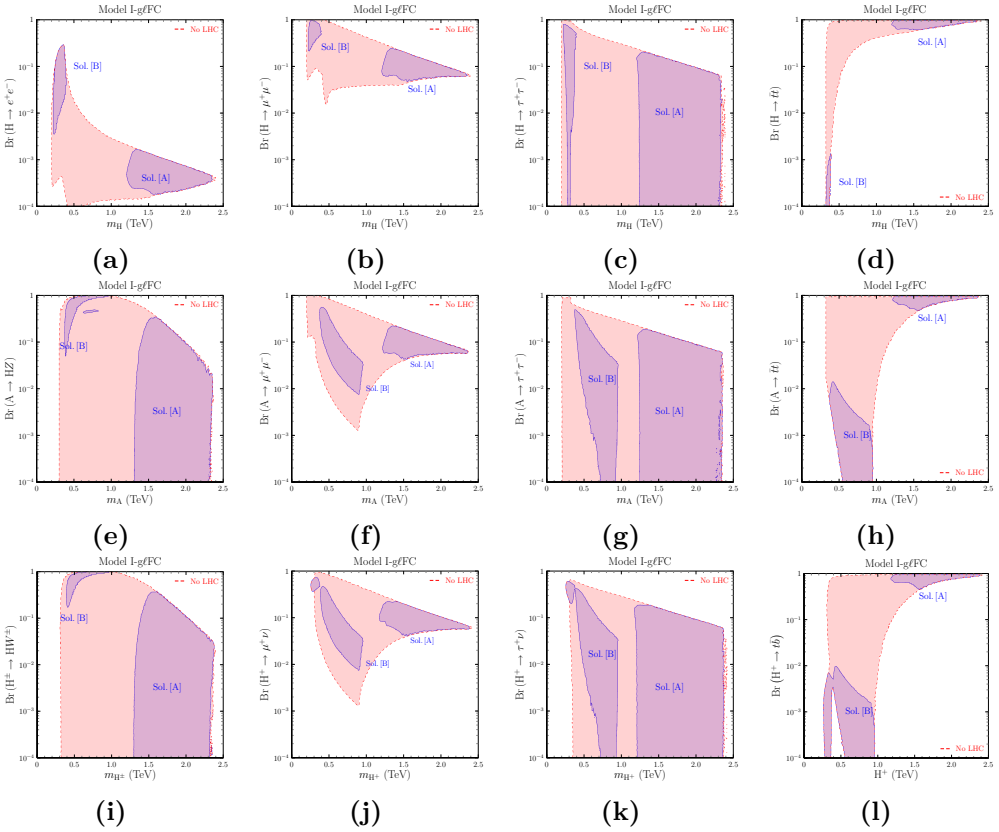

Figure 9.8: Dominant decay channels of H, A, $H^{\pm}$.

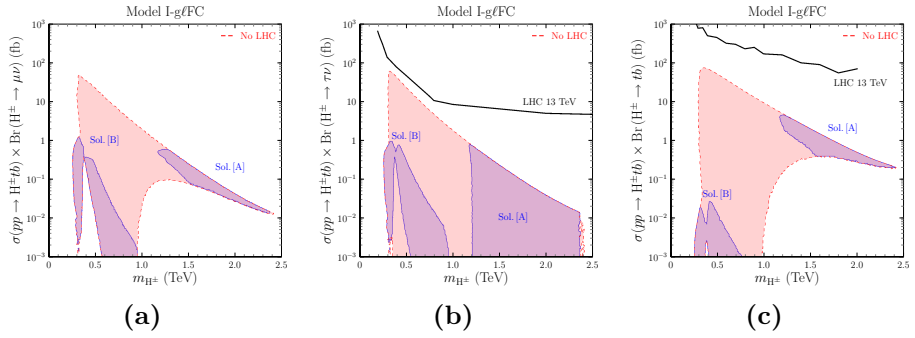

Figure 9.9: $pp \to H^{\pm}(tb) \to \ell\nu, tb$ versus $m_{H^{\pm}}$.

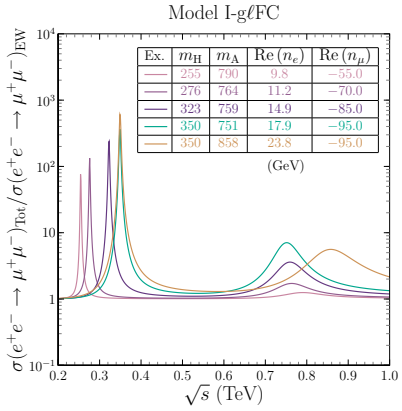

Figure 9.10: $e^+e^- \to \mu^+\mu^-$ for $\sqrt{s} \in [0.2; 1.0]$ TeV, examples of solution [B] in model I-gℓFC.

Conclusions

Along the present thesis different aspects of the Two Higgs Doublet Models have been studied, both from the theoretical and phenomenological points of view. The Flavor Changing Neutral Couplings have been a recurring theme since it is one of the most constrained features that are introduced when the Standard Model is enlarged with extra scalars. The question of general Flavor Conserving 2HDM and the effect of one loop Renormalization Group Evolution of the Yukawa matrices on these scenarios is addressed. Regarding the quarks some well known models as the Type I and II has been discussed as well as the case of a model with a Cabibbo-like quark mixing matrix. It is worth stressing that in the absence of right-handed neutrinos, gFC in the lepton sector is stable.

At a phenomenological level we have studied the parameter space through a numerical analysis for the different fermion sectors. We have put our attention in the flavor conserving processes related to the Higgs and we have imposed the constraints provided by the current experimental data. Processes as the direct $q\bar{q} \to$ h production which are negligible in the SM but may receive a big contribution from the new scalar particles are also considered.

The fact that the gFC models in the leptonic sector allow a decoupling of the electron, muon and tau Yukawa interactions opens the possibility of a simultaneous explanation for the electron and muon (g-2) anomalies. This is possible since lepton flavor universality is broken beyond the mass proportionality. We have considered two of these general flavor conserving models in the leptonic sector, I-gℓFC and II-gℓFC, that differ in the quark Yukawa couplings, which coincide, respectively, with the ones in type I and in type II 2HDMs. We have found two sets of solutions

that are able to reproduce both anomalies together with constraints coming from LEP and LHC, including LFU observables, flavor and electroweak measurements and the usual theoretical requirements in the scalar sector. In the first solution new the scalar particles live in the mass range 1–2.5 TeV, t_β is close to one and both anomalies are dominated by two loop Barr-Zee contributions. This solution arises in both models, I-gℓFC and II-gℓFC. Howeever, in the second solution, the one loop diagram is the dominant one in the muon anomaly. In this case, the scalar particles masses are below the 1 TeV and the VEVs differ substantially from each other (t_β in the 10–100 range). The pseudoscalar neutral Higgs A is heavier (400–900 GeV) than the heavy scalar H (210–390 GeV). Due to the EW constraints, the charged Higgs $H^\pm$ is almost degenerate in mass with one of the neutral ones. This second solution is only available in the I-gℓFC models. In both solutions, soft breaking of the $\mathbb{Z}_2$ symmetry of the Higgs potential is required, together with lepton Yukawa couplings with values from 1 to 100 GeV. These results imply for LHC searches, in the light scalar solution, that it should be easier to find both charged and neutral Higgses in the muonic channel. The heavy channels, like the top quark channels, are more suited to searches addressing the heavy scalars solution.

With a different approach, we have worked in a set of models where the Flavor Changing Neutral Couplings are controlled instead of being canceled as in the general Flavor Conserving case. We have shown that the well-known BGL models can be generalized into what we have named as gBGL. These new models are generated by a new $\mathbb{Z}_2$ symmetry so they keep the feature of being renomalizable. This symmetry is the same as the one proposed by Glashow and Weinberg in NFC models but differs in the way the quark fields transform under it. We have seen as well that BGL models are contained as special cases in the gBGL. In such scenarios, the Lagrangian acquire a larger symmetry, in particular a U(1) or a $\mathbb{Z}_4$ symmetry (this depends on the neutrino being Dirac or Majorana). However, gBGL models do not math the MFV conditions as the BGLs do. The gBGL models introduce 4 new parameters with respect to the BGL models which is still a great reduction compared with the general 2HDM. The models also introduced SCFNC at tree level

in both the down and the up sectors but in a controlled way. We have shown that gBGL model can safely overcome the present experimental constraints on SFCNC. Finally we have shown as well that gBGL models can introduce enough CP violation to explain the BAU observations. This happens since the WB invariant controlling the CP violation appear at much lower order of mass than in the SM.

We have also discussed the possibility of relating the CKM and PMNS complex phases in the gBGL framework. In general there is no relation since the Yukawa sector for the quarks and leptons are independent. We have investigated the possibility of generating this connection via the complex vacuum phase while the Yukawa couplings remain real. That is, in this framework, CP is spontaneously broken. In order to generate realistic mixing matrices, it is mandatory to have SFCNC in all the fermion sectors. The gBGL models are a great candidate since they produce the desired SFCNC while keeping them controlled. We have proved that in some special cases it is possible to relate $\delta_{\rm CKM}$ and $\delta_{\rm PMNS}$. The interplay among CPV and the existence of SFCNC makes that these relations are quite involved implying connections or predictions for processes mediated by SFCNC in all the sectors: up, down quarks and charged leptons [3]. Because of this we have studied a subclass of the general model following two hints:

- an experimental fact: the absence of any convincing evidence of the presence of SFCNC at the actual level of precision
- a theoretical discovery: the necessity of having at least one type of SFCNC in each sector: quarks up and down, charged leptons and even in the neutrino sector.

We have studied models with the minimal amount of SFCNC needed to keep SCPV. Because of this, these models verify the MFV conditions. This election is reflected on the unit vectors $\hat{r}_{[\rm u]}$, $\hat{r}_{[\rm d]}$, $\hat{r}_{[\nu]}$, $\hat{r}_{[\ell]}$, by canceling one of their three entries. Among the $3^4 = 81$ possible models of this type only one is capable of generation both the

[3] SFCNC involving neutrinos, being proportional to the neutrino masses are not experimentally accessible.

desired connection between phases and realistic (in agreement with experiment) mixing matrices, as discussed in section 5.5.

Finally we have performed a scan over the different 2HDM obtained by Abelian symmetries, consistent with non-zero quarks masses and non-diagonal CKM [145], supplemented by the right or left conditions at eq. (6.2) and eq. (6.5) respectively. With the left conditions we have recovered the well-known G-W and BGL models as well as the gBGL and we have found a new model that we have named jBGL. Concerning the right conditions, six models in addition to the G-W model meet them. All these models have been parametrized in terms of fermion masses, $\tan\beta$, elements of the CKM matrix and unit vectors containing the rest of the parametric freedom.

Resum de la Tesi

El 12 de juny del 2012 ATLAS i CMS confirmaven el descobriment del bosó de Higgs completant l'última peça que mancava en el Model Estàndard (SM per les seues sigles en anglés [4]). Actualment, el SM de la física de partícules és la teoria més simple que pot descriure amb gran èxit els components fonamentals de la matèria i les seues interaccions Malgrat això, el SM no pot ser la *teoria definitiva* ja que hi ha certs aspectes teòrics i evidències experimentals que no és capaç d'explicar. Aquest fet és el que motiva la present tesi en la qual s'han explorat models de Nova Física (NP) que són capaços de donar explicació a alguns dels problemes del SM.

La tesi, redactada en anglés excepte aquest resum, està organitzada de la següent forma. A la Part I s'introdueixen les bases teòriques que sustenten la tesi. En el capítol 1 es descriu amb cert nivell de detall el SM, és a dir, es presenten les partícules elementals i les seues interaccions que venen descrites pel Lagrangià es mostra. A més, es fa una revisió dels problemes teòrics i les evidències experimentals que donen peu a l'estudi de física més enllà del SM. Al segon capítol es presenta una extensió mínima del SM, coneguda com model de dos doblets de Higgs (2HDM) en la qual s'estén el sector escalar amb un segon doblet de Higgs. En aquest capítol es revisen les diferents formes de restringir els corrents neutres amb canvi de sabor, una de les restriccions experimentals més fortes d'aquest tipus de models.

En la Part II es concentren els aspectes teòrics dels treballs d'investigació duts a terme durant el període doctoral. En particular ens centrem en estudiar les extensions del sector escalars del SM que no generen contribucions importants als processos que contenen corrents neutres amb canvi de sabor. Aquests processos

[4] D'ara en avant es suposa que totes les sigles es deriven dels termes en anglés.

estan molt suprimits tant al SM com experimentalment i qualsevol extensió del SM ha de suprimir-los per a ser compatible amb les observacions. La condició perquè no hi haja corrents neutres amb canvi de sabor a nivell arbre (primer ordre de teoria de pertorbacions) implica que les matrius de Yukawa es puguen diagonalitzar simultàniament. Els models que compleixen això han sigut àmpliament estudiats a la literatura i són coneguts com a models amb conservació de sabor natural (NFC). Per exemple, al model 2HDM alineat s'imposa que les matrius de Yukawa siguen proporcionals entre elles a una determinada escala d'energia però, en general, aquesta condició no es satisfà a altres escales degut a les correccions quàntiques, com s'estudia en el capítol 3.

En el capítol 4 es desenvolupa una generalització dels models coneguts com a BGL. Mentre que els models BGL compleixen les condicions de violació mínima de sabor (MFV), els gBGL no ho fan, però contenen corrents neutres amb canvi de sabor en els dos sectors de quarks dalt i baix però controlades per elements de la matriu de barreja dels quarks (anomenada matriu CKM). Generat per la mateixa simetria que dona lloc als models BGL generalitzats del capítol anterior, en el capítol 5 es presenta un model que ofereix una connexió entre les fases de les matrius de barreja de quarks i leptons. A partir de la parametrització de les matrius de Yukawa dels models anomenats gBGL, en el capítol 6 es fa un estudi sistemàtic dels diferents models generats a partir de simetries abelianes i que poden ser parametritzats de manera anàloga als models BGL i gBGL.

En la Part III es concentren els aspectes fenomenològics abordats en aquesta tesi. En el capítol 7 és possible trobar tots els resultats experimentals que s'utilitzen en els següents capítols a l'hora d'ajustar l'espai de paràmetres dels models presentats en la Part II. En el capítol 8 es recull una anàlisis general de l'espai de paràmetres dels models gFC. Finalment, en el capítol 9 s'estudien dos casos particulars del model conegut com gFC, on les anomalies del moment magnètic de l'electró i el muó s'expliquen simultàniament.

A continuació es recullen els objectius, metodologia, resultats i conclusions de la tesi.

Motivació i Objectius

El SM és una teoria gauge basada en el grup de simetria $\mathrm{SU}(3)_c \times \mathrm{SU}(2)_L \times \mathrm{U}(1)_Y$. Les partícules elementals poden ser classificades en fermions, on trobem els quarks i els leptons, amb espí 1/2 i bosons, on trobem els bosons gauge i el bosó de Higgs, amb espí 1 i 0, respectivament. Aquests estats fonamentals són representacions de la simetria Lorentz. Els fermions es divideixen en dos grups segons la seua càrrega sota la simetria $\mathrm{SU}(3)_c$: els quarks són triplets sota $SU(3)_C$ amb càrrega 1 i els leptons sense càrrega sota aquesta simetria són singlets sota aquest mateix grup. Pel que fa a la càrrega elèctrica, els quarks poden tindre càrrega elèctrica 2/3 o −1/3 mentre que els leptons tenen càrrega −1 o 0. Els leptons de càrrega nulůla són coneguts com a neutrins. A més, els fermions tenen quiralitat definida i apareixen en diferents representacions de $\mathrm{SU}(2)_L$. Els de quiralitat levogira són doblets mentre que els de quiralitat dextrogira són singlets.

$$\begin{aligned} Q_L^0 &= \begin{pmatrix} u_L^0 \\ d_L^0 \end{pmatrix}, \qquad u_R^0\,, \qquad d_R^0\,, \\ L_L^0 &= \begin{pmatrix} \nu_L^0 \\ \ell_L^0 \end{pmatrix}, \qquad \ell_R^0\,. \end{aligned} \tag{1.1}$$

De cada un dels fermions hi ha tres còpies, conegudes com famílies. Els fermions interaccionen entre ells mitjançant intercanvi de bosons, que són els portadors de les interaccions. El SM descriu tres de les quatre forces fonamentals, en particular, la força forta, la feble i l'electromagnetisme, quedant fora la gravetat. Els boson de gauge d'aquestes forces són els gluons, associats a la simetria $\mathrm{SU}(3)_c$, que són els mediadors de la interacció forta, i els bosons febles, $W^\pm$ i Z, i el fotó, associats a la simetria $\mathrm{SU}(2)_L \times \mathrm{U}(1)_Y$, que són els mediadors de la interacció feble i l'electromagnetisme, respectivament. La descripció d'aquestes últimes interaccions s'unifica en la teoria electrofeble. Totes aquestes partícules elementals i les seues principals característiques es recullen en la taula R.1.

En la teoria electrofeble els bosons de gauge són, per construcció, partícules sense massa. Experimentalment es conegut que en el cas dels bososns febles, $W^\pm$ i Z això no és cert. De la mateixa manera, un terme de massa per als fermions

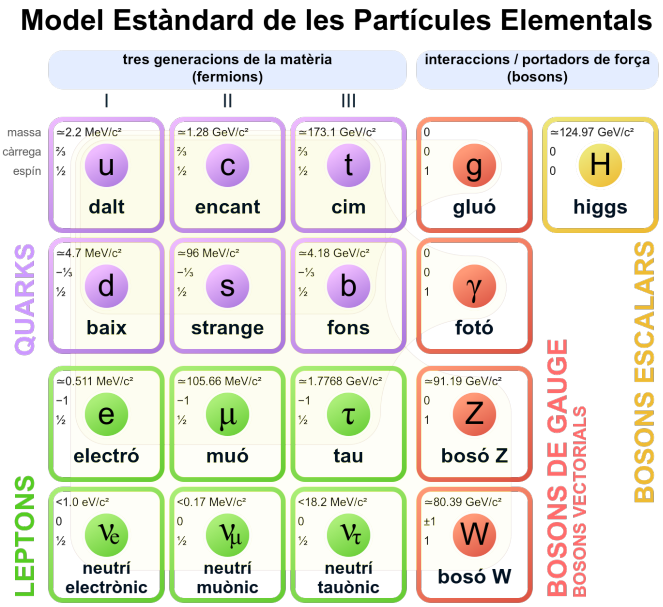

Table R.1: Partícules elementals del Model Estàndard. S'ha traduït la gràfica de [14]

trencaria la invariància gauge del Lagrangià. Aquests dos problemes se solucionen simultàniament amb el conegut com a mecanisme de Higgs. Aquest mecanisme es basa en el fet que l'estat fonamental o buit del potencial escalar no és simètric sota la simetria gauge. Aquest fet condueix a l'aparició d'un nou camp escalar, el bosó de Higgs. L'estat fonamental d'aquest camp té un valor no nul, la qual cosa indueix una ruptura espontània de la simetria electrofeble. La ruptura dels generadors de la simetria atorga massa als bosons febles i gràcies al camp de Higgs permet escriure termes de massa per als fermions. A més, s'introdueixen barreges entre les diferents famílies de quarks, parametritzades per la matriu CKM.

El SM ha aconseguit reproduir la gran majoria de resultats experimentals obtinguts fins al moment. Malgrat això, hi ha diversos elements teòrics que no és capaç d'explicar, així com algunes mesures experiementals que podrien apuntar cap a la necessitat de cercar un model de física més enllà del SM. Entre les qüestions experimentals trobem:

- **Masses dels neutrins**

  En el SM els neutrins són partícules sense massa, però des de fa temps sabem experimentalment que això no pot ser cert. Els neutrins oscilůlen entre un

sabor i un altre i aquest efecte és proporcional al quadrat de la diferència de les masses, la qual cosa implica que almenys dos dels sabors han de tindre una massa no nulůla. El SM es pot estendre per donar massa als neutrins, però encara no s'ha descobert experimentalment quin és el mecanisme escollit per la natura que ho faria possible.

- **Anomalies en mesons B**

  Alguns experiments de sabor com el LHCb, Babar i Belle han trobat desviacions del SM en les desintegracions de mesons B. Aquestes desviacions no són encara estadísticament significatives com per afirmar categòricament el descobriment de nova física, però sembla haver-hi un patró en diversos canals de desintegració que podrien apuntar en la direcció de violació d'universalitat en acoblaments leptònics.

- **g-2 de l'electró i el muó**

  Recentment s'ha tornat a mesurar la constant d'estructura fina, relacionada amb el moment anòmal de l'electró, i ha generat una nova discrepància amb la predicció del SM. D'altra banda, el $g-2$ del muó presenta una anomalia que s'ha mantes al llarg del temps i de les noves mesures experimentals. A més, durant l'escriptura d'aquesta tesi, la colůlaboració Muó g-2 de Fermilab, va presentar una nova mesura per al moment magnètic anòmal del muó que augmenta la tensió en la mesura d'aquest observable.

- **Asimetria matèria-antimatèria**

  L'univers observat està compost gairebé completament de matèria. Aquest fet no pot ser explicat únicament amb el SM, ja que aquest prediu que en l'univers primerenc matèria i antimatèria es crearen van haver de crear-se aproximadament en la mateixa quantitat. A més, tot i que la violació de la simetria CP podria explicar aquesta asimetria, al SM la simetria CP no es viola en una quantitat suficientment gran com per a explicar tota l'asimetria. Per tant, per a explicar aquesta observació, el SM hauria de ser estés.

- **Sector fosc**

  Gràcies a les mesures cosmològiques sabem que només el 5% del univers observable està format per matèria regular, és a dir, descrita pel SM (taula R.1). Per a poder entendre les velocitats dels cúmuls galàctics, al voltant d'un 26% ha de ser *matèria fosca*. S'anomena fosca perquè es tracta de matèria que no interacciona electromagnèticament (tampoc fortament). A més, per a entendre el ritme d'acceleració de l'expansió de l'univers ha d'haver-hi un 69% d'un component desconegut anomenat energia fosca.

D'altra banda, des d'un punt de vista teòric tenim els problemes següents:

- **Gravetat**

  El SM descriu totes les forces fonamentals conegudes excepte la gravetat. Des d'un punt de vista teòric seria desitjable tindre una teoria capaç de descriure tota la matèria i les seues interaccions. El SM hauria de ser estés per descriure la gravetat quàntica.

- **El sector de sabor**

  No hi ha una raó fonamental per la qual existisquen tres, i sol tres, famílies de fermions. Tampoc no hi ha cap motiu teòric pel qual les matrius de massa per als quarks i els leptons carregats i la matriu de CKM tinguen una estructura jeràrquica mentre que la dels neutrins i la matriu PMNS (la matriu de mescla dels neutrins) no.[5]

- **El problema de la jerarquia**

  En les extensions del SM poden aparèixer contribucions importants a la massa del bosó de Higgs com conseqüència de les correccions radiatives, que són proporcionals a l'escala de nova física. Aquestes correccions haurien de cancelůlar-se amb el paràmetre de massa del Lagrangià per donar el valor experimental de 125 GeV, fet que comportaria un ajust molt fi dels paràmetres. Tradicionalment l'ajust fi s'ha entés com un problema de la teoria.

[5]Estrictament parlant, el SM no inclou masses i angles de mescla dels neutrins, però aquestes quantitats s'han mesurat experimentalment i no tenen una estructura anàloga al sector dels quarks.

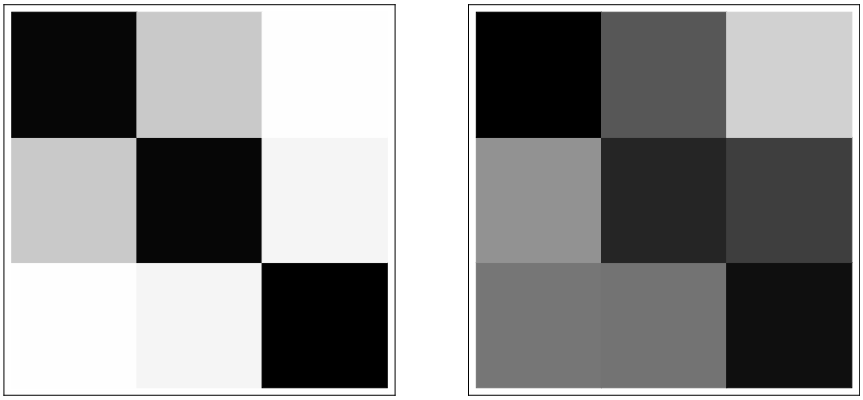

(a) Patró de la matriu CKM **(b)** Patró de la matriu PMNS

Figure 1.6: Patrons jeràrquics mesurats de les matrius CKM (9.11a) i PMNS (9.11b). Els elements més clars indiquen que estan més suprimits en comparació amb els més foscos. Figura de [63].

- **Problema de la fase forta de CP**

  El Lagrangià de les interaccions fortes permet la violació de la simetria CP. Aquesta violació ajudaria a solucionar el problema de l'asimetria matèria-antimatèria. Experimentalment s'observa que d'haver-hi violació en la part forta del SM, aquesta seria molt menuda. No hi ha una explicació teòrica en el SM per la qual això haja de ser així.

- **Gran Unificació**

  Els acoblaments de les interaccions varien amb l'escala d'energia a les quals són mesurats. En el SM, els acoblaments de les forces forta, feble i electromagnètica són aproximadament iguals a escales d'energia molt altes. Aquest fet podria assenyalar cap a un mecanisme més general en què aquestes forces s'unifiquen en una sola, com passa amb l'electromagnetisme i la força feble. Els models que intenten explicar aquest fet són coneguts com a Teories de Gran Unificació.

Una vegada que s'ha descobert el bosó de Higgs, no hi ha cap raó perquè hi haja únicament un doblet de $\mathrm{SU}(2)_L$, llevat el principi de minimalisme. La presència de doblets extra augmenta les possibilitats del sector de sabor i per tant s'han abordat estudis de sabor amb models que contenen diversos Higgs, així com la corresponent fenomenologia associada a tots els sectors. Això inclou, per descomptat, violació de

la simetria CP i les possibles implicacions per a l'asimetria bariònica de l'univers (BAU). En particular, aquesta tesi se centra en els 2HDM per intentar explicar alguns dels problemes anteriors. Aquests models es discuteixen en detall en els capítols 2, 3, 4, 5 i 6 i es resumeixen en la secció 9.3, on es presenta la metodologia utilitzada en la tesi. També s'han abordat algunes de les qüestions experimentals resumides en aquesta secció. En particular, en el capítol 9 es presenten els resultats d'un model que és capaç d'explicar simultàniament les anomalies experimentals del (g-2) del muó i de l'electró.

Metodología

Com s'ha comentat anteriorment, no hi ha cap raó teòrica que restringisca el sector escalar a un únic doblet de Higgs. De fet, l'extensió d'aquest sector inclou característiques com ara nous termes de violació de CP que podrien explicar alguns dels problemes observats en el SM. A més, el sector escalar de certs models com els models supersimètrics contenen sectors escalars més complexos que el SM. És a dir, l'estudi de models com el 2HDM no només té interés en si mateix, sinó que pot servir com un estudi parcial d'uns altres models més complexos que el contenen.

En els models 2HDM tenim dos doblets escalars de $\mathrm{SU}(2)_L$, és a dir, quatre nous camps reals. Això es tradueix, després de la ruptura espontània de la simetria que atorga masses als bosons gauge, en un total de cinc camps físics, quatre més que el SM. D'aquestes quatre noves partícules dos són neutres (una parella i l'altra senar sota transformacions de CP) i dos són carregades. Apareixen també nous termes al Lagrangià de Yukawa associat al nou doblet. En general les noves matrius de Yukawa i les del SM no tenen per què ser diagonalitzables simultàniament. Aquest fet introdueix corrents neutres amb canvi de sabor (FCNC), és a dir, acoblaments de fermions amb diferent sabor però igual càrrega a través d'un Higgs neutre. Això és, potencialment, un problema, ja que experimentalment les FCNC estan molt restringides.

En la literatura es recullen dos mecanismes mitjançant els quals evitar que aquests models siguen descartats experimentalment per produir FCNC massa grans.

El primer és conegut com a conservació natural del sabor i en ells les FCNC s'anulůlen com en el SM. Entre els models amb NFC es troben els 2HDM de tipus I, II, X i Y, generats mitjançant una simetria $\mathbb{Z}_2$. En aquests models, els fermions d'una certa càrrega, s'acoblen només a un dels dos doblets, fet que evita l'existència de FCNC. Un altre model similar a aquests i també àmpliament estudiat en la literatura és el 2HDM alineat, en el qual les matrius de Yukawa són proporcionals entre elles. Aquesta condició s'aplica a certa escala d'energia, però no es compleix a altres escales, on apareixen FCNC. Això passa perquè aquest model no es genera per cap simetria. Tots aquests models s'expliquen amb detall en la secció 2.4. L'altra opció per tal de tindre models fenomenològicament segurs és, en comptes de suprimir les FCNC, restringir-les. Dins d'aquesta categoria es troben els models de violació mínima del sabor (MFV). En aquests models, els acoblaments que violen sabor són proporcionals a elements de la matriu CKM. Els models BGL utilitzen aquest mecanisme i, a més, només presenten FCNC en el sector dels quarks dalt o baix, però no en els dos simultàniament. Els 6 models (36 si s'estenen al sector leptònic) són generats mitjançant una simetria $\mathrm{U}(1)$. Aquests models es presenten a la secció 2.5.

En relació amb els models NFC, en el capítol 3 es presenta un estudi sobre l'estabilitat de les condicions que han de satisfer les matrius de Yukawa perquè siguen diagonalitzables simultàniament sota les equacions del grup de renormalització (RGE). Aquesta condició és més general que la dels models alineats, on sabem que les FCNC apareixen si ens trobem a una escala diferent a l'escala en la qual s'imposa la condició d'alineament. Estudiant l'evolució de la condició imposada es recuperen els models NFC i s'obtenen alguns resultats interessants, com un model amb una matriu CKM amb la forma de la matriu de Cabibbo. A més, ressaltem que en el sector leptònic, amb neutrins sense massa, una matriu N_ℓ (veure eq. (2.29)) diagonal i arbitrària conserva sabor independentment de l'escala. Aquesta qualitat ha estat utilitzada en una anàlisi que es presenta posteriorment, ja que aquests models permeten explicar simultàniament les anomalies del (g-2) de l'electró i del muó.

D'altra banda, en el capítol 4 es presenta una generalització dels models BGL. En aquests models, es restringeix la simetria contínua $\mathrm{U}(1)$ que dona lloc als models

BGL a una simetria discreta $\mathbb{Z}_2$. Mitjançant aquest canvi, no només s'obtenen tots els models BGL sinó que s'obté un espectre continu de models en els quals es tenen FCNC controlades tant en el sector dels quarks dalt com en el dels quarks baix. A més, aquests models introdueixen noves fonts de violació de CP que augmenten significativament la generació d'asimetria bariònica de l'univers respecte al SM.

Si u assumeix que la violació de CP sorgeix d'acoblaments de Yukawa complexos als dos sectors: quarks i de leptons, la connexió entre les fases CKM i PMNS no és possible en general, ja que els acoblaments Yukawa dels dos sectors tenen estructures de sabor independents. No obstant això, en el capítol 5 es demostra que en certs casos i generant la violació de CP a través de la fase complexa de l'buit, la connexió és possible. En particular, es presenta un model a partir de la mateixa simetria $\mathbb{Z}_2$ que dona lloc als models gBGL que és capaç de generar aquesta connexió.

Inspirats per la parametrització de les matrius N_f en els models gBGL (vegeu eqs. (4.40)–(4.43)), en el capítol 6 es presenta un estudi de models 2HDM amb simetries abelianes i que es poden parametritzar de manera similar al gBGL. Aquestes condicions condueixen a una reducció notable en el nombre de paràmetres respecte al model general.

Finalment, en el capítol 7 es descriuen les dades experimentals utilitzades i la forma d'ajustar els nostres models a elles. En particular, s'explora l'espai de paràmetres emprant una cadena de Markov mitjançant tècniques Monte Carlo. Per a fer-ho s'obté el corresponent $\chi^2_{\mathcal{O}} = \left(\frac{\mathcal{O}_{\mathrm{Th}}-\mathcal{O}_{\mathrm{Exp}}}{\sigma_{\mathrm{Exp}}}\right)^2$ per a cada observable $\mathcal{O}$, on $\mathcal{O}_{\mathrm{Exp}}$ és el valor de la mesura experimental amb una incertesa σ_{Exp} y $\mathcal{O}_{\mathrm{Th}}$ la predicció teòrica del model en qüestió. Finalment es presenten les regions paramètriques permeses a diferents intervals de confiança.

Resultats i Conclusions

Al llarg de la tesi s'han presentat diferents resultats associats als models estudiats, i que han estat resumits en la secció anterior. Molts dels models presentats en aquesta tesi poden considerar-se com un resultat per si mateix, però en aquesta secció ens centrem en els resultats fenomenològics.

BAU als models gBGL

Un dels primers a destacar s'inclou en el capítol 4. Els models gBGL inclouen noves fonts de violació de sabor i de CP, la qual cosa pot augmentar la contribució a l'asimetria bariònica de l'Univers (BAU) respecte al SM. El primer invariant WB amb part imaginària no nulůla apareix a ordre 4 en els gBGL

$$\mathrm{Im}\left(\mathrm{Tr}\left\{\mathrm{N}_d^0\mathrm{M}_d^{0\dagger}\mathrm{M}_u^0\mathrm{M}_u^{0\dagger}\right\}\right), \tag{4.74}$$

el que produeix un augment respecte al SM

$$\frac{\mathrm{BAU_{gBGL}}}{\mathrm{BAU_{SM}}} \sim (t_\beta + t_\beta^{-1})\left|\hat{n}_{[\mathrm{d}]3}\hat{n}^*_{[\mathrm{d}]2}\right|\sin\alpha\,\frac{|V_{ts}|}{J}\frac{E^8}{m_t^2m_b^2m_c^2m_s^2}$$
$$\sim 10^{16}(t_\beta + t_\beta^{-1})\left|\hat{n}_{[\mathrm{d}]3}\hat{n}^*_{[\mathrm{d}]2}\right|\sin\alpha\,. \tag{4.84}$$

Per tant aquests models prodrien donar solució a un dels problemes del SM.

Fenomenologia dels gFC

El capítol 8 conté una anàlisi fenomenològic general de models GFC és a dir, models on les matrius N_f estan definides com:

$$\mathrm{N}_d = \begin{pmatrix} n_d & 0 & 0 \\ 0 & n_s & 0 \\ 0 & 0 & n_b \end{pmatrix},\ \mathrm{N}_u = \begin{pmatrix} n_u & 0 & 0 \\ 0 & n_c & 0 \\ 0 & 0 & n_t \end{pmatrix},\ \mathrm{N}_\ell = \begin{pmatrix} n_e & 0 & 0 \\ 0 & n_\mu & 0 \\ 0 & 0 & n_\tau \end{pmatrix}, \tag{3.4}$$

amb $n_j \in \mathbb{C}$. Es posa especial atenció en els observables que involucren el menor nombre de nous paràmetres (respecte al SM) i els que proveeixen restriccions directes de les mesures existents. S'imposa que els acoblaments n_j romanguen pertorbatius, així com les restriccions provinents de la producció i desintegració del Higgs i les provinents dels moments dipolars elèctrics.

En les figures 8.3 i 8.4 es presenten els resultats obtinguts. En particular, en la 8.3 es representen les regions permeses s a 68, 95 y 99% de valor de confiança (CL) per als acoblaments $|n_f|$ en funció de $c_{\alpha\beta}$. En aquestes figures cal destacar:

- Com era desperar, per a $c_{\alpha\beta} \in 0$, desapareixen les restriccions a n_f.

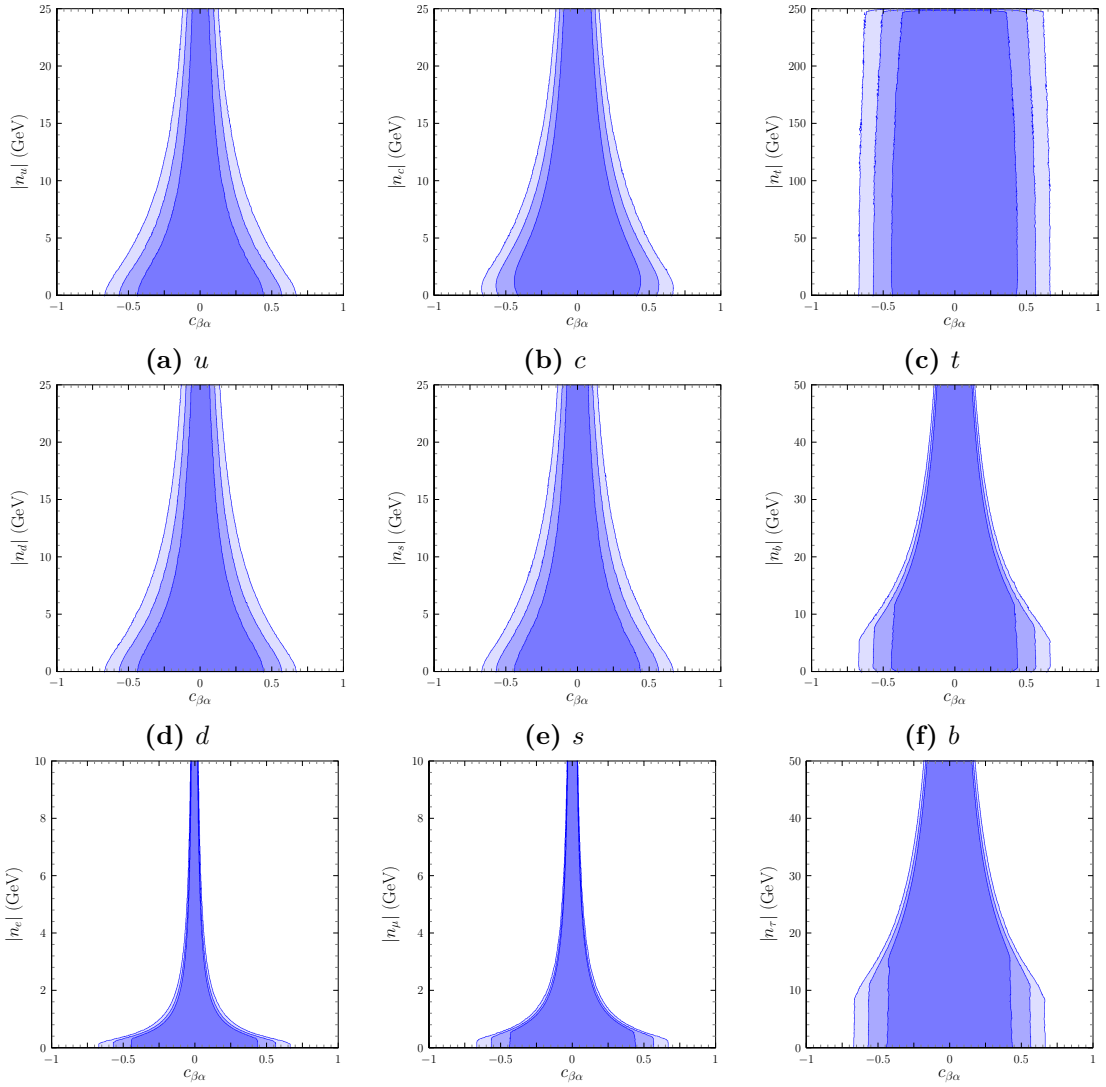

(a) u **(b)** c **(c)** t

(d) d **(e)** s **(f)** b

(g) e **(h)** μ **(i)** τ

Figure 8.3: $|n_f|$ vs. $c_{\alpha\beta}$ per als diferents fermions f; les regions més fosques a les més clares corresponen a 68, 95 and 99% CL.

- Per a quarks u, c, d i s, les regions permeses són gairebé idèntiques, com es podria anticipar pel seu paper irrellevant, al SM, en la producció disponible × decaïment del Higgs. Els n_f corresponents semblen estar eficaçment limitats per les contribucions a l'amplada de Higgs.

- Sorprenentment, $|n_t|$ sembla ser independent de $c_{\alpha\beta}$.

- Els casos de n_b i n_τ també són similars, amb regions permeses diferents dels casos de u, c, d, s per $|n_q|$ és inferior a 10-15 GeV i $c_{\alpha\beta}$ no menuts.

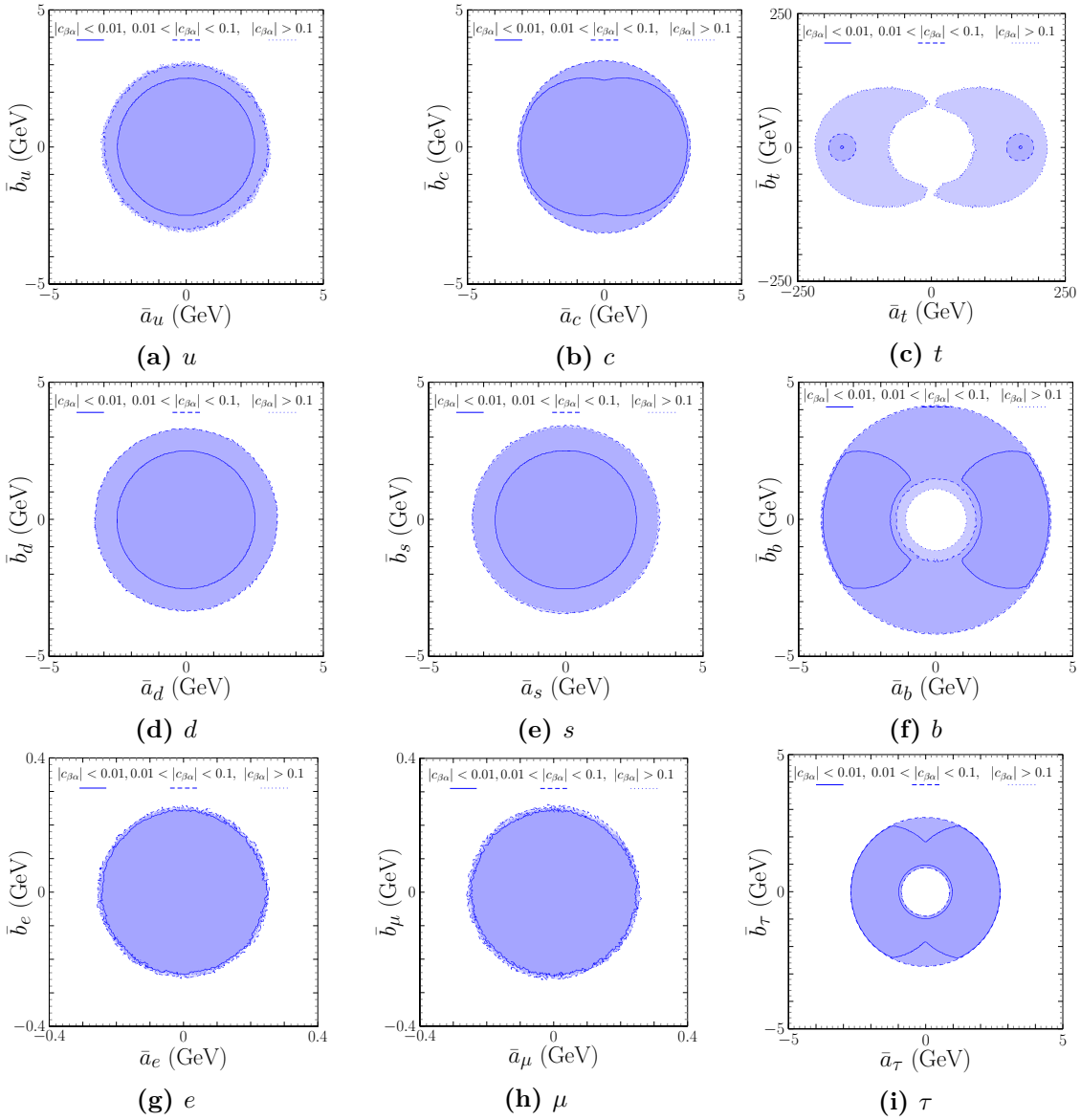

(a) u **(b)** c **(c)** t

(d) d **(e)** s **(f)** b

(g) e **(h)** μ **(i)** τ

Figure 8.4: Regions permesa a un 99% CL en els acopamientros escalars vs. pseudoescalars per als diferents fermions f amb $\mathscr{L}_{\mathrm{h}\bar{f}f} = -\frac{\mathrm{h}}{v}\bar{f}(\bar{a}_f + i\bar{b}_f\gamma_5)f$.

- Per a n_e i n_μ, les regions permeses estan molt més restringides a causa dels límits establerts per $pp \to \mathrm{h} \to e^+e^-$, $\mu^+\mu^-$ anàlisis com ara [266, 267].

Tot i que la figura 8.3 mostra límits absoluts a $|n_f|$, no proporciona informació sobre $\arg(n_f)$ i no es pot llegir directament en termes dels acoblaments escalar i pseudosscalar de h a eqs. (7.9)–(7.10). Tenint en compte això, la figura 8.4 mostra $\bar{b}_f$ vs $\bar{a}_f$. A més, per mantenir informació sobre $c_{\alpha\beta}$, es mostren les regions corresponents a $|c_{\alpha\beta}| < 0.01$, a $0.01 < |c_{\alpha\beta}| < 0.1$ i a $0.1 < |c_{\alpha\beta}|$ permeses. Es pot notar això

- per a la primera i segona generació de fermions, no hi ha dependència en $\arg(n_f)$, ja que només les desintegracions proporcionals a $|\bar{a}_f|^2 + |\bar{b}_f|^2$, són rellevants. Per als quarks, la regió permesa per $|c_{\alpha\beta}| < 0.01$ és més menuda: això es deu simplement al requisit de pertorbativitat de eq. (8.1).

- Per al quark t, es permeten dues regions separades: això també s'espera ja que canvis de signes tant a $\bar{a}_t$ com a $\bar{b}_t$ (juntament amb els canvis de signes a $c_{\alpha\beta}$, $s_{\alpha\beta}$) no alteren les prediccions. Per a $|c_{\alpha\beta}| < 0.01$, les regions permeses es redueixen i es situen al voltant de $(\bar{a}_t, \bar{b}_t) = (\pm m_t, 0)$; amb $0.01 < |c_{\alpha\beta}| < 0.1$ la seua mida augmenta i només per $|c_{\alpha\beta}| > 0.1$ la interacció de (i) contribucions pseudoscalars a $gg \to \mathrm{h}$ i $\mathrm{h} \to \gamma\gamma$ i (ii) la interferència W-cima (escalar) en $\mathrm{h} \to \gamma\gamma$ dona lloc a regions més grans.

- Per b i τ, les regions per a mescles no massa menudes, $|c_{\alpha\beta}| > 0.01$, tenen forma d'anell; m_b i m_τ estableixen els radis d'aquestes regions, com es podia esperar de la restricció imposada per $\mathrm{h} \to b\bar{b}$ i $\mathrm{h} \to \tau\bar{\tau}$. Per a mescles xicotetes, $|c_{\alpha\beta}| < 0.01$, el requisit de pertorbativitat de $|n_b|$, $Absn_\tau$ limita la separació respecte de $(\bar{a}_f, \bar{b}_f) = (\pm m_f, 0)$, donant de fet, per al cas b, dues regions disjuntes.

Solució del (g-2) del muó i l'electró

En el capítol 9 es proposa una explicació simultània de les anomalies experimentals observades en els moments anòmals magnètics de l'electró i del muó. S'ha observat una tensió amb el SM a l'electró.

$$\delta a_e \equiv a_e^{\mathrm{Exp}} - a_e^{\mathrm{SM}} = -(8.7 \pm 3.6) \times 10^{-13}\,, \tag{1.74}$$

i al muó

$$\delta a_\mu \equiv a_\mu^{\mathrm{Exp}} - a_\mu^{\mathrm{SM}} = (2.7 \pm 0.9) \times 10^{-9}\,. \tag{1.76}$$

Cal destacar que aquestes anomalies tenen sentits oposats. Aquest fet fa que una gran majoria de models de nova física siguen descartats com solució de les dues

anomalies alhora. En particular, en molts models l'anomalia escala amb el quadrat de la massa del leptó, el que genera un δa_e massa gran i amb el signe equivocat. Alguns autors [269] defensen que si l'origen de les dues anomalies es pot explicar amb física més enllà del SM, el model corresponent ha d'incorporar algun tipus de desacoblament efectiu entre μ i e. Això no passa en la majoria dels models de dos doblets de Higgs, ja que els acoblaments Yukawa solen ser proporcionals a la massa.

No obstant això, en el capítol 3 es presenta un dels resultats obtinguts en aquesta tesi que compleix la condició anterior. Al sector leptònic la matriu N_ℓ = diag(n_e, n_μ, n_τ) (amb n_i quantitats arbitraris) és estable sota les equacions de grup de renormalització. És a dir, no només es conserva sabor en corrents neutres a l'escala de la condició sinó a totes les escales. Com que els factors n_i són arbitràris en aquests models sense FCNC, tenim el desacoblament entre el muó i l'electró necessari per a ajustar les dues anomalies. En resum, un model en el qual el sector dels quark és Tipus I o II i el leptònic és gFC és estable sota RGE i els anomenarem I- i II-gℓFC.

Hi ha dos tipus de solucions que reprodueixen completament tant les dues anomalies com les dades experimentals de LEP i LHC, la universalitat de sabor leptònica, els tests de física electrofeble i de sabor i els requeriments teòrics sobre el sector escalar.

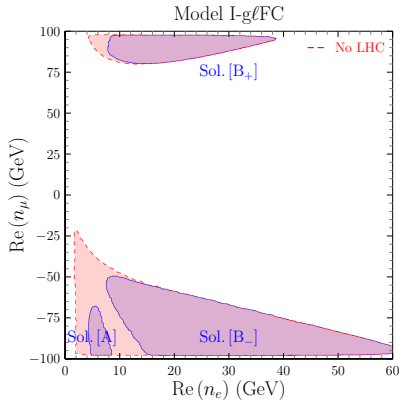

Figure 9.3: Re (n_μ) vs. Re (n_e).

En una de les dues solucions (solució A), tots els nous escalars tenen masses en el rang 1–2.5 TeV, els valors esperats del buit (VEVs) són bastant similars ($t_\beta \approx 1$)

i les dues anomalies estan dominades per la contribució del diagrama Barr-Zee a dos llaços. Aquesta solució apareix en els dos models, I- i II-gℓFC.

A la segona solució (solució B) el diagrama que contribueix principalment en l'anomalia del muó és a un llaç. Els nous escalars són lleugers, amb masses menors que 1 TeV i els VEVs són molt diferents (el quocient, t_β està en el rang 10-100). Entre els nous escalars, el neutre i parell sota CP, H, és el més lleuger, amb una massa en la franja 210-390 GeV, mentre que el pseudoescalar, A, és més pesat amb una massa en el rang 400-900 GeV. L'escalar carregat està gairebé degenerat en massa amb el pseudoescalar. Aquesta solució només està present en el model I-gℓFC.

Les dues solucions requereixen un trencament suau de la simetria $\mathbb{Z}_2$ del potencial de Higgs juntament amb valors per als acoblaments Yukawa d'entre 1 i 100 GeV. Aquests resultats en la solució d'escalars lleugers impliquen que hauria de ser més fàcil trobar els ecalares carregats i neutres en un canal de desintegració muònic a les cerques directes del LHC. Per contra, canals més pesats com els que involucren el quark top són més probables a la solució d'escalars pesats.

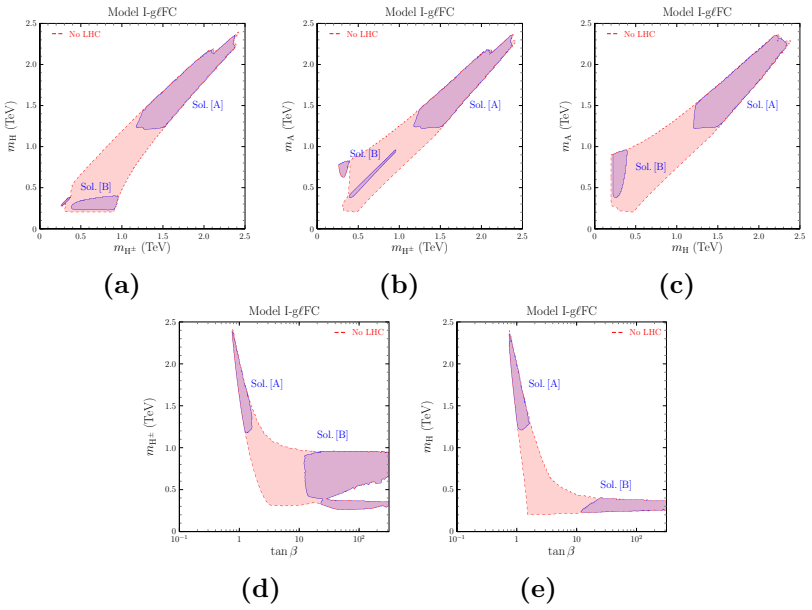

Figure 9.5: Sector Escalar

–I wonder if people will ever say, "Let's hear about Frodo and the Ring,"and they'll say, "Yes, that's one of my favorite stories. Frodo was really courageous, wasn't he, Dad?" "Yes, my boy, the most famousest of hobbits. And that's saying a lot."– SAM
–You left out one of the chief characters: SAMwise the Brave. I want to hear more about SAM. Frodo wouldn't have got far without SAM.– Frodo

— SAMwise Gamgee and Frodo Baggins
The Lord of the Rings, J. R. R. Tolkien

Agradecimientos

En primer lugar, quiero agradecer a mis directores, Quico Botella y Miguel Nebot, todo el esfuerzo y tiempo que me han dedicado así como la pasión y conocimientos que me han transmitido. Además, quiero agradecer a Quico el darme la oportunidad de venir a Valencia a iniciar mi carrera investigadora y a Miguel el haberme hecho sentir como en casa en las estancias en Lisboa. Ambos han puesto atención no solo en mi formación científica si no también en mi bienestar personal y este segundo aspecto es muchas veces olvidado en la academia, siendo, en mi opinión, igual de importante que el primero.

Quiero agradecer también a todos los miembros del IFIC en general y a los del grupo de LHCb en particular, por la acogida y por todos los momentos que hemos compartido. No puedo olvidarme del Escuadrón IFIC y de todos los cafés, comidas y cervezas que hemos compartido. Habéis estado ahí desde mi primer día en el IFIC, cuando Ana nos presentó, hasta que el virus, que nos ha privado de unas cuantas *picaetas*, nos ha cortado el ritmo. Cuando parte de tu familia está lejos los amigos desempeñan un papel más fundamental si cabe aun.

No puedo olvidarme de mis compañeros de despacho, de tesis y , me atrevería a decir, de vida: Ana, Víctor y Félix. No podría haber imaginado unas mejores personas para compartir estos años. Ana, gracias porque ya fuiste una gran amiga incluso antes de conocernos e hiciste que mi adaptación aquí fuese muy cómoda. He disfrutado y aprendido mucho de las conversaciones de física que hemos tenido. Víctor, por todos los buenos ratos que hemos pasado juntos, por el buen ambiente que has creado en el despacho y por estar siempre disponible para echar una mano.

Se nos ha quedado pendiente tener un paper los tres juntos (junto con Clara) para dejarlo inmortalizado en el muro, pero quien sabe, igual la vida nos presenta otra oportunidad. Y Félix, nos has dado ese punto de alegría y locura que todo físico necesita para mantenerse cuerdo mientras hace la tesis. Además has organizado las fiestas y barbacoas más épicas [6]. Sabed los tres que donde quiera que acabe estando, tendréis una casa a la que ir.

Quiero agradecer también a toda mi familia. A mis padres, Esther María y Fernando, sin los cuales esta tesis no existiría y no solo por la obviedad de que yo mismo no lo haría si no porque sin ellos yo no sería físico ni probablemente tampoco me habría lanzado a esta aventura. Todo empezó cuando os pregunté que qué significaba la rayita que había delante del 1 en el botón del garaje en el ascensor y mirad hasta donde ha llegado la curiosidad. Además han estado siempre apoyándome en la distancia y en la cercanía. A mi hermano Alberto y a Ana, por haber buscado siempre la manera de pasar días juntos. Aunque no hubiera video, no se me olvidaría la sorpresa que me disteis al venir a casa. Tengo que acordarme también de Elvira y Gustavo y agradecerles, entre otras cosas, todo el tiempo que pasé es su casa durante en confinamiento. Esta tesis se ha forjado parcialmente en La Herradura. Y de nuevo a Elvira, por entender en el momento más difícil, lo complicado que es escribir una tesis. Os quiero a todos.

Y por último y en un párrafo aparte no porque no sea familia, que ya lo es (y pronto lo será también oficialmente), si no porque se merece un párrafo y más. Un lector atento se habrá dado cuenta que en todas las citas de las cabeceras de los capítulos cuando escribo SAMwise (SAMsagaz) Gamgee, lo hago con las letras en mayúsculas. Es intencionado puesto que en este caso SAM no son otra cosa que unas siglas y por tanto así han de escribirse. Y es que como en *El Señor de los Anillos* es bien sabido que Frodo (con el que comparto inicial) no habría llegado a Mordor sin su compañero y amigo Sam, yo tampoco habría llegado a escribir esta tesis sin mi compañera y amiga Sara Arrojo Montilla (SAM). Y es que desde que nos embarcamos en esta aventura hace algo más de cuatro años, ella ha estado en

[6] Te lo he agradecido en español porque si no te acomodas y se te olvida!

los días sombríos y los brillantes. En Valencia, Granada, La Herradura y Lisboa. Estuvo celebrando el primer paper y a mi lado cuando las cosas no salían. Ha estado conmigo incluso cuando ni siquiera ella estaba consigo. Por todo esto, aunque en la primera página de este libro solo este escrito mi nombre, ella es tan protagonista de esta historia como yo. Gracias por todo. Te quiero.

Acknowledgements

I would like to thank all the agents that have made economically possible the development of this thesis. During the PhD period I have been financially supported by Severo Ochoa Excellence Center Project SEV-2014-0398, by Generalitat Valenciana under grant GVPROMETEOII 2014-049 (CPI-16-295) from 11/16 to 12/17, by the Spanish SEPE and my parents (Fernando and Esther M.) from 1/18 to 6/18 and by Ministerio de Ciencia, Innovación y Universidades, Spain, under grant BES-2017-080070 from 7/18 until now. This thesis is also partially supported by a Short-Term Scientific Mission Grant from the COST Action CA15108.

Appendices

A
RGE details

The analysis of the RGE of the quark Yukawa couplings and the stability of the gFC scenario in eq. (3.4) has been presented in detail for the set $\{Y_{d,\alpha}Y^{\dagger}_{d,\beta}\}$ in section 3.2.1 and 3.2.2. We reproduce in this appendix the equations relevant for $\{Y_{d,\alpha}Y^{\dagger}_{d,\beta}\}$ and also for $\{Y^{\dagger}_{d,\alpha}Y_{d,\beta}\}$, $\{Y_{u,\alpha}Y^{\dagger}_{u,\beta}\}$ and $\{Y^{\dagger}_{u,\alpha}Y_{u,\beta}\}$, omitted for conciseness in section 3.2. In correspondence with eqs. (3.12), (3.13) and (3.14),

$$\begin{aligned}
\mathcal{D}(Y_{d,\alpha}Y^{\dagger}_{d,\beta}) &= f^{[\mathrm{d_L}]}_{\alpha\beta}(Y_d) + g^{[\mathrm{d_L}]}_{\alpha\beta}(Y_d, Y_u)\,,\\
\mathcal{D}(Y_{u,\alpha}Y^{\dagger}_{u,\beta}) &= f^{[\mathrm{u_L}]}_{\alpha\beta}(Y_u) + g^{[\mathrm{u_L}]}_{\alpha\beta}(Y_d, Y_u)\,,\\
\mathcal{D}(Y^{\dagger}_{d,\alpha}Y_{d,\beta}) &= f^{[\mathrm{d_R}]}_{\alpha\beta}(Y_d) + g^{[\mathrm{d_R}]}_{\alpha\beta}(Y_d, Y_u)\,,\\
\mathcal{D}(Y^{\dagger}_{u,\alpha}Y_{u,\beta}) &= f^{[\mathrm{u_R}]}_{\alpha\beta}(Y_u) + g^{[\mathrm{u_R}]}_{\alpha\beta}(Y_d, Y_u)\,,
\end{aligned} \tag{A.1}$$

with

$$\begin{aligned}
f^{[\mathrm{d_L}]}_{\alpha\beta}(Y_d) &= 2a_d Y_{d,\alpha}Y^{\dagger}_{d,\beta} + \sum_{\rho=1}^{n=2}\left[T^{d}_{\alpha,\rho}Y_{d,\rho}Y^{\dagger}_{d,\beta} + T^{d*}_{\beta,\rho}Y_{d,\alpha}Y^{\dagger}_{d,\rho}\right]\\
&\qquad + 2Y_{d,\alpha}Y^{R}_{d}Y^{\dagger}_{d,\beta} + \frac{1}{2}Y^{L}_{d}Y_{d,\alpha}Y^{\dagger}_{d,\beta} + \frac{1}{2}Y_{d,\alpha}Y^{\dagger}_{d,\beta}Y^{L}_{d}\,,\\
g^{[\mathrm{d_L}]}_{\alpha\beta}(Y_d, Y_u) &= \frac{1}{2}Y^{L}_{u}Y_{d,\alpha}Y^{\dagger}_{d,\beta} + \frac{1}{2}Y_{d,\alpha}Y^{\dagger}_{d,\beta}Y^{L}_{u} -\\
&\qquad 2\sum_{\rho=1}^{n=2}\left[Y_{u,\rho}Y^{\dagger}_{u,\alpha}Y_{d,\rho}Y^{\dagger}_{d,\beta} + Y_{d,\alpha}Y^{\dagger}_{d,\rho}Y_{u,\beta}Y^{\dagger}_{u,\rho}\right],
\end{aligned} \tag{A.2}$$

$$
\begin{aligned}
f^{[\mathrm{d_R}]}_{\alpha\beta}(Y_d) &= 2a_d Y^\dagger_{d,\alpha} Y_{d,\beta} + \sum_{\rho=1}^{n=2}\left[T^{d*}_{\alpha,\rho} Y^\dagger_{d,\rho} Y_{d,\beta} + T^{d}_{\beta,\rho} Y^\dagger_{d,\alpha} Y_{d,\rho}\right] \\
&\quad + Y^\dagger_{d,\alpha} Y^L_d Y_{d,\beta} + Y^R_d Y^\dagger_{d,\alpha} Y_{d,\beta} + Y^\dagger_{d,\alpha} Y_{d,\beta} Y^R_d\,, \\
g^{[\mathrm{d_R}]}_{\alpha\beta}(Y_d, Y_u) &= Y^\dagger_{d,\alpha} Y^L_u Y_{d,\beta} - 2\sum_{\rho=1}^{n=2}\left[Y^\dagger_{d,\rho} Y_{u,\alpha} Y^\dagger_{u,\rho} Y_{d,\beta} + Y^\dagger_{d,\alpha} Y_{u,\rho} Y^\dagger_{u,\beta} Y_{d,\rho}\right],
\end{aligned}
\tag{A.3}
$$

$$
\begin{aligned}
f^{[\mathrm{u_L}]}_{\alpha\beta}(Y_u) &= 2a_u Y_{u,\alpha} Y^\dagger_{u,\beta} + \sum_{\rho=1}^{n=2}\left[T^{u}_{\alpha,\rho} Y_{u,\rho} Y^\dagger_{u,\beta} + T^{d*}_{\beta,\rho} Y_{u,\alpha} Y^\dagger_{u,\rho}\right] + 2Y_{u,\alpha} Y^R_u Y^\dagger_{u,\beta} \\
&\quad + \frac{1}{2} Y^L_u Y_{u,\alpha} Y^\dagger_{u,\beta} + \frac{1}{2} Y_{u,\alpha} Y^\dagger_{u,\beta} Y^L_u\,, \\
g^{[\mathrm{u_L}]}_{\alpha\beta}(Y_d, Y_u) &= \frac{1}{2} Y^L_d Y_{u,\alpha} Y^\dagger_{u,\beta} + \frac{1}{2} Y_{u,\alpha} Y^\dagger_{u,\beta} Y^L_d \\
&\quad - 2\sum_{\rho=1}^{n=2}\left[Y_{d,\rho} Y^\dagger_{d,\alpha} Y_{u,\rho} Y^\dagger_{u,\beta} + Y_{u,\alpha} Y^\dagger_{u,\rho} Y_{d,\beta} Y^\dagger_{d,\rho}\right],
\end{aligned}
\tag{A.4}
$$

and

$$
\begin{aligned}
f^{[\mathrm{u_R}]}_{\alpha\beta}(Y_d) &= 2a_u Y^\dagger_{u,\alpha} Y_{u,\beta} + \sum_{\rho=1}^{n=2}\left[T^{u*}_{\alpha,\rho} Y^\dagger_{u,\rho} Y_{u,\beta} + T^{u}_{\beta,\rho} Y^\dagger_{u,\alpha} Y_{u,\rho}\right] \\
&\quad + Y^\dagger_{u,\alpha} Y^L_u Y_{u,\beta} + Y^R_u Y^\dagger_{u,\alpha} Y_{u,\beta} + Y^\dagger_{u,\alpha} Y_{u,\beta} Y^R_u\,, \\
g^{[\mathrm{u_R}]}_{\alpha\beta}(Y_d, Y_u) &= Y^\dagger_{u,\alpha} Y^L_d Y_{u,\beta} - 2\sum_{\rho=1}^{n=2}\left[Y^\dagger_{u,\rho} Y_{d,\alpha} Y^\dagger_{d,\rho} Y_{u,\beta} + Y^\dagger_{u,\alpha} Y_{d,\rho} Y^\dagger_{d,\beta} Y_{u,\rho}\right].
\end{aligned}
\tag{A.5}
$$

The RGE of the commutation relations of eq. (3.3) reads

$$
\begin{aligned}
\mathcal{D}\left[Y_{d,\alpha} Y^\dagger_{d,\beta}\,,\, Y_{d,\gamma} Y^\dagger_{d,\delta}\right] &= \left[g^{[\mathrm{d_L}]}_{\alpha\beta}(Y_d, Y_u)\,,\, Y_{d,\gamma} Y^\dagger_{d,\delta}\right] + \left[Y_{d,\alpha} Y^\dagger_{d,\beta}\,,\, g^{[\mathrm{d_L}]}_{\gamma\delta}(Y_d, Y_u)\right], \\
\mathcal{D}\left[Y^\dagger_{d,\alpha} Y_{d,\beta}\,,\, Y^\dagger_{d,\gamma} Y_{d,\delta}\right] &= \left[g^{[\mathrm{d_R}]}_{\alpha\beta}(Y_d, Y_u)\,,\, Y^\dagger_{d,\gamma} Y_{d,\delta}\right] + \left[Y^\dagger_{d,\alpha} Y_{d,\beta}\,,\, g^{[\mathrm{d_R}]}_{\gamma\delta}(Y_d, Y_u)\right], \\
\mathcal{D}\left[Y_{u,\alpha} Y^\dagger_{u,\beta}\,,\, Y_{u,\gamma} Y^\dagger_{u,\delta}\right] &= \left[g^{[\mathrm{u_L}]}_{\alpha\beta}(Y_d, Y_u)\,,\, Y_{u,\gamma} Y^\dagger_{u,\delta}\right] + \left[Y_{u,\alpha} Y^\dagger_{u,\beta}\,,\, g^{[\mathrm{u_L}]}_{\gamma\delta}(Y_d, Y_u)\right], \\
\mathcal{D}\left[Y^\dagger_{u,\alpha} Y_{u,\beta}\,,\, Y^\dagger_{u,\gamma} Y_{u,\delta}\right] &= \left[g^{[\mathrm{u_R}]}_{\alpha\beta}(Y_d, Y_u)\,,\, Y^\dagger_{u,\gamma} Y_{d,\delta}\right] + \left[Y^\dagger_{u,\alpha} Y_{u,\beta}\,,\, g^{[\mathrm{u_R}]}_{\gamma\delta}(Y_d, Y_u)\right],
\end{aligned}
\tag{A.6}
$$

which, following the discussion in section 3.2.2, lead to (summation over $h = 1, 2$ understood)

$$
\begin{aligned}
\{d_L\} \equiv \frac{v^2}{2}\mathcal{U}^\dagger_{d_L}&\left(\mathcal{D}\left[T^0_{[\mathrm{d}]i} T^{0\dagger}_{[\mathrm{d}]j}\,,\, T^0_{[\mathrm{d}]k} T^{0\dagger}_{[\mathrm{d}]l}\right]\right)\mathcal{U}_{d_L} = \\
&T_{[\mathrm{d}]i} T^\dagger_{[\mathrm{d}]j} V^\dagger T_{[\mathrm{u}]h} T^\dagger_{[\mathrm{u}]h} V\, T_{[\mathrm{d}]k} T^\dagger_{[\mathrm{d}]l} - T_{[\mathrm{d}]k} T^\dagger_{[\mathrm{d}]l} V^\dagger T_{[\mathrm{u}]h} T^\dagger_{[\mathrm{u}]h} V\, T_{[\mathrm{d}]i} T^\dagger_{[\mathrm{d}]j} \\
&- 2\left[V^\dagger T_{[\mathrm{u}]h} T^\dagger_{[\mathrm{u}]i} V\,,\, T_{[\mathrm{d}]k} T^\dagger_{[\mathrm{d}]l}\right] T_{[\mathrm{d}]h} T^\dagger_{[\mathrm{d}]j} - 2T_{[\mathrm{d}]i} T^\dagger_{[\mathrm{d}]h}\left[V^\dagger T_{[\mathrm{u}]j} T^\dagger_{[\mathrm{u}]h} V\,,\, T_{[\mathrm{d}]k} T^\dagger_{[\mathrm{d}]l}\right] \\
&+ 2\left[V^\dagger T_{[\mathrm{u}]h} T^\dagger_{[\mathrm{u}]k} V\,,\, T_{[\mathrm{d}]i} T^\dagger_{[\mathrm{d}]j}\right] T_{[\mathrm{d}]h} T^\dagger_{[\mathrm{d}]l} + 2T_{[\mathrm{d}]k} T^\dagger_{[\mathrm{d}]h}\left[V^\dagger T_{[\mathrm{u}]l} T^\dagger_{[\mathrm{u}]h} V\,,\, T_{[\mathrm{d}]i} T^\dagger_{[\mathrm{d}]j}\right],
\end{aligned}
\tag{A.7}
$$

$$\{d_R\} \equiv \frac{v^2}{2}\mathcal{U}_{d_R}^\dagger \left(\mathcal{D}\left[T^{0\dagger}_{[\mathrm{d}]i}T^0_{[\mathrm{d}]j}\,,\, T^{0\dagger}_{[\mathrm{d}]k}T^0_{[\mathrm{d}]l}\right]\right)\mathcal{U}_{d_R} =$$
$$\left[T^\dagger_{[\mathrm{d}]i}V^\dagger T_{[\mathrm{u}]h}T^\dagger_{[\mathrm{u}]h}V\,T_{[\mathrm{d}]j}\,,\, T^\dagger_{[\mathrm{d}]k}T_{[\mathrm{d}]l}\right] - \left[T^\dagger_{[\mathrm{d}]k}V^\dagger T_{[\mathrm{u}]h}T^\dagger_{[\mathrm{u}]h}V\,T_{[\mathrm{d}]l}\,,\, T^\dagger_{[\mathrm{d}]i}T_{[\mathrm{d}]j}\right]$$
$$-2\left[T^\dagger_{[\mathrm{d}]h}V^\dagger T_{[\mathrm{u}]i}T^\dagger_{[\mathrm{u}]h}V\,T_{[\mathrm{d}]j}\,,\, T^\dagger_{[\mathrm{d}]k}T_{[\mathrm{d}]l}\right] - 2\left[T^\dagger_{[\mathrm{d}]i}V^\dagger T_{[\mathrm{u}]h}T^\dagger_{[\mathrm{u}]j}V\,T_{[\mathrm{d}]h}\,,\, T^\dagger_{[\mathrm{d}]k}T_{[\mathrm{d}]l}\right]$$
$$+2\left[T^\dagger_{[\mathrm{d}]h}V^\dagger T_{[\mathrm{u}]k}T^\dagger_{[\mathrm{u}]h}V\,T_{[\mathrm{d}]l}\,,\, T^\dagger_{[\mathrm{d}]i}T_{[\mathrm{d}]j}\right] + 2\left[T^\dagger_{[\mathrm{d}]k}V^\dagger T_{[\mathrm{u}]h}T^\dagger_{[\mathrm{u}]l}V\,T_{[\mathrm{d}]h}\,,\, T^\dagger_{[\mathrm{d}]i}T_{[\mathrm{d}]j}\right], \tag{A.8}$$

$$\{u_L\} \equiv \frac{v^2}{2}\mathcal{U}_{u_L}^\dagger \left(\mathcal{D}\left[T^0_{[\mathrm{u}]i}T^{0\dagger}_{[\mathrm{u}]j}\,,\, T^0_{[\mathrm{u}]k}T^{0\dagger}_{[\mathrm{u}]l}\right]\right)\mathcal{U}_{u_L} =$$
$$T_{[\mathrm{u}]i}T^\dagger_{[\mathrm{u}]j}VT_{[\mathrm{d}]h}T^\dagger_{[\mathrm{d}]h}V^\dagger T_{[\mathrm{u}]k}T^\dagger_{[\mathrm{u}]l} - T_{[\mathrm{u}]k}T^\dagger_{[\mathrm{u}]l}VT_{[\mathrm{d}]h}T^\dagger_{[\mathrm{d}]h}V^\dagger T_{[\mathrm{u}]i}T^\dagger_{[\mathrm{u}]j}$$
$$-2\left[VT_{[\mathrm{d}]h}T^\dagger_{[\mathrm{d}]i}V^\dagger\,,\, T_{[\mathrm{u}]k}T^\dagger_{[\mathrm{u}]l}\right]T_{[\mathrm{u}]h}T^\dagger_{[\mathrm{u}]j} - 2T_{[\mathrm{u}]i}T^\dagger_{[\mathrm{u}]h}\left[VT_{[\mathrm{d}]j}T^\dagger_{[\mathrm{d}]h}V^\dagger\,,\, T_{[\mathrm{u}]k}T^\dagger_{[\mathrm{u}]l}\right]$$
$$+2\left[VT_{[\mathrm{d}]h}T^\dagger_{[\mathrm{d}]k}V^\dagger\,,\, T_{[\mathrm{u}]i}T^\dagger_{[\mathrm{u}]j}\right]T_{[\mathrm{u}]h}T^\dagger_{[\mathrm{u}]l} + 2T_{[\mathrm{u}]k}T^\dagger_{[\mathrm{u}]h}\left[VT_{[\mathrm{d}]l}T^\dagger_{[\mathrm{d}]h}V^\dagger\,,\, T_{[\mathrm{u}]i}T^\dagger_{[\mathrm{u}]j}\right], \tag{A.9}$$

and

$$\{u_R\} \equiv \frac{v^2}{2}\mathcal{U}_{u_R}^\dagger \left(\mathcal{D}\left[T^{0\dagger}_{[\mathrm{u}]i}T^0_{[\mathrm{u}]j}\,,\, T^{0\dagger}_{[\mathrm{u}]k}T^0_{[\mathrm{u}]l}\right]\right)\mathcal{U}_{u_R} =$$
$$\left[T^\dagger_{[\mathrm{u}]i}VT_{[\mathrm{d}]h}T^\dagger_{[\mathrm{d}]h}V^\dagger T_{[\mathrm{u}]j}\,,\, T^\dagger_{[\mathrm{u}]k}T_{[\mathrm{u}]l}\right] - \left[T^\dagger_{[\mathrm{u}]k}VT_{[\mathrm{d}]h}T^\dagger_{[\mathrm{d}]h}V^\dagger T_{[\mathrm{u}]l}\,,\, T^\dagger_{[\mathrm{u}]i}T_{[\mathrm{u}]j}\right]$$
$$-2\left[T^\dagger_{[\mathrm{u}]h}VT_{[\mathrm{d}]i}T^\dagger_{[\mathrm{d}]h}V^\dagger T_{[\mathrm{u}]j}\,,\, T^\dagger_{[\mathrm{u}]k}T_{[\mathrm{u}]l}\right] - 2\left[T^\dagger_{[\mathrm{u}]i}VT_{[\mathrm{d}]h}T^\dagger_{[\mathrm{d}]j}V^\dagger T_{[\mathrm{u}]h}\,,\, T^\dagger_{[\mathrm{u}]k}T_{[\mathrm{u}]l}\right]$$
$$+2\left[T^\dagger_{[\mathrm{u}]h}VT_{[\mathrm{d}]k}T^\dagger_{[\mathrm{d}]h}V^\dagger T_{[\mathrm{u}]l}\,,\, T^\dagger_{[\mathrm{u}]i}T_{[\mathrm{u}]j}\right] + 2\left[T^\dagger_{[\mathrm{u}]k}VT_{[\mathrm{d}]h}T^\dagger_{[\mathrm{d}]l}V^\dagger T_{[\mathrm{u}]h}\,,\, T^\dagger_{[\mathrm{u}]i}T_{[\mathrm{u}]j}\right]. \tag{A.10}$$

In order to compute the matrix elements of eqs. (A.7)–(A.10), we notice that

$$\left(\left[V^\dagger T_{[\mathrm{u}]i}T^\dagger_{[\mathrm{u}]j}V\,,\, T^\dagger_{[\mathrm{d}]k}T_{[\mathrm{d}]l}\right]\right)_{ab} = \sum_{q=1}^{3} V^*_{qa}V_{qb}t^{\mathrm{u}}_{i,q}t^{\mathrm{u}*}_{j,q}(t^{\mathrm{d}*}_{k,b}t^{\mathrm{d}}_{l,b} - t^{\mathrm{d}*}_{k,a}t^{\mathrm{d}}_{l,a}), \tag{A.11}$$

and

$$\left(\left[VT_{[\mathrm{d}]i}T^\dagger_{[\mathrm{d}]j}V^\dagger\,,\, T_{[\mathrm{u}]k}T^\dagger_{[\mathrm{u}]l}\right]\right)_{ab} = \sum_{q=1}^{3} V_{aq}V^*_{bq}t^{\mathrm{d}}_{i,q}t^{\mathrm{d}*}_{j,q}(t^{\mathrm{u}}_{k,b}t^{\mathrm{u}*}_{l,b} - t^{\mathrm{u}}_{k,a}t^{\mathrm{u}*}_{l,a}). \tag{A.12}$$

Then, with the parameters in eq. (3.28), the matrix elements (a, b) of eqs. (A.7)–(A.10) read

$$\{d_L\}_{ab} = \sum_{q=1}^{3}\sum_{\mathrm{h}=1}^{n=2} V^*_{qa}V_{qb}\Big\{\left|t^{\mathrm{u}}_{h,q}\right|^2\left(t^{\mathrm{d}}_{i,a}t^{\mathrm{d}*}_{j,a}t^{\mathrm{d}}_{k,b}t^{\mathrm{d}*}_{l,b} - t^{\mathrm{d}}_{i,b}t^{\mathrm{d}*}_{j,b}t^{\mathrm{d}}_{k,a}t^{\mathrm{d}*}_{l,a}\right) \tag{A.13}$$
$$-2\left(t^{\mathrm{u}}_{h,q}t^{\mathrm{u}*}_{i,q}t^{\mathrm{d}}_{h,b}t^{\mathrm{d}*}_{j,b} + t^{\mathrm{u}}_{j,q}t^{\mathrm{u}*}_{h,q}t^{\mathrm{d}}_{i,a}t^{\mathrm{d}*}_{h,a}\right)\left(t^{\mathrm{d}}_{k,b}t^{\mathrm{d}*}_{l,b} - t^{\mathrm{d}}_{k,a}t^{\mathrm{d}*}_{l,a}\right)$$
$$+2\left(t^{\mathrm{u}}_{h,q}t^{\mathrm{u}*}_{k,q}t^{\mathrm{d}}_{h,b}t^{\mathrm{d}*}_{l,b} + t^{\mathrm{u}}_{l,q}t^{\mathrm{u}*}_{h,q}t^{\mathrm{d}}_{k,a}t^{\mathrm{d}*}_{h,a}\right)\left(t^{\mathrm{d}}_{i,b}t^{\mathrm{d}*}_{j,b} - t^{\mathrm{d}}_{i,a}t^{\mathrm{d}*}_{j,a}\right)\Big\}.$$

$$\{d_R\}_{ab} = \tag{A.14}$$
$$\sum_{q=1}^{3}\sum_{\mathrm{h}=1}^{n=2} V_{qa}^{*}V_{qb}\Big\{\left(t_{k,b}^{\mathrm{d}*}t_{l,b}^{\mathrm{d}}-t_{k,a}^{\mathrm{d}*}t_{l,a}^{\mathrm{d}}\right)\left(\left|t_{h,q}^{\mathrm{u}}\right|^2 t_{i,a}^{\mathrm{d}*}t_{j,b}^{\mathrm{d}}-2t_{i,q}^{\mathrm{u}}t_{h,q}^{\mathrm{u}*}t_{h,a}^{\mathrm{d}*}t_{j,b}^{\mathrm{d}}-2t_{h,q}^{\mathrm{u}}t_{j,q}^{\mathrm{u}*}t_{i,a}^{\mathrm{d}*}t_{h,b}^{\mathrm{d}}\right)$$
$$-\left(t_{i,b}^{\mathrm{d}*}t_{j,b}^{\mathrm{d}}-t_{i,a}^{\mathrm{d}*}t_{j,a}^{\mathrm{d}}\right)\left(\left|t_{h,q}^{\mathrm{u}}\right|^2 t_{k,a}^{\mathrm{d}*}t_{l,b}^{\mathrm{d}}-2t_{k,q}^{\mathrm{u}}t_{h,q}^{\mathrm{u}*}t_{h,a}^{\mathrm{d}*}t_{l,b}^{\mathrm{d}}-2t_{h,q}^{\mathrm{u}}t_{l,q}^{\mathrm{u}*}t_{k,a}^{\mathrm{d}*}t_{h,b}^{\mathrm{d}}\right)\Big\},$$

$$\{u_L\}_{ab} = \sum_{q=1}^{3}\sum_{\mathrm{h}=1}^{n=2} V_{aq}V_{bq}^{*}\Big\{\left|t_{h,q}^{\mathrm{d}}\right|^2\left(t_{i,a}^{\mathrm{u}}t_{j,a}^{\mathrm{u}*}t_{k,b}^{\mathrm{u}}t_{l,b}^{\mathrm{u}*}-t_{i,b}^{\mathrm{u}}t_{j,b}^{\mathrm{u}*}t_{k,a}^{\mathrm{u}}t_{l,a}^{\mathrm{u}*}\right)$$
$$-2\left(t_{h,q}^{\mathrm{d}}t_{i,q}^{\mathrm{d}*}t_{h,b}^{\mathrm{u}}t_{j,b}^{\mathrm{u}*}+t_{j,q}^{\mathrm{d}}t_{h,q}^{\mathrm{d}*}t_{i,a}^{\mathrm{u}}t_{h,a}^{\mathrm{u}*}\right)\left(t_{k,b}^{\mathrm{u}}t_{l,b}^{\mathrm{u}*}-t_{k,a}^{\mathrm{u}}t_{l,a}^{\mathrm{u}*}\right) \tag{A.15}$$
$$+2\left(t_{h,q}^{\mathrm{d}}t_{k,q}^{\mathrm{d}*}t_{h,b}^{\mathrm{u}}t_{l,b}^{\mathrm{u}*}+t_{l,q}^{\mathrm{d}}t_{h,q}^{\mathrm{d}*}t_{k,a}^{\mathrm{u}}t_{h,a}^{\mathrm{u}*}\right)\left(t_{i,b}^{\mathrm{u}}t_{j,b}^{\mathrm{u}*}-t_{i,a}^{\mathrm{u}}t_{j,a}^{\mathrm{u}*}\right)\Big\},$$

and

$$\{u_R\}_{ab} =$$
$$\sum_{q=1}^{3}\sum_{\mathrm{h}=1}^{n=2} V_{aq}V_{bq}^{*}\Big\{\left(t_{k,b}^{\mathrm{u}*}t_{l,b}^{\mathrm{u}}-t_{k,a}^{\mathrm{u}*}t_{l,a}^{\mathrm{u}}\right)\left(\left|t_{h,q}^{\mathrm{d}}\right|^2 t_{i,a}^{\mathrm{u}*}t_{j,b}^{\mathrm{u}}-2t_{i,q}^{\mathrm{d}}t_{h,q}^{\mathrm{d}*}t_{h,a}^{\mathrm{u}*}t_{j,b}^{\mathrm{u}}-2t_{h,q}^{\mathrm{d}}t_{j,q}^{\mathrm{d}*}t_{i,a}^{\mathrm{u}*}t_{h,b}^{\mathrm{u}}\right)$$
$$-\left(t_{i,b}^{\mathrm{u}*}t_{j,b}^{\mathrm{u}}-t_{i,a}^{\mathrm{u}*}t_{j,a}^{\mathrm{u}}\right)\left(\left|t_{h,q}^{\mathrm{d}}\right|^2 t_{k,a}^{\mathrm{u}*}t_{l,b}^{\mathrm{u}}-2t_{k,q}^{\mathrm{d}}t_{h,q}^{\mathrm{d}*}t_{h,a}^{\mathrm{u}*}t_{l,b}^{\mathrm{u}}-2t_{h,q}^{\mathrm{d}}t_{l,q}^{\mathrm{d}*}t_{k,a}^{\mathrm{u}*}t_{h,b}^{\mathrm{u}}\right)\Big\}. \tag{A.16}$$

For diagonal elements, $a = b$, the right-hand sides of eqs. (A.13)–(A.16) are identically zero. For $i = j$ and $k = l$, by construction, we have in addition $\{q_X\}_{ba} = -\{q_X\}_{ab}^{*}$ ($q = u, d$, $X = L, R$). For illustration, we show in the following eqs. (A.13)–(A.16) for 2HDM and $i = j = 1$, $k = l = 2$.

$$\{d_L\}_{d_a d_b} = \sum_{u_q=1}^{3} V_{u_q d_a}^{*}V_{u_q d_b}\Big\{\left(m_{u_q}^2+\left|n_{u_q}\right|^2\right)\left(m_{d_a}^2\left|n_{d_b}\right|^2-m_{d_b}^2\left|n_{d_a}\right|^2\right)$$
$$-2\left(\left|n_{d_b}\right|^2-\left|n_{d_a}\right|^2\right)\left(m_{u_q}m_{d_b}\left(m_{u_q}m_{d_b}+n_{u_q}n_{d_b}\right)+m_{u_q}m_{d_a}\left(m_{u_q}m_{d_a}+n_{u_q}^{*}n_{d_a}^{*}\right)\right)$$
$$+2\left(m_{d_b}^2-m_{d_a}^2\right)\left(n_{u_q}^{*}n_{d_b}^{*}\left(m_{u_q}m_{d_b}+n_{u_q}n_{d_b}\right)+n_{u_q}n_{d_a}\left(m_{u_q}m_{d_a}+n_{u_q}^{*}n_{d_a}^{*}\right)\right)\Big\}, \tag{A.17}$$

$$\{d_R\}_{d_a d_b} = \sum_{u_q=1}^{3} V_{u_q d_a}^{*}V_{u_q d_b}\Big\{\left(\left|n_{d_b}\right|^2-\left|n_{d_a}\right|^2\right)\left(m_{u_q}^2+\left|n_{u_q}\right|^2\right)m_{d_a}m_{d_b}$$
$$-2\left(\left|n_{d_b}\right|^2-\left|n_{d_a}\right|^2\right)\left(m_{u_q}m_{d_b}\left(m_{u_q}m_{d_a}+n_{u_q}^{*}n_{d_a}^{*}\right)+m_{u_q}m_{d_a}\left(m_{u_q}m_{d_b}+n_{u_q}n_{d_b}\right)\right)$$
$$+2\left(m_{d_b}^2-m_{d_a}^2\right)\left(n_{u_q}n_{d_b}\left(m_{u_q}m_{d_a}+n_{u_q}^{*}n_{d_a}^{*}\right)+n_{u_q}^{*}n_{d_a}^{*}\left(m_{u_q}m_{d_b}+n_{u_q}n_{d_b}\right)\right)$$
$$-\left(m_{d_b}^2-m_{d_a}^2\right)\left(m_{u_q}^2+\left|n_{u_q}\right|^2\right)n_{d_a}^{*}n_{d_b}\Big\},$$

$$\{u_L\}_{u_a u_b} = \sum_{d_q=1}^{3} V_{u_a d_q}V_{u_b d_q}^{*}\Big\{\left(m_{d_q}^2+\left|n_{d_q}\right|^2\right)\left(m_{u_a}^2\left|n_{u_b}\right|^2-m_{u_b}^2\left|n_{u_a}\right|^2\right)$$
$$-2\left(\left|n_{u_b}\right|^2-\left|n_{u_a}\right|^2\right)\left(m_{d_q}m_{u_b}\left(m_{d_q}m_{u_b}+n_{d_q}n_{u_b}\right)+m_{d_q}m_{u_a}\left(m_{d_q}m_{u_a}+n_{d_q}^{*}n_{u_a}^{*}\right)\right)$$
$$+2\left(m_{u_b}^2-m_{u_a}^2\right)\left(n_{d_q}^{*}n_{u_b}^{*}\left(m_{d_q}m_{u_b}+n_{d_q}n_{u_b}\right)+n_{d_q}n_{u_a}\left(m_{d_q}m_{u_a}+n_{d_q}^{*}n_{u_a}^{*}\right)\right)\Big\}, \tag{A.18}$$

and

$$\begin{aligned}\{u_R\}_{u_a u_b} = \sum_{q=1}^{3} V_{u_a d_q} V^*_{u_b d_q} \Big\{ &\left(|n_{u_b}|^2 - |n_{u_a}|^2\right)\left(m^2_{d_q} + \left|n_{d_q}\right|^2\right) m_{u_a} m_{u_b} \\ &- 2\left(|n_{u_b}|^2 - |n_{u_a}|^2\right)\left(m_{d_q} m_{u_b}\left(m_{d_q} m_{u_a} + n^*_{d_q} n^*_{u_a}\right) + m_{d_q} m_{u_a}\left(m_{d_q} m_{u_b} + n_{d_q} n_{u_b}\right)\right) \\ &+ 2\left(m^2_{u_b} - m^2_{u_a}\right)\left(n_{d_q} n_{u_b}\left(m_{d_q} m_{u_a} + n^*_{d_q} n^*_{u_a}\right) + n^*_{d_q} n^*_{u_a}\left(m_{d_q} m_{u_b} + n_{d_q} n_{u_b}\right)\right) \\ &- \left(m^2_{u_b} - m^2_{u_a}\right)\left(m^2_{d_q} + \left|n_{d_q}\right|^2\right) n^*_{u_a} n_{u_b} \Big\}. \end{aligned} \tag{A.19}$$

B

Necessary and Suficient conditions for gBGL models

We complete in this appendix the proof of the sufficient conditions in the following general result: *the WB invariant matrix conditions*

$$\begin{aligned} Y_{d,2}^\dagger Y_{d,1} = 0, \quad Y_{d,2}^\dagger Y_{u,1} = 0, \\ Y_{u,2}^\dagger Y_{u,1} = 0, \quad Y_{u,2}^\dagger Y_{d,1} = 0, \end{aligned} \tag{4.10}$$

are the necessary and sufficient conditions to define gBGL models or a type I 2HDM[1]*, provided there are no massless quarks.*

It is always possible, in general, to write

$$Y_{d,i} = W_{d_i}\, D_{d_i}\, U_{d_i}^\dagger, \qquad Y_{u,i} = W_{u_i}\, D_{u_i}\, U_{u_i}^\dagger, \tag{B.1}$$

where W_{d_i}, W_{u_i}, U_{d_i} and U_{u_i} are unitary matrices, and D_{d_i} and D_{u_i} are diagonal ones. From $Y_{u,2}^\dagger Y_{u,1} = 0$ it is straightforward that $[Y_{u,1}Y_{u,1}^\dagger, Y_{u,2}Y_{u,2}^\dagger] = 0$ and thus one can choose

$$W_{u_1} = W_{u_2} = W_u\,, \tag{B.2}$$

[1]Since we are not specifying the leptonic sector, with type I we also refer to type X 2HDM.

while from $Y_{d,2}^\dagger Y_{d,1} = 0$ it follows that $[Y_{d,1}Y_{d,1}^\dagger, Y_{d,2}Y_{d,2}^\dagger] = 0$ and therefore we can also choose

$$W_{d_1} = W_{d_2} = W_d\,. \tag{B.3}$$

Now, in $Y_{u,2}^\dagger Y_{u,1} = 0$, W_u simplifies away and we have

$$D_{u_2}^\dagger D_{u_1} = 0\,, \tag{B.4}$$

and similarly, for $Y_{d,2}^\dagger Y_{d,1} = 0$,

$$D_{d_2}^\dagger D_{d_1} = 0\,. \tag{B.5}$$

If there are no massless quarks, there are two kinds of solutions for eq. (B.4),

(a) type I 2HDM

$$D_{u_1} = \begin{pmatrix} 0 & 0 & 0 \\ 0 & 0 & 0 \\ 0 & 0 & 0 \end{pmatrix}, \quad D_{u_2} = \begin{pmatrix} u_1 & 0 & 0 \\ 0 & u_2 & 0 \\ 0 & 0 & u_3 \end{pmatrix}, \tag{B.6}$$

with $u_i \neq 0$ in order to have massive up quarks. Notice that interchanging $D_{u_1} \leftrightarrows D_{u_2}$ will give rise to the same model, as explained later.

(b) gBGL

$$D_{u_1} = \begin{pmatrix} u_1 & 0 & 0 \\ 0 & 0 & 0 \\ 0 & 0 & 0 \end{pmatrix}, \quad D_{u_2} = \begin{pmatrix} 0 & 0 & 0 \\ 0 & u_2 & 0 \\ 0 & 0 & u_3 \end{pmatrix}, \tag{B.7}$$

with $u_i \neq 0$ again. As above, exchanging $D_{u_1} \leftrightarrows D_{u_2}$ does not introduce new models. We should also take into account the possibility that $u_1 \neq 0$ is in a different position in the diagonal of D_{u_1} while respecting $D_{u_2}^\dagger D_{u_1} = 0$, which is ensured with a corresponding permutation of the diagonal elements of D_{u_2}.

Similarly to the up sector, we have different solutions of eq. (B.5), and we consider three possibilities.

(a) First,

$$D_{d_1} = \begin{pmatrix} 0 & 0 & 0 \\ 0 & 0 & 0 \\ 0 & 0 & 0 \end{pmatrix}, \quad D_{d_2} = \begin{pmatrix} d_1 & 0 & 0 \\ 0 & d_2 & 0 \\ 0 & 0 & d_3 \end{pmatrix}, \tag{B.8}$$

with $d_i \neq 0$. Notice that eq. (B.6) together with eq. (B.8) with interchanged $D_{d_1} \leftrightarrows D_{d_2}$ do not match in order to be a solution of eqs. (4.10).

(b) Second, D_{d_1} and D_{u_1} have equal rank, and we could consider in general permutations of the diagonal elements, for example

$$D_{d_1} = \begin{pmatrix} 0 & 0 & 0 \\ 0 & d_2 & 0 \\ 0 & 0 & 0 \end{pmatrix}, \quad D_{d_2} = \begin{pmatrix} d_1 & 0 & 0 \\ 0 & 0 & 0 \\ 0 & 0 & d_3 \end{pmatrix}. \tag{B.9}$$

Then, of course, the rank of D_{d_2} is equal to the rank of D_{u_2}.

(c) Third, D_{d_1} and D_{u_1} have different rank (and therefore D_{d_2} and D_{u_2} also have different rank), for example

$$D_{d_1} = \begin{pmatrix} d_1 & 0 & 0 \\ 0 & d_2 & 0 \\ 0 & 0 & 0 \end{pmatrix}, \quad D_{d_2} = \begin{pmatrix} 0 & 0 & 0 \\ 0 & 0 & 0 \\ 0 & 0 & d_3 \end{pmatrix}. \tag{B.10}$$

We have to explore now which solutions to eqs. (4.10) arise from the available possibilities in eqs. (B.6)–(B.7) and eqs. (B.8)–(B.10).

- $D_{d_1} = 0$ if and only if $D_{u_1} = 0$, which corresponds to a type I or X 2HDM. The proof is simple: if $D_{d_1} = 0$, D_{d_2} has rank 3, and thus $Y_{d,2}$ has rank 3. Since $Y_{d,2}^\dagger Y_{u,1} = 0$, all column vectors of $Y_{u,1}$ are in the null-space of $Y_{d,2}^\dagger$ (they are all non-zero vectors transformed into the zero or null vector), but since $\text{rank}(Y_{d,2}^\dagger) = 3$, according to the rank-nullity theorem, the null-space of $Y_{d,2}^\dagger$ has dimension $3 - 3 = 0$, and thus $Y_{u,1} = 0$, that is $D_{u_1} = 0$. eqs. (4.10) are then trivially verified. Of course, there is also the solution $D_{d_2} = D_{u_2} = 0$, which is completely equivalent with a trivial relabelling of the scalar doublets $\Phi_1 \leftrightarrows \Phi_2$.

- Next we show that concerning eq. (B.7) and eqs. (B.9)–(B.10), the ranks of the Yukawa matrices should match in the following manner: $\text{rank}(D_{d_1}) = \text{rank}(D_{u_1})$ and $\text{rank}(D_{d_2}) = \text{rank}(D_{u_2})$. Consider for definiteness D_{u_1} and D_{u_2} as in eq. (B.7). First, since $Y_{u,2}^\dagger Y_{d,1} = 0$ and $Y_{d,2}^\dagger Y_{u,1} = 0$, with $W = W_u^\dagger W_d$,

$$D_{u_2}^\dagger \, W \, D_{d_1} = 0, \qquad D_{d_2}^\dagger \, W^\dagger \, D_{u_1} = 0 \,. \tag{B.11}$$

$D_{u_2}^\dagger W$ has rank 2, and thus its null-space has dimension 1; according to the first equation above, if D_{d_1} had rank 2, then the null-space of $D_{u_2}^\dagger W$

would have at least dimension 2 in contradiction with the first statement: consequently, the rank of D_{d_1} has to be 1. Then $\text{rank}(D_{d_1}) = \text{rank}(D_{u_1}) = 1$ and $\text{rank}(D_{d_2}) = \text{rank}(D_{u_2}) = 2$. That is, the matrices in eq. (B.9) match the ones in eq. (B.7) for solutions of eqs. (4.10) while eqs. (B.9) and (B.7) do not match. Finally, relabelling of scalar doublets $\Phi_1 \leftrightarrows \Phi_2$ gives equivalent solutions with $\text{rank}(D_{d_1}) = \text{rank}(D_{u_1}) = 2$ and $\text{rank}(D_{d_2}) = \text{rank}(D_{u_2}) = 1$.

- The following step is to show that the most general case can be taken to be

$$D_{u_1} = \begin{pmatrix} u_1 & 0 & 0 \\ 0 & 0 & 0 \\ 0 & 0 & 0 \end{pmatrix}, \quad D_{u_2} = \begin{pmatrix} 0 & 0 & 0 \\ 0 & u_2 & 0 \\ 0 & 0 & u_3 \end{pmatrix},$$
$$D_{d_1} = \begin{pmatrix} d_1 & 0 & 0 \\ 0 & 0 & 0 \\ 0 & 0 & 0 \end{pmatrix}, \quad D_{d_2} = \begin{pmatrix} 0 & 0 & 0 \\ 0 & d_2 & 0 \\ 0 & 0 & d_3 \end{pmatrix}. \tag{B.12}$$

  It is trivial to check that with the insertion of

$$P_{12} = \begin{pmatrix} 0 & 1 & 0 \\ 1 & 0 & 0 \\ 0 & 0 & 1 \end{pmatrix}, \tag{B.13}$$

  in $Y_{d,i} = W_d\, P_{12} P_{12}\, D_{d_i}\, P_{12} P_{12}\, U_d^\dagger = W'_d\, (P_{12}\, D_{d_i}\, P_{12})\, U_d'^\dagger$, one can redefine $W'_d = W_d\, P_{12}$ and $U'_d = U_d P_{12}$, while P_{12} in $P_{12}\, D_{d_i}\, P_{12}$ permutes the first and second elements in the diagonal. This would bring, for example, eq. (B.9) to the desired form, matching with eq. (B.7).

- Finally, substituting eq. (B.12) in $D_{u_1}^\dagger\, W\, D_{d_2} = 0$,

$$u_1^* \begin{pmatrix} 0 & d_2 W_{12} & d_3 W_{13} \\ 0 & 0 & 0 \\ 0 & 0 & 0 \end{pmatrix} = 0\,, \tag{B.14}$$

  we get $W_{12} = W_{13} = 0$, while from $D_{u_2}^\dagger\, W\, D_{d_1} = 0$,

$$d_1 \begin{pmatrix} 0 & 0 & 0 \\ u_2^* W_{21} & 0 & 0 \\ u_3^* W_{31} & 0 & 0 \end{pmatrix} = 0\,, \tag{B.15}$$

  we have $W_{21} = W_{31} = 0$. Then W has the block structure

$$W = W_u^\dagger W_d = e^{i\omega} \begin{pmatrix} 1 & 0 & 0 \\ 0 & W_{22} & W_{23} \\ 0 & W_{32} & W_{33} \end{pmatrix}. \tag{B.16}$$

One can now complete the proof; going back to eq. (B.1):

$$
\begin{aligned}
Y_{u,1} &= W_u \begin{pmatrix} u_1 & 0 & 0 \\ 0 & 0 & 0 \\ 0 & 0 & 0 \end{pmatrix} U_{u_1}^\dagger = W_u \begin{pmatrix} \times & \times & \times \\ 0 & 0 & 0 \\ 0 & 0 & 0 \end{pmatrix}, \\
Y_{u,2} &= W_u \begin{pmatrix} 0 & 0 & 0 \\ 0 & u_2 & 0 \\ 0 & 0 & u_3 \end{pmatrix} U_{u_2}^\dagger = W_u \begin{pmatrix} 0 & 0 & 0 \\ \times & \times & \times \\ \times & \times & \times \end{pmatrix},
\end{aligned}
\tag{B.17}
$$

$$
\begin{aligned}
Y_{d,1} &= W_d \begin{pmatrix} d_1 & 0 & 0 \\ 0 & 0 & 0 \\ 0 & 0 & 0 \end{pmatrix} U_{d_1}^\dagger = W_u W \begin{pmatrix} \times & \times & \times \\ 0 & 0 & 0 \\ 0 & 0 & 0 \end{pmatrix} = W_u \begin{pmatrix} \times & \times & \times \\ 0 & 0 & 0 \\ 0 & 0 & 0 \end{pmatrix}, \\
Y_{d,2} &= W_d \begin{pmatrix} 0 & 0 & 0 \\ 0 & d_2 & 0 \\ 0 & 0 & d_3 \end{pmatrix} U_{d_2}^\dagger = W_u W \begin{pmatrix} 0 & 0 & 0 \\ \times & \times & \times \\ \times & \times & \times \end{pmatrix} = W_u \begin{pmatrix} 0 & 0 & 0 \\ \times & \times & \times \\ \times & \times & \times \end{pmatrix}.
\end{aligned}
\tag{B.18}
$$

With a WB transformation given by $Q_L \mapsto W_u Q_L$ we arrive to the equivalent gBGL structures in eqs. (4.5).

C

CKM and PMNS fits

The PDG parametrization [20, 321] of the CKM and PMNS matrices is

$$\mathcal{R}_{23}(\theta_{23})\varphi_3(\delta)\mathcal{R}_{13}(\theta_{13})\varphi_3(-\delta)\mathcal{R}_{12}(\theta_{12}) = \begin{pmatrix} c_{12}c_{13} & s_{12}c_{13} & s_{13}e^{-i\delta} \\ -s_{12}c_{23} - c_{12}s_{13}s_{23}e^{i\delta} & c_{12}c_{23} - s_{12}s_{13}s_{23}e^{i\delta} & c_{13}s_{23} \\ s_{12}s_{23} - c_{12}s_{13}c_{23}e^{i\delta} & -c_{12}s_{23} - s_{12}s_{13}c_{23}e^{i\delta} & c_{13}c_{23} \end{pmatrix}, \quad \text{(C.1)}$$

where rephasings allow to reduce the parameter ranges to $\theta_{ij} \in [0; \pi/2]$ and $\delta \in [0; 2\pi[$. For CKM we use the values [20]

$$\begin{aligned} &\sin\theta^q_{12} = 0.2265 \pm 0.0005\,, && \sin\theta^q_{13} = (3.61 \pm 0.10) \times 10^{-3}\,, \\ &\sin\theta^q_{23} = (4.05 \pm 0.07) \times 10^{-2}\,, && \delta_q = (66.9 \pm 2.0)^\circ\,. \end{aligned} \quad \text{(C.2)}$$

For the PMNS matrix, we use

$$\sin^2\theta^\ell_{12} = 0.32^{+0.020}_{-0.016}\,, \quad \sin^2\theta^\ell_{13} = (2.16^{+0.063}_{-0.066}) \times 10^{-2}\,, \quad \sin^2\theta^\ell_{23} = 0.547^{+0.020}_{-0.030}\,. \quad \text{(C.3)}$$

Although results corresponding to normal ordering and inverted ordering of neutrino masses differ slightly, and results quoted by several groups differ too [20, 198, 199], these differences are unsubstantial for the scope of this work.

To illustrate how one fits the CKM and PMNS matrices, in the models under consideration, to the experimental information condensed in eqs. (C.2) and (C.3), let us consider the CKM case. In terms of the parameters of the particular model

under consideration, a CKM matrix V is computed. Then, one computes (for simplicity, we use here $1,2,3$ indices rather than u,c,t,d,s,b)

$$s_{13}^2 = |V_{13}|^2\,, \qquad s_{12}^2 = \frac{|V_{12}|^2}{1-|V_{13}|^2}, \qquad s_{23}^2 = \frac{|V_{23}|^2}{1-|V_{13}|^2}, \tag{C.4}$$

and

$$\delta = \arg\left(\frac{V_{12}V_{13}^*V_{23}V_{22}^*}{|V_{12}V_{13}V_{23}|\,(1-|V_{13}|^2)} + |V_{12}V_{13}V_{23}|\right). \tag{C.5}$$

These are the values, obtained in a rephasing invariant manner, to be compared with eq. (C.2) (in the actual fit, this comparison gives the usual likelihood function of the model parameters, which is maximized). For the PMNS matrix, we follow the same procedure with the values in eq. (C.3), and include no constraint on the phase δ_ℓ, as discussed in section 5.5.

It is to be mentioned that while the PDG parametrization of CKM and PMNS is such that one can reduce the ranges of θ_{ij} to $[0;\pi/2]$ (while $\delta \in [0;2\pi[$ through rephasings, in our case the ranges of the parameters p_1^f, p_2^f in the different orthogonal matrices O_{f_L} entering CKM and PMNS, require some care since they cannot be completely reduced to those ranges (the form of V and U in eqs. (5.13), (5.23)-(5.26), is different from eq. (C.1)).

D
jBGL

D.1 Details on model identification

D.1.1 Rows and columns

Recall the arguments in sections 6.2.2 and 6.3.2. Consider the *Left condition*

$$\mathrm{N}_q^0 = (\ell_1 \mathrm{P}_1 + \ell_2 \mathrm{P}_2 + \ell_3 \mathrm{P}_3)\, \mathrm{M}_q^0 = \begin{pmatrix} \ell_1 & 0 & 0 \\ 0 & \ell_2 & 0 \\ 0 & 0 & \ell_3 \end{pmatrix} \mathrm{M}_q^0, \tag{D.1}$$

and eq. (2.29) for M_q^0 and N_q^0 ($q = d, u$) expressed in terms of the Yukawa matrices $Y_{d,1}, Y_{d,2}$ and $Y_{u,1}, Y_{u,2}$, respectively for $q = d$ and $q = u$. If there were non-zero elements $(Y_{d,1})_{ia} \neq 0$ and $(Y_{d,2})_{ib} \neq 0$ (or $(Y_{u,1})_{ia} \neq 0$ and $(Y_{u,2})_{ib} \neq 0$) in the same row i of both Yukawa matrices, it would follow that

$$\left(\mathrm{N}_q^0\right)_{ia} = \ell_i \left(\mathrm{M}_q^0\right)_{ia} \Rightarrow \ell_i = t_\beta \quad \text{and} \quad \left(\mathrm{N}_q^0\right)_{ib} = \ell_i \left(\mathrm{M}_q^0\right)_{ib} \Rightarrow \ell_i = -t_\beta^{-1}\,, \tag{D.2}$$

which is not possible. That is, the rows of the M_d^0 and N_d^0 matrices (M_u^0 and N_u^0 matrices) come either from $Y_{d,1}$ or from $Y_{d,2}$ (from $Y_{u,1}$ or from $Y_{u,2}$), never from both. In other words, each doublet Q_{Li}^0 couples to one and only one doublet Φ_j.
For the *Right condition*

$$\mathrm{N}_q^0 = \mathrm{M}_q^0 \left(r_1 \mathrm{P}_1 + r_2 \mathrm{P}_2 + r_3 \mathrm{P}_3\right) = \mathrm{M}_q^0 \begin{pmatrix} r_1 & 0 & 0 \\ 0 & r_2 & 0 \\ 0 & 0 & r_3 \end{pmatrix}, \tag{D.3}$$

it follows similarly that each singlet d^0_{Ri}, u^0_{Rj}, couples to one and only one doublet Φ_k. However, contrary to *Left conditions*, this holds separately for the up and down sectors. Notice, finally, that the only values that the parameters ℓ_j and r_j can take, following eq. (D.2) are either t_β or $-t_\beta^{-1}$.

D.1.2 Models

The models discussed in sections 6.2 and 6.3 are representative examples within each class. In the following we briefly comment on some other details on these classes of models.

Starting with the BGL models of subsection 6.2.3, it is to be noticed that in eq. (6.19) one singles out both the third generation and the down quarks. This leads to a model, the "bottom" BGL model, where tree level FCNC are absent in the down sector and are controlled by products of CKM elements $V_{ib}V^*_{jb}$ in the up sector. By choosing for example the second generation, the "strange" BGL model, one obtains again tree level FCNC in the up sector but controlled by $V_{is}V^*_{js}$ instead. Furthermore, if instead of the down sector one chooses the up sector, that is

$$\Phi_2 \mapsto e^{i\theta}\Phi_2, \quad Q^0_{L3} \mapsto e^{i\theta}Q^0_{L3}, \quad u^0_{R3} \mapsto e^{i2\theta}u^0_{R3}, \quad \theta \neq 0, \pi\,, \tag{D.4}$$

instead of eq. (6.19), one obtains the "top" BGL model, with no tree level FCNC in the up sector and FCNC controlled by $V_{ti}V^*_{tj}$ in the down sector. Overall, considering the quark sector alone, there are 6 BGL models, one per quark type.

For all the remaining models, shaped by either *Left* or *Right* conditions, the situation is different. Consider for example the generalised BGL model given by eq. (6.26). The transformation singles out the third generation with $Q^0_{L3} \mapsto -Q^0_{L3}$. The only trace of that election in eq. (6.32) is the fact that the unitary vector $\hat{n}_{[\mathrm{q}]}$ is given by the third row of the unitary matrix $\mathcal{U}_{q_L}$. However, if we start with $Q^0_{L2} \mapsto -Q^0_{L2}$ instead, the form of N_d and N_u remains exactly the same, but with a different interpretation of $\hat{n}_{[\mathrm{q}]}$ (the second row of $\mathcal{U}_{q_L}$ in that case). With $\hat{n}_{[\mathrm{q}]}$ free to vary – either $q = d$ or $q = u$, the other fixed via CKM, eq. (6.33) –, it is clear that the generic parametrization in terms of $\hat{n}_{[\mathrm{q}]}$ covers simultaneously all

three initial possibilities $Q^0_{Lj} \mapsto -Q^0_{Lj}$, $j = 1, 2, 3$. This consideration concerning the generalised BGL model is applicable to the remaining cases: the parametrisation of the N_d and N_u matrices involving unitary vectors $\hat{n}_{[\mathrm{q}]}$ or $\hat{r}_{[\mathrm{q}]}$ encompasses all initial symmetry assignments. It is to be noticed of course, that despite this fact, the models discussed in different classes are distinct: for example the jBGL model in eq. (6.37) *cannot* be obtained from the gBGL model in eq. (6.32) with some election of $\hat{n}_{[\mathrm{q}]}$; they have a different dependence on t_β. The same kind of distinction applies to eq. (6.49) versus eq. (6.53) and to eq. (6.72) versus eq. (6.76).

D.1.3 Identifying Φ_1 and model discrimination

In the most general 2HDM there is nothing to disentangle Φ_1 from Φ_2. Indeed, one can mix them through a unitary transformation without any physical consequence. The situation changes once one introduces a symmetry through some specific form. We start by noticing that the form of the Abelian symmetry chosen in eq. (6.1) already singles out Φ_1; it is the field which remains invariant under the symmetry. Given any generic Abelian symmetry, this choice can always be made by an appropriate basis transformation in the space of scalar doublets. Before that choice is made, the sub-indices $k = 1, 2$ in Φ_k (and, thus, in $Y_{d,k}$, $Y_{u,k}$, and the vevs v_k) are just unphysical labels. One should notice that models are not yet unequivocally defined, even after the basis choice is made such that the Abelian symmetry is expressed as $\Phi_1 \mapsto \Phi_1$. This is most easily seen in the simple context of the $\mathbb{Z}_2$ Natural Flavor Conservation models of Glashow-Weinberg [112]. In that context, after a scalar basis choice is made such that the scalars transform as $\Phi_1 \mapsto \Phi_1$ and $\Phi_2 \mapsto -\Phi_2$, one can still choose for the right handed quarks the transformations (the same for all quarks of a given charge)

$$d_R \mapsto d_R\,, \qquad u_R \mapsto u_R\,, \tag{D.5}$$

$$d_R \mapsto -d_R\,, \qquad u_R \mapsto -u_R\,, \tag{D.6}$$

$$d_R \mapsto d_R\,, \qquad u_R \mapsto -u_R\,, \tag{D.7}$$

$$d_R \mapsto -d_R\,, \qquad u_R \mapsto u_R\,. \tag{D.8}$$

In the first two equations, the up and down quarks couple to the same field (be it Φ_1 or Φ_2; it does not matter). This is known as Type I. In the last two equations, the up and down quarks couple to the different fields; which is known as Type II. Denoting a field by Φ_1 or Φ_2 has no physical meaning. The most direct counting can be obtained by choosing (say) Φ_2 as the field which couples to the up quarks. This is what attributes physical meaning to the labels 1 and 2. With this choice, the sub-indices of the Yukawa matrices ($Y_{d,k}$ and $Y_{u,k}$) acquire physical meaning. The same happens with the vevs v_k [322]. Subsequent changes in the basis for fermions will alter the form of the Yukawa matrices, but not their rank.

A similar analysis can be made for the models discussed in chapter 6, except that here the right handed up quarks do not couple all to the same doublet. However, as can be seen from the form of the matrices shown, $\text{rank}\,(Y_{d,1}) + \text{rank}\,(Y_{d,2}) = 3$ and $\text{rank}\,(Y_{u,1}) + \text{rank}\,(Y_{u,2}) = 3$. As a result, one can define physically the label in Φ_1 as the scalar which couples to most of the up quarks. All subsequent choices are physically meaningful. Alternatively, one can define Φ_1 as the field which obeys $\Phi_1 \to \Phi_1$ under the Abelian symmetry, at the price of an apparent but illusory doubling of the number of model types. This is shown explicitly for the *Right* models in Table D.1 [1].

rank $Y_{d,k}$ \ rank $Y_{u,k}$	3,0	0,3	2,1	1,2
3,0	Type I	Type II	Type A	Type B
0,3	Type II	Type I	Type B	Type A
2,1	Type C	Type D	Type E	Type F
1,2	Type D	Type C	Type F	Type E

Table D.1: Identification of the *Right* models (and the usual Type I and Type II), in terms of the ranks of the Yukawa matrices, in the order $Y_{u,1}, Y_{u,2}$ (in columns), and $Y_{d,1}, Y_{d,2}$ (in rows).

In this analysis, we have used the fact that, if for example $Y_{u,1}$ has two columns and $Y_{u,2}$ the third, it is immaterial their placement and, moreover, their placement

[1] Due to eq. (D.2), the change $1 \leftrightarrow 2$ implies a change $t_\beta \leftrightarrow -t_\beta^{-1}$ in the parametrization of the N_q matrices. Thus, models which could seem to differ by such a change, do in fact correspond to the same model.

with respect to the placement of the columns which appear in $Y_{d,1}$ and $Y_{d,2}$. To be specific, let us consider the Type A matrices of eq. (6.44), where we have chosen $Y_{u,1}$ to have the first two columns and $Y_{u,2}$ the last, while $Y_{d,1}$ has all columns. We could have chosen $Y_{u,1}$ to have the first and last column, with $Y_{u,2}$ having the second column. The different permutations refer only to the labels in the space of right handed up quarks (which is completely detached from the space of right handed down quarks). Such choices are indistinguishable.

The situation is easier for *Left* models, because left up quark and left down quark fields belong to the same doublet, leading to the restriction in eq. (6.33). Hence, as seen in section 6.2, the possible ranks of $(Y_{d,1}, Y_{d,2})$ are only $(1,2)$ and $(2,1)$. Thus, instead of Table D.1 one obtains the much simpler Table D.2. We are now ready to

rank $Y_{d,k}$ \ rank $Y_{u,k}$	2,1	1,2
2,1	gBGL	jBGL
1,2	jBGL	gBGL

Table D.2: Identification of the *Left* models in terms of the ranks of the Yukawa matrices, in the order $Y_{u,1}, Y_{u,2}$ (in columns), and $Y_{d,1}, Y_{d,2}$ (in rows).

develop basis invariant conditions for the determination of the various models.

D.1.4 Invariant conditions

Here, we present conditions for the identification of the various types of models discussed in this article, which are invariant under basis transformations in the spaces of left-handed doublets and of up-type and down-type right-handed singlets. For BGL and generalised BGL models, the following matrix conditions hold [1]:

$$\begin{aligned}
\text{BGL models:}\quad & Y_{d,1}^\dagger Y_{d,2} = 0, \quad Y_{u,1}^\dagger Y_{u,2} = 0, \quad Y_{d,1}^\dagger Y_{u,2} = 0, \quad Y_{d,2}^\dagger Y_{u,1} = 0, \\
& \text{and} \quad Y_{d,1} Y_{d,2}^\dagger = 0 \ \text{(dBGL)} \quad \text{or} \quad Y_{u,1} Y_{u,2}^\dagger = 0 \ \text{(uBGL)}, \\
\text{gBGL models:}\quad & Y_{d,1}^\dagger Y_{d,2} = 0, \quad Y_{u,1}^\dagger Y_{u,2} = 0, \quad Y_{d,1}^\dagger Y_{u,2} = 0, \quad Y_{d,2}^\dagger Y_{u,1} = 0. \qquad \text{(D.9)}
\end{aligned}$$

Their importance resides in the fact that, under a weak basis transformation (WBT) of the fermion fields

$$Q_L \mapsto W_{\rm L}\, Q_L, \quad d_R \mapsto W_{\rm d_R}\, d_R, \quad u_R \mapsto W_{\rm u_R}\, u_R, \quad W_{\rm L}, W_{\rm d_R}, W_{\rm u_R} \in U(3), \tag{D.10}$$

the Yukawa coupling matrices are transformed as

$$Y_{d,i} \mapsto W_{\rm L}^\dagger\, Y_{d,i}\, W_{\rm d_R}, \quad Y_{u,i} \mapsto W_{\rm L}^\dagger\, Y_{u,i}\, W_{\rm u_R}\,, \tag{D.11}$$

and, although the WBT in eqs. (D.10)–(D.11) may hide the symmetry under the Abelian transformations in eq. (6.1), the conditions in eqs. (D.9) are in any case invariant. In general, the different combinations of $Y_{d,i}$, $Y_{u,j}$, which are invariant under some of the WBT are the following.

- Invariant under $W_{\rm L}$ WBT,

$$\begin{aligned} Y_{d,i}^\dagger Y_{d,j} &\mapsto W_{\rm d_R}^\dagger\, Y_{d,i}^\dagger Y_{d,j}\, W_{\rm d_R}, \\ Y_{u,i}^\dagger Y_{u,j} &\mapsto W_{\rm u_R}^\dagger\, Y_{u,i}^\dagger Y_{u,j}\, W_{\rm u_R}, \\ Y_{d,i}^\dagger Y_{u,j} &\mapsto W_{\rm d_R}^\dagger\, Y_{d,i}^\dagger Y_{u,j}\, W_{\rm u_R}, \end{aligned} \tag{D.12}$$

  (and, of course, $Y_{u,i}^\dagger Y_{d,j} = (Y_{d,j}^\dagger Y_{u,i})^\dagger$).

- Invariant under $W_{\rm d_R}$ and $W_{\rm u_R}$ WBT,

$$\begin{aligned} Y_{d,i} Y_{d,j}^\dagger &\mapsto W_{\rm L}^\dagger\, Y_{d,i} Y_{d,j}^\dagger\, W_{\rm L}, \\ Y_{u,i} Y_{u,j}^\dagger &\mapsto W_{\rm L}^\dagger\, Y_{u,i} Y_{u,j}^\dagger\, W_{\rm L}. \end{aligned} \tag{D.13}$$

Considering in addition the *Left* and *Right conditions* of eqs. (6.2) and (6.5), respectively, we can straightforwardly obtain invariant conditions. This is what we turn to next.

Left conditions

In terms of the Yukawa matrices, the *Left conditions* are

$$Y_{d,1} = e^{-i\xi_1}\frac{\sqrt{2}}{v}s_\beta(t_\beta^{-1}\mathbf{1} + \mathrm{L}_\mathrm{d}^0)\mathrm{M}_d^0, \qquad Y_{d,2} = -e^{-i\xi_2}\frac{\sqrt{2}}{v}c_\beta(-t_\beta\mathbf{1} + \mathrm{L}_\mathrm{d}^0)\mathrm{M}_d^0, \tag{D.14}$$

$$Y_{u,1} = e^{i\xi_1}\frac{\sqrt{2}}{v}s_\beta(t_\beta^{-1}\mathbf{1} + \mathrm{L}_\mathrm{u}^0)\mathrm{M}_u^0, \qquad Y_{u,2} = -e^{i\xi_2}\frac{\sqrt{2}}{v}c_\beta(-t_\beta\mathbf{1} + \mathrm{L}_\mathrm{u}^0)\mathrm{M}_u^0, \tag{D.15}$$

where we have used equations (2.29) Then,

$$Y_{d,1}^\dagger Y_{d,2} = -s_\beta c_\beta e^{i\xi}\frac{2}{v^2}\mathrm{M}_d^{0\dagger}(t_\beta^{-1}\mathbf{1} + \mathrm{L}_\mathrm{d}^0)(-t_\beta\mathbf{1} + \mathrm{L}_\mathrm{d}^0)\mathrm{M}_d^0\,, \tag{D.16}$$

where

$$(t_\beta^{-1}\mathbf{1} + \mathrm{L}_\mathrm{d}^0)(-t_\beta\mathbf{1} + \mathrm{L}_\mathrm{d}^0) = \sum_{j=1}^3(\ell_j^{[d]} + t_\beta^{-1})(\ell_j^{[d]} - t_\beta)P_j = 0 \tag{D.17}$$

since $\ell_j^{[d]}$ is equal either to $-t_\beta^{-1}$ or to t_β, thus giving $Y_{d,1}^\dagger Y_{d,2} = 0$. For the up Yukawa matrices, the conclusion is identical, and thus the conditions in eqs. (D.12) involving separately the up and down quark sectors are trivially

$$Y_{d,1}^\dagger Y_{d,2} = 0, \quad Y_{u,1}^\dagger Y_{u,2} = 0\,. \tag{D.18}$$

For the conditions involving Yukawa matrices from both sectors, proceeding along similar lines, one finds

$$\begin{aligned}
e^{-i2\xi_1}\frac{v^2}{2}Y_{d,1}^\dagger Y_{u,1} &= s_\beta^2\,\mathrm{M}_d^{0\dagger}\left[\sum_{j=1}^3(\ell_j^{[d]} + t_\beta^{-1})(\ell_j^{[u]} + t_\beta^{-1})P_R j\right]\mathrm{M}_u^0,\\
-e^{-i(\xi_1+\xi_2)}\frac{v^2}{2}Y_{d,1}^\dagger Y_{u,2} &= s_\beta c_\beta\,\mathrm{M}_d^{0\dagger}\left[\sum_{j=1}^3(\ell_j^{[d]} + t_\beta^{-1})(\ell_j^{[u]} - t_\beta)P_R j\right]\mathrm{M}_u^0,\\
-e^{-i(\xi_1+\xi_2)}\frac{v^2}{2}Y_{d,2}^\dagger Y_{u,1} &= s_\beta c_\beta\,\mathrm{M}_d^{0\dagger}\left[\sum_{j=1}^3(\ell_j^{[d]} - t_\beta)(\ell_j^{[u]} + t_\beta^{-1})P_R j\right]\mathrm{M}_u^0,\\
e^{-i2\xi_2}\frac{v^2}{2}Y_{d,2}^\dagger Y_{u,2} &= c_\beta^2\,\mathrm{M}_d^{0\dagger}\left[\sum_{j=1}^3(\ell_j^{[d]} - t_\beta)(\ell_j^{[u]} - t_\beta)P_R j\right]\mathrm{M}_u^0,
\end{aligned} \tag{D.19}$$

and one can readily obtain the additional conditions

$$\begin{aligned}
&\text{BGL and gBGL models:} \quad Y_{d,1}^\dagger Y_{u,2} = 0, \quad Y_{d,2}^\dagger Y_{u,1} = 0,\\
&\text{jBGL models:} \qquad\qquad\quad Y_{d,1}^\dagger Y_{u,1} = 0, \quad Y_{d,2}^\dagger Y_{u,2} = 0.
\end{aligned} \tag{D.20}$$

The remaining matrix products, including $Y_{d,1}Y_{d,2}^\dagger$, $Y_{u,1}Y_{u,2}^\dagger$, are different from 0 and do not give invariant conditions like eqs. (D.18) and (D.20).

Right conditions

For models with *Right conditions*, the analog of eq. (D.18) is simply

$$Y_{d,1}Y_{d,2}^{\dagger} = 0, \quad Y_{u,1}Y_{u,2}^{\dagger} = 0\,. \tag{D.21}$$

One could naively think that conditions such as $Y_{d,2}Y_{u,1}^{\dagger}$ could be used to distinguish among different models. But, such conditions cannot be used, for they are not covariant under WBT. Fortunately, the different *Right* models can be distinguished in a basis invariant way by the rank of the $Y_{d,1}$ and $Y_{u,1}$ matrices.

Summary

We summarize in Table D.3 the invariant conditions associated with all models discussed in this article.

Model	Invariant Conditions
dBGL	$Y_{d,1}^{\dagger}Y_{d,2} = 0,\ Y_{u,1}^{\dagger}Y_{u,2} = 0,\ Y_{d,1}^{\dagger}Y_{u,2} = 0,\ Y_{d,2}^{\dagger}Y_{u,1} = 0,\ Y_{d,1}Y_{d,2}^{\dagger} = 0$
uBGL	$Y_{d,1}^{\dagger}Y_{d,2} = 0,\ Y_{u,1}^{\dagger}Y_{u,2} = 0,\ Y_{d,1}^{\dagger}Y_{u,2} = 0,\ Y_{d,2}^{\dagger}Y_{u,1} = 0,\ Y_{u,1}Y_{u,2}^{\dagger} = 0$
gBGL	$Y_{d,1}^{\dagger}Y_{d,2} = 0,\ Y_{u,1}^{\dagger}Y_{u,2} = 0,\ Y_{d,1}^{\dagger}Y_{u,2} = 0,\ Y_{d,2}^{\dagger}Y_{u,1} = 0$
jBGL	$Y_{d,1}^{\dagger}Y_{d,2} = 0,\ Y_{u,1}^{\dagger}Y_{u,2} = 0,\ Y_{d,1}^{\dagger}Y_{u,1} = 0,\ Y_{d,2}^{\dagger}Y_{u,2} = 0$
Type A	$Y_{d,1}Y_{d,2}^{\dagger} = 0,\ Y_{u,1}Y_{u,2}^{\dagger} = 0,\ \mathrm{rank}(Y_{d,1}) = 3,\ \mathrm{rank}(Y_{u,1}) = 2$
Type B	$Y_{d,1}Y_{d,2}^{\dagger} = 0,\ Y_{u,1}Y_{u,2}^{\dagger} = 0,\ \mathrm{rank}(Y_{d,1}) = 3,\ \mathrm{rank}(Y_{u,1}) = 1$
Type C	$Y_{d,1}Y_{d,2}^{\dagger} = 0,\ Y_{u,1}Y_{u,2}^{\dagger} = 0,\ \mathrm{rank}(Y_{d,1}) = 2,\ \mathrm{rank}(Y_{u,1}) = 3$
Type D	$Y_{d,1}Y_{d,2}^{\dagger} = 0,\ Y_{u,1}Y_{u,2}^{\dagger} = 0,\ \mathrm{rank}(Y_{d,1}) = 2,\ \mathrm{rank}(Y_{u,1}) = 0$
Type E	$Y_{d,1}Y_{d,2}^{\dagger} = 0,\ Y_{u,1}Y_{u,2}^{\dagger} = 0,\ \mathrm{rank}(Y_{d,1}) = 2,\ \mathrm{rank}(Y_{u,1}) = 2$
Type F	$Y_{d,1}Y_{d,2}^{\dagger} = 0,\ Y_{u,1}Y_{u,2}^{\dagger} = 0,\ \mathrm{rank}(Y_{d,1}) = 2,\ \mathrm{rank}(Y_{u,1}) = 1$

Table D.3: Summary of invariant conditions.

E

Contributions to $(g-2)_\ell$

E.1 One loop contributions

Yukawa interactions (of neutral scalars S) of the form

$$\mathscr{L}_{S\ell\ell} = -\frac{m_\ell}{v} S\bar{\ell}(a_\ell^S + ib_\ell^S\gamma_5)\ell\,, \tag{E.1}$$

give one loop contributions to the anomalous magnetic moment of lepton ℓ of the form

$$\Delta a_\ell^{(1)} = \frac{1}{8\pi^2}\frac{m_\ell^2}{v^2}\sum_S \left\{[a_\ell^S]^2\left(2I_2(x_{\ell S}) - I_3(x)\right) - [b_\ell^S]^2 I_3(x_{\ell S})\right\}, \tag{E.2}$$

with $x_{\ell S} \equiv m_\ell^2/m_S^2$ and

$$I_2(x) = 1 + \frac{1-2x}{2x\sqrt{1-4x}}\ln\left(\frac{1+\sqrt{1-4x}}{1-\sqrt{1-4x}}\right) + \frac{1}{2x}\ln x, \tag{E.3}$$

$$I_3(x) = \frac{1}{2} + \frac{1}{x} + \frac{1-3x}{2x^2\sqrt{1-4x}}\ln\left(\frac{1+\sqrt{1-4x}}{1-\sqrt{1-4x}}\right) + \frac{1-x}{2x^2}\ln x. \tag{E.4}$$

For $x \ll 1$,

$$I_2(x) \simeq x\left(-\frac{3}{2} - \ln x\right) + x^2\left(-\frac{16}{3} - 4\ln x\right) + \mathcal{O}(x^3), \tag{E.5}$$

$$I_3(x) \simeq x\left(-\frac{11}{6} - \ln x\right) + x^2\left(-\frac{89}{12} - 5\ln x\right) + \mathcal{O}(x^3), \tag{E.6}$$

and thus, for $m_\ell \ll m_S$,

$$\Delta a_\ell^{(1)} = \frac{1}{8\pi^2}\frac{m_\ell^2}{m_S^2}\frac{m_\ell^2}{v^2}\left\{-[a_\ell^S]^2\left(\frac{7}{6} + \ln\left(\frac{m_\ell^2}{m_S^2}\right)\right) + [b_\ell^S]^2\left(\frac{11}{6} + \ln\left(\frac{m_\ell^2}{m_S^2}\right)\right)\right\}. \tag{E.7}$$

Yukawa interactions (of charged scalars $C^{\pm}$) of the form

$$\mathscr{L}_{C\ell\nu} = -C^{-}\bar{\ell}(a_\ell^C + ib_\ell^C\gamma_5)\nu - C^{+}\bar{\nu}(a_\ell^{C*} + ib_\ell^{C*}\gamma_5)\ell\,, \tag{E.8}$$

give one loop contributions to the anomalous magnetic moment of lepton ℓ of the form

$$\Delta a_\ell^{(1)} = -\frac{1}{8\pi^2}\sum_C \left\{\left|a_\ell^C\right|^2 + \left|b_\ell^C\right|^2\right\} H(x_{\ell C})\,, \tag{E.9}$$

where $x_{\ell C} = m_\ell^2/m_{C^{\pm}}^2$, and

$$H(x) = -\frac{1}{2} + \frac{1}{x} + \frac{1-x}{x^2}\ln(1-x)\,, \quad H(x) \simeq \frac{x}{6} + \frac{x^2}{12} + \mathcal{O}(x^3) \text{ for } x \ll 1. \tag{E.10}$$

E.2 Two loop contributions

In addition to eq. (E.1), Yukawa interactions of the form

$$\mathscr{L}_{S\bar{f}f} = -\frac{m_f}{v}S\bar{f}(\alpha_f^S + i\beta_f^S\gamma_5)f\,, \tag{E.11}$$

give the following type of two loop Barr-Zee contributions to the anomalous magnetic moment of lepton ℓ:

$$\Delta a_\ell^{(2)} = -\frac{\alpha^2}{4\pi^2 s_W^2}\frac{m_\ell^2}{M_W^2}\sum_f\sum_S N_c^f Q_f^2\left\{a_\ell^S\alpha_f^S f(z_{fS}) - b_\ell^S\beta_f^S g(z_{fS})\right\}\,. \tag{E.12}$$

The sum over fermions f corresponds to the different fermions appearing in the closed fermion loop (with N_c^f the number of colors of f and Q_f its electric charge and $z_{fS} = m_f^2/m_S^2$), while the sum over scalars S corresponds to the different neutral scalars connecting the closed fermion loop with the external lepton line, as Figure E.1 illustrates. The functions $f(z)$ and $g(z)$ (see the discussion in section 9.1) read:

$$f(z) = \frac{z}{2}\int_0^1 dx\,\frac{1-2x(1-x)}{x(1-x)-z}\,\ln\left(\frac{x(1-x)}{z}\right)\,, \tag{E.13}$$

$$g(z) = \frac{z}{2}\int_0^1 dx\,\frac{1}{x(1-x)-z}\,\ln\left(\frac{x(1-x)}{z}\right)\,. \tag{E.14}$$

For other 2 loop contributions see [296].

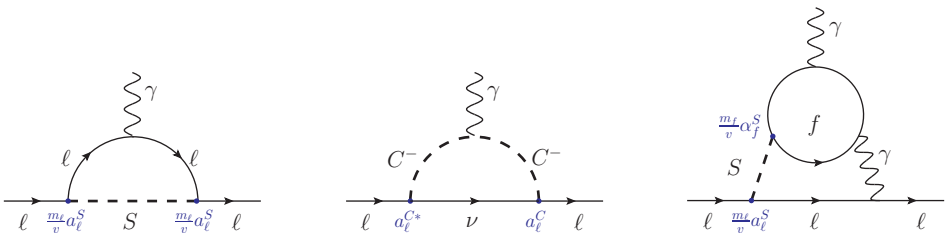

Figure E.1: Illustrative 1 and 2 loop contributions to δa_ℓ.

References

[1] J. M. Alves, F. J. Botella, G. C. Branco, F. Cornet-Gomez, and M. Nebot. "Controlled Flavour Changing Neutral Couplings in Two Higgs Doublet Models". In: *Eur. Phys. J. C* 77.9 (2017), p. 585. arXiv: 1703.03796 [hep-ph].

[2] F. J. Botella, F. Cornet-Gomez, and M. Nebot. "Flavor conservation in two-Higgs-doublet models". In: *Phys. Rev. D* 98.3 (2018), p. 035046. arXiv: 1803.08521 [hep-ph].

[3] J. M. Alves, F. J. Botella, G. C. Branco, F. Cornet-Gomez, M. Nebot, and J. P. Silva. "Symmetry Constrained Two Higgs Doublet Models". In: *Eur. Phys. J. C* 78.8 (2018), p. 630. arXiv: 1803.11199 [hep-ph].

[4] F. J. Botella, F. Cornet-Gomez, and M. Nebot. "Electron and muon $g-2$ anomalies in general flavour conserving two Higgs doublets models". In: *Phys. Rev. D* 102.3 (2020), p. 035023. arXiv: 2006.01934 [hep-ph].

[5] J. M. Alves, F. J. Botella, G. C. Branco, F. Cornet-Gomez, and M. Nebot. "The framework for a common origin of δ_{CKM} and δ_{PMNS}". In: *Eur. Phys. J. C* 81.8 (2021), p. 727. arXiv: 2105.14054 [hep-ph].

[6] F. J. Botella Olcina, F. Cornet-Gomez, and M. Nebot. "(g-2)l in the General Flavour Conserving 2HDM". In: *PoS* CORFU2019 (2020), p. 038.

[7] S. L. Glashow. "Partial Symmetries of Weak Interactions". In: *Nucl. Phys.* 22 (1961), pp. 579–588.

[8] S. Weinberg. "A Model of Leptons". In: *Phys. Rev. Lett.* 19 (1967), pp. 1264–1266.

[9] A. Salam. "Weak and Electromagnetic Interactions". In: *Conf. Proc. C* 680519 (1968), pp. 367–377.

[10] S. L. Glashow, J. Iliopoulos, and L. Maiani. "Weak Interactions with Lepton-Hadron Symmetry". In: *Phys. Rev. D* 2 (1970), pp. 1285–1292.

[11] A. Pich. "The Standard Model of Electroweak Interactions". In: *2010 European School of High Energy Physics*. Jan. 2012. arXiv: 1201.0537 [hep-ph].

[12] M. Herrero. "The Standard model". In: *NATO Sci. Ser. C* 534 (1999). Ed. by T. Ferbel, pp. 1–59. arXiv: hep-ph/9812242.

[13] P. Langacker. *The standard model and beyond; 1st ed.* Series in high energy physics, cosmology, and gravitation. Boca Raton, FL: Taylor and Francis, 2010. URL: https://cds.cern.ch/record/1226768.

[14] Such, MissMJ. *Standard Model of Elementary Particles*. [Online; accessed 20-April-2021]. 2020. URL: https://en.wikipedia.org/wiki/File:Standard_Model_of_Elementary_Particles.svg.

[15] D. J. Gross and F. Wilczek. "Ultraviolet Behavior of Nonabelian Gauge Theories". In: *Phys. Rev. Lett.* 30 (1973). Ed. by J. C. Taylor, pp. 1343–1346.

[16] S. Weinberg. “Nonabelian Gauge Theories of the Strong Interactions”. In: *Phys. Rev. Lett.* 31 (1973), pp. 494–497.

[17] H. Fritzsch, M. Gell-Mann, and H. Leutwyler. “Advantages of the Color Octet Gluon Picture”. In: *Phys. Lett. B* 47 (1973), pp. 365–368.

[18] H. D. Politzer. “Reliable Perturbative Results for Strong Interactions?” In: *Phys. Rev. Lett.* 30 (1973). Ed. by J. C. Taylor, pp. 1346–1349.

[19] J. Ellis. “TikZ-Feynman: Feynman diagrams with TikZ”. In: *Comput. Phys. Commun.* 210 (2017), pp. 103–123. arXiv: 1601.05437 [hep-ph].

[20] P. A. Zyla et al. “Review of Particle Physics”. In: *PTEP* 2020.8 (2020), p. 083C01.

[21] G. S. Guralnik, C. R. Hagen, and T. W. B. Kibble. “Global Conservation Laws and Massless Particles”. In: *Phys. Rev. Lett.* 13 (1964). Ed. by J. C. Taylor, pp. 585–587.

[22] P. W. Higgs. “Broken Symmetries and the Masses of Gauge Bosons”. In: *Phys. Rev. Lett.* 13 (1964). Ed. by J. C. Taylor, pp. 508–509.

[23] F. Englert and R. Brout. “Broken Symmetry and the Mass of Gauge Vector Mesons”. In: *Phys. Rev. Lett.* 13 (1964). Ed. by J. C. Taylor, pp. 321–323.

[24] T. W. B. Kibble. “Symmetry breaking in nonAbelian gauge theories”. In: *Phys. Rev.* 155 (1967). Ed. by J. C. Taylor, pp. 1554–1561.

[25] J. Goldstone, A. Salam, and S. Weinberg. “Broken Symmetries”. In: *Phys. Rev.* 127 (1962), pp. 965–970.

[26] J. Goldstone. “Field Theories with Superconductor Solutions”. In: *Nuovo Cim.* 19 (1961), pp. 154–164.

[27] G. Aad et al. “Observation of a new particle in the search for the Standard Model Higgs boson with the ATLAS detector at the LHC”. In: *Phys. Lett. B* 716 (2012), pp. 1–29. arXiv: 1207.7214 [hep-ex].

[28] S. Chatrchyan et al. “Observation of a New Boson at a Mass of 125 GeV with the CMS Experiment at the LHC”. In: *Phys. Lett. B* 716 (2012), pp. 30–61. arXiv: 1207.7235 [hep-ex].

[29] N. Cabibbo. “Unitary Symmetry and Leptonic Decays”. In: *Phys. Rev. Lett.* 10 (1963), pp. 531–533.

[30] M. Kobayashi and T. Maskawa. “CP Violation in the Renormalizable Theory of Weak Interaction”. In: *Prog. Theor. Phys.* 49 (1973), pp. 652–657.

[31] B. Pontecorvo. “Inverse beta processes and nonconservation of lepton charge”. In: *Zh. Eksp. Teor. Fiz.* 34 (1957), p. 247.

[32] Z. Maki, M. Nakagawa, and S. Sakata. “Remarks on the unified model of elementary particles”. In: *Prog. Theor. Phys.* 28 (1962), pp. 870–880.

[33] L. Wolfenstein. “Parametrization of the Kobayashi-Maskawa Matrix”. In: *Phys. Rev. Lett.* 51 (1983), p. 1945.

[34] J. Charles, A. Hocker, H. Lacker, S. Laplace, F. R. Le Diberder, J. Malcles, J. Ocariz, M. Pivk, and L. Roos. “CP violation and the CKM matrix: Assessing the impact of the asymmetric B factories”. In: *Eur. Phys. J. C* 41.1 (2005), pp. 1–131. arXiv: hep-ph/0406184.

[35] M. Bona et al. "The Unitarity Triangle Fit in the Standard Model and Hadronic Parameters from Lattice QCD: A Reappraisal after the Measurements of Delta m(s) and BR(B —> tau nu(tau))". In: *JHEP* 10 (2006), p. 081. arXiv: hep-ph/0606167.

[36] L. D. Faddeev and V. N. Popov. "Feynman Diagrams for the Yang-Mills Field". In: *Phys. Lett. B* 25 (1967). Ed. by J.-P. Hsu and D. Fine, pp. 29–30.

[37] J. N. Bahcall, A. M. Serenelli, and S. Basu. "New solar opacities, abundances, helioseismology, and neutrino fluxes". In: *Astrophys. J. Lett.* 621 (2005), pp. L85–L88. arXiv: astro-ph/0412440.

[38] B. Aharmim et al. "Combined Analysis of all Three Phases of Solar Neutrino Data from the Sudbury Neutrino Observatory". In: *Phys. Rev. C* 88 (2013), p. 025501. arXiv: 1109.0763 [nucl-ex].

[39] K. Abe et al. "Solar Neutrino Measurements in Super-Kamiokande-IV". In: *Phys. Rev. D* 94.5 (2016), p. 052010. arXiv: 1606.07538 [hep-ex].

[40] S. Abe et al. "Precision Measurement of Neutrino Oscillation Parameters with KamLAND". In: *Phys. Rev. Lett.* 100 (2008), p. 221803. arXiv: 0801.4589 [hep-ex].

[41] C. Arpesella et al. "Direct Measurement of the Be-7 Solar Neutrino Flux with 192 Days of Borexino Data". In: *Phys. Rev. Lett.* 101 (2008), p. 091302. arXiv: 0805.3843 [astro-ph].

[42] Y. Ashie et al. "A Measurement of atmospheric neutrino oscillation parameters by SUPER-KAMIOKANDE I". In: *Phys. Rev. D* 71 (2005), p. 112005. arXiv: hep-ex/0501064.

[43] M. H. Ahn et al. "Measurement of Neutrino Oscillation by the K2K Experiment". In: *Phys. Rev. D* 74 (2006), p. 072003. arXiv: hep-ex/0606032.

[44] P. Adamson et al. "Improved search for muon-neutrino to electron-neutrino oscillations in MINOS". In: *Phys. Rev. Lett.* 107 (2011), p. 181802. arXiv: 1108.0015 [hep-ex].

[45] R. H. Parker, C. Yu, W. Zhong, B. Estey, and H. Müller. "Measurement of the fine-structure constant as a test of the Standard Model". In: *Science* 360 (2018), p. 191. arXiv: 1812.04130 [physics.atom-ph].

[46] H. Davoudiasl and W. J. Marciano. "Tale of two anomalies". In: *Phys. Rev. D* 98.7 (2018), p. 075011. arXiv: 1806.10252 [hep-ph].

[47] T. Aoyama, M. Hayakawa, T. Kinoshita, and M. Nio. "Tenth-Order QED Contribution to the Electron g-2 and an Improved Value of the Fine Structure Constant". In: *Phys. Rev. Lett.* 109 (2012), p. 111807. arXiv: 1205.5368 [hep-ph].

[48] T. Aoyama, M. Hayakawa, T. Kinoshita, and M. Nio. "Complete Tenth-Order QED Contribution to the Muon g-2". In: *Phys. Rev. Lett.* 109 (2012), p. 111808. arXiv: 1205.5370 [hep-ph].

[49] S. Laporta. "High-precision calculation of the 4-loop contribution to the electron g-2 in QED". In: *Phys. Lett. B* 772 (2017), pp. 232–238. arXiv: 1704.06996 [hep-ph].

[50] T. Aoyama, T. Kinoshita, and M. Nio. "Revised and Improved Value of the QED Tenth-Order Electron Anomalous Magnetic Moment". In: *Phys. Rev. D* 97.3 (2018), p. 036001. arXiv: 1712.06060 [hep-ph].

[51] S. Volkov. "Calculating the five-loop QED contribution to the electron anomalous magnetic moment: Graphs without lepton loops". In: *Phys. Rev. D* 100.9 (2019), p. 096004. arXiv: 1909.08015 [hep-ph].

[52] H. Terazawa. "Convergence of Perturbative Expansion Series in QED and the Muon g-2: One of the Oldest Problems in Quantum Field Theory and of the Latest Problems in the Standard Model". In: *Nonlin. Phenom. Complex Syst.* 21.3 (2018), pp. 268–272.

[53] G. W. Bennett et al. "Final Report of the Muon E821 Anomalous Magnetic Moment Measurement at BNL". In: *Phys. Rev. D* 73 (2006), p. 072003. arXiv: hep-ex/0602035.

[54] F. Jegerlehner and A. Nyffeler. "The Muon g-2". In: *Phys. Rept.* 477 (2009), pp. 1–110. arXiv: 0902.3360 [hep-ph].

[55] M. Davier, A. Hoecker, B. Malaescu, and Z. Zhang. "Reevaluation of the Hadronic Contributions to the Muon g-2 and to alpha(MZ)". In: *Eur. Phys. J. C* 71 (2011). [Erratum: Eur.Phys.J.C 72, 1874 (2012)], p. 1515. arXiv: 1010.4180 [hep-ph].

[56] M. Davier, A. Hoecker, B. Malaescu, and Z. Zhang. "A new evaluation of the hadronic vacuum polarisation contributions to the muon anomalous magnetic moment and to $\boldsymbol{\alpha(m_Z^2)}$". In: *Eur. Phys. J. C* 80.3 (2020). [Erratum: Eur.Phys.J.C 80, 410 (2020)], p. 241. arXiv: 1908.00921 [hep-ph].

[57] T. Blum, P. A. Boyle, V. Gülpers, T. Izubuchi, L. Jin, C. Jung, A. Jüttner, C. Lehner, A. Portelli, and J. T. Tsang. "Calculation of the hadronic vacuum polarization contribution to the muon anomalous magnetic moment". In: *Phys. Rev. Lett.* 121.2 (2018), p. 022003. arXiv: 1801.07224 [hep-lat].

[58] T. Aoyama et al. "The anomalous magnetic moment of the muon in the Standard Model". In: *Phys. Rept.* 887 (2020), pp. 1–166. arXiv: 2006.04822 [hep-ph].

[59] P. Roig and P. Sanchez-Puertas. "Axial-vector exchange contribution to the hadronic light-by-light piece of the muon anomalous magnetic moment". In: *Phys. Rev. D* 101.7 (2020), p. 074019. arXiv: 1910.02881 [hep-ph].

[60] L. Morel, Z. Yao, P. Cladé, and S. Guellati-Khélifa. "Determination of the fine-structure constant with an accuracy of 81 parts per trillion". In: *Nature* 588.7836 (2020), pp. 61–65.

[61] B. Abi et al. "Measurement of the Positive Muon Anomalous Magnetic Moment to 0.46 ppm". In: *Phys. Rev. Lett.* 126.14 (2021), p. 141801. arXiv: 2104.03281 [hep-ex].

[62] A. D. Sakharov. "Violation of CP Invariance, C asymmetry, and baryon asymmetry of the universe". In: *Pisma Zh. Eksp. Teor. Fiz.* 5 (1967), pp. 32–35.

[63] J. Fuentes Martn. "New Physics adventures in the LHC age". PhD thesis. Valencia U., IFIC, 2017.

[64] C. A. Baker et al. "An Improved experimental limit on the electric dipole moment of the neutron". In: *Phys. Rev. Lett.* 97 (2006), p. 131801. arXiv: hep-ex/0602020.

[65] H. P. Nilles. "Supersymmetry, Supergravity and Particle Physics". In: *Phys. Rept.* 110 (1984), pp. 1–162.

[66] T. D. Lee. "A Theory of Spontaneous T Violation". In: *Phys. Rev. D* 8 (1973). Ed. by G. Feinberg, pp. 1226–1239.

[67] G. C. Branco. "Spontaneous CP Violation in Theories with More Than Four Quarks". In: *Phys. Rev. Lett.* 44 (1980), p. 504.

[68] G. C. Branco. "Spontaneous CP Nonconservation and Natural Flavor Conservation: A Minimal Model". In: *Phys. Rev. D* 22 (1980), p. 2901.

[69] N. Turok and J. Zadrozny. "Electroweak baryogenesis in the two doublet model". In: *Nucl. Phys. B* 358 (1991), pp. 471–493.

[70] G. W. Anderson and L. J. Hall. "The Electroweak phase transition and baryogenesis". In: *Phys. Rev. D* 45 (1992), pp. 2685–2698.

[71] J. M. Cline, K. Kainulainen, and A. P. Vischer. "Dynamics of two Higgs doublet CP violation and baryogenesis at the electroweak phase transition". In: *Phys. Rev. D* 54 (1996), pp. 2451–2472. arXiv: `hep-ph/9506284`.

[72] L. Lopez Honorez, E. Nezri, J. F. Oliver, and M. H. G. Tytgat. "The Inert Doublet Model: An Archetype for Dark Matter". In: *JCAP* 02 (2007), p. 028. arXiv: `hep-ph/0612275`.

[73] R. Barbieri, L. J. Hall, and V. S. Rychkov. "Improved naturalness with a heavy Higgs: An Alternative road to LHC physics". In: *Phys. Rev. D* 74 (2006), p. 015007. arXiv: `hep-ph/0603188`.

[74] R. D. Peccei and H. R. Quinn. "CP Conservation in the Presence of Instantons". In: *Phys. Rev. Lett.* 38 (1977), pp. 1440–1443.

[75] R. D. Peccei and H. R. Quinn. "Constraints Imposed by CP Conservation in the Presence of Instantons". In: *Phys. Rev. D* 16 (1977), pp. 1791–1797.

[76] G. C. Branco, P. M. Ferreira, L. Lavoura, M. N. Rebelo, M. Sher, and J. P. Silva. "Theory and phenomenology of two-Higgs-doublet models". In: *Phys. Rept.* 516 (2012), pp. 1–102. arXiv: `1106.0034 [hep-ph]`.

[77] I. P. Ivanov. "Building and testing models with extended Higgs sectors". In: *Prog. Part. Nucl. Phys.* 95 (2017), pp. 160–208. arXiv: `1702.03776 [hep-ph]`.

[78] S. Chatrchyan et al. "Observation of a New Boson at a Mass of 125 GeV with the CMS Experiment at the LHC". In: *Phys. Lett. B* 716 (2012), pp. 30–61. arXiv: `1207.7235 [hep-ex]`.

[79] H. E. Haber, G. L. Kane, and T. Sterling. "The Fermion Mass Scale and Possible Effects of Higgs Bosons on Experimental Observables". In: *Nucl. Phys. B* 161 (1979), pp. 493–532.

[80] J. F. Donoghue and L. F. Li. "Properties of Charged Higgs Bosons". In: *Phys. Rev. D* 19 (1979), p. 945.

[81] L. F. Abbott, P. Sikivie, and M. B. Wise. "Constraints on Charged Higgs Couplings". In: *Phys. Rev. D* 21 (1980), p. 1393.

[82] L. J. Hall and M. B. Wise. "Flavor Changing Higgs - Boson Couplings". In: *Nucl. Phys. B* 187 (1981), pp. 397–408.

[83] V. D. Barger, J. L. Hewett, and R. J. N. Phillips. "New Constraints on the Charged Higgs Sector in Two Higgs Doublet Models". In: *Phys. Rev. D* 41 (1990), pp. 3421–3441.

[84] D. Atwood, L. Reina, and A. Soni. "Phenomenology of two Higgs doublet models with flavor changing neutral currents". In: *Phys. Rev. D* 55 (1997), pp. 3156–3176. arXiv: hep-ph/9609279.

[85] A. Wahab El Kaffas, P. Osland, and O. M. Ogreid. "Constraining the Two-Higgs-Doublet-Model parameter space". In: *Phys. Rev. D* 76 (2007), p. 095001. arXiv: 0706.2997 [hep-ph].

[86] F. Cornet and W. Hollik. "Pair Production of Two-Higgs-Doublet Model Light Higgs Bosons in gamma gamma Collisions". In: *Phys. Lett. B* 669 (2008), pp. 58–61. arXiv: 0808.0719 [hep-ph].

[87] M. Aoki, S. Kanemura, K. Tsumura, and K. Yagyu. "Models of Yukawa interaction in the two Higgs doublet model, and their collider phenomenology". In: *Phys. Rev. D* 80 (2009), p. 015017. arXiv: 0902.4665 [hep-ph].

[88] F. Mahmoudi and O. Stal. "Flavor constraints on the two-Higgs-doublet model with general Yukawa couplings". In: *Phys. Rev. D* 81 (2010), p. 035016. arXiv: 0907.1791 [hep-ph].

[89] O. Deschamps, S. Descotes-Genon, S. Monteil, V. Niess, S. T'Jampens, and V. Tisserand. "The Two Higgs Doublet of Type II facing flavour physics data". In: *Phys. Rev. D* 82 (2010), p. 073012. arXiv: 0907.5135 [hep-ph].

[90] A. Crivellin, A. Kokulu, and C. Greub. "Flavor-phenomenology of two-Higgs-doublet models with generic Yukawa structure". In: *Phys. Rev. D* 87.9 (2013), p. 094031. arXiv: 1303.5877 [hep-ph].

[91] A. Broggio, E. J. Chun, M. Passera, K. M. Patel, and S. K. Vempati. "Limiting two-Higgs-doublet models". In: *JHEP* 11 (2014), p. 058. arXiv: 1409.3199 [hep-ph].

[92] D. Das. "New limits on tan β for 2HDMs with $\mathbb{Z}_2$ symmetry". In: *Int. J. Mod. Phys. A* 30.26 (2015), p. 1550158. arXiv: 1501.02610 [hep-ph].

[93] R. Gaitán, J. H. Montes de Oca, E. A. Garcés, and R. Martinez. "Rare top decay $t \to c\gamma$ with flavor changing neutral scalar interactions in two Higgs doublet model". In: *Phys. Rev. D* 94.9 (2016), p. 094038. arXiv: 1503.04391 [hep-ph].

[94] B. Altunkaynak, W.-S. Hou, C. Kao, M. Kohda, and B. McCoy. "Flavor Changing Heavy Higgs Interactions at the LHC". In: *Phys. Lett. B* 751 (2015), pp. 135–142. arXiv: 1506.00651 [hep-ph].

[95] A. Arhrib, R. Benbrik, C.-H. Chen, M. Gomez-Bock, and S. Semlali. "Two-Higgs-doublet type-II and -III models and $t \to ch$ at the LHC". In: *Eur. Phys. J. C* 76.6 (2016), p. 328. arXiv: 1508.06490 [hep-ph].

[96] C. S. Kim, Y. W. Yoon, and X.-B. Yuan. "Exploring top quark FCNC within 2HDM type III in association with flavor physics". In: *JHEP* 12 (2015), p. 038. arXiv: 1509.00491 [hep-ph].

[97] T. Enomoto and R. Watanabe. "Flavor constraints on the Two Higgs Doublet Models of $\mathbb{Z}_2$ symmetric and aligned types". In: *JHEP* 05 (2016), p. 002. arXiv: 1511.05066 [hep-ph].

[98] R. Benbrik, C.-H. Chen, and T. Nomura. "$h, Z \to \ell_i \bar{\ell}_j$, Δa_μ, $\tau \to (3\mu, \mu\gamma)$ in generic two-Higgs-doublet models". In: *Phys. Rev. D* 93.9 (2016), p. 095004. arXiv: 1511.08544 [hep-ph].

[99] J. M. Cline. "Scalar doublet models confront τ and b anomalies". In: *Phys. Rev. D* 93.7 (2016), p. 075017. arXiv: 1512.02210 [hep-ph].

[100] L. Wang, F. Zhang, and X.-F. Han. "Two-Higgs-doublet model of type-II confronted with the LHC run-I and run-II data". In: *Phys. Rev. D* 95.11 (2017), p. 115014. arXiv: 1701.02678 [hep-ph].

[101] S. Gori, H. E. Haber, and E. Santos. "High scale flavor alignment in two-Higgs doublet models and its phenomenology". In: *JHEP* 06 (2017), p. 110. arXiv: 1703.05873 [hep-ph].

[102] A. Arbey, F. Mahmoudi, O. Stal, and T. Stefaniak. "Status of the Charged Higgs Boson in Two Higgs Doublet Models". In: *Eur. Phys. J. C* 78.3 (2018), p. 182. arXiv: 1706.07414 [hep-ph].

[103] N. G. Deshpande and E. Ma. "Pattern of Symmetry Breaking with Two Higgs Doublets". In: *Phys. Rev. D* 18 (1978), p. 2574.

[104] M. Bona et al. "The 2004 UTfit collaboration report on the status of the unitarity triangle in the standard model". In: *JHEP* 07 (2005), p. 028. arXiv: hep-ph/0501199.

[105] F. J. Botella, G. C. Branco, M. Nebot, and M. N. Rebelo. "New physics and evidence for a complex CKM". In: *Nucl. Phys. B* 725 (2005), pp. 155–172. arXiv: hep-ph/0502133.

[106] H.-K. Guo, Y.-Y. Li, T. Liu, M. Ramsey-Musolf, and J. Shu. "Lepton-Flavored Electroweak Baryogenesis". In: *Phys. Rev. D* 96.11 (2017), p. 115034. arXiv: 1609.09849 [hep-ph].

[107] K. Fuyuto, W.-S. Hou, and E. Senaha. "Electroweak baryogenesis driven by extra top Yukawa couplings". In: *Phys. Lett. B* 776 (2018), pp. 402–406. arXiv: 1705.05034 [hep-ph].

[108] I. F. Ginzburg and M. Krawczyk. "Symmetries of two Higgs doublet model and CP violation". In: *Phys. Rev. D* 72 (2005), p. 115013. arXiv: hep-ph/0408011.

[109] S. Davidson and H. E. Haber. "Basis-independent methods for the two-Higgs-doublet model". In: *Phys. Rev. D* 72 (2005). [Erratum: Phys.Rev.D 72, 099902 (2005)], p. 035004. arXiv: hep-ph/0504050.

[110] H. Georgi and D. V. Nanopoulos. "Suppression of Flavor Changing Effects From Neutral Spinless Meson Exchange in Gauge Theories". In: *Phys. Lett. B* 82 (1979), pp. 95–96.

[111] F. J. Botella and J. P. Silva. "Jarlskog - like invariants for theories with scalars and fermions". In: *Phys. Rev. D* 51 (1995), pp. 3870–3875. arXiv: hep-ph/9411288.

[112] S. L. Glashow and S. Weinberg. "Natural Conservation Laws for Neutral Currents". In: *Phys. Rev. D* 15 (1977), p. 1958.

[113] A. Stange, W. J. Marciano, and S. Willenbrock. "Higgs bosons at the Fermilab Tevatron". In: *Phys. Rev. D* 49 (1994), pp. 1354–1362. arXiv: hep-ph/9309294.

[114] M. A. Diaz and T. J. Weiler. "Decays of a fermiophobic Higgs". In: *3rd Annual Southern Association for High-energy Physics Meeting*. Jan. 1994. arXiv: hep-ph/9401259.

[115] V. D. Barger, N. G. Deshpande, J. L. Hewett, and T. G. Rizzo. "A Separate Higgs?" In: *Workshop on Physics at Current Accelerators and the Supercollider*. Nov. 1992. arXiv: hep-ph/9211234.

[116] O. Eberhardt, U. Nierste, and M. Wiebusch. "Status of the two-Higgs-doublet model of type II". In: *JHEP* 07 (2013), p. 118. arXiv: 1305.1649 [hep-ph].

[117] J. Baglio, O. Eberhardt, U. Nierste, and M. Wiebusch. "Benchmarks for Higgs Pair Production and Heavy Higgs boson Searches in the Two-Higgs-Doublet Model of Type II". In: *Phys. Rev. D* 90.1 (2014), p. 015008. arXiv: 1403.1264 [hep-ph].

[118] R. M. Barnett, G. Senjanovic, and D. Wyler. "Tracking Down Higgs Scalars With Enhanced Couplings". In: *Phys. Rev. D* 30 (1984), p. 1529.

[119] R. M. Barnett, G. Senjanovic, L. Wolfenstein, and D. Wyler. "Implications of a Light Higgs Scalar". In: *Phys. Lett. B* 136 (1984), pp. 191–195.

[120] J. Cao, P. Wan, L. Wu, and J. M. Yang. "Lepton-Specific Two-Higgs Doublet Model: Experimental Constraints and Implication on Higgs Phenomenology". In: *Phys. Rev. D* 80 (2009), p. 071701. arXiv: 0909.5148 [hep-ph].

[121] A. Crivellin, J. Heeck, and P. Stoffer. "A perturbed lepton-specific two-Higgs-doublet model facing experimental hints for physics beyond the Standard Model". In: *Phys. Rev. Lett.* 116.8 (2016), p. 081801. arXiv: 1507.07567 [hep-ph].

[122] X.-F. Han, T. Li, L. Wang, and Y. Zhang. "Simple interpretations of lepton anomalies in the lepton-specific inert two-Higgs-doublet model". In: *Phys. Rev. D* 99.9 (2019), p. 095034. arXiv: 1812.02449 [hep-ph].

[123] L. Wang, J. M. Yang, M. Zhang, and Y. Zhang. "Revisiting lepton-specific 2HDM in light of muon $g-2$ anomaly". In: *Phys. Lett. B* 788 (2019), pp. 519–529. arXiv: 1809.05857 [hep-ph].

[124] V. Barger, H. E. Logan, and G. Shaughnessy. "Identifying extended Higgs models at the LHC". In: *Phys. Rev. D* 79 (2009), p. 115018. arXiv: 0902.0170 [hep-ph].

[125] A. Pich and P. Tuzon. "Yukawa Alignment in the Two-Higgs-Doublet Model". In: *Phys. Rev. D* 80 (2009), p. 091702. arXiv: 0908.1554 [hep-ph].

[126] P. M. Ferreira, L. Lavoura, and J. P. Silva. "Renormalization-group constraints on Yukawa alignment in multi-Higgs-doublet models". In: *Phys. Lett. B* 688 (2010), pp. 341–344. arXiv: 1001.2561 [hep-ph].

[127] M. Jung, A. Pich, and P. Tuzon. "Charged-Higgs phenomenology in the Aligned two-Higgs-doublet model". In: *JHEP* 11 (2010), p. 003. arXiv: 1006.0470 [hep-ph].

[128] F. J. Botella, G. C. Branco, A. M. Coutinho, M. N. Rebelo, and J. I. Silva-Marcos. "Natural Quasi-Alignment with two Higgs Doublets and RGE Stability". In: *Eur. Phys. J. C* 75 (2015), p. 286. arXiv: 1501.07435 [hep-ph].

[129] A. Peñuelas and A. Pich. "Flavour alignment in multi-Higgs-doublet models". In: *JHEP* 12 (2017), p. 084. arXiv: 1710.02040 [hep-ph].

[130] C. B. Braeuninger, A. Ibarra, and C. Simonetto. "Radiatively induced flavour violation in the general two-Higgs doublet model with Yukawa alignment". In: *Phys. Lett. B* 692 (2010), pp. 189–195. arXiv: 1005.5706 [hep-ph].

[131] A. Pich. "Flavour constraints on multi-Higgs-doublet models: Yukawa alignment". In: *Nucl. Phys. B Proc. Suppl.* 209 (2010). Ed. by G. Ricciardi, G. De Nardo, M. Merola, and C. Sciacca, pp. 182–187. arXiv: 1010.5217 [hep-ph].

[132] J. Bijnens, J. Lu, and J. Rathsman. "Constraining General Two Higgs Doublet Models by the Evolution of Yukawa Couplings". In: *JHEP* 05 (2012), p. 118. arXiv: 1111.5760 [hep-ph].

[133] G. C. Branco, W. Grimus, and L. Lavoura. "Relating the scalar flavor changing neutral couplings to the CKM matrix". In: *Phys. Lett. B* 380 (1996), pp. 119–126. arXiv: hep-ph/9601383.

[134] A. J. Buras, P. Gambino, M. Gorbahn, S. Jager, and L. Silvestrini. "Universal unitarity triangle and physics beyond the standard model". In: *Phys. Lett. B* 500 (2001), pp. 161–167. arXiv: hep-ph/0007085.

[135] G. D'Ambrosio, G. F. Giudice, G. Isidori, and A. Strumia. "Minimal flavor violation: An Effective field theory approach". In: *Nucl. Phys. B* 645 (2002), pp. 155–187. arXiv: hep-ph/0207036.

[136] V. Cirigliano, B. Grinstein, G. Isidori, and M. B. Wise. "Minimal flavor violation in the lepton sector". In: *Nucl. Phys. B* 728 (2005), pp. 121–134. arXiv: hep-ph/0507001.

[137] A. J. Buras. "Minimal flavor violation". In: *Acta Phys. Polon. B* 34 (2003). Ed. by M. Praszalowicz, pp. 5615–5668. arXiv: hep-ph/0310208.

[138] F. J. Botella, G. C. Branco, and M. N. Rebelo. "Minimal Flavour Violation and Multi-Higgs Models". In: *Phys. Lett. B* 687 (2010), pp. 194–200. arXiv: 0911.1753 [hep-ph].

[139] L. Lavoura. "Models of CP violation exclusively via neutral scalar exchange". In: *Int. J. Mod. Phys. A* 9 (1994), pp. 1873–1888.

[140] F. J. Botella, G. C. Branco, M. Nebot, and M. N. Rebelo. "Two-Higgs Leptonic Minimal Flavour Violation". In: *JHEP* 10 (2011), p. 037. arXiv: 1102.0520 [hep-ph].

[141] F. J. Botella, G. C. Branco, A. Carmona, M. Nebot, L. Pedro, and M. N. Rebelo. "Physical Constraints on a Class of Two-Higgs Doublet Models with FCNC at tree level". In: *JHEP* 07 (2014), p. 078. arXiv: 1401.6147 [hep-ph].

[142] G. Bhattacharyya, D. Das, and A. Kundu. "Feasibility of light scalars in a class of two-Higgs-doublet models and their decay signatures". In: *Phys. Rev. D* 89 (2014), p. 095029. arXiv: 1402.0364 [hep-ph].

[143] F. J. Botella, G. C. Branco, M. Nebot, and M. N. Rebelo. "Flavour Changing Higgs Couplings in a Class of Two Higgs Doublet Models". In: *Eur. Phys. J. C* 76.3 (2016), p. 161. arXiv: 1508.05101 [hep-ph].

[144] G. Bhattacharyya, D. Das, P. B. Pal, and M. N. Rebelo. "Scalar sector properties of two-Higgs-doublet models with a global U(1) symmetry". In: *JHEP* 10 (2013), p. 081. arXiv: 1308.4297 [hep-ph].

[145] P. M. Ferreira and J. P. Silva. "Abelian symmetries in the two-Higgs-doublet model with fermions". In: *Phys. Rev. D* 83 (2011), p. 065026. arXiv: 1012.2874 [hep-ph].

[146] H. Serôdio. "Yukawa sector of Multi Higgs Doublet Models in the presence of Abelian symmetries". In: *Phys. Rev. D* 88.5 (2013), p. 056015. arXiv: 1307.4773 [hep-ph].

[147] P. Ko, Y. Omura, and C. Yu. "A Resolution of the Flavor Problem of Two Higgs Doublet Models with an Extra $U(1)_H$ Symmetry for Higgs Flavor". In: *Phys. Lett. B* 717 (2012), pp. 202–206. arXiv: 1204.4588 [hep-ph].

[148] M. D. Campos, D. Cogollo, M. Lindner, T. Melo, F. S. Queiroz, and W. Rodejohann. "Neutrino Masses and Absence of Flavor Changing Interactions in the 2HDM from Gauge Principles". In: *JHEP* 08 (2017), p. 092. arXiv: 1705.05388 [hep-ph].

[149] R. Gatto, G. Morchio, and F. Strocchi. "Natural Flavor Conservation in the Neutral Currents and the Determination of the Cabibbo Angle". In: *Phys. Lett. B* 80 (1979), pp. 265–268.

[150] R. Gatto, G. Morchio, G. Sartori, and F. Strocchi. "Natural Flavor Conservation in Higgs Induced Neutral Currents and the Quark Mixing Angles". In: *Nucl. Phys. B* 163 (1980), pp. 221–253.

[151] G. Sartori. "Discrete Symmetries, Natural Flavor Conservation and Weak Mixing Angles". In: *Phys. Lett. B* 82 (1979), pp. 255–259.

[152] W. Grimus and G. Ecker. "On the Simultaneous Diagonalizability of Matrices". In: *J. Phys. A* 19 (1986), p. 3917.

[153] R. Barbieri, R. Gatto, and F. Strocchi. "Quark Mass Matrix and Discrete Symmetries in the SU(2) X U(1) Model". In: *Phys. Lett. B* 74 (1978), pp. 344–346.

[154] G. Sartori. "The Concrete Realization Of The Symmetries Responsible For Natural Flavor Conservation Laws". In: *Nuovo Cim. A* 55 (1980), p. 377.

[155] R. Gatto, G. Morchio, and F. Strocchi. "Symmetries Leading To Flavor Conservation In Higgs Induced Neutral Currents And Implications On The Cabibbo Angle". In: *Phys. Lett. B* 83 (1979), pp. 348–350.

[156] G. Segre and H. A. Weldon. "Natural Flavor Conservation and the Absence of Radiatively Induced Cabibbo Angles". In: *Phys. Lett. B* 86 (1979), pp. 291–293.

[157] G. Segre and H. A. Weldon. "The Conflict Between Natural Flavor Conservation of Higgs Couplings and Cabibbo Mixing in $SU(2)_L \times U(1)$". In: *Annals Phys.* 124 (1980), p. 37.

[158] A. C. Rothman and K. Kang. "Natural Flavor Conservation". In: *Phys. Rev. D* 23 (1981), p. 2657.

[159] K. Kang and A. C. Rothman. "Generalized Mixing Angles in Gauge Theories With Natural Flavor Conservation". In: *Phys. Rev. D* 24 (1981), p. 167.

[160] M. Leurer, Y. Nir, and N. Seiberg. "Mass matrix models". In: *Nucl. Phys. B* 398 (1993), pp. 319–342. arXiv: hep-ph/9212278.

[161] G. Ecker, W. Grimus, and H. Neufeld. "Spontaneous CP Violation And Neutral Flavor Conservation". In: *Phys. Lett. B* 228 (1989), pp. 401–405.

[162] H. Serodio. "Yukawa Alignment in a Multi Higgs Doublet Model: An effective approach". In: *Phys. Lett. B* 700 (2011), pp. 133–138. arXiv: 1104.2545 [hep-ph].

[163] I. de Medeiros Varzielas. "Family symmetries and alignment in multi-Higgs doublet models". In: *Phys. Lett. B* 701 (2011), pp. 597–600. arXiv: 1104.2601 [hep-ph].

[164] M. B. Wise. "Radiatively Induced Flavor Changing Neutral Higgs Boson Couplings". In: *Phys. Lett. B* 103 (1981), pp. 121–123.

[165] J. M. Frere and Y.-P. Yao. "Naturalness For Multiscalar Models And Radiative Stability". In: *Phys. Rev. Lett.* 55 (1985), p. 2386.

[166] G. Cvetic, S. S. Hwang, and C. S. Kim. "One loop renormalization group equations of the general framework with two Higgs doublets". In: *Int. J. Mod. Phys. A* 14 (1999), pp. 769–798. arXiv: hep-ph/9706323.

[167] G. Cvetic, C. S. Kim, and S. S. Hwang. "Higgs mediated flavor changing neutral currents in the general framework with two Higgs doublets: An RGE analysis". In: *Phys. Rev. D* 58 (1998), p. 116003. arXiv: hep-ph/9806282.

[168] Y. H. Ahn and C.-H. Chen. "New charged Higgs effects on $\Gamma_{K_{e2}}/\Gamma_{K_2}$, f_{D_s} and $\mathcal{B}(B^+ \to \tau^+\nu)$ in the Two-Higgs-Doublet model". In: *Phys. Lett. B* 690 (2010), pp. 57–61. arXiv: 1002.4216 [hep-ph].

[169] S. Pakvasa and H. Sugawara. "Discrete Symmetry and Cabibbo Angle". In: *Phys. Lett. B* 73 (1978), pp. 61–64.

[170] D. Wyler. "The Cabibbo Angle in the $SU(2)_L\times$ U(1) Gauge Theories". In: *Phys. Rev. D* 19 (1979), p. 330.

[171] M. Nebot and J. P. Silva. "Self-cancellation of a scalar in neutral meson mixing and implications for the LHC". In: *Phys. Rev. D* 92.8 (2015), p. 085010. arXiv: 1507.07941 [hep-ph].

[172] W. Grimus and L. Lavoura. "Renormalization of the neutrino mass operators in the multi-Higgs-doublet standard model". In: *Eur. Phys. J. C* 39 (2005), pp. 219–227. arXiv: hep-ph/0409231.

[173] T. P. Cheng, E. Eichten, and L.-F. Li. "Higgs Phenomena in Asymptotically Free Gauge Theories". In: *Phys. Rev. D* 9 (1974), p. 2259.

[174] V. Andreev et al. "Improved limit on the electric dipole moment of the electron". In: *Nature* 562.7727 (2018), pp. 355–360.

[175] T. Han, S. K. Kang, and J. Sayre. "Muon $g-2$ in the aligned two Higgs doublet model". In: *JHEP* 02 (2016), p. 097. arXiv: 1511.05162 [hep-ph].

[176] G. C. Branco and M. N. Rebelo. "The Higgs Mass in a Model With Two Scalar Doublets and Spontaneous CP Violation". In: *Phys. Lett. B* 160 (1985), pp. 117–120.

[177] A. G. Akeroyd, A. Arhrib, and E.-M. Naimi. "Note on tree level unitarity in the general two Higgs doublet model". In: *Phys. Lett. B* 490 (2000), pp. 119–124. arXiv: hep-ph/0006035.

[178] I. F. Ginzburg and I. P. Ivanov. "Tree-level unitarity constraints in the most general 2HDM". In: *Phys. Rev. D* 72 (2005), p. 115010. arXiv: hep-ph/0508020.

[179] B. Grinstein, C. W. Murphy, and P. Uttayarat. "One-loop corrections to the perturbative unitarity bounds in the CP-conserving two-Higgs doublet model with a softly broken $\mathbb{Z}_2$ symmetry". In: *JHEP* 06 (2016), p. 070. arXiv: 1512.04567 [hep-ph].

[180] V. Cacchio, D. Chowdhury, O. Eberhardt, and C. W. Murphy. "Next-to-leading order unitarity fits in Two-Higgs-Doublet models with soft $\mathbb{Z}_2$ breaking". In: *JHEP* 11 (2016), p. 026. arXiv: 1609.01290 [hep-ph].

[181] G. Blankenburg, J. Ellis, and G. Isidori. "Flavour-Changing Decays of a 125 GeV Higgs-like Particle". In: *Phys. Lett. B* 712 (2012), pp. 386–390. arXiv: 1202.5704 [hep-ph].

[182] M. Aaboud et al. "Search for top-quark decays $t \to Hq$ with 36 fb^{-1} of pp collision data at $\sqrt{s} = 13$ TeV with the ATLAS detector". In: *JHEP* 05 (2019), p. 123. arXiv: 1812.11568 [hep-ex].

[183] A. M. Sirunyan et al. "Search for the flavor-changing neutral current interactions of the top quark and the Higgs boson which decays into a pair of b quarks at $\sqrt{s} = 13$ TeV". In: *JHEP* 06 (2018), p. 102. arXiv: 1712.02399 [hep-ex].

[184] G. Aad et al. "Search for top quark decays $t \to qH$ with $H \to \gamma\gamma$ using the ATLAS detector". In: *JHEP* 06 (2014), p. 008. arXiv: 1403.6293 [hep-ex].

[185] V. Khachatryan et al. "Searches for heavy Higgs bosons in two-Higgs-doublet models and for $t \to ch$ decay using multilepton and diphoton final states in pp collisions at 8 TeV". In: *Phys. Rev. D* 90 (2014), p. 112013. arXiv: 1410.2751 [hep-ex].

[186] V. Khachatryan et al. "Search for top quark decays via Higgs-boson-mediated flavor-changing neutral currents in pp collisions at $\sqrt{s} = 8$ TeV". In: *JHEP* 02 (2017), p. 079. arXiv: 1610.04857 [hep-ex].

[187] F. J. Botella, G. C. Branco, and M. N. Rebelo. "Invariants and Flavour in the General Two-Higgs Doublet Model". In: *Phys. Lett. B* 722 (2013), pp. 76–82. arXiv: 1210.8163 [hep-ph].

[188] J. Bernabeu, G. C. Branco, and M. Gronau. "CP Restrictions on Quark Mass Matrices". In: *Phys. Lett. B* 169 (1986), pp. 243–247.

[189] M. Trodden. "Electroweak baryogenesis". In: *Rev. Mod. Phys.* 71 (1999), pp. 1463–1500. arXiv: hep-ph/9803479.

[190] D. E. Morrissey and M. J. Ramsey-Musolf. "Electroweak baryogenesis". In: *New J. Phys.* 14 (2012), p. 125003. arXiv: 1206.2942 [hep-ph].

[191] C. Jarlskog. "Commutator of the Quark Mass Matrices in the Standard Electroweak Model and a Measure of Maximal CP Violation". In: *Phys. Rev. Lett.* 55 (1985), p. 1039.

[192] R. Acciarri et al. "Long-Baseline Neutrino Facility (LBNF) and Deep Underground Neutrino Experiment (DUNE): Conceptual Design Report, Volume 1: The LBNF and DUNE Projects". In: (Jan. 2016). arXiv: 1601.05471 [physics.ins-det].

[193] K. Abe et al. "Constraint on the matterantimatter symmetry-violating phase in neutrino oscillations". In: *Nature* 580.7803 (2020). [Erratum: Nature 583, E16 (2020)], pp. 339–344. arXiv: 1910.03887 [hep-ex].

[194] M. A. Acero et al. "First Measurement of Neutrino Oscillation Parameters using Neutrinos and Antineutrinos by NOvA". In: *Phys. Rev. Lett.* 123.15 (2019), p. 151803. arXiv: 1906.04907 [hep-ex].

[195] M. Bona et al. "The UTfit collaboration report on the status of the unitarity triangle beyond the standard model. I. Model-independent analysis and minimal flavor violation". In: *JHEP* 03 (2006), p. 080. arXiv: hep-ph/0509219.

[196] M. Nebot, F. J. Botella, and G. C. Branco. "Vacuum Induced CP Violation Generating a Complex CKM Matrix with Controlled Scalar FCNC". In: *Eur. Phys. J. C* 79.8 (2019), p. 711. arXiv: 1808.00493 [hep-ph].

[197] G. D'Ambrosio, G. F. Giudice, G. Isidori, and A. Strumia. "Minimal flavor violation: An Effective field theory approach". In: *Nucl. Phys. B* 645 (2002), pp. 155–187. arXiv: hep-ph/0207036.

[198] P. F. de Salas, D. V. Forero, S. Gariazzo, P. Martnez-Miravé, O. Mena, C. A. Ternes, M. Tórtola, and J. W. F. Valle. "2020 global reassessment of the neutrino oscillation picture". In: *JHEP* 02 (2021), p. 071. arXiv: 2006.11237 [hep-ph].

[199] I. Esteban, M. C. Gonzalez-Garcia, M. Maltoni, T. Schwetz, and A. Zhou. "The fate of hints: updated global analysis of three-flavor neutrino oscillations". In: *JHEP* 09 (2020), p. 178. arXiv: 2007.14792 [hep-ph].

[200] A. M. Sirunyan et al. "Search for the flavor-changing neutral current interactions of the top quark and the Higgs boson which decays into a pair of b quarks at $\sqrt{s}$ = 13 TeV". In: *JHEP* 06 (2018), p. 102. arXiv: 1712.02399 [hep-ex].

[201] M. Aaboud et al. "Search for top-quark decays $t \to Hq$ with 36 fb^{-1} of pp collision data at $\sqrt{s}$ = 13 TeV with the ATLAS detector". In: *JHEP* 05 (2019), p. 123. arXiv: 1812.11568 [hep-ex].

[202] A. M. Baldini et al. "Search for the lepton flavour violating decay $\mu^+ \to e^+\gamma$ with the full dataset of the MEG experiment". In: *Eur. Phys. J. C* 76.8 (2016), p. 434. arXiv: 1605.05081 [hep-ex].

[203] S. M. Barr and A. Zee. "Electric Dipole Moment of the Electron and of the Neutron". In: *Phys. Rev. Lett.* 65 (1990). [Erratum: Phys.Rev.Lett. 65, 2920 (1990)], pp. 21–24.

[204] D. Chang, W. S. Hou, and W.-Y. Keung. "Two loop contributions of flavor changing neutral Higgs bosons to mu —> e gamma". In: *Phys. Rev. D* 48 (1993), pp. 217–224. arXiv: hep-ph/9302267.

[205] A. M. Sirunyan et al. "Search for lepton-flavor violating decays of the Higgs boson in the $\mu\tau$ and eτ final states in proton-proton collisions at $\sqrt{s} = 13$ TeV". In: (May 2021). arXiv: 2105.03007 [hep-ex].

[206] A. M. Sirunyan et al. "Search for lepton flavour violating decays of the Higgs boson to $\mu\tau$ and eτ in proton-proton collisions at $\sqrt{s}$ = 13 TeV". In: *JHEP* 06 (2018), p. 001. arXiv: 1712.07173 [hep-ex].

[207] G. Aad et al. "Searches for lepton-flavour-violating decays of the Higgs boson in $\sqrt{s}$ = 13 TeV pp collisions with the ATLAS detector". In: *Phys. Lett. B* 800 (2020), p. 135069. arXiv: 1907.06131 [hep-ex].

[208] T. Davidek and L. Fiorini. "Search for Lepton-Flavor-Violating Decays of Bosons With the ATLAS Detector". In: *Front. in Phys.* 8 (2020), p. 149.

[209] A. S. Joshipura and S. D. Rindani. "Naturally suppressed flavor violations in two Higgs doublet models". In: *Phys. Lett. B* 260 (1991), pp. 149–153.

[210] A. S. Joshipura. "Neutral Higgs and CP violation". In: *Mod. Phys. Lett. A* 6 (1991), pp. 1693–1700.

[211] I. P. Ivanov and J. P. Silva. "Tree-level metastability bounds for the most general two Higgs doublet model". In: *Phys. Rev. D* 92.5 (2015), p. 055017. arXiv: 1507.05100 [hep-ph].

[212] S. Kanemura, T. Kubota, and E. Takasugi. "Lee-Quigg-Thacker bounds for Higgs boson masses in a two doublet model". In: *Phys. Lett. B* 313 (1993), pp. 155–160. arXiv: hep-ph/9303263.

[213] J. Horejsi and M. Kladiva. "Tree-unitarity bounds for THDM Higgs masses revisited". In: *Eur. Phys. J. C* 46 (2006), pp. 81–91. arXiv: hep-ph/0510154.

[214] S. Kanemura and K. Yagyu. "Unitarity bound in the most general two Higgs doublet model". In: *Phys. Lett. B* 751 (2015), pp. 289–296. arXiv: 1509.06060 [hep-ph].

[215] M. Nebot. "Bounded masses in two Higgs doublets models, spontaneous CP violation and $\mathbb{Z}_2$ symmetry". In: *Phys. Rev. D* 102.11 (2020), p. 115002. arXiv: 1911.02266 [hep-ph].

[216] W. Grimus, L. Lavoura, O. M. Ogreid, and P. Osland. "A Precision constraint on multi-Higgs-doublet models". In: *J. Phys. G* 35 (2008), p. 075001. arXiv: 0711.4022 [hep-ph].

[217] W. Grimus, L. Lavoura, O. M. Ogreid, and P. Osland. "The Oblique parameters in multi-Higgs-doublet models". In: *Nucl. Phys. B* 801 (2008), pp. 81–96. arXiv: 0802.4353 [hep-ph].

[218] G. Aad et al. "Measurements of Higgs Bosons Decaying to Bottom Quarks from Vector Boson Fusion Production with the ATLAS Experiment at $\sqrt{s}$ = 13 TeV". In: (Nov. 2020). arXiv: 2011.08280 [hep-ex].

[219] G. Aad et al. "Measurements of WH and ZH production in the $H \to b\bar{b}$ decay channel in pp collisions at 13 TeV with the ATLAS detector". In: *Eur. Phys. J. C* 81.2 (2021), p. 178. arXiv: 2007.02873 [hep-ex].

[220] "Measurement of the Higgs boson decaying to b-quarks produced in association with a top-quark pair in pp collisions at $\sqrt{s}$ = 13 TeV with the ATLAS detector". In: (Nov. 2020).

[221] "Measurement of the properties of Higgs boson production at $\sqrt{s}$=13 TeV in the $H \to \gamma\gamma$ channel using 139 fb^1 of pp collision data with the ATLAS experiment". In: (Aug. 2020).

[222] G. Aad et al. "A search for the dimuon decay of the Standard Model Higgs boson with the ATLAS detector". In: *Phys. Lett. B* 812 (2021), p. 135980. arXiv: 2007.07830 [hep-ex].

[223] "A combination of measurements of Higgs boson production and decay using up to 139 fb^{-1} of proton–proton collision data at $\sqrt{s}$ = 13 TeV collected with the ATLAS experiment". In: (Aug. 2020).

[224] G. Aad et al. "Measurement of the production cross section for a Higgs boson in association with a vector boson in the $H \to WW^* \to \ell\nu\ell\nu$ channel in pp collisions at $\sqrt{s} = 13$ TeV with the ATLAS detector". In: *Phys. Lett. B* 798 (2019), p. 134949. arXiv: 1903.10052 [hep-ex].

[225] G. Aad et al. "Higgs boson production cross-section measurements and their EFT interpretation in the 4ℓ decay channel at $\sqrt{s}$ =13 TeV with the ATLAS detector". In: *Eur. Phys. J. C* 80.10 (2020). [Erratum: Eur.Phys.J.C 81, 29 (2021)], p. 957. arXiv: 2004.03447 [hep-ex].

[226] CMS. *Combined Higgs boson production and decay measurements with up to 137 fb-1 of proton-proton collision data at sqrts = 13 TeV*. Tech. rep. Geneva: CERN, 2020. URL: http://cds.cern.ch/record/2706103.

[227] CMS. "Search for the standard model Higgs boson produced through vector boson fusion and decaying to bb with proton-proton collisions at sqrt(s) = 13 TeV". In: (2016). URL: http://cds.cern.ch/record/2160154.

[228] A. M. Sirunyan et al. "Measurements of Higgs boson production cross sections and couplings in the diphoton decay channel at $\sqrt{s}$ = 13 TeV". In: (Mar. 2021). arXiv: 2103.06956 [hep-ex].

[229] A. M. Sirunyan et al. "Evidence for Higgs boson decay to a pair of muons". In: *JHEP* 01 (2021), p. 148. arXiv: 2009.04363 [hep-ex].

[230] A. M. Sirunyan et al. "Measurements of production cross sections of the Higgs boson in the four-lepton final state in proton-proton collisions at $\sqrt{s}$ = 13 TeV". In: (Mar. 2021). arXiv: 2103.04956 [hep-ex].

[231] N. Kauer and G. Passarino. "Inadequacy of zero-width approximation for a light Higgs boson signal". In: *JHEP* 08 (2012), p. 116. arXiv: 1206.4803 [hep-ph].

[232] G. Aad et al. "Constraints on the off-shell Higgs boson signal strength in the high-mass ZZ and WW final states with the ATLAS detector". In: *Eur. Phys. J. C* 75.7 (2015), p. 335. arXiv: 1503.01060 [hep-ex].

[233] V. Khachatryan et al. "Search for Higgs boson off-shell production in proton-proton collisions at 7 and 8 TeV and derivation of constraints on its total decay width". In: *JHEP* 09 (2016), p. 051. arXiv: 1605.02329 [hep-ex].

[234] J. F. Gunion, H. E. Haber, G. L. Kane, and S. Dawson. *The Higgs Hunter's Guide*. Vol. 80. 2000.

[235] A. Djouadi. "The Anatomy of electro-weak symmetry breaking. I: The Higgs boson in the standard model". In: *Phys. Rept.* 457 (2008), pp. 1–216. arXiv: hep-ph/0503172.

[236] M. Spira, A. Djouadi, D. Graudenz, and P. M. Zerwas. "Higgs boson production at the LHC". In: *Nucl. Phys. B* 453 (1995), pp. 17–82. arXiv: hep-ph/9504378.

[237] S. Dittmaier et al. "Handbook of LHC Higgs Cross Sections: 1. Inclusive Observables". In: (Jan. 2011). arXiv: 1101.0593 [hep-ph].

[238] S. Dittmaier et al. "Handbook of LHC Higgs Cross Sections: 2. Differential Distributions". In: (Jan. 2012). arXiv: 1201.3084 [hep-ph].

[239] J. R. Andersen et al. "Handbook of LHC Higgs Cross Sections: 3. Higgs Properties". In: (July 2013). Ed. by S. Heinemeyer, C. Mariotti, G. Passarino, and R. Tanaka. arXiv: 1307.1347 [hep-ph].

[240] D. de Florian et al. "Handbook of LHC Higgs Cross Sections: 4. Deciphering the Nature of the Higgs Sector". In: 2/2017 (Oct. 2016). arXiv: 1610.07922 [hep-ph].

[241] Z.-z. Xing, H. Zhang, and S. Zhou. "Impacts of the Higgs mass on vacuum stability, running fermion masses and two-body Higgs decays". In: *Phys. Rev. D* 86 (2012), p. 013013. arXiv: 1112.3112 [hep-ph].

[242] H. M. Georgi, S. L. Glashow, M. E. Machacek, and D. V. Nanopoulos. "Higgs Bosons from Two Gluon Annihilation in Proton Proton Collisions". In: *Phys. Rev. Lett.* 40 (1978), p. 692.

[243] R. V. Harlander and W. B. Kilgore. "Next-to-next-to-leading order Higgs production at hadron colliders". In: *Phys. Rev. Lett.* 88 (2002), p. 201801. arXiv: hep-ph/0201206.

[244] V. Ravindran, J. Smith, and W. L. van Neerven. "NNLO corrections to the total cross-section for Higgs boson production in hadron hadron collisions". In: *Nucl. Phys. B* 665 (2003), pp. 325–366. arXiv: hep-ph/0302135.

[245] A. Pak, M. Rogal, and M. Steinhauser. "Production of scalar and pseudo-scalar Higgs bosons to next-to-next-to-leading order at hadron colliders". In: *JHEP* 09 (2011), p. 088. arXiv: 1107.3391 [hep-ph].

[246] R. V. Harlander and W. B. Kilgore. "Production of a pseudoscalar Higgs boson at hadron colliders at next-to-next-to leading order". In: *JHEP* 10 (2002), p. 017. arXiv: hep-ph/0208096.

[247] C. Anastasiou and K. Melnikov. "Pseudoscalar Higgs boson production at hadron colliders in NNLO QCD". In: *Phys. Rev. D* 67 (2003), p. 037501. arXiv: hep-ph/0208115.

[248] T. Ahmed, M. Bonvini, M. C. Kumar, P. Mathews, N. Rana, V. Ravindran, and L. Rottoli. "Pseudo-scalar Higgs boson production at N^3 LO_A $+N^3$ LL $'$". In: *Eur. Phys. J. C* 76.12 (2016), p. 663. arXiv: 1606.00837 [hep-ph].

[249] Y. Kuno and Y. Okada. "Muon decay and physics beyond the standard model". In: *Rev. Mod. Phys.* 73 (2001), pp. 151–202. arXiv: hep-ph/9909265.

[250] M. Tanabashi et al. "Review of Particle Physics". In: *Phys. Rev. D* 98.3 (2018), p. 030001.

[251] P. A. Zyla et al. "Review of Particle Physics". In: *PTEP* 2020.8 (2020), p. 083C01.

[252] V. Cirigliano and I. Rosell. "Two-loop effective theory analysis of pi (K) —> e anti-nu/e [gamma] branching ratios". In: *Phys. Rev. Lett.* 99 (2007), p. 231801. arXiv: 0707.3439 [hep-ph].

[253] A. Pich. "Precision Tau Physics". In: *Prog. Part. Nucl. Phys.* 75 (2014), pp. 41–85. arXiv: 1310.7922 [hep-ph].

[254] M. Misiak et al. "Estimate of $\mathcal{B}(\bar{B} \to X_s\gamma)$ at $O(\alpha_s^2)$". In: *Phys. Rev. Lett.* 98 (2007), p. 022002. arXiv: hep-ph/0609232.

[255] J. F. Gunion and H. E. Haber. "The CP conserving two Higgs doublet model: The Approach to the decoupling limit". In: *Phys. Rev. D* 67 (2003), p. 075019. arXiv: hep-ph/0207010.

[256] A. D. Martin, W. J. Stirling, R. S. Thorne, and G. Watt. "Parton distributions for the LHC". In: *Eur. Phys. J. C* 63 (2009), pp. 189–285. arXiv: 0901.0002 [hep-ph].

[257] R. G. Leigh, S. Paban, and R. M. Xu. "Electric dipole moment of electron". In: *Nucl. Phys. B* 352 (1991), pp. 45–58.

[258] J. F. Gunion and R. Vega. "The Electron electric dipole moment for a CP violating neutral Higgs sector". In: *Phys. Lett. B* 251 (1990), pp. 157–162.

[259] D. Chang, W.-Y. Keung, and T. C. Yuan. "Two loop bosonic contribution to the electron electric dipole moment". In: *Phys. Rev. D* 43 (1991), R14–R16.

[260] C. Kao and R.-M. Xu. "Charged Higgs loop contribution to the electric dipole moment of electron". In: *Phys. Lett. B* 296 (1992), pp. 435–439.

[261] V. Ilisie. "New Barr-Zee contributions to $(\mathbf{g-2})_\mu$ in two-Higgs-doublet models". In: *JHEP* 04 (2015), p. 077. arXiv: 1502.04199 [hep-ph].

[262] S. Inoue, M. J. Ramsey-Musolf, and Y. Zhang. "CP-violating phenomenology of flavor conserving two Higgs doublet models". In: *Phys. Rev. D* 89.11 (2014), p. 115023. arXiv: 1403.4257 [hep-ph].

[263] W. Altmannshofer, J. Brod, and M. Schmaltz. "Experimental constraints on the coupling of the Higgs boson to electrons". In: *JHEP* 05 (2015), p. 125. arXiv: 1503.04830 [hep-ph].

[264] L. Bian, T. Liu, and J. Shu. "Cancellations Between Two-Loop Contributions to the Electron Electric Dipole Moment with a CP-Violating Higgs Sector". In: *Phys. Rev. Lett.* 115 (2015), p. 021801. arXiv: 1411.6695 [hep-ph].

[265] M. Jung and A. Pich. "Electric Dipole Moments in Two-Higgs-Doublet Models". In: *JHEP* 04 (2014), p. 076. arXiv: 1308.6283 [hep-ph].

[266] V. Khachatryan et al. "Search for a standard model-like Higgs boson in the $\mu^+\mu^-$ and e^+e^- decay channels at the LHC". In: *Phys. Lett. B* 744 (2015), pp. 184–207. arXiv: 1410.6679 [hep-ex].

[267] M. Aaboud et al. "Search for the dimuon decay of the Higgs boson in pp collisions at $\sqrt{s} = 13$ TeV with the ATLAS detector". In: *Phys. Rev. Lett.* 119.5 (2017), p. 051802. arXiv: 1705.04582 [hep-ex].

[268] G. F. Giudice, P. Paradisi, and M. Passera. "Testing new physics with the electron g-2". In: *JHEP* 11 (2012), p. 113. arXiv: 1208.6583 [hep-ph].

[269] A. Crivellin, M. Hoferichter, and P. Schmidt-Wellenburg. "Combined explanations of $(g-2)_{\mu,e}$ and implications for a large muon EDM". In: *Phys. Rev. D* 98.11 (2018), p. 113002. arXiv: 1807.11484 [hep-ph].

[270] J. Liu, C. E. M. Wagner, and X.-P. Wang. "A light complex scalar for the electron and muon anomalous magnetic moments". In: *JHEP* 03 (2019), p. 008. arXiv: 1810.11028 [hep-ph].

[271] M. Endo and W. Yin. "Explaining electron and muon $g-2$ anomaly in SUSY without lepton-flavor mixings". In: *JHEP* 08 (2019), p. 122. arXiv: 1906.08768 [hep-ph].

[272] M. Bauer, M. Neubert, S. Renner, M. Schnubel, and A. Thamm. "Axionlike Particles, Lepton-Flavor Violation, and a New Explanation of a_μ and a_e". In: *Phys. Rev. Lett.* 124.21 (2020), p. 211803. arXiv: 1908.00008 [hep-ph].

[273] M. Badziak and K. Sakurai. "Explanation of electron and muon g – 2 anomalies in the MSSM". In: *JHEP* 10 (2019), p. 024. arXiv: 1908.03607 [hep-ph].

[274] G. Hiller, C. Hormigos-Feliu, D. F. Litim, and T. Steudtner. "Anomalous magnetic moments from asymptotic safety". In: *Phys. Rev. D* 102.7 (2020), p. 071901. arXiv: 1910.14062 [hep-ph].

[275] A. E. Cárcamo Hernández, Y. Hidalgo Velásquez, S. Kovalenko, H. N. Long, N. A. Pérez-Julve, and V. V. Vien. "Fermion spectrum and $g-2$ anomalies in a low scale 3-3-1 model". In: *Eur. Phys. J. C* 81.2 (2021), p. 191. arXiv: 2002.07347 [hep-ph].

[276] N. Haba, Y. Shimizu, and T. Yamada. "Muon and electron $g-2$ and the origin of the fermion mass hierarchy". In: *PTEP* 2020.9 (2020), 093B05. arXiv: 2002.10230 [hep-ph].

[277] I. Bigaran and R. R. Volkas. "Getting chirality right: Single scalar leptoquark solutions to the $(g-2)_{e,\mu}$ puzzle". In: *Phys. Rev. D* 102.7 (2020), p. 075037. arXiv: 2002.12544 [hep-ph].

[278] L. Calibbi, M. L. López-Ibáñez, A. Melis, and O. Vives. "Muon and electron $g-2$ and lepton masses in flavor models". In: *JHEP* 06 (2020), p. 087. arXiv: 2003.06633 [hep-ph].

[279] C.-H. Chen and T. Nomura. "Electron and muon $g-2$, radiative neutrino mass, and $\ell' \to \ell\gamma$ in a $U(1)_{e-\mu}$ model". In: *Nucl. Phys. B* 964 (2021), p. 115314. arXiv: 2003.07638 [hep-ph].

[280] S. Jana, V. P. K., and S. Saad. "Resolving electron and muon $g-2$ within the 2HDM". In: *Phys. Rev. D* 101.11 (2020), p. 115037. arXiv: 2003.03386 [hep-ph].

[281] C. Hati, J. Kriewald, J. Orloff, and A. M. Teixeira. "Anomalies in ^{8}Be nuclear transitions and $(g-2)_{e,\mu}$: towards a minimal combined explanation". In: *JHEP* 07 (2020), p. 235. arXiv: 2005.00028 [hep-ph].

[282] B. Dutta, S. Ghosh, and T. Li. "Explaining $(g-2)_{\mu,e}$, the KOTO anomaly and the MiniBooNE excess in an extended Higgs model with sterile neutrinos". In: *Phys. Rev. D* 102.5 (2020), p. 055017. arXiv: 2006.01319 [hep-ph].

[283] D. Sabatta, A. S. Cornell, A. Goyal, M. Kumar, B. Mellado, and X. Ruan. "Connecting muon anomalous magnetic moment and multi-lepton anomalies at LHC". In: *Chin. Phys. C* 44.6 (2020), p. 063103. arXiv: 1909.03969 [hep-ph].

[284] S.-P. Li, X.-Q. Li, Y.-Y. Li, Y.-D. Yang, and X. Zhang. "Power-aligned 2HDM: a correlative perspective on $(g-2)_{e,\mu}$". In: *JHEP* 01 (2021), p. 034. arXiv: 2010.02799 [hep-ph].

[285] S. Fajfer, J. F. Kamenik, and M. Tammaro. "Interplay of New Physics effects in (g – 2) and h $\to \ell^+\ell$ lessons from SMEFT". In: *JHEP* 06 (2021), p. 099. arXiv: 2103.10859 [hep-ph].

[286] A. E. Cárcamo Hernández, C. Espinoza, J. Carlos Gómez-Izquierdo, and M. Mondragón. "Fermion masses and mixings, dark matter, leptogenesis and $g-2$ muon anomaly in an extended 2HDM with inverse seesaw". In: (Apr. 2021). arXiv: 2104.02730 [hep-ph].

[287] X.-F. Han, T. Li, H.-X. Wang, L. Wang, and Y. Zhang. "Lepton-specific inert two-Higgs-doublet model confronted with the new results for muon and electron g-2 anomalies and multi-lepton searches at the LHC". In: (Apr. 2021). arXiv: 2104.03227 [hep-ph].

[288] C.-H. Chen, C.-W. Chiang, and T. Nomura. "Muon $g-2$ in two-Higgs-doublet model with type-II seesaw mechanism". In: (Apr. 2021). arXiv: 2104.03275 [hep-ph].

[289] A. Jueid, J. Kim, S. Lee, and J. Song. "Type-X two Higgs doublet model in light of the muon $\mathbf{g-2}$: confronting Higgs and collider data". In: (Apr. 2021). arXiv: 2104.10175 [hep-ph].

[290] H.-X. Wang, L. Wang, and Y. Zhang. "muon $g-2$ anomaly and μ-τ-philic Higgs doublet with a light CP-even component". In: (Apr. 2021). arXiv: 2104.03242 [hep-ph].

[291] A. E. Cárcamo Hernández, S. Kovalenko, M. Maniatis, and I. Schmidt. "Fermion mass hierarchy and g-2 anomalies in an extended 3HDM Model". In: (Apr. 2021). arXiv: 2104.07047 [hep-ph].

[292] W. Rodejohann and U. Saldaña-Salazar. "Multi-Higgs-Doublet Models and Singular Alignment". In: *JHEP* 07 (2019), p. 036. arXiv: 1903.00983 [hep-ph].

[293] J. P. Leveille. "The Second Order Weak Correction to (g-2) of the Muon in Arbitrary Gauge Models". In: *Nucl. Phys. B* 137 (1978), pp. 63–76.

[294] K.-m. Cheung, C.-H. Chou, and O. C. W. Kong. "Muon anomalous magnetic moment, two Higgs doublet model, and supersymmetry". In: *Phys. Rev. D* 64 (2001), p. 111301. arXiv: hep-ph/0103183.

[295] K. Cheung, O. C. W. Kong, and J. S. Lee. "Electric and anomalous magnetic dipole moments of the muon in the MSSM". In: *JHEP* 06 (2009), p. 020. arXiv: 0904.4352 [hep-ph].

[296] A. Cherchiglia, P. Kneschke, D. Stöckinger, and H. Stöckinger-Kim. "The muon magnetic moment in the 2HDM: complete two-loop result". In: *JHEP* 01 (2017), p. 007. arXiv: 1607.06292 [hep-ph].

[297] G. Aad et al. "Measurements of the Higgs boson production and decay rates and constraints on its couplings from a combined ATLAS and CMS analysis of the LHC pp collision data at $\sqrt{s} = 7$ and 8 TeV". In: *JHEP* 08 (2016), p. 045. arXiv: 1606.02266 [hep-ex].

[298] M. Aaboud et al. "Evidence for the $H \to b\bar{b}$ decay with the ATLAS detector". In: *JHEP* 12 (2017), p. 024. arXiv: 1708.03299 [hep-ex].

[299] A. M. Sirunyan et al. "Evidence for the Higgs boson decay to a bottom quarkantiquark pair". In: *Phys. Lett. B* 780 (2018), pp. 501–532. arXiv: 1709.07497 [hep-ex].

[300] A. M. Sirunyan et al. "Observation of the Higgs boson decay to a pair of τ leptons with the CMS detector". In: *Phys. Lett. B* 779 (2018), pp. 283–316. arXiv: 1708.00373 [hep-ex].

[301] E. J. Chun and J. Kim. "Leptonic Precision Test of Leptophilic Two-Higgs-Doublet Model". In: *JHEP* 07 (2016), p. 110. arXiv: 1605.06298 [hep-ph].

[302] S. Schael et al. "Fermion pair production in e^+e^- collisions at 189-209-GeV and constraints on physics beyond the standard model". In: *Eur. Phys. J. C* 49 (2007), pp. 411–437. arXiv: hep-ex/0609051.

[303] M. Aaboud et al. "Search for new high-mass phenomena in the dilepton final state using 36 fb^1 of proton-proton collision data at $\sqrt{s}$ = 13 TeV with the ATLAS detector". In: *JHEP* 10 (2017), p. 182. arXiv: 1707.02424 [hep-ex].

[304] M. Aaboud et al. "Search for scalar resonances decaying into $\mu^+\mu^-$ in events with and without b-tagged jets produced in proton-proton collisions at $\sqrt{s}$ = 13 TeV with the ATLAS detector". In: *JHEP* 07 (2019), p. 117. arXiv: 1901.08144 [hep-ex].

[305] A. M. Sirunyan et al. "Search for MSSM Higgs bosons decaying to μ + μ − in proton-proton collisions at s=13TeV". In: *Phys. Lett. B* 798 (2019), p. 134992. arXiv: 1907.03152 [hep-ex].

[306] M. Aaboud et al. "Search for additional heavy neutral Higgs and gauge bosons in the ditau final state produced in 36 fb^1 of pp collisions at $\sqrt{s}$ = 13 TeV with the ATLAS detector". In: *JHEP* 01 (2018), p. 055. arXiv: 1709.07242 [hep-ex].

[307] V. Khachatryan et al. "Search for heavy resonances decaying to tau lepton pairs in proton-proton collisions at $\sqrt{s}$ = 13 TeV". In: *JHEP* 02 (2017), p. 048. arXiv: 1611.06594 [hep-ex].

[308] A. M. Sirunyan et al. "Search for additional neutral MSSM Higgs bosons in the $\tau\tau$ final state in proton-proton collisions at $\sqrt{s}$ = 13 TeV". In: *JHEP* 09 (2018), p. 007. arXiv: 1803.06553 [hep-ex].

[309] M. Aaboud et al. "Search for charged Higgs bosons produced in association with a top quark and decaying via $H^\pm \to \tau\nu$ using pp collision data recorded at $\sqrt{s}$ = 13 TeV by the ATLAS detector". In: *Phys. Lett. B* 759 (2016), pp. 555–574. arXiv: 1603.09203 [hep-ex].

[310] M. Aaboud et al. "Search for charged Higgs bosons decaying into top and bottom quarks at $\sqrt{s}$ = 13 TeV with the ATLAS detector". In: *JHEP* 11 (2018), p. 085. arXiv: 1808.03599 [hep-ex].

[311] A. M. Sirunyan et al. "Search for charged Higgs bosons in the $H^\pm \to \tau^\pm\nu_\tau$ decay channel in proton-proton collisions at $\sqrt{s}$ = 13 TeV". In: *JHEP* 07 (2019), p. 142. arXiv: 1903.04560 [hep-ex].

[312] A. M. Sirunyan et al. "Search for a charged Higgs boson decaying into top and bottom quarks in events with electrons or muons in proton-proton collisions at $\sqrt{s}$ = 13 TeV". In: *JHEP* 01 (2020), p. 096. arXiv: 1908.09206 [hep-ex].

[313] A. M. Sirunyan et al. "Search for charged Higgs bosons decaying into a top and a bottom quark in the all-jet final state of pp collisions at $\sqrt{s}$ = 13 TeV". In: *JHEP* 07 (2020), p. 126. arXiv: 2001.07763 [hep-ex].

[314] M. Flechl, R. Klees, M. Kramer, M. Spira, and M. Ubiali. "Improved cross-section predictions for heavy charged Higgs boson production at the LHC". In: *Phys. Rev. D* 91.7 (2015), p. 075015. arXiv: 1409.5615 [hep-ph].

[315] C. Degrande, M. Ubiali, M. Wiesemann, and M. Zaro. "Heavy charged Higgs boson production at the LHC". In: *JHEP* 10 (2015), p. 145. arXiv: 1507.02549 [hep-ph].

[316] J. Alwall, R. Frederix, S. Frixione, V. Hirschi, F. Maltoni, O. Mattelaer, H. .-. Shao, T. Stelzer, P. Torrielli, and M. Zaro. "The automated computation of tree-level and next-to-leading order differential cross sections, and their matching to parton shower simulations". In: *JHEP* 07 (2014), p. 079. arXiv: 1405.0301 [hep-ph].

[317] A. Alloul, N. D. Christensen, C. Degrande, C. Duhr, and B. Fuks. "FeynRules 2.0 - A complete toolbox for tree-level phenomenology". In: *Comput. Phys. Commun.* 185 (2014), pp. 2250–2300. arXiv: 1310.1921 [hep-ph].

[318] C. Degrande. "Automatic evaluation of UV and R2 terms for beyond the Standard Model Lagrangians: a proof-of-principle". In: *Comput. Phys. Commun.* 197 (2015), pp. 239–262. arXiv: 1406.3030 [hep-ph].

[319] C. Degrande. "Automated Two Higgs Doublet Model at NLO". In: *PoS* Charged2014 (2015). Ed. by O. Stål and E. Bergeaas Kuutmann, p. 024. arXiv: 1412.6955 [hep-ph].

[320] F. Faro, J. C. Romao, and J. P. Silva. "Nondecoupling in Multi-Higgs doublet models". In: *Eur. Phys. J. C* 80.7 (2020), p. 635. arXiv: 2002.10518 [hep-ph].

[321] L.-L. Chau and W.-Y. Keung. "Comments on the Parametrization of the Kobayashi-Maskawa Matrix". In: *Phys. Rev. Lett.* 53 (1984), p. 1802.

[322] H. E. Haber and D. O'Neil. "Basis-independent methods for the two-Higgs-doublet model. II. The Significance of tanβ". In: *Phys. Rev. D* 74 (2006). [Erratum: Phys.Rev.D 74, 059905 (2006)], p. 015018. arXiv: hep-ph/0602242.